Functional and molecular characterization of the phylogenetically related *ERF102* to *ERF105* transcription factor genes in *Arabidopsis thaliana*

Inaugural–Dissertation

to obtain the academic degree

Doctor rerum naturalium (Dr. rer. nat.)

submitted to the Department of Biology, Chemistry and Pharmacy

of Freie Universität Berlin

by

Sylvia Bolt

from Bernau (Germany)

Berlin 2017

The investigations described in the following thesis were performed from March 2012 to June 2017 under supervision of Prof. Dr. Thomas Schmülling at the Institute of Biology, Department of Applied Genetics of the Freie Universität Berlin.

1st Reviewer: Prof. Dr. Thomas Schmülling (FU Berlin)

2nd Reviewer: Prof. Dr. Wolfgang Schuster (FU Berlin)

Date of defense: 12th October 2017

Table of contents

List of tables

List of figures

List of abbreviations

SI units, symbols and abbreviations from the statistic, or the periodic table as well as country codes according to ISO 3166 are not listed in this table.

24-epiBL	24-epi-brassinolide
3-AT	3-amino-1,2,4-triazole
7'-OH-ABA	7'-hydroxy-ABA
A	Absorbance
AAO3	*ABSCISIC ALDEHYDE OXIDASE 3*
ABA	Abscisic acid
ABA	*ABA DEFICIENT*
ABA-GE	ABA-glucose ester
ABF	*ABA-BINDING FACTOR*
ABI	*ABA INSENSITIVE*
ABRE	ABA-responsive element
ACC	1-Aminocyclopropane-1-carboxylic acid
ACC14	14 days acclimated
ACC21	21 days acclimated
ACT2	*ACTIN 2*
AGL68	*AGAMOUS-LIKE 68*
AHK	*ARABIDOPSIS HISTIDINE KINASE*
AHP	*ARABIDOPSIS HISTIDINE PHOSPHOTRANSFER PROTEIN*
amiRNA	Artificial micro RNA
ANS	Anthocyanin synthase
AP2	*APETALA 2*
APX	Ascorbate peroxidase
AREB	ABA-RESPONSIVE ELEMENT-BINDING PROTEIN
Arg	Arginine
ARR	*ARABIDOPSIS RESPONSE REGULATOR*
ATP	Adenosine triphosphate
BA	N6-Benzyladenine
bHLH	Basic helix-loop-helix
BiFC	Bimolecular fluorescence complementation
bp	Base pair(s)
BR	Brassinoteroid
BRAVO	*BRASSINOSTEROIDS AT VASCULAR AND ORGANIZING CENTER*
bZIP	Basic leucine-zipper
CAM	Crassulacean acid metabolism
CAMTA3	*CALMODULIN-BINDING TRANSCRIPTION ACTIVATOR 3*
CaMV	Cauliflower mosaic virus
CAT	Catalase

CBF	*C-REPEAT-BINDING FACTOR*
cDNA	Complementary desoxyribonucleic acid
CHI	Chalcone isomerase
ChIP	Chromatin immunoprecipitation
CHS	Chalcone synthase
CK	Cytokinin
CM2	Conserved motif 2
Co-IP	Co-immunoprecipitation
Col-0	Ecotype/accession Columbia-0
COR	*COLD-REGULATED*
CRISPR/CAS	Clustered regularly interspaced short palindromic repeats/CRISPR-associated protein
CRF	*CYTOKININ RESPONSE FACTOR*
CRT	C-repeat element
CSD1	*COPPER/ZINC SUPEROXIDE DISMUTASE 1*
CTAB	Cetyl trimethylammonium bromide
CYP707A	*CYTOCHROME P450, FAMILY 707, SUBFAMILY A, POLYPEPTIDE*
ddH2O	double deionized water
DFR	Dihydroflavonol 4-reductase
DHAP	dihydroxyacetone phosphate
DHAR	Dehydroascorbate reductase
DMSO	Dimethyl sulfoxide
DNA	Desoxyribonucleic acid
dNTP	Desoxyribonucleoside-tri-phosphate
DPA	Dihydrophaseic acid
DRE	Dehydration-responsive element
DREB	Dehydration response element-binding protein
DTT	Dithiothreitol
EAR	ERF-associated amphiphilic repression
e. g.	*exempli gratia* (Latin: for example)
EDTA	Ethylenediaminetetraacetic acid
EF1A	*TRANSLATION ELONGATION FACTOR EF1A*
EIL1	*ETHYLENE-INSENSITIVE3-LIKE 1*
EIN3	*ETHLYENE-INSENSITIVE3*
ERE-box	Ethylene-responsive element box
EREBP	ETHYLENE-RESPONSIVE ELEMENT-BINDING PROTEIN
ERF	*ETHYLENE RESPONSE FACTOR*
ESK1	*ESKIMO 1*
ET	Ethylene
et al.	*et alii* (Latin: and others)
ETR1	*ETHYLENE RESPONSE 1*
EX1	*EXECUTER 1*
eY1H	Enhanced yeast one-hybrid
F_1, F_2, F_3	First, second, third filial generation after a crossing

F3H	Flavanone 3-Hydroxylase
F3'H	Flavonoid 3' Hydroxylase
Fig./Figs	Figure/figures
flg22	Flagellin22
FLS	Flavonol synthase
F	Forward
Fru	Fructose
FSD	Fe superoxide dismutase
GA	Gibberellin
GA20OX	Gibberellin 20-oxidase
GA2OX	Gibberellin 2-oxidase
GA3OX	Gibberellin 3 beta-hydroxylase
GAPDH	Glyceraldehyde 3-phosphate dehydrogenase
GFP	Green fluorescent protein
Glc	Glucose
Glu	Glutamine
GR	Glutathione reductase
GUS	β-glucoronidase
HEPES	4-(2-Hydroxyethyl)piperazineethanesulfonic acid
His	Histidine
HOS1	*HIGH EXPRESSION OF OSMOTICALLY RESPONSIVE GENES 1*
HPAEC	High performance anion exchange chromatography
ICE	*INDUCER OF C-REPEAT-BINDING FACTOR EXPRESSION*
IDP	Intrinsically disordered protein
Inc	Incorporated
JA	Jasmonic acid
kb	Kilobase pair(s)
LB	Luria and Broth
LC-MS	Liquid chromatography-mass spectrometry
LD	Long day (light/dark: 16 h/8 h)
LDOX	Leucoanthocyanidin dioxygenase
LEA	*LATE EMBRYOGENESIS ABUNDANT*
Leu	Leucine
LOS4	*LOW EXPRESSION OF OSMOTICALLY RESPONSIVE GENES 4*
MBW	MYB-bHLH-WD40
MDA	Malondialdehyde
MDAR	Monodehydroascorbate reductase
MeJa	Methyl jasmonate
MES	2-(N-morpholino)ethanesulfonic acid
MPK	*MITOGEN-ACTIVATED PROTEIN KINASE*
MPKK	*MITOGEN-ACTIVATED PROTEIN KINASE KINASE*
MS	Murashige and Skoog
MU	Methylumbelliferone
MYBRS	MYB transcription factor recognition sequence

MYCRS	MYC transcription factor recognition sequence
NA	Non-acclimated
NAA	1-Naphthaleneacetic acid
NAD(P)H	Reduced nicotinamide adenine dinucleotide (phosphate)
NBT	Nitroblue tetrazolium
NCBI	National Center for Biotechnology Information
NCED3	*NINE-CIS-EPOXYCAROTENOID DIOXYGENASE 3*
neoPA	Neophaseic acid
NLS	Nuclear localization signal
OD	Optical density
OMT	O-Methyltransferase
ORA59	*OCTADECANOID-RESPONSIVE ARABIDOPSIS AP2/ERF 59*
OST1	*OPEN STOMATA 1*
P	Phosphorylation
PA	Phaseic acid
PAP	Purple acid phosphatase
PCR	Polymerase chain reaction
PCRE	PIN cytokinin response element
PDF1.2	*PLANT DEFENSIN 1.2*
PEG	Polyethylenglycol
PIN	*PIN-FORMED*
PIPES	Piperazine-N,N′-bis(2-ethanesulfonic acid)
PLT	*PLETHORA*
PP2AA2	*PROTEIN PHOSPHATASE 2A SUBUNIT A2*
PR	Pathogenesis-related
Pro	Proline
PVP	Polyvinylpyrrolidone
QC	Quiescent center
qRT-PCR	Quantitative real-time polymerase chain reaction
R	Reverse
RAB18	*ARABIDOPSIS RAB GTPASE HOMOLOG B18*
Raf	Raffinose
RAM	Root apical meristem
RBOH	RESPIRATORY BURST OXIDASE HOMOLOGUE
RD	*RESPONSIVE TO DESSICATION*
RNA	Ribonucleic acid
RNAi	Ribonucleic acid interference
ROS	Reactive oxygen species
ROX	6-Carboxyl-X-rhodamine
rpm	Rounds per minute
RT	Room temperature
RT-PCR	Reverse transcription polymerase chain reaction
RTTF1	*REDOX RESPONSIVE TRANSCRIPTION FACTOR 1*
S	Sumoylation

SA	Salicylic acid
SAM	Shoot apical meristem
SCR	*SCARECROW*
SD	Short-day (light/dark: 8 h/16 h)
SDS	Sodium dodecyl sulfate
SHR	*SHORT ROOT*
SIGnAL	Salk Institute Genomic Analysis Laboratory
SLAC1	*SLOW ANION CHANNEL-ASSOCIATED 1*
SOD	Superoxide dismutase
SOS	*SALT OVERLY SENSITIVE*
STZ	*SALT TOLERANCE ZINC FINGER*
T1, T2, T3	First, second, third generation after a transformation
Tab.	Table
TAE	Tris acetate ethylenediaminetetraacetic acid
TAIR	The *Arabidopsis* Information Resource
TALEN	Transcription activator-like effector nucleases
TBA	Thiobarbituric acid
TCA	Trichloroacetic acid
T-DNA	Transfer desoxyribonucleic acid
TGA3	*TGA1A-RELATED GENE 3*
Ti	Tumor inducing
TM	Trademark
TPT	Triosephosphate translocator
Tris	tris(hydroxymethyl)aminomethane
Trp	Tryptophane
TT	*TRANSPARENT TESTA*
TTG	*TRANSPARENT TESTA GLABRA*
U	Unit
U	Ubiquitination
UBC10	*UBIQUITIN-CONJUGATING ENZYME 10*
UGT	UDP-glycosyltransferase
UPLC-ESI-MS/MS	Ultra-performance liquid chromatography-electrospray ionisation tandem mass spectrometry
Ura	Uracil
VTC2	*VITAMIN C DEFECTIVE 2*
WMD3	Web MicroRNA Designer 3
WT	Wild type
X-Gluc	5-Bromo-4-chloro-1H-indol-3-yl β-D-glucopyranosiduronic acid
Y1H	Yeast one-hybrid
Y2H	Yeast two-hybrid
YNB	Yeast nitrogen base
ZAT	*ZINC FINGER OF ARABIDOPSIS THALIANA*

1 INTRODUCTION

For plant development, regulated growth and clearly determined differentiation steps are of decisive importance. The growth and yield of plants are strongly dependent on external conditions. As for all living beings, it is essential for the survival of plants to be able to respond to a variety of abiotic and biotic environmental influences. All these processes require numerous physiological and metabolic mechanisms. Plants are able to perceive environmental factors and translate them into altered gene expression patterns by the usage of signal transduction processes, with the participation of phytohormones and transcription factors, for instance, ETHYLENE RESPONSE FACTORs (ERFs), which enable the stress response and stress tolerance of plants (Sakuma *et al*., 2002).

This work is dealing with the characterization of four closely related *ERF* transcription factor genes, namely *ERF102* (AT5G47230; also known as *ERF5*), *ERF103* (AT4G17490; identical to *ERF6*), *ERF104* (AT5G61600) and *ERF105* (AT5G51190) (Nakano *et al*., 2006). In the course of the study it turned out that all four *ERF* genes play a role in abiotic stress. Therefore, the following sections will first introduce ERF transcription factors and then abiotic stress responses focusing on cold and drought stress, since these stresses played a major role in this study.

1.1 AP2/ERF transcription factors

The *APETALA2/ETHYLENE RESPONSE FACTOR* (*AP2/ERF)* genes form a large, plant-specific transcription factor gene (super)family. As the first gene of this superfamily, the floral homeotic plant gene *APETALA2* (*AP2*) was identified in *Arabidopsis thaliana* (Jofuku *et al*., 1994). In contrast to other identity genes of floral meristems and floral organs, of which most have a MADS domain (Davies and Schwarz-Sommer, 1994), the AP2 protein was found to have two copies of a new DNA-binding motif, the AP2 domain (Jofuku *et al*., 1994). Shortly after, four DNA-binding proteins that bind to a sequence, the ethylene-responsive element box (ERE-box) or GCC-box, which is essential for the response to the plant hormone ethylene (ET), were identified from tobacco (*Nicotiana tabacum*). These proteins were designated as ETHYLENE-RESPONSIVE ELEMENT-BINDING PROTEIN 1, 2, 3, and 4 (EREBP1, 2, 3, and 4), later renamed as ETHYLENE RESPONSE FACTOR 1, 2, 3, and 4 (ERF1, 2, 3, and 4) (Ohme-Takagi and Shinshi, 1995). The DNA-binding domain of EREBP2 was mapped to a region that was common to all four proteins (Ohme-Takagi and Shinshi, 1995) and that was found to have strong sequence similarity to the AP2 domain (Weigel, 1995).

Meanwhile, AP2/ERF transcription factors are found throughout the entire plant kingdom (Zhou *et al*., 1997; Liu *et al*., 2011). However, they are not found in mammalian, fungi, or yeast (Weigel, 1995).

Recent phylogenetic analyses based on sequence comparisons revealed that there are 147 AP2/ERF transcription factors in *Arabidopsis thaliana* (Nakano *et al*., 2006). Based on the number of existing AP2/ERF domains and the sequence similarities, the AP2/ERF transcription factors can be phylogenetically divided into four families (Fig. 1): the AP2 family, the RAV family, the ERF family, and a single gene (AT4G13040). AT4G13040 possesses an AP2/ERF-like domain sequence, but its homology is quite low in comparison with the other *AP2/ERF* genes. Members of the AP2 family have two AP2/ERF domains linked by a conserved sequence of 25 amino acids (Riechmann and Meyerowitz, 1998). RAV transcription factors are characterized by containing a single AP2/ERF domain and a B3 domain (Kagaya *et al*., 1999), which is a DNA-binding domain conserved in other plant-specific transcription factors. The ERF family proteins contain a single AP2/ERF domain (Sakuma *et al*., 2002) and can be divided into the C-REPEAT-BINDING FACTOR/DEHYDRATION RESPONSE ELEMENT-BINDING PROTEIN (CBF/DREB) and ERF subfamilies and these in turn into different groups (Nakano *et al*., 2006).

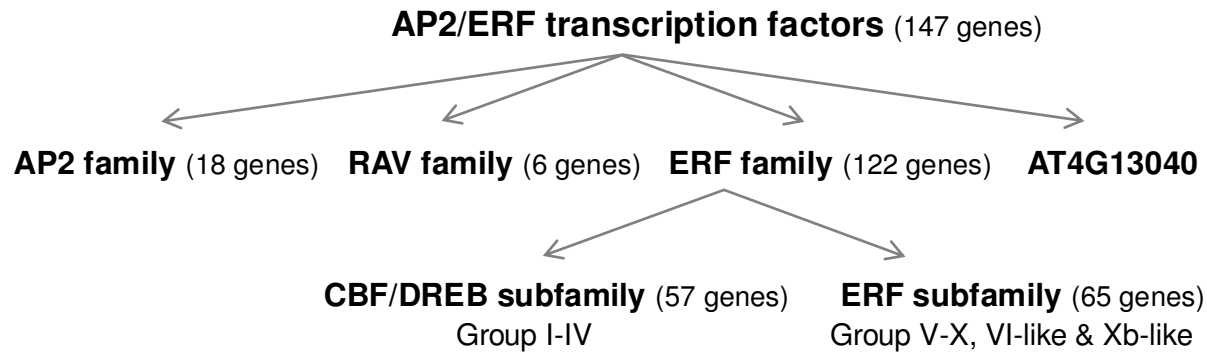

Figure 1. AP2/ERF transcription factors in *Arabidopsis thaliana*. Schematic presentation of classification by Nakano *et al.* (2006). The AP2/ERF transcription factor superfamily in *Arabidopsis thaliana* can be phylogenetically divided into the AP2, RAV, ERF family and AT4G13040. The ERF family can be divided into two subfamilies, the CBF/DREB and the ERF subfamily, including the groups I up to IV and V up to X, respectively. Numbers of genes of the respective transcription factor family are parenthesized.

1.1.1 The AP2/ERF domain

The AP2/ERF transcription factors are plant-specific transcription factors. However, it is unclear whether the origin of the AP2/ERF domain is eukaryotic, bacterial or viral. Studies on the evolution of the AP2/ERF domain revealed homologies to the homing endonucleases, mobile genetic elements, identified in the cyanobacterium *Trichodesmium erythraeum*, the ciliate *Tetrahymena thermophila,* and in the viruses *Enterobacteria phage Rb49* and *Bacteriophage Felix 01* (Gimble, 2000; Magnani *et al*., 2004). The hypothesis that the

AP2/ERF domain exists as a DNA-binding domain in non-plant species was supported by demonstrating that the *T. erythraeum* AP2/ERF domain can selectively bind stretches of poly(dG)/poly(dC). It is therefore assumed that the origin of the AP2/ERF domain is the lateral gene transfer of a homing endonuclease and its transposition and homing (Magnani *et al*., 2004).

The AP2/ERF domains of AP2/ERF transcription factors comprise 58 to 70 amino acids (Ohme-Takagi and Shinshi, 1995; Riechmann and Meyerowitz, 1998) and are more related to the members within the families (AP2, RAV and ERF family) than between the families. Common characteristics of the AP2/ERF domains of all families are the two conserved YRG and RAYD elements named after their conserved amino acids (Fig. 2). The N-terminal YRG element has a length of about 20 amino acids and is postulated as the DNA-binding domain, due to its hydrophilic and basic character. The C-terminal RAYD element of about 40 amino acids contains a stretch of 18 amino acids capable of forming an amphipathic α-helix that is proposed to be involved in protein-protein interactions and has also been considered for DNA binding (Jofuku *et al*., 1994; Okamuro *et al*., 1997). More recent analyses of the 3D solution structure of the AP2/ERF domain of AtERF1 (ERF100) revealed that the DNA-binding domain is composed of a three-stranded anti-parallel β-sheet packed along the α-helix. This structure is stabilized by an extensive number of hydrophobic contacts (Allen *et al*., 1998). It is suggested that the three-stranded β-sheet bind to the target sequence in the major groove of the DNA double helix (Fig. 2). This binding is essentially achieved by the seven highly conserved amino acids Arg150, Arg152, Trp154, Glu160, Arg162, Arg170 and Trp172 (Allen *et al*., 1998).

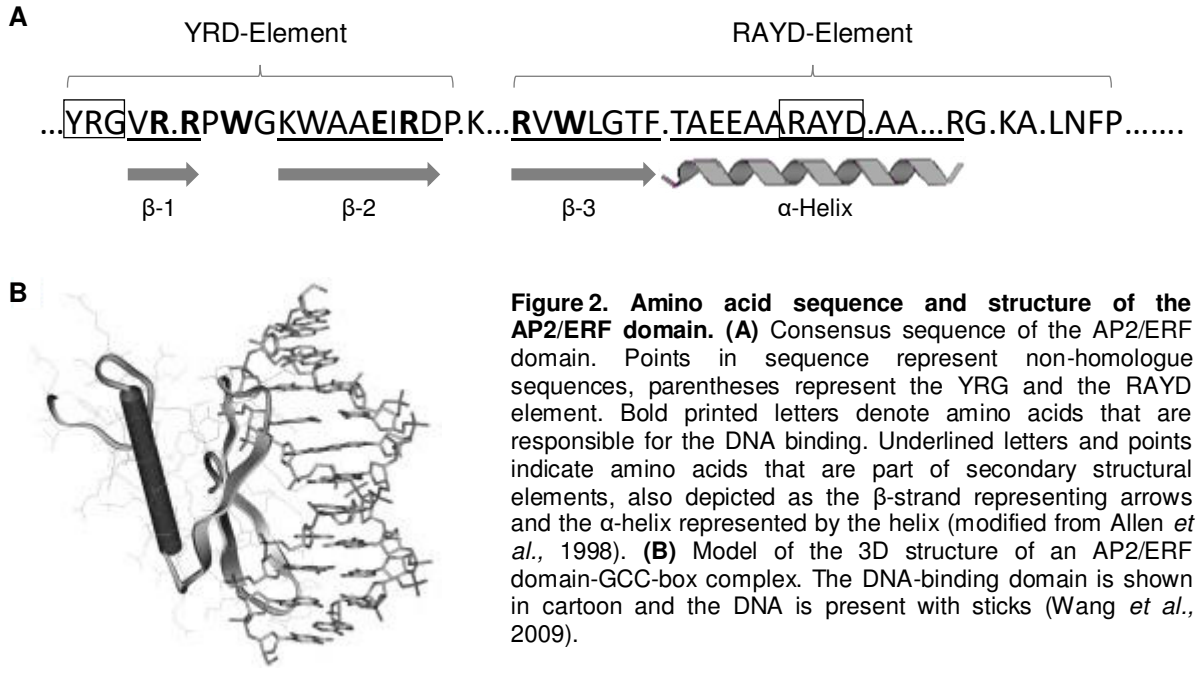

Figure 2. Amino acid sequence and structure of the AP2/ERF domain. (A) Consensus sequence of the AP2/ERF domain. Points in sequence represent non-homologue sequences, parentheses represent the YRG and the RAYD element. Bold printed letters denote amino acids that are responsible for the DNA binding. Underlined letters and points indicate amino acids that are part of secondary structural elements, also depicted as the β-strand representing arrows and the α-helix represented by the helix (modified from Allen *et al.,* 1998). **(B)** Model of the 3D structure of an AP2/ERF domain-GCC-box complex. The DNA-binding domain is shown in cartoon and the DNA is present with sticks (Wang *et al.,* 2009).

The AP2/ERF domains have been shown to bind to different *cis*-elements. The floral homeotic protein AP2 in *Arabidopsis* binds as monomer to a motif which includes an AT-rich element that is directly contacted by the second AP2/ERF repeat (Dinh *et al*., 2012). The AP2/ERF domain in RAV1 binds a CAACA motif (Kagaya *et al*., 1999). Many CBF/DREB proteins have been shown to bind to the dehydration-responsive element (DRE) with the core sequence 5'-A/GCCGAC-3', which is often associated with ABA, drought and cold-responsive genes (Stockinger *et al*., 1997; Liu *et al*., 1998, Sakuma *et al*., 2002). Conversely, members of the ERF subfamily specifically bind to the 5'-TAAGAGCCGCC-3' sequence, named the GCC-box, with the core element 5'-AGCCGCC-3', and the first G, the fourth G, and the sixth C exhibit highest binding specificity (Hao *et al*., 1998). This sequence is often found in the promoters of genes that respond to ET, pathogens and wounding (Ohme-Takagi and Shinshi, 1995). Other bases within the GCC-box exhibit modulated binding specificity varying from protein to protein, implying that these positions are important for differential binding by distinct ERF transcription factors (Hao *et al*., 1998). Single members of the CBF/DREB and ERF subfamilies have been reported to bind DRE and GCC elements (Sun *et al*., 2008) or even novel DNA elements that diverge significantly from these two (Welsch *et al*., 2007; Shaikhali *et al*., 2008).

1.1.2 The ERF family in Arabidopsis thaliana

1.1.2.1 The phylogeny of ERF transcription factors

In 2002, Sakuma *et al*. subdivided 121 ERF proteins from *Arabidopsis thaliana* according to the similarity of their AP2/ERF domain into two main groups, the CBF/DREB family and the ERF family, each further separable into six subgroups. Four years later, Nakano *et al*. (2006) refined Sakuma's classification taking into account the intron-exon structure of the *ERF* genes and the occurrence of additional motifs. In this way, they found 122 ERF proteins which were subdivided into twelve groups that substantially matched the classification provided by Sakuma *et al*. (2002). A phylogenetic tree of ERF transcription factors in *Arabidopsis thaliana* is shown in Figure 3.

Most of the *ERF* genes have no introns. Only 20 of the 122 *ERF* genes in *Arabidopsis* were found to have a single intron in their open reading frame region. These genes are associated with groups IV, V, VII, X, and Xb-like with the position of the intron being conserved in the respective group (Nakano *et al*., 2006). As already mentioned above, besides the AP2/ERF domain and the intron-exon structure, further conserved motifs were incorporated into the phylogenetic study of Nakano *et al*. (2006). Generally, regions outside the DNA-binding domain in transcription factors comprise functionally important domains involved in, for instance, protein-protein interaction, transcriptional activity or nuclear localization (Liu *et al*., 1999). Motif analyses revealed that some ERF proteins contain the ERF-associated

amphiphilic repression (EAR) motif, which has been shown to function as a repression domain (Ohta *et al*., 2001; Kagale and Rozwadowski, 2011). Those proteins are associated in group VIII of the ERF family (Nakano *et al*., 2006). A putative zinc finger motif, which is suggested to enable protein-DNA or protein-protein interactions, is conserved in the N-terminal region of ERF109 (AT4G34410) of group Xb as well as in members of group Xb-like (Nakano *et al*., 2006). Further putative functional motifs that were identified in most of the ERF proteins are acidic amino acid-rich sequences which are often designated as transcriptional activation domains (Liu *et al*., 1999), and putative phosphorylation sites found in groups VI, VII and IXb (Nakano *et al*., 2006). The functions of most of these and further identified conserved motifs have not been rigorously demonstrated.

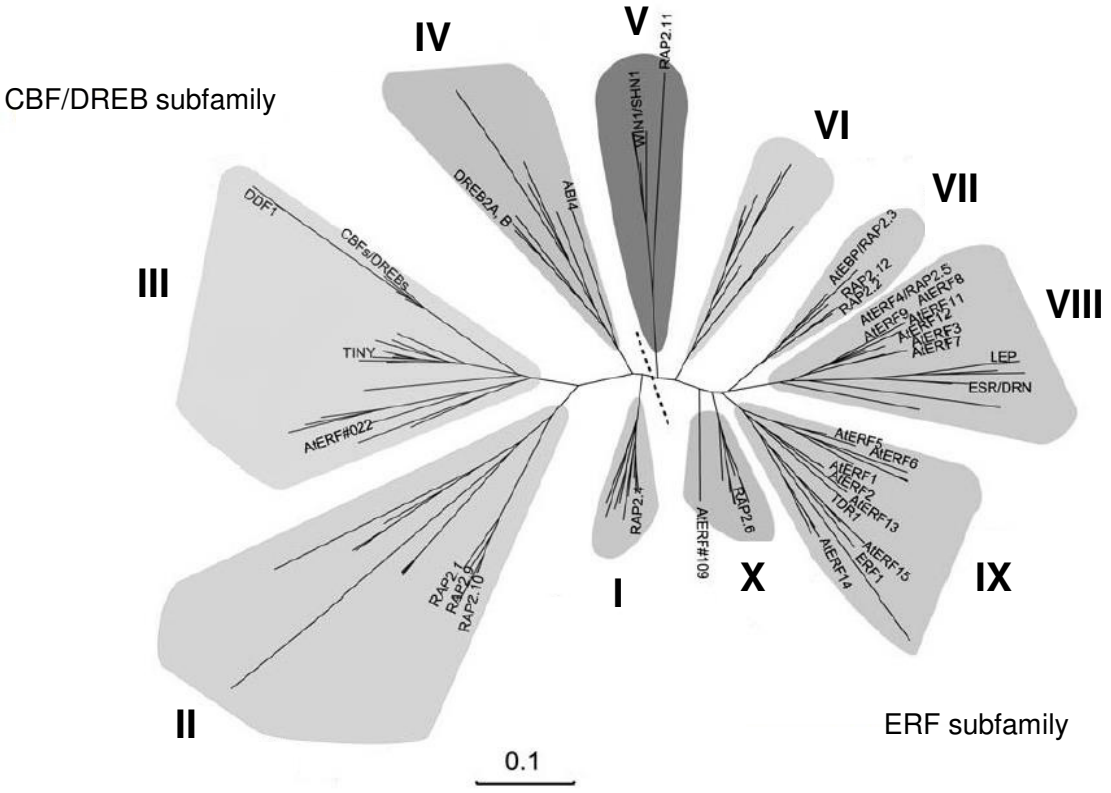

Figure 3. Phylogenetic tree of ERF transcription factors in *Arabidopsis thaliana*. An unrooted phylogenetic tree showing the CBF/DREB and ERF subfamily which are divided with a dashed line. The amino acid sequences of the AP2/ERF domain, except members of group VI-like and Xb-like, were aligned. The names of exemplary *ERF* genes that have already been reported are indicated (modified from Nakano *et al.,* 2006).

The number of *ERF* genes and their sequence similarities can be explained by the numerous polyploidy and duplication events of the *Arabidopsis* genome during evolution (Vision *et al*., 2000; Blanc *et al*., 2003; Bowers *et al*., 2003). The 122 *ERF* genes are distributed on all five chromosomes. About 75 % of the *ERF* genes are known to be the result of segment duplications (Nakano *et al*., 2006).

1.1.2.2 Functions of ERF family transcription factors

ERF proteins were originally identified as transcription factors that bind to the promoter regions of pathogenesis-related (PR) protein genes in an ET-dependent manner (Ohme-Takagi and Shinshi, 1995). Meanwhile, it is known that the *ERF* genes can be induced by biotic and abiotic stresses, including pathogen infection, salt stress, osmotic stress, wounding, drought, hypoxia, temperature stress, and the stress-related hormones such as ET, jasmonic acid (JA) or abscisic acid (ABA) (Licausi *et al*., 2013).

The most intensely studied ERF proteins are members of the CBF/DREB subfamily. Three of the four *CBF/DREB1* genes, namely *CBF1* (*DREB1B*), *CBF2* (*DREB1C*) and *CBF3* (*DREB1A*) which are linked tandemly in the *Arabidopsis* genome, are rapidly induced in response to cold stress and, when ectopically expressed, improve tolerance to freezing (Jaglo-Ottosen *et al*., 1998; Liu *et al*., 1998; Kasuga *et al*., 1999). In contrast, *Arabidopsis* RNAi lines for *CBF1* or *CBF3* have reduced freezing tolerance (Novillo *et al*., 2007). Recently, *cbf* triple mutants have been shown to be extremely sensitive to freezing stress and salt stress as well as defective in early development (Jia *et al*., 2016b; Zhao and Zhu, 2016).

DREB2A and DREB2B have been shown to be inducible by dehydration, high salinity and heat in an ABA-independent manner (Liu *et al*., 1998; Nakashima *et al*., 2000; Sakuma *et al*., 2006b). Overexpression of constitutive active DREB2A exhibits improved tolerance to drought, high salinity and heat stresses (Sakuma *et al*., 2006a, b). In contrast, mutants of DREB2A are more sensitive to heat stress (Sakuma *et al*., 2006b).

Among the ERF subfamily the members ERF1 and OCTADECANOID-RESPONSIVE ARABIDOPSIS AP2/ERF 59 (ORA59) have been most extensively characterized. Both are key regulators in the defense against necrotrophic pathogens, which are in turn regulated by ETHYLENE-INSENSITIVE3 (EIN3) and ETHYLENE-INSENSITIVE3-LIKE 1 (EIL1), whereas the JA and ET signaling pathways synergize to activate a specific set of defense genes including *PLANT DEFENSIN 1.2* (*PDF1.2*) (Solano *et al*., 1998; Lorenzo *et al*., 2003; Pre *et al*., 2008; Zarei *et al*., 2011). Recently, it has been demonstrated that salicylic acid (SA) reduces ORA59 levels mediated by EIN3 binding to and targeting of ORA59 for proteasomal degradation, thus suggesting the ORA59 pool as a coordination node for the antagonistic function of ET/JA and SA (He *et al*., 2017).

The functionality of ERF-VI and ERF-VI-like proteins was first identified as genes induced in response to the hormone cytokinin (CK), and therefore these genes were designated as *CYTOKININ RESPONSE FACTORs* (*CRF*s). Although, it has been shown that not all *CRF*s are transcriptionally regulated by CK, such as *CRF1*, *CRF3* and *CRF4* (Rashotte *et al*., 2006; Rashotte and Goerzen, 2010; Cutcliffe *et al*., 2011). Functional examinations of CRFs have

been performed to reveal that these proteins interact with the ARABIDOPSIS HISTIDINE PHOSPHOTRANSFER PROTEINs (AHPs) of the cytokinin two-component signaling pathway and induce many of the same target genes such as the ARABIDOPSIS RESPONSE REGULATORs (ARRs) type-B transcription factors (Rashotte *et al.*, 2006; Cutcliffe *et al.*, 2011). The CRFs are involved in diverse processes in plants and influence a subset of cytokinin responses. CRFs regulate the embryo development, the development of both the root and the shoot, they function as negative regulators of rosette size, but positive regulators of root growth, acting at least in part by regulating the size of the root apical meristem (Raines *et al.*, 2016) and regulate the onset of leaf senescence (Zwack *et al.*, 2013; Raines *et al.*, 2016). Recently, it has been demonstrated that CRF2, CRF3 and CRF6 modulate the auxin response by transcriptional control of genes encoding PIN-FORMED (PIN) auxin transporters through recognition of the 5'-AGCAGAC-3' motif, namely PIN cytokinin response element (PCRE) (Simásková *et al.*, 2015). Thus, CRFs play a pivotal role in auxin-cytokinin crosstalk, for instance, during female reproductive organ development (Cucinotta *et al.*, 2016) or root development (Simásková *et al.*, 2015). Furthermore, several CRFs appear to be induced by abiotic stresses such as cold or oxidative stress (Zwack *et al.*, 2013; Jeon *et al.*, 2016; Zwack *et al.*, 2016).

1.1.2.3 The ERF102 *to* ERF105 *genes*

In addition to the known *CRF* genes, four phylogenetically closely related *ERF* genes were identified to be similarly regulated by CK in a microarray study (Brenner *et al.*, 2005). These genes, *ERF102* (AT5G47230; also known as *ERF5*), *ERF103* (AT4G17490; identical to *ERF6*), *ERF104* (AT5G61600) and *ERF105* (AT5G51190) are members of group IXb of the ERF family (Fig. 4A) (Nakano *et al.*, 2006).

According to 'The *Arabidopsis* Information Resource' (TAIR) (Huala *et al.*, 2001), *ERF102* to *ERF105* are relatively small, intronless genes with a gene size of 1.191 bp (*ERF102*), 1.044 bp (*ERF103*), 1.045 bp (*ERF104*) and 833 bp (*ERF105*). The coding sequences are predicted to encode proteins of 300 (ERF102), 282 (ERF103), 241 (ERF104) and 221 (ERF105) amino acids. Like all AP2/ERF transcription factors they possess the characteristic AP2/ERF domain and are those proteins in the group IX with one (ERF102 and ERF103) or two (ERF104 and ERF105) putative MITOGEN-ACTIVATED PROTEIN KINASE (MPK) phosphorylation sites (Nakano *et al.*, 2006). Moreover, ERF102 to ERF105 possess acidic regions that might function as transcriptional activation domains (Fujimoto *et al.*, 2000). According to WoLF PSORT (Horton *et al.*, 2007), a program predicting the subcellular localization of proteins, ERF103 has a single nuclear localization signal (NLS) whereas ERF102, ERF104 and ERF105 have two NLS (Fig. 4B).

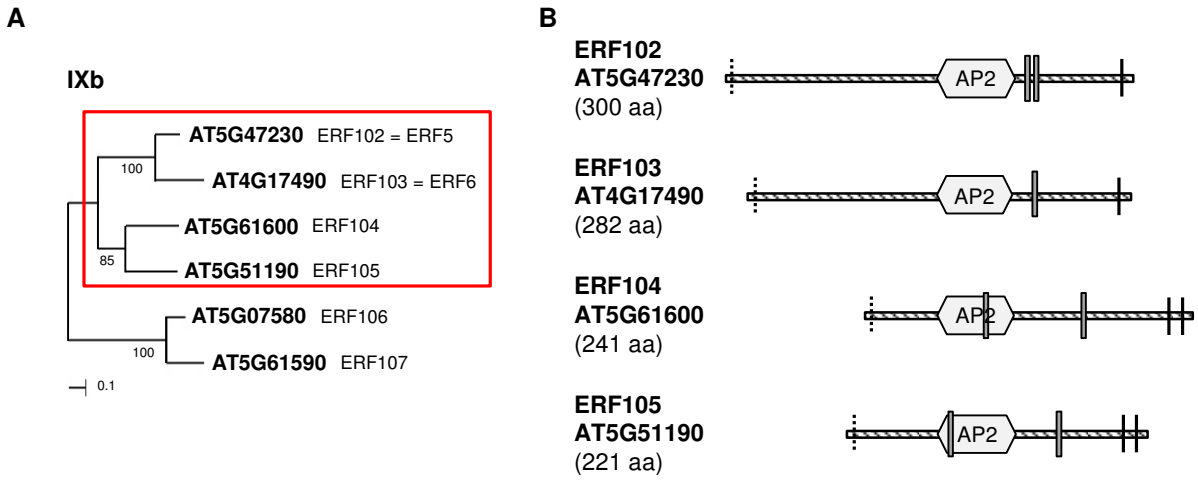

Figure 4. Description of the ERF102 to ERF105 proteins of *Arabidopsis thaliana*. (A) An unrooted phylogenetic tree of group IXb ERF transcription factors showing the close evolutionary relationship between ERF102 to ERF105 (red box) that are studied. The phylogenetic tree was constructed using MEGA6. **(B)** Structure of the *Arabidopsis* ERF102 to ERF105 proteins. The schematic representation shows the protein structures of ERF102 to ERF105 according to Nakano *et al.* (2006). The striped lines represent the protein sequences, the hexagons indicate the AP2/ERF DNA-binding domain, black lines putative phosphorylation sites, dashed lines the putative transactivation domains and grey boxes the nuclear localization signals determined with WoLF PSORT.

In the beginning of this study, the biological functions of the four *ERF* genes were basically unknown. One study was published about *ERF104* revealing its function in plant basal immunity. Bethke *et al.* (2009) showed the flagellin22- (flg22) mediated activation of MPK6 that phosphorylates ERF104 and on a separate branch flg22 stimulates ET production. The produced ET triggers a yet unknown mechanism (that is dependent on EIN2 and the EIN3/EIL members) for the substrate release of ERF104 from MPK6, presumably allowing the liberated ERF104 to access target genes and to control defense responses. In a microarray analysis with *ERF104* overexpressing plants, *PDF1.2, PDF1.2b, PATHOGENESIS-RELATED GENE 5* (*PR5*), *MITOGEN-ACTIVATED PROTEIN KINASE KINASE 4 (MKK4), RESPIRATORY BURST OXIDASE HOMOLOGUE D (RBOHD), ERF4, WRKY33, TGA1A-RELATED GENE 3 (TGA3)*, and other PR and defense signaling genes were identified as putative targets of ERF104. Overexpression of *ERF104* and the *erf104* mutant showed reduced immunity against *B. cinerea* and the non-adapted *P. syringae* pv. phaseolicola 1448A and enhanced the growth inhibition response to flg22 suggesting ERF104 must be maintained at an optimal level and any alterations of this crucial threshold can tip the signaling balance (Bethke *et al.*, 2009).

In the following years *ERF102* and *ERF103* have been demonstrated to play a role in plant immunity as well. *ERF102* plays opposing roles in the control of plant defense: ERF102 negatively regulates chitin signaling and plant defense against necrotrophic fungal pathogens and positively regulates SA signaling and plant defense against biotrophic bacterial pathogens (Son *et al.*, 2012). ERF102 and ERF103 are phosphorylated by MPK3 and MPK6

(Popescu *et al*., 2009; Son *et al*., 2012; Meng *et al*., 2013; Wang *et al*., 2013). Overexpressing lines of *ERF103* as well as plants overexpressing a phospho-mimicking ERF103 showed an increased resistance to *B. cinerea*, whereas dominant negative ERF103-EAR plants were highly susceptible to *B. cinerea* (Moffat *et al*., 2012; Meng *et al*., 2013). The upregulation of *ERF103* is not altered in the ET signaling mutants *etr1* and *ein2* in response to *B. cinerea* infection, indicating that ERF103 activates ET-independently the expression of PR genes such as *PDF1.2* by acting downstream of the MPK3/MPK6 signaling cascade (Meng *et al*., 2013).

ERF102 to *ERF105* have also been reported to be involved in the response to abiotic stress. *ERF102* and *ERF103*, which have recently been identified as being cold-induced together with the *CBF* genes (Park *et al*., 2015), are central regulators of leaf growth inhibition upon mild osmotic stress (Dubois *et al*., 2013; 2015). It was suggested that mild osmotic stress triggers the accumulation of ET in the actively growing leaves. ET further activates the signaling pathway involving MPK3 and MPK6 which phosphorylate a basal amount of ERF102 and ERF103 proteins present in the cell prior to stress exposure. Thus, activated ERF102 and ERF103 initiate transcription of the *GA2OX6* gene encoding a gibberellin (GA)-degrading enzyme, thereby decreasing the bioactive GA concentration and stabilizing the DELLA proteins and repressing growth. In parallel, ERF102 and ERF103 activation initiates the expression of stress-related genes such as *STZ*, *WRKY33* and *MYB51* (Dubois *et al*., 2013).

ERF103 also induces the expression of the transcriptional repressor ERF11 (ERF076) that counteracts the action of ERF103 and represses at least some of the ERF103-induced genes by directly competing for the target gene promoters to maintain a balance between plant growth and stress defense (Dubois *et al*., 2015).

ERF103 has also been described as a regulator of oxidative stress (Wang *et al*., 2013; Sewelam *et al*., 2013). Mutant analyses revealed that the reactive oxygen species (ROS)-producing NADPH oxidase RBOHD and calcium signaling are required for ROS-responsive expression of *ERF103*. *erf103* mutants showed a reduced growth and increased H_2O_2 and anthocyanin levels under normal growth conditions. Expression analyses of selected ROS-responsive genes in the *erf103* mutant revealed that a number of ROS-responsive genes such as *ZAT12*, *RBOHs*, *WRKYs*, *MPKs*, *DHAR1*, *APX4*, and *CAT1* were more strongly induced by H_2O_2 in *erf103* mutants than in wild type. In contrast, *CAT3, MDAR3*, *VTC2,* and *EX1* showed lower expression levels in the *erf103* mutant. These results suggest that *ERF103* is required for controlled ROS production during plant growth as well as during stress signaling (Sewelam *et al*., 2013).

Moreover, *ERF103* as well as *ERF104* and *ERF105* have been elucidated to be involved in the fast retrograde signaling response and acclimation response to high light (Vogel *et al*.,

2014; Moore *et al*., 2014). The acclimation response to high light is initiated within seconds as indicated by the rapid upregulation of the four AP2/ERF transcription factor genes *ERF103*, *ERF104*, *ERF105* and *RRTF1* (*ERF109*) with a maximum at ten minutes. In an attempt to link those AP2/ERF transcription factors transcript accumulation to retrograde signaling, *Arabidopsis* mutants with defects in proposed chloroplast-to-nucleus signaling pathways were analyzed. These experiments revealed an involvement of the triosephosphate translocator (TPT) and MPK6. Accordingly, it was suggested that within a few seconds after the light shift, the cytosolic level of dihydroxyacetone phosphate (DHAP) and subsequently of linked metabolites such as ATP and NADPH, change as a consequence of translocation of DHAP from the chloroplast to the cytosol by the TPT. These changes activate phosphorylation of MPK6 which in turn phosphorylates constitutive but inactive transcription factors initiating the expression of the four *AP2/ERF* transcription factor genes. These accumulated *AP2/ERF* transcription factor genes and their subsequent translation together with higher H_2O_2 levels and H_2O_2-dependent signaling amplify the high light acclimation response (Vogel *et al*., 2014; Moore *et al*., 2014).

Most recently, ERF105 has been identified to play an important role in *Arabidopsis* freezing tolerance and cold acclimation which is in detail described in this study and briefly by Bolt *et al*. (2017).

From the above-mentioned functions of the *ERF102* to *ERF105* genes, it appears that they are involved in response to biotic and, in particular, abiotic stress. Therefore, the following section will deal with abiotic stress.

1.2 Abiotic stress

Plants are sessile organisms and must cope with constantly changing environments that are often unfavorable or stressful for growth and development. These adverse environmental conditions include biotic stress such as pathogen infection and herbivore attack, and abiotic stress such as drought, low/high temperature, salinity, acidic conditions, light intensity, flooding, anaerobiosis, nutrient starvation and toxic metals in the soil. Abiotic stress conditions, particularly drought, salt, and temperature stresses are major environmental factors that affect the geographical distribution of plants, limit plant productivity in agriculture, and threaten food security (Zhu *et al*., 2016). However, in the field, crops and other plants are generally subjected to a combination of different abiotic stresses (Mittler, 2006). For instance, in drought-stricken areas, many crops encounter a combination of drought and heat or salinity (Heyne and Brunson, 1940; Moffat, 2002). To cope with these stresses, plants have evolved unique mechanisms. Each of these different abiotic stresses requires responses with distinct characteristics which determine whether or not the plant will survive.

Notably, stress responses are not always exclusive to a single stress; there are also general plant stress responses (Mittler, 2006).

In the following chapters, two abiotic stresses, namely cold and drought stress will be briefly introduced since these stresses played a major role in this study.

1.2.1 Cold stress

1.2.1.1 Cold stress and its consequences

Cold stress can be defined into two distinct categories. The first is characterized by the exposure of plants to low temperature ranging from 0 °C to 10 °C causing chilling stress (Solanke and Sharma, 2008). Chilling stress affects the life cycle, growth and development of plants. A key response to chilling temperatures is growth repression, which has been shown to be regulated, for instance, by the phytohormones SA and GA (Scott *et al.*, 2004; Archard *et al.*, 2008). Growth arrest is thought to be utilized to relocate resources from growth to increase cold tolerance (Scott *et al.*, 2004). Cold also contributes to break seed dormancy by inducing GA accumulation (Derkx *et al.*, 1994; Yamauchi *et al.*, 2004). Many temperate species only flower after they have experienced a longer cold period, a process known as vernalization, which aligns flowering with the favourable conditions of spring (Henderson and Dean, 2004). Physiological changes caused by chilling stress are a decreased membrane fluidity due to fatty acid unsaturation in membrane lipids, changes in composition and ratios of lipids to proteins in the cell membrane (Wang *et al.*, 2006b). Low non-freezing temperature also leads to dehydration, mainly due to reduction in water uptake by roots and an impediment to close stomata (Solanke and Sharma, 2008). Chilling stress leads to cold acclimation, since these conditions often prepare many temperate plants for future cold stress, specifically freezing stress (Xin and Browse, 2000). As a consequence of cold acclimation, plants can survive freezing at temperatures ranging from -5 °C to -30 °C, depending on the species (McKhann *et al.*, 2008). Non-acclimated wheat, for instance, is killed at subzero temperatures around -5 °C whereas cold-acclimated wheat is able to survive temperatures down to -20 °C (McKhann *et al.*, 2008). Cold acclimation involves the induction of protective mechanisms such as accumulation of osmoprotectants or antioxidants which will be described further later in this thesis.

The second category is freezing stress which is characterized by the exposure of plants to less than or equal to 0 °C temperatures. Freezing stress is most detrimental to plant survival since it can cause protein denaturation and severe cellular dehydration, associated with ice formation and even physical disruption of cells and tissues (Uemura *et al.*, 1995; Solanke and Sharma, 2008). Depending on the freezing temperature and freezing duration, different forms of membrane damages can occur, including expansion-induced lysis, lamellar-to-

hexagonal-II phase transition and fracture jump lesion (Steponkus *et al*., 1993; Uemura *et al*., 1997). Both low and freezing temperatures lead to generation of ROS which disequilibrate the electron transfer reactions and disturb accompanying biochemical reactions. Consequently, generation of ROS results in damage of photosystem II reaction centre and membrane lipids and ultimately leads to the death of plants (Prasad *et al*., 1994; Suzuki and Mittler, 2006).

1.2.1.2 The CBF cold signaling pathway

Plants probably sense low temperatures through membrane rigidification, changes in protein and nucleic acid conformation and/or metabolite concentration, which might induce a calcium influx in the cytosol and activate protein kinases (Chinnusamy *et al*., 2007). Thus, the MPK cascade is involved in the regulation of cold signaling. The MITOGEN-ACTIVATED PROTEIN KINASE KINASE 2 (MKK2) phosphorylates and activates MPK4 and MPK6 in response to cold (Teige *et al*., 2004). A further kinase, namely OPEN STOMATA 1 (OST1), has been shown to phosphorylate the MYC-type bHLH (basic helix-loop-helix) transcription factor INDUCER OF C-REPEAT-BINDING FACTOR EXPRESSION 1 (ICE1). OST1 interferes with the interaction between ICE1 and HIGH EXPRESSION OF OSMOTICALLY RESPONSIVE GENES 1 (HOS1) (Ding *et al*., 2015). HOS1, an E3-ligase, mediates the ubiquitination and proteosomal degradation of ICE1 (Dong *et al*., 2006; Kim *et al*., 2015). The *ICE1* gene is constitutively expressed and its gene product is activated by cold stress through sumoylation by the E3 SUMO-protein ligase SIZ1, which stabilizes the protein under freezing conditions (Miura *et al*., 2007). ICE1 in turn activates the transcription of the CBF regulon as central regulatory element of the cold signaling pathway. The CBF regulon comprises of the *CBF1* to *CBF3* genes (Chinnusamy *et al*., 2003), also referred to as *DREB1B*, *DREB1C* and *DREB1A*, respectively (Liu *et al*., 1998). Besides ICE1, expression of the cold-regulated *CBF* genes are positively controlled by several other transcription factors including ICE2 and CALMODULIN-BINDING TRANSCRIPTION ACTIVATOR 3 (CAMTA3) (Fursova *et al*., 2009; Doherty *et al*., 2009). Negative regulators of the CBF regulon are, for instance, the C2H2 zinc finger transcription factor ZAT12 (Vogel *et al*., 2005) and MYB15 (Agarwal *et al*., 2006). MYB15 is in turn negatively regulated by ICE1 (Agarwal *et al*., 2006) and phosphorylation of MYB15 by MPK6 reduces its affinity to bind to the *CBF3* promoter (Kim *et al*., 2017). The CBF proteins regulate the expression of the *COLD-REGULATED* (*COR*) genes that finally confer cold acclimation (Thomashow, 1999; Yamaguchi-Shinozaki and Shinozaki, 2006).

A schematic overview of the cold-responsive transcriptional network with the components mentioned above is depicted in the figure below.

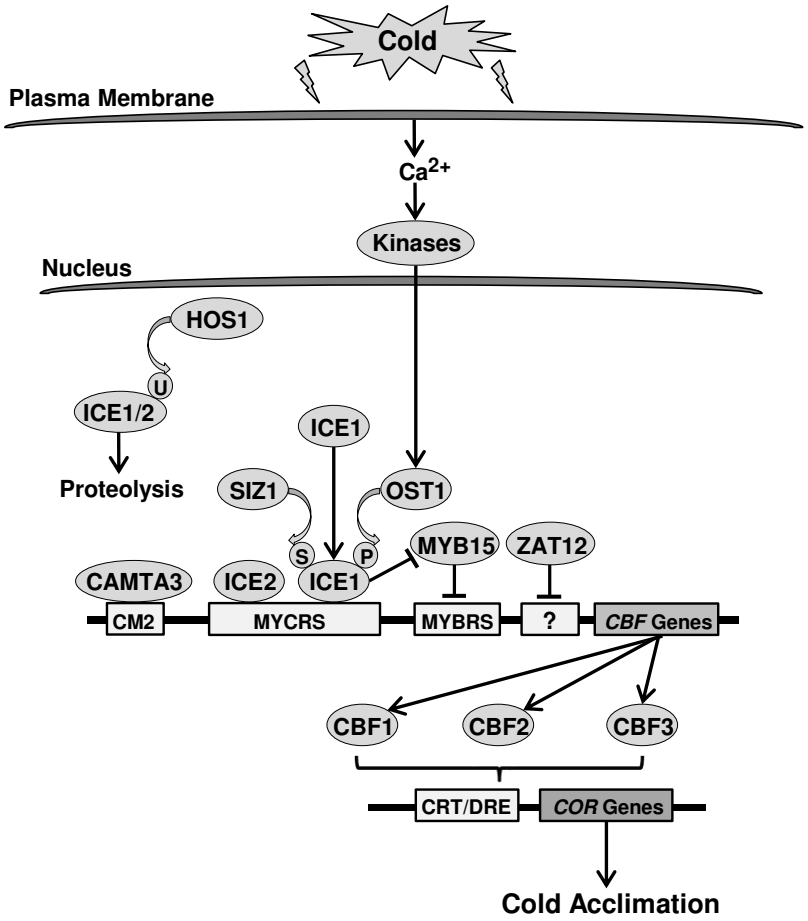

Figure 5. The CBF cold signaling pathway. Some major components involved in the CBF cold signaling pathway are shown. Plants probably sense low temperatures through membrane rigidification and/or other cellular changes, which might induce a calcium influx in the cytosol and activate protein kinases. Constitutively expressed ICE1 is activated through sumoylation by SIZ1 and phosphorylation by OST1, which is critical for transcription of the CBF regulon and repression of MYB15, a negative regulator of the CBF regulon. Expression of the *CBF* genes is positively controlled by several other transcription factors, including ICE2 and CAMTA3. HOS1 mediates the ubiquitination and proteosomal degradation of ICE1 and ICE2 and, thus, negatively regulates the CBF regulon. ZAT12 also represses the CBF regulon. The CBFs regulate the expression of *COR* genes that confer cold acclimation.
Arrows indicate positive regulation, lines ending with a bar indicate negative regulation. Question mark denotes an unknown regulatory *cis*-element. Abbreviations: ICE1/2, INDUCER OF C-REPEAT-BINDING FACTOR EXPRESSION 1/2; OST1, OPEN STOMATA 1; CAMTA3, CALMODULIN-BINDING TRANSCRIPTION ACTIVATOR 3; HOS1, HIGH EXPRESSION OF OSMOTICALLY RESPONSIVE GENES 1; ZAT12, ZINC FINGER OF ARABIDOPSIS THALIANA 12; CBF, C-REPEAT-BINDING FACTOR; COR, COLD-REGULATED; CRT/DRE, C-repeat element/dehydration-responsive element; MYBRS, MYB transcription factor recognition sequence; MYCRS, MYC transcription factor recognition sequence; CM2, conserved motif 2; U, ubiquitination; S, sumoylation; P, phosphorylation (Chinnusamy *et al*., 2007; Doherty *et al*., 2009; Ding *et al*., 2015).

Recently, it was suggested that plants efficiently control the acquisition of cold tolerance using a different set of activated genes of the CBF cold signaling pathway in response to a gradual temperature decrease during seasonal changes and a sudden temperature drop during the night (Kidokoro *et al*., 2017).

Overall the transcriptional response to cold is complex. In the last two decades, many further genes have been identified that are involved in the cold signaling pathway, including genes of the circadian clock (Bieniawska *et al*., 2008; Catalá *et al*., 2011), light signaling (Kim *et al*., 2002; Catalá *et al*., 2011; Kidokoro *et al*., 2017), or hormonal signaling (Eremina *et al*.,

2016). The cold signaling network affects more than 2000 genes (Park *et al*., 2015). Of these, about 12 % are controlled by the CBF regulon (Fowler and Thomashow, 2002), indicating that additional transcription factors and signaling modules must be involved to orchestrate the response to cold and acquire freezing tolerance. Genetic studies have shown that CBF-independent regulation exists, for instance by analysis of the *esk1* mutant (Xin *et al*., 2007). Further, the cold-responsive transcriptome appears to be different in different tissues (Kreps *et al*., 2002). Together, this suggests the existence of additional transcriptionally controlled signaling pathways in cold signaling.

1.2.1.3 Cold acclimation

Many temperate plants have evolved mechanisms to acquire freezing tolerance through cold acclimation, a process in which upon exposure to low non-freezing temperatures, the ability to survive freezing temperatures increases (Thomashow, 1999). During the process of cold acclimation, the plant transcriptome and metabolome are massively reprogrammed (Cook *et al*., 2004; Kaplan *et al*., 2004; 2007). This reprogramming is to a significant part regulated by the CBF signaling cascade (Chinnusamy *et al*., 2007). The CBF transcription factors activate many downstream target genes, including genes encoding enzymes involved in compatible solute biosynthesis and as described above the *COR* genes. The best characterized COR proteins are the highly homologue COR15A and COR15B proteins which belong to the group of LATE EMBRYOGENESIS ABUNDANT (LEA) proteins. LEA proteins were first described as proteins that accumulate late in plant seed development (Dure *et al*., 1981). However, they are also abundant in vegetative plant tissues following environmental stresses such as cold or drought (Hundertmark and Hincha, 2008). Like most LEA proteins, COR15A and COR15B are intrinsically disordered proteins (IDPs) under fully hydrated conditions that gain a predominantly α-helical structure during dehydration and/or in the presence of membranes. Thus, it has been shown that both proteins accumulate in the chloroplast stroma during cold and fold into amphipathic α-helices and associate with the chloroplast inner envelope membrane. The protein-binding stabilizes the inner envelope membrane against the formation of hexagonal II phase lipid domains (Steponkus *et al*., 1998; Nakayama *et al*., 2007).

It is generally accepted that the key function of cold acclimation is to stabilize membranes against freezing injury (Steponkus, 1984; Krause *et al*., 1988; Hincha *et al*., 1987). Detailed lipid analyses of the plasma membrane revealed that, during cold acclimation, an increase in the relative amounts of diunsaturated species of phosphatidylcholine takes place in the plasma membrane. This leads to increased freezing stability of protoplasts (Uemura and Yoshida, 1984; Uemura *et al*., 1995). Similarly, complex changes have also been described for the lipid composition of the inner and outer chloroplast envelope membranes during cold

acclimation. However, the specific function of these changes has to be determined yet (Uemura and Steponkus, 1997). Another effect often seen in response to cold stress is the accumulation of sucrose and other simple soluble sugars, which are presumed to contribute to the stabilization of membranes as these molecules can protect membranes against freeze-induced damage *in vitro* (Anchordoguy *et al*., 1987; Strauss and Hauser, 1986). Flavononoids that typically accumulate with cold acclimation are suggested to stabilize membranes upon cold stress as well (Schulz *et al*., 2015). Additionally, flavonoids are considered to function as UV screens (Emiliani *et al*., 2013) and antioxidants (Winkel-Shirley 2002), although the latter role is not undisputed (Hernandez *et al*., 2009). Moreover, soluble sugars as well as accumulated organic acids, polyamines, amino acids such as proline can function as signaling molecules for regulating gene expression, as mediators of osmotic adjustment, as stabilizers of subcellular structures, as scavengers of free radicals, and as energy sources (Schobert and Tschesche, 1978; Levitt 1980; Handa *et al*.,1986; Smirnoff and Cumbes, 1989; Guy, 1990; Saradhi and Saradhi, 1991; Saradhi *et al*.,1995; Hincha and Hagemann, 2004). Furthermore, the levels of the phytohormone ABA are transiently elevated in response to cold (Chen *et al*., 1983). Exogenous application of ABA at non-acclimating temperatures can enhance freezing tolerance (Lang *et al*., 1994) and induces many of the cold-responsive genes (Heino *et al*., 1990; Gilmour and Thomashow 1991). The induction of genes encoding molecular chaperones typically occurs with cold acclimation, which could have protective effects (Thomashow, 1999). Due to the above-mentioned tolerance mechanisms, plants can survive in a vegetative state through the winter by either allow ice to crystallize in the apoplast (freeze tolerance) or prevent the crystallization of ice within their tissues (freeze avoidance). Freeze avoidance involves supercooling, which means plants can avoid freezing damage by preventing extracellular ice formation below the equilibrium freezing temperature. Thus, some specialized cell types and organs do use supercooling as a strategy to overwinter: the xylem ray parenchyma cells and floral primordia of many trees supercool to about -40 °C (Quamme, 1974; George and Burke, 1977; Smallwood and Bowles, 2002).

1.2.2 Drought stress

Drought, cold and salinity are those environmental stressors which affect plants in many respects and which, due to their wide-spread occurrence, cause most economic losses in agriculture (Beck *et al*., 2007). In particular drought, which results from the global warming, is the major challenge in agriculture and food security (Adams *et al*., 1998). For this reason, the effects of drought have been studied extensively, ranging from the whole plant to the molecular level and from the description of the damages to the tolerance mechanisms.

1.2.2.1 Drought stress and its consequences

Drought severely affects plant growth and development. The response of plants to drought is dependent on the extent and rate of water loss. A slow rate of water loss permits acclimation to the water deficit and limits the extent of injury, while a rapid rate of loss precludes acclimation (Bray, 1997). Drought causes loss of turgor, changes in plasma membrane fluidity and compositions, denaturation of proteins (Bray, 1997). It further impairs germination (Harris *et al*., 2002), mitosis, cell elongation and expansion resulting in reduced growth and yield (Hussain *et al*., 2008). Moreover, drought stress leads to formation of ROS resulting in oxidative damage (Anjum *et al*., 2011).

Drought induces the biosynthesis and the accumulation of ABA in roots. The *de novo* synthesized ABA is then transferred to the leaves through the transpiration stream (Zhang and Outlaw, 2008). This drought-induced root-to-leaf signaling which is promoted by soil drying results in stomatal closure. ABA promotes the efflux of K^+ ions from the guard cells leading to the loss of turgor pressure and consequently leading to stomatal closure (Fan *et al*., 2004). The stomatal closure deprives the leaves of CO_2 and declines the internal CO_2 concentration in the plant. As a result, the photosynthetic carbon assimilation is decreased in favor of photorespiration (Farquhar and Sharkey, 1982). The non-stomatal limitations of photosynthesis include reductions in chlorophyll content, structural damage and functional disturbances of chloroplasts and metabolic impairments (Haupt-Herting and Fock, 2002; Lawlor and Cornic, 2002; Li *et al*., 2006).

1.2.2.2 Drought signaling pathway

The perception of drought is not yet concluded. No drought stress-specific plant receptor has been identified. Although, the two-component ARABIDOPSIS HISTIDINE KINASE 1 (AHK1) is thought to function as an osmosensor and probably contributes to the transfer of the drought signal indirectly (Urao *et al*., 1999; Wohlbach *et al*., 2008; Kumar *et al*., 2012). In contrast to signal perception, many *cis*-regulatory elements and genes involved in the drought signaling cascade have been identified. Molecular analyses have revealed that ABA not only triggers the stomatal closure but induces the expression of drought stress-related genes as well. Presently, several transcription factors belonging to the MYB, MYC and ABA-RESPONSIVE ELEMENT-BINDING PROTEIN/ABA-BINDING FACTOR (AREB/ABF) families, together with the corresponding stress-responsive *cis*-acting regulatory elements MYB-/MYC-recognition sequences (MYBR/MYCR) and ABA-responsive element (ABRE) have been demonstrated to be involved in the ABA-dependent drought signaling pathway (Shinozaki *et al*., 2003). CBF4, a homolog of the CBF1, CBF2, and CBF3 proteins plays also an equivalent role during drought adaptation. In contrast to the three *CBF* homologs, which are induced under cold stress, *CBF4* gene expression is upregulated by drought stress and

ABA, but not by low temperature (Haake *et al.*, 2002). The ABA-independent pathway involves activation of CBF/DREB transcription factors. Prominent examples are DREB2A and DREB2B which has been already described above (1.1.2.2) (Liu *et al.*, 1998; Nakashima *et al.*, 2000; Sakuma *et al.*, 2006b).

Many genes of the drought and cold signaling pathway are induced by both drought and cold stress, suggesting the existence of a complex gene network for specificity and crosstalk in abiotic stress-responsive gene expression. One example is the above-mentioned serine/threonine proteine kinase OST1, which phosphorylates ICE1 and promotes the expression of downstream cold-responsive genes (Ding *et al.*, 2015). OST1 was first identified in the context of ABA-dependent stomatal closure (Mustilli *et al.*, 2002). Under stress conditions, OST1 can phosphorylate AREB/ABF proteins to regulate the expression of drought stress-responsive genes (Furihata *et al.*, 2006) and it can phosphorylate the S-type anion channel SLAC1 to control stomatal movement in plants (Geiger *et al.*, 2009).

1.2.2.3 Drought response mechanisms and adaptations

Plants have evolved numerous strategies to cope with water deficit. Similar to cold stress, under drought, plants accumulate compatible solutes in cytoplasm, including proline, sucrose, soluble carbohydrates, glycine betaine and other solutes improving, for instance, water uptake from drying soil, protein and membrane stabilization and radical scavenging (Ingram and Bartels, 1996). The accumulation of antioxidant enzymes to scavenge ROS (Sharma and Dubey, 2005) as well as the accumulation of protective proteins including mainly the LEA, LEA-like and heat shock proteins play also decisive roles in the drought response (Shinozaki and Yamaguchi-Shinozaki, 2007). Heat shock proteins have been shown to function as molecular chaperones. They are key components responsible for protein folding, assembly, translocation and degradation under stress conditions (Lindquist and Craig, 1988; Lindquist, 1986; Wang *et al.*, 2004). Functions of LEA proteins are binding to RNA or DNA, water or ion binding, antioxidative activity or sugar stabilization in the dry state and stabilization of enzymes (Tunnacliffe and Wise 2007; Hincha and Thalhammer, 2012). One of the best studied function of LEA proteins is membrane stabilization through, for instance, COR15A as it is decribed above (Thalhammer *et al.*, 2014a).

To withstand long drought periods, plants have evolved numerous physiological adaptations and in the following, a few examples are mentioned: Stomatal transpiration is the main cause for water loss in plants. It occurs during photosynthesis when stomata are open for diffusion of CO_2 into leaves (Cowan *et al.*, 1978). C4 and CAM plants have evolved strategies to fix CO_2 with minimal water loss (reviewed in Yamori *et al.*, 2014). Xerophytic plants have developed morphological adaptations to aride conditions such as waxy stomata, spines, succulent stems, hairy leaves (Kozlowski, 1968). Many annual herbaceous plants complete

their life cycles before the annual drought period (van der Valk, 2009). A small group of vascular angiosperm plants, termed resurrection plants, have evolved unique mechanisms of desiccation tolerance and can tolerate severe water loss by diminishing their metabolic functions. The metabolic functions are resumed if the water potential increases (Dinakar and Bartels, 2013). Many bromeliads have developed specific morphological structures for rainwater impounding by tightly overlapping their leaf bases (Krömer *et al*., 2006). Since plants obtain their water and mineral nutrients from roots, one crucial aspect for drought adaptation in plants are morphological changes in plant root systems. Drought inhibits lateral root growth (Khan *et al*., 2016). In contrast, deep and vigorous root systems have been demonstrated in drought-tolerant plants to maximize water uptake (Taylor *et al*., 1979; Ober and Sharp, 2003; Jaleel *et al*., 2008).

1.3 Aim of the study

The aim of the present work was to elucidate the molecular functions of four phylogenetically closely related *ERF* genes, which were identified in a microarray study to have a similar response to cytokinin (Brenner *et al*., 2005). These genes, *ERF102*, *ERF103*, *ERF104*, and *ERF105* are members of group IXb of the ERF family (Fig. 4A) (Nakano *et al*., 2006). In the beginning of this study, the biological functions of the four *ERF* genes were basically unknown. Therefore, it was of interest to characterize these four *ERF* genes and to probably connect their function to cytokinin. To do so, the transcriptional responses of *ERF102* to *ERF105* by different hormones and abiotic stresses, the tissue-specific expressions of *ERF102:GUS* to *ERF105:GUS*, the subcellular localizations and protein interactions of ERF102 to ERF105 proteins were analyzed. In order to identify specific roles of *ERF102* to *ERF105* in plant development and/or the response to stress, loss-of-function and gain-of-function lines were analyzed for their growth characteristics. To explore potential redundant roles of the four *ERF* genes, double loss-of-function mutants were additionally evaluated.
During the course of the study, several functions of *ERF102*, *ERF103* and *ERF104* have been published. Thus, the focus of this thesis has been set on the detailed characterization of the molecular functions of *ERF105*.

2 MATERIAL & METHODS

2.1 Databases and software

The databases and software used in the present study are listed in Table 1.

Table 1. Databases and software.

Name	Company, internet link and/or reference	Purpose of use
AB 7500 Software v2.0.6	Applied Biosystems/Thermo Fisher Scientific, Waltham, US	Quantitative real-time PCRs (qRT-PCRs)
ATTED-II	atted.jp Obayashi *et al*., 2007	Analysis of co-expressed genes
Chromas Lite 2.1.1		Analysis of chromatograms
CorelDRAW 2014	Corel Corporation, Ottawa, CA	Figure design
Excel	Microsoft Corporation, Redmond, US	Calculation and graph design
Genevestigator	https://genevestigator.com/gv/ Zimmermann *et al*., 2004	Analysis of gene expression patterns
GraphPad Prism3	GraphPad Software, Inc., La Jolla, US	Analysis of electrolyte leakage
GraphPad Instat	GraphPad Software, Inc., La Jolla, US	Statistical analyses
ImageJ	Abràmoff *et al*., 2004	Image analyses
MEGA6	Tamura *et al*., 2013	Generation of a phylogenetic tree
MeV 4.9	Howe *et al*., 2010	Generation of heat maps
MUSCLE	http://www.ebi.ac.uk/Tools/msa/muscle/ Edgar, 2004	Sequence alignment
NASC	http://arabidopsis.info/	Ordering *Arabidopsis* seeds
NCBI	http://www.ncbi.nlm.nih.gov/	Literature (PubMed)
PowerPoint	Microsoft Corporation, Redmond, US	Figure design
QuantPrime	http://www.quantprime.de/ Arvidsson *et al*., 2008	Primer design for qRT-PCRs
SAS	http://www.sas.com/en_us/software/analytics/stat.html	Statistical analyses
SIGnAL	http://signal.salk.edu/cgi-bin/tdnaexpress	Search for *Arabidopsis* T-DNA insertion lines
TAIR	http://www.arabidopsis.org/ Huala *et al*., 2001	Search for *Arabidopsis* gene information
Vector NTI 9.0	Invitrogen/Thermo Fisher Scientific, Waltham US Lu and Moriyama, 2004	Search for restriction sites and generation of vector maps
WMD3	http://wmd3.weigelworld.org/cgi-bin/webapp.cgi Ossowski *et al*., 2008	Generation of artificial microRNAs
WoLF PSORT	http://www.genscript.com/wolf-psort.html Horton *et al*., 2007	Protein localization predictor

2.2 Chemicals and consumables

The main distributers for chemicals and consumables are listed below:

Applichem (Darmstadt, DE), Bioline (London, UK), Bio-Rad (Munich, DE), Boehringer Mannheim (Mannheim, DE), Duchefa Biochemie (Haarlem, NL), Eppendorf (Hamburg, DE), Fluka (Buchs, CH), Greiner Bio-One (Frickenhausen, DE), Invitrogen/Thermo Fisher Scientific (Waltham, US), Macherey-Nagel (Düren, DE), Merck (Darmstadt, DE), Peqlab (Erlangen, DE), Qiagen (Hilden, DE), Roche (Mannheim, DE), Roth (Karlsruhe, DE), Sarstedt (Nümbrecht-Rommelsdorf, DE), Sigma Aldrich (Steinheim, DE).

2.3 Kits, enzymes and DNA ladders

The kits, enzymes and DNA ladders that were used in this study are listed in Table 2.

Table 2. Kits, enzymes and DNA ladders.

Name	Manufacturer
DNase I	Thermo Fisher Scientific, Waltham, US
Gateway® BP Clonase™ enzyme mix	Invitrogen/Thermo Fisher Scientific, Waltham, US
Gateway® LR Clonase™ enzyme mix	Invitrogen/Thermo Fisher Scientific, Waltham, US
Gateway® LR Clonase™ II Plus enzyme mix	Invitrogen/Thermo Fisher Scientific, Waltham, US
HyperLadder™ I	Bioline, Luckenwalde, DE
Immolase DNA Polymerase	Bioline, Luckenwalde, DE
NucleSpin RNA Plant	Macherey-Nagel, Düren, DE
Phusion High-Fidelity DNA Polymerase	Thermo Fisher Scientific, Waltham, US
P805 (100 bp DNA ladder)	MBBL, Bielefeld, DE
QIAGEN Plasmid Mini Kit	Qiagen, Hilden, DE
QIAGEN OneStep RT-PCR Kit	Qiagen, Hilden, DE
Restriction enzymes	Thermo Fisher Scientific, Waltham, US
SuperScript® III Reverse Transcriptase	Invitrogen/Thermo Fisher Scientific, Waltham, US
Taq DNA Polymerase	AG Schuster, Institute of Biology/Applied Genetics, FU Berlin, DE
Wizard® SV Gel and PCR Clean-Up System	Promega, Mannheim, DE

2.4 Antibiotics, herbicides, amino acids and hormones

The antibiotics, herbicides, amino acids and hormones that were used in this study are listed in Table 3.

Table 3. Antibiotics, herbicides, amino acids and hormones.

Antibiotic/herbicide	**1000x Stock solution**
Carbenicillin	50 mg/ml in ddH_2O
Chloramphenicol	34 mg/ml in 100 % ethanol
Gentamycin	25 mg/ml in ddH_2O
Hygromycin B	15 mg/ml in HEPES
Kanamycine	50 mg/ml in ddH_2O
Phosphinothricin	12 mg/ml in ddH_2O
Rifampicin	50 mg/ml in ddH_2O
Spectinomycin	50 mg/ml in ddH_2O
Sulfadiazine	10 mg/ml in DMSO
Tetracycline	10 mg/ml in 100 % ethanol
Amino acids	**10x Stock solution**
L-Histidine HCl	2 mg/ml in ddH_2O
L-Leucine	10 mg/ml in ddH_2O
L-Tryptophane	2 mg/ml in ddH_2O
Uracil (pH 5.8)	2 mg/ml in ddH_2O
Hormones/Hormonal substitutes	**freshly prepared in**
(+)-abscisic acid	100 % ethanol
1-Aminocyclopropane-1-carboxylic acid	ddH_2O
1-Naphthaleneacetic acid	ddH_2O
24-epi-brassinolide	DMSO
6-Benzyladenine	1N KOH
Gibberellic acid (GA_3)	DMSO
Gibberellic acid (GA_4:GA_7=65:35)	DMSO
Methyl jasmonate	100 % acetone
Salicylic acid	ddH_2O

2.5 Cloning vectors

The following vectors were used in this study (Table 4).

Table 4. Cloning vectors.

Vector	**Reference**	**Purpose of use**
pRS300	Ossowski *et al*., 2008	Template for generation of artificial microRNAs
pDONR221	Invitrogen/Thermo Fisher Scientific, Waltham, US	Gateway® donor vector for cloning
pDONR P4-P1R	Invitrogen/Thermo Fisher Scientific, Waltham, US	Gateway® donor vector for cloning
pEN-L1-SI-L2	Karimi *et al*., 2007a	Gateway® entry clone with GUS intron
pBWGFS7	Karimi *et al*., 2007b	Gateway® destination vector, binary vector for promoter analyses (GFP-GUS)

Table 4. Continued.

Vector	Reference	Purpose of use
pH2GW7	Karimi *et al*., 2007b	Gateway® destination vector, binary vector for overexpression in plants
pK7WGF2	Karimi *et al*., 2007b	Gateway® destination vector, binary vector for over-expression in plants with N-terminal GFP-fusion
pK7FWG2	Karimi *et al*., 2007b	Gateway® destination vector, binary vector for over-expression in plants with C-terminal GFP-fusion
pORE-E4	Coutu *et al*., 2007	binary vector for overexpression in plants
pK7m24GW,3	Karimi *et al*., 2005	MultiSite Gateway® destination vector, two fragment recombination
pACT2-GW	pACT2 Clonetech®, modified by Dortay *et al*., 2006	Gateway® destination vector, protein expression in yeast, prey vector for the yeast two-hybrid system
pACT2-GW-empty	pACT2 Clonetech®, modified by Dortay *et al*., 2006	empty pACT2-GW vector for testing autoactivation in the yeast two-hybrid system
pBTM-116-D9-GW	Goehler *et al*., 2004, modified by Dortay *et al*., 2006	Gateway® destination vector, protein expression in yeast, bait vector for the yeast two-hybrid system
pBTM-116-D9-GW-empty	Goehler *et al*., 2004, modified by Dortay *et al*., 2006	empty pBTM-116-D9-GW vector for testing autoactivation in the yeast two-hybrid system

2.6 Organisms

2.6.1 Bacteria and yeast strains

The bacteria and yeast strains used in this study are listed in Table 5.

Table 5. Bacteria and yeast strains.

Organism/strain	Genotype, reference	Purpose of use
A. tumefaciens GV3101::pMP90	Rifampicin resistent, gentamycin resistent Koncz and Schell, 1986	Transient and stable plant transformation
E. coli DB3.1	F$^-$ *gyr*A462 *end*A1 *gln*V44 Δ(*sr*1-*rec*A) *mcr*B *mrr hsd* S20 (r$_B^-$, m$_B^-$) *ara*14 *gal*K2 *lac*Y1 *pro*A2 *rps*L20 *(Smr) xyl*5 Δ*leu mtl*1 Bernard and Couturier, 1992	Propagation of plasmids containing *ccdB* gene
E. coli DH5α	F$^-$ *end*A1 *gln*V44 *thi*-1 *rec*A1 *rel*A1 *gyr*A96 *deo*R *nup*G Φ80d *lac*ZΔM15 Δ(*lac*ZYA-*arg*F)U169*hsd*R17 (r$_K^-$ m$_K^+$), λ– Hanahan, 1983	Plasmid amplification
S. cerevisiae L40ccua	*MATa his3Δ200 trp1-901 leu2-3,112 LYS::(lexAop)$_4$-HIS3 URA3::(lexAop)8-lacZ ADE2::(lexAop)$_8$- URA3 GAL4 gal80 can1 cyh2* Goehler *et al*., 2004	Yeast two-hybrid

2.6.2 Plants

In the present study *Nicotiana benthamiana* and *Arabidopsis thaliana* ecotype Columbia-0 (Col-0) plants were used. *N. benthamiana* wild-type plants were used for transient protein expression and *A. thaliana* was used in all other plant experiments. The *Arabidopsis* T-DNA insertion lines *erf102* (SAIL_46_C02) and *erf105* (GABI_680C11) were obtained from the 'European *Arabidopsis* Stock Centre' (NASC). After selection of homozygous plants, the location of the T-DNA insertion was verified by sequencing and plants were backcrossed twice with Col-0 to eliminate possible multiple insertions and other background mutations. Transgenic plants that were generated in this study are described in chapter 2.11.

2.7 Growth conditions

All described media and solutions were autoclaved at 1 bar for 15–20 min at 120 °C. Heat instable components (antibiotics, amino acids and hormones) were sterile filtrated and added to the autoclaved media according to the plasmid requirements of the respective cultures or other experimental demands.

2.7.1 Bacteria growth conditions

For plasmid selection or plasmid propagation, *E. coli* and *A. tumefaciens* strains were grown in liquid or on solid Luria Broth (LB) media (10 g/l tryptone, 5 g/l yeast extract, 5 g/l NaCl and 15 g/l agar for solid LB-medium; pH 7.5) as described by Bertani (1951). Liquid SOB medium (20 g/l tryptone, 5 g/l yeast extract, 500 mg/l NaCl, 2.5 mM KCl, 10 mM $MgSO_4$, 10 mM $MgCl_2$; pH 7.4) was used for the production of chemically competent *E. coli* DH5α cells (Hanahan, 1983). Liquid YEBS medium (1 g/l yeast extract, 5 g/l beef extract, 5 g/l sucrose, 5 g/l bacto-peptone, 0.5 g/l $MgSO_4$; pH 7.0) was used for the propagation of *A. tumefaciens* cells which were used for plant transformation (Davis *et al.*, 2009). *E. coli* strains were grown at 37 °C overnight and *A. tumefaciens* at 28 °C for two days. Liquid cultures were grown while shaking at 200 rpm for *E. coli* or 160 rpm for *A. tumefaciens.* For plasmid selection, the appropriate antibiotics were added to the medium.

For cryoconservations, 1 ml of an overnight culture was mixed with 500 µl 70 % sterile glycerole, shock frozen in liquid nitrogen and stored at -80 °C.

2.7.2 Yeast growth conditions

S. cerevisiae was grown at 30 °C in liquid or on solid complete YPD medium (10 g/l yeast extract, 20g/l peptone, 20 g/l glucose; pH 5.8) or minimal SD medium (6.7 g/l YNB (yeast nitrogen base without amino acids), 20 g/l glucose; pH 5.8) (Sambrook *et al.*, 2001). 10 g/l

agar was added for solid medium. Liquid cultures were grown while shaking with 150 rpm. For plasmid selection, the appropriate amino acids were added to SD medium and for autoactivation tests, different concentrations of 3-amino-1,2,4-triazole (3-AT, a competitive inhibitor of the product of the *HIS3* gene) were added to SD medium.

2.7.3 Plant growth conditions

2.7.3.1 In vitro *culture*

For growth of *Arabidopsis* seedlings under sterile conditions, seeds were surface-sterilized by shaking for 5 min in 70 % ethanol containing 0.01 % (v/v) Triton X-100. Afterwards, seeds were rinsed twice with 70 % ethanol under a clean bench and transferred for drying to a sterile filter paper. For *in vitro* cultures, plants were grown in petri dishes in liquid or on solid Murashige and Skoog (MS) medium (4.3 g/l MS basal salt mixture, 0.5 g/l MES, 30 g/l sucrose; pH 5.7) (Murashige and Skoog, 1962). Depending on the experimental requirements (2.15) a different composition of the medium was used. After stratification at 4 °C for two days, plants were transferred to a climate chamber and cultivated under long day (LD) conditions (16 h light/8 h dark) at 110–140 µmol m^{-2} s^{-1} and 21 °C.

2.7.3.2 Growth on soil

Arabidopsis seeds were sown on a watered mixture of P- and T-soil and sand (2:2:1). After stratification at 4 °C for two days, plants were transferred to a climate chamber or the greenhouse. Twelve days after germination, seedlings were singled out onto soil containing P- and T-soil and Perligran G (2:2:1). If not otherwise specified, plants were grown under long day (LD) conditions (16 h light/8 h dark) at 130–160 µE m^{-2} s^{-1} and 21 °C.

N. benthamiana was grown under 14 h light/10 h dark conditions at 24 °C.

2.8 Genetic Crossings

To perform genetic crossings, two parental plants were grown until they reached the stage of flowering. Open flowers from the receptive “mother” plant as well as flower buds which were not used for crossings were removed. Afterwards, a flower bud was opened and emasculated by removing sepals, petals and all six stamens. Anthers of an opened flower of the pollinating “father” plant were used to fertilize the receptive gynoeceum by brushing the anthers over the stigma of the receptive plant. Genetic crossings were performed on three flower buds per plant and in both directions (reciprocal crossings) to determine whether or not a gene is sex linked. Finally, the developed siliques were harvested and used for propagation.

2.9 Transformation techniques

2.9.1 Preparation and transformation of bacteria

2.9.1.1 Preparation and transformation of chemically competent E. coli *cells*

Preparation of chemically competent *E. coli* cells was performed according to the protocol from Inoue *et al.* (1990) with slight modifications. A 5 ml overnight culture was transferred into 200 ml SOB medium and incubated at 37 °C on a shaker. Growth was monitored spectrophotometrically at 600 nm with a spectrophotometer (Thermo Fisher Scientific, Waltham, US). After reaching an OD_{600} of 0.5, cells were cooled down on ice for 10 min and centrifuged at 4.000 rpm for 15 min at 4 °C. The pellet was resuspended in 16 ml TP buffer (10 mM PIPES, 15 mM $CaCl_2$ x 2 H_2O, 250 mM KCl, $MnCl_2$ x 4 H_2O; pH 6.7) using a cooled glass pipette. 7 % DMSO were added and mixed to the cell suspension. After an incubation of 10 min on ice, cells were aliquoted in portions of 100 µl, shock frozen in liquid nitrogen and stored at -80 °C.

For heat shock transformation of plasmid DNA to chemically competent *E. coli* cells, cells were thawed on ice for 5 min. 20–100 ng plasmid DNA were added to 100 µl *E. coli* cells and thoroughly mixed. The cell suspension was incubated 30 min on ice, then incubated at 42 °C in a water bath for 45 s and immediately transferred on ice for 2 min. 400 µl of SOC medium (20 g/l tryptone, 5 g/l yeast extract, 500 mg/l NaCl, 2.5 mM KCl, 10 mM $MgSO_4$, 10 mM $MgCl_2$, 20 mM glucose; pH 7.4) were added and incubated on a shaker at 37 °C for 60 min. Aliquots of the transformation mix were plated on selection medium and incubated at 37 °C overnight.

2.9.1.2 Preparation and transformation of electrocompetent A. tumefaciens *cells*

For the preparation of electrocompetent *A. tumefaciens* cells, a 25 ml starting culture was transferred to 200 ml LB medium (without NaCl) and grown on a shaker at 28 °C until an OD_{600} of 0.5–1.0. Cells were centrifuged at 4.000 rpm for 5 min at 4 °C. The pellet was resuspended in 30 ml ice-cold water and centrifuged at 4.000 rpm for 5 min at 4 °C. The pellet was then resuspended in 30 ml 10 % ice-cold glycerole. The centrifugation step was repeated and the pellet was finally resuspended in 2 ml 10 % ice-cold glycerole, aliquoted in portions of 50 µl, shock frozen in liquid nitrogen and stored at -80 °C.

Transformation of *A. tumefaciens* cells was done by electroporation. Therefore, a 50 µl aliquot of electrocompetent *A. tumefaciens* cells was thawed on ice for 5 min, before 50–150 ng plasmid DNA were added. The transformation mixture was transferred into a pre-cooled electroporation cuvette and an electric pulse (200 Ω, 1.8 kV, 2.5 to 5 ms) was applied by using the Genepulser II (Bio-Rad, Munich, DE). Subsequently, 950 µl of LB medium was

added to the transformation. The mixture was transferred into a 2 ml reaction tube, shaken at 28 °C for 2 h, plated on selection medium and incubated at 28 °C for two days.

2.9.2 Preparation and transformation of yeast

Yeast transformation was performed according to the protocol from Gietz and Woods (2002) with modifications: Since the metabolism of *S. cerevisiae* is strongly reduced at temperatures lower 20 °C which impairs the competence, a freshly grown 4 ml *S. cerevisiae* culture was used to adjust 50 ml YPD medium to an OD_{600} of 0.3. This starting culture was incubated on a shaker at 30 °C. After reaching an OD_{600} of 0.6–0.9, cells were centrifuged at 2.000 rpm for 5 min at RT. The pellet was resuspended by pivoting in 10 ml freshly made Mix 1 solution (0.1 M LiAc, 1 M sorbitol, 0.5 mM EDTA 5 mM, Tris/HCl pH 7.5) and centrifuged at 2.000 rpm for 5 min at RT. The pellet was resuspended in 1 ml Mix 1 and incubated at RT for 10 min. In a 2 ml reaction tube 1 µg transforming plasmid, 15 µl (10 µg/µl) carrier DNA (DNA from salmon testes), 700 µl Mix 2 solution (0.1 M LiAc, 40 % PEG 3350, 1 mM EDTA, 10 mM Tris/HCl pH 7.5) and 100 µl of the in Mix 1 resuspended cells were pipetted and thoroughly mixed. The transformation mixture was incubated at 30 °C for 30 min. After incubation, 30 µl DMSO were added, mixed and heat shock transformation was conducted in a waterbath at 42 °C for 30 min. The transformed cell suspension was centrifuged at 4.000 rpm for 3 min at RT, resuspended in 200 µl ddH_2O, plated on SD media lacking the appropriate amino acid and incubated at 30 °C for two or three days.

2.9.3 Stable transformation of **Arabidopsis thaliana**

Stable transformation of *Arabidopsis thaliana* was achieved by *agrobacterium*-mediated transformation using the floral dip method according to the protocol from Davis *et al.* (2009). Transformants were selected using appropriate antibiotics or herbicides.

2.9.4 Transient transformation of **Nicotiana benthamiana**

For transient transformation of *Nicotiana benthamiana*, leaves of six-week-old *N. benthamiana* plants were infiltrated with *A. tumefaciens* as described by Sparkes *et al.* (2006).

2.10 Nucleic acid methods

2.10.1 Nucleic acid extraction methods

2.10.1.1 Extraction of plasmid DNA from bacteria

Small scale plasmid isolation from bacteria was conducted with the QIAGEN Plasmid Mini Kit Qiagen (Hilden, DE), according to the manufacturer's instructions. Extracted plasmids were stored at -20 °C.

2.10.1.2 Extraction of RNA from Arabidopsis

In order to isolate RNA from *Arabidopsis*, plant material was shock frozen in liquid nitrogen and homogenized using a Retsch mill (Retsch, Haan, DE). Total RNA was extracted from tissues using the NucleoSpin RNA Plant Kit (Macherey-Nagel, Düren, DE) according to the manufacturer's instructions, including an on-column DNase digestion.

The RNA quantity and quality were measured photometrically using the NanoDrop ND-1000 spectrophotometer (PeqLab, Erlangen, DE). The RNA was considered clean if the ratios of 260/280 and 260/230 were both ~2. Extracted RNA was stored at -80 °C.

2.10.1.3 Extraction of genomic DNA from Arabidopsis

Genomic DNA was isolated from *Arabidopsis* using the CTAB method (Weigel and Glazebrook, 2002), if DNA was used for PCR amplification and cloning. Therefore, ~100 mg leave material were harvested and homogenized using a Retsch mill (Retsch, Haan, DE). 200 µl extraction buffer (2 % CTAB, 20 mM EDTA pH 8.0, 1.4 M NaCl, 1 % PVP, 100 mM Tris/HCl pH 8.0) were added, thoroughly mixed and the sample was incubated at 65 °C for 30 min. Subsequently, one volume of chloroform/isoamyl alcohol (24:1) was added, thoroughly mixed and the sample was centrifuged at 13.000 rpm for 3 min at RT. Three volumes of 96 % ice-cold ethanol were added to the supernatant. For DNA precipitation, the sample was incubated at -20 °C for 20 min and then centrifuged at 13.000 rpm for 15 min at 4 °C. The supernatant was discarded and the pellet was washed with 70 % ethanol, air dried and resuspended in 50 µl ddH_2O. Extracted DNA was stored at -20 °C.

A quick extraction method was used, if the genomic DNA was used for genotyping. One or two younger leaves were harvested and homogenized in 400 µl extraction buffer (250 mM NaCl, 25 mM EDTA, 0.5 % (w/v) SDS, 200 mM Tris/HCl pH 7.5) using a Retsch mill (Retsch, Haan, DE). The sample was centrifuged at 13.000 rpm for 3 min at RT. The supernatant was transferred into a new reaction tube and one volume of isopropyl alcohol was added, thoroughly mixed, incubated for 2 min at RT and centrifuged at 10.000 rpm for 5 min at RT.

The supernatant was discarded and the pellet was washed twice with 70 % ethanol, air dried and resuspended in 50 µl ddH_2O. Extracted DNA was stored at -20 °C.

2.10.2 Polymerase chain reaction (PCR)

Standard polymerase chain reaction (PCR) (Mullis and Faloona, 1987) was performed for genotyping plants and validation of bacterial or yeast clones by using the house-made *Taq* polymerase and 10x *Taq* PCR buffer (500 mM KCl, 1 % (v/v) Triton X-100, 100 mM Tris/HCl pH 9.0). PCR was also performed for amplification of DNA, used for cloning, by using the Phusion high-fidelity DNA polymerase (Thermo Fisher Scientific, Waltham, US). The compositions of the PCR reaction mixtures are shown in Table 6.

Table 6. PCR reaction mixtures. For genotyping plants or amplification of promoters used for cloning, 1 µl DNA (50–100 ng) was used as template. For amplification of genes used for cloning, 10 µl cDNA (50 ng) was used as template. For genotyping bacteria or yeast, a single colony was picked with a pipette tip and stirred in the PCR reaction mixture.

Component	Volume for *Taq* PCR	Volume for Phusion PCR
Buffer (Taq buffer: 10x, Phusion HF buffer: 5x)	2 µl	4 µl
100 mM $MgCl_2$	0.4 µl	–
5 mM dNTPs	0.8 µl	0.8 µl
50 µM forward primer	0.25 µl	0.25 µl
50 µM reverse primer	0.25 µl	0.25 µl
Polymerase (*Taq*: 1 U/µl, Phusion: 2 U/µl)	0.5 µl	0.2 µl
DNA/cDNA	x µl/1 colony	x µl/1 colony
ddH_2O	ad 20 µl	ad 20 µl

Different PCR programs were used depending on the template, the enzyme, the length of the amplification product and the annealing temperature of primers (Table 7).

Table 7. PCR programs. The time for the initial step was either 1 min for pure DNA or 5 min, if bacteria or yeast colonies were used. The annealing temperature of primers depended on the melting temperature of the primers and was calculated 5 °C lower than the averaged melting temperature of forward and reverse primer.

PCR step	Temperature	Time
Initial denaturation step	95 °C	1 or 5 min
Denaturation	95 °C	30 s
Primer annealing	53–56 °C	30 s
Elongation	72 °C (*Taq* polymerase)	1 min/kb
	72 °C (Phusion polymerase)	30 s/kb
Final elongation	72 °C (*Taq* polymerase)	twice as long as the amplicon-specific elongation time
	72 °C (Phusion polymerase)	

Lists of primers used for PCRs can be found in the respective chapters.

2.10.3 Reverse transcription (RT)-PCR

The reverse transcription (RT)-PCR was used to determine whether the ordered T-DNA insertion lines are loss-of-function mutants by analyzing RNA samples for the presence of transcripts for the genes of interest. Therefore, total RNA was extracted from tissues using the NucleoSpin RNA Plant Kit (Macherey-Nagel, Düren, DE) according to the manufacturer's instructions, including an on-column DNase digestion. For RT-PCR, 500 ng RNA were reverse transcribed using the QIAGEN OneStep RT-PCR Kit (Qiagen, Hilden, DE) according to the manufacturer's information. The sequences of primers are shown in Table 8.

Table 8. Primer sequences for reverse transcription (RT)-PCR.

Purpose of use	Forward sequence (5'-3')	Reverse sequence (5'-3')
Determination of the transcript abundance of *ERF102* (AT5G47230)	CTGCACTTTGGTTCATCGAG	GAGATAACGGCGACAGAAGC
Determination of the transcript abundance of *ERF105* (AT5G51190)	GCAAGAACAAGACCAGTCAGC	TCCAAGAGATGGACAAGGAGA
Determination of the transcript abundance of *ACTIN 2* (AT3G18780)	TACAACGAGCTTCGTGTTGC	GATTGATCCTCCGATCCAGA

2.10.4 Agarose gel electrophoresis

Agarose gel electrophoresis was performed to detect DNA after PCRs (2.10.2), to separate DNA fragments by size after restriction digests (2.10.7) or to check RNA quality. Depending on the expected DNA/RNA fragment size, 1 % or 2 % agarose gels in 1x TAE buffer (40 mM Tris, 20 mM acetic acid, 1 mM EDTA pH 8.0) were used and 0.2 µg/ml ethidium bromide were added to the agarose gel to enable the visualization of DNA/RNA fragments. 1x TAE buffer was used as running buffer. Prior to electrophoresis the samples were mixed with a suitable volume of Orange G loading dye (2 M sucrose, 4 mg/ml Orange G, 0.5 M EDTA pH 8.0). For DNA size determination, the HyperLadder™ I (Bioline, Luckenwalde, DE) or the 100 bp DNA ladder P805 (MBBL, Bielefeld, DE) were used. Gels were running at 80–100 V for 45–60 min. Visualization and pictures of agarose gels were taken by using an ultraviolet transilluminator (SynGene Bioimaging system, Merck, Darmstadt, DE).

2.10.5 Purification of PCR products

In order to purify PCR products or to isolate DNA fragments from agarose gels, the Wizard® SV Gel and PCR Clean-Up System (Promega, Mannheim, DE) was used according to manufacturer's instructions. The DNA concentration was measured photometrically using the NanoDrop ND-1000 spectrophotometer (PeqLab, Erlangen, DE).

2.10.6 Gateway® cloning

The first step of Gateway® cloning was to amplify DNA fragments with attached attB-sites. Therefore, primers with the complete attB-sites were designed (listed in Table 9).

Table 9. Primer sequences for Gateway® cloning. Small letters in the primer sequences indicate the integrated attB4- or attB1-sites for cloning DNA fragments into pDONR P4-P1R. Small italic letters in the primer sequences indicate the integrated attB1- or attB2-sites for cloning DNA fragments into pDONR221. Underlined letters are the nucleotides added to keep the sequence in the right frame.

Amplification of	Primer sequences (5'-3')
Promoter	F: ggggacaactttgtatagaaaagttgCGTTGATTCATTCTACAAACCAG
of *ERF102* (AT5G47230)	R: ggggactgctttttgtacaaacttgTGATAAAATTTTCAAAAAGC
Promoter	F: ggggacaactttgtatagaaaagttgGTTGTGGATTCTGGCATTTG
of *ERF103* (AT4G17490)	R: ggggactgctttttgtacaaacttgTTTGGAGGAAACAGAGAATTG
Promoter	F: ggggacaactttgtatagaaaagttgTGATGAGTGGTCGCTTCTTT
of *ERF104* (AT5G61600)	R: ggggactgctttttgtacaaacttgCTTCACTCTACTTGATTGAC
Promoter	F: *ggggacaagtttgtacaaaaaagcaggct*TGGTGGTTCCGCCTTATAGA
of *ERF105* (AT5G51190)	R: *ggggaccactttgtacaagaaagctgggt*AGATGATGAATTATGTTGGAG
ERF102 (AT5G47230)	F: *ggggacaagtttgtacaaaaaagcaggct*CAATGGCGACTCCTAACGAAG
for N-terminal fusion	R: *ggggaccactttgtacaagaaagctgggt*GTAATCAAACAACGGTCAACTGG
for C-terminal fusion	R: *ggggaccactttgtacaagaaagctgggt*AAACAACGGTCAACTGGGAA
ERF103 (AT4G17490)	F: *ggggacaagtttgtacaaaaaagcaggct*CGGAAATGGCTACACCAAACGAA
for N-terminal fusion	R: *ggggaccactttgtacaagaaagctgggt*CTCAAACAACGGTCAATTGTG
for C-terminal fusion	R: *ggggaccactttgtacaagaaagctgggt*AAACAACGGTCAATTGTGGAT
ERF104 (AT5G61600)	F: *ggggacaagtttgtacaaaaaagcaggct*CGATGGCAACTAAACAAGAAGCTTTA
for N-terminal fusion	R: *ggggaccactttgtacaagaaagctgggt*CGTTTTAAGTGACGGAGATAACGGAAA
for C-terminal fusion	R: *ggggaccactttgtacaagaaagctgggt*AAGTGACGGAGATAACGGAAA
ERF105 (AT5G51190)	F: *ggggacaagtttgtacaaaaaagcaggct*CGATGGCTTCTTCACATCAACAAC
for N-terminal fusion	R: *ggggaccactttgtacaagaaagctgggt*CACCCTCTGAAGCTTAAGTAACTACG
for C-terminal fusion	R: *ggggaccactttgtacaagaaagctgggt*AAGTAACTACGAGTTGAGAGTGTCC
MPK6 (AT2G43790)	F: *ggggacaagtttgtacaaaaaagcaggct*TGATGGACGGTGGTTCAGGTC
for N-terminal fusion	R: *ggggaccactttgtacaagaaagctgggt*CTCAAACTATTGCTGATATTCTGGA

The cloning of constructs in Gateway® compatible vectors was performed according to the manufacturer's instructions (Invitrogen/Thermo Fisher Scientific, Waltham, US) with slight modifications: For a modified BP reaction 60–120 ng attB-PCR product, 30–60 ng of the donor vector, 1 µl BP buffer and 1 µl BP clonase were filled up with ddH_2O to 10 µl. After incubation of at least 2 h, the BP reaction was stopped by adding 0.5 µl proteinase K and incubation at 37 °C for 10 min. Finally, proteinase K was inactivated by incubation at 65 °C for 10 min.

For a modified LR reaction 100–300 ng of the entry clone, 50–150 ng of the destination vector, 1 µl LR buffer and 1 µl LR clonase were filled up with ddH_2O to 10 µl. After incubation of at least 2 h, the LR reaction was stopped by adding 0.5 µl proteinase K and incubation at 37 °C for 10 min. Finally, proteinase K was inactivated by incubation at 65 °C for 10 min.

For MultiSite Gateway® cloning the Gateway® LR Clonase™ II Plus enzyme mix was used according to the manufacturer's instructions (Invitrogen/Thermo Fisher Scientific, Waltham, US).

Gateway® vectors which were used in this study are listed in Table 4.

2.10.7 Restriction digestion

Restriction digestions were performed for examination of bacterial plasmids for their identity. Restriction enzymes were obtained from Thermo Fisher Scientific (Waltham, US) and used with supplied buffers. In general, a restriction digestion consisted of 100–800 ng DNA with 10 U of the appropriate enzyme, the recommend 1x reaction buffer and ddH_2O to a final volume of 20 µl. The reaction mixture was incubated for at least 2 h at the recommended temperature.

2.10.8 Sequencing of DNA

DNA sequencing of purified plasmids was done by the company GATC Biotech (Konstanz, DE).

2.10.9 Genotyping of plants

T-DNA insertion lines were genotyped after ordering seeds from NASC by selection on antibiotic containing medium and by PCR (2.10.2). Genotyping of T-DNA insertion lines by PCR was conducted using two primer pairs. One pair comprised of a gene-specific primer (starting with the start codon of the respective gene) and a T-DNA-specific primer (binding to the left boarder of the T-DNA) used to amplify the mutant allele. The second primer pair was used to amplify the entire gene from start to stop codon to amplify the wild-type allele.

Generated homozygous *promoter:GUS*-, amiRNA- and overexpressing lines were identified by selection on antibiotic containing medium. Therefore, seeds from transformed plants were sown on medium with the appropriate antibiotic or herbicide. Antibiotic/herbicide resistant T_1 plants were harvested and seeds (T_2) were used for segregation analyses to identify plants with an 1:3 segregation, with one insertion, respectively. Finally, T_2 seedlings with one insertion were grown until ripening and harvested. Their seeds (T_3) were used for segregation analyses to identify plants that do not segregate, homozygous plants, respectively.

Complementation lines were generated by crossings of T-DNA insertion lines and overexpressing lines. The progeny (F_2) of the double heterozygous F_1 plants were used for genotyping. To identify double homozygous complementation lines, the following genotyping strategy was performed: One primer pair comprised of a gene-specific primer (starting with

the start codon of the respective gene) and a T-DNA-specific primer (binding to the left boarder of the T-DNA) used to amplify the mutant allele. The second primer pair was used to amplify the respective gene from the 5' upstream region to stop codon to amplify the wild-type allele. Primer pairs one and two were used to identify the homozygous knockout. A third primer pair was used to examine the presence of the overexpression construct and comprised a primer binding to the cauliflower mosaic virus (CaMV) *35S* promoter and a primer binding to the stop codon region of the respective gene. F_3 plants were finally used to analyze segregation on antibiotic containing medium regarding the homozygosity of the overexpression construct.

All primers used for genotyping are listed in the following Table 10.

Table 10. Primer sequences for genotyping.

Primer	Sequence (5'-3')	Purpose of use
ERF102 ATG	ATGGCGACTCCTAACGAAGT	Genotyping of *erf102*
ERF102 TGA	TCAAACAACGGTCAACTGGG	Genotyping of *erf102*
ERF105 ATG	ATGGCTTCTTCACATCAACAACA	Genotyping of *erf105*
ERF105 TAA	TTAAGTAACTACGAGTTGAGAGTGTC	Genotyping of *erf105*
IT-LB	GCCTTTTCAGAAATGGATAAATAGCCTTGCTTCC	Genotyping of SAIL lines, e.g. *erf102*
GABI-LB	ATATTGACCATCATACTCATTGC	Genotyping of GABI lines, e.g. *erf105*
ERF102 upstream	GACTTGGCGAAGCCTCATAA	Genotyping of erf102comp lines
ERF105 upstream	TAATCCACAGTGTGCCCAAA	Genotyping of erf105comp lines
35S	GGAAGTTCATTTCATTTGGAG	Genotyping of complementation lines

2.10.10 cDNA synthesis

For quantitative real-time PCR analyses, 1 µg RNA was transcribed into cDNA by SuperScript® III Reverse Transcriptase (Invitrogen/Thermo Fisher Scientific, Waltham, US) according to the manufacturer's instructions with slight modifications: 1 µg RNA was mixed with 2 µl dNTPs (5 mM), 1 µl oligo(dT) primers (50 µM), 1.8 µl random hexamers (50 µM) and 14.5 µl ddH_2O and incubated at 65 °C for 5 min. Afterwards, the reaction mixture was placed on ice and 5 µl 5x first strand buffer, 1 µl DTT (0.1 M) and 0.5 µl SuperScript® III (200 U/µl) were added. The final reaction mixture was incubated at 25 °C for 5 min, at 50 °C for 60 min and at 70 °C for 15 min. After cDNA synthesis, the cDNA was diluted 1:10 (5 ng/µl) and stored at -20 °C.

2.10.11 Quantitative real-time PCR (qRT-PCR)

Quantitative real-time PCRs (qRT-PCRs) were performed on an ABI PRISM 7500 sequence detection system (Applied Biosystems/Thermo Fisher Scientific, Waltham, US). Quality of cDNA was assessed by qRT-PCR using intron-specific primers of *AGL68* (AT5G65080) to

confirm the absence of genomic DNA contamination. A second quality check of cDNA was performed using primers which amplify 5' and 3' regions of *GAPDH* (AT1G13440). The qRT-PCR reactions with a final volume of 10 µl contained 10 ng cDNA as template, 0.01 U/µl Immolase DNA-Polymerase (Bioline, Luckenwalde, DE), the corresponding 1x buffer, 2 mM $MgCl_2$, 100 µM each dNTP, 0.1x SYBR Green I (Fluka, Buchs, CH), 50 nM ROX as internal reference dye (Sigma, Buchs, CH) and primers. All primers used for qRT-PCR are listed below in Table 11. Primer concentrations varied, depending on their tested efficiency. Primer efficiency was calculated by determining a standard curve with 2 µl of cDNA dilutions. Dilution series were made using two-fold dilutions with the 1:10 diluted cDNA (5 ng/µl) as highest template concentration. Six dilutions were used plus one water control. All dilutions were measured in technical triplicates using the "standard" qRT-PCR program. Primer efficiency was calculated with the Applied Biosystems 7500 Software v2.0.6. Primers were defined as suitable if their efficiency was ≥ 90 %. For qRT-PCRs, the "fast" cycling set up of the Applied Biosystems 7500 Software was used. After heat activation of the DNA-Polymerase (95 °C, 15 min), 40 PCR cycles followed comprised of denaturation (95 °C, 5 s), annealing (55 °C, 15 s) and elongation (72 °C, 15 s). Subsequently, a dissociation curve was generated to analyze the specificity of amplification. The relative transcript abundance of each gene of interest was normalized against at least two different reference genes (*Actin2*, *PP2AA2*, *EF1A, UBC10*) according to Vandesompele *et al.* (2002) and is presented relative to the control treatment. Four biological replicates were performed for each experiment.

Table 11. Primer sequences for quantitative real-time PCR. Primers were designed using the QuantPrime software (Arvidsson *et al.*, 2008). If applicable, primers were designed to be intron spanning. Most primers were used in a final concentration of 300 nM. * These primers were used in a 450 nM final concentration; ** these primers were used in a 600 nM final concentration.

Gene	AGI number	Forward sequence (5'-3')	Reverse sequence (5'-3')
AAO3	AT2G27150	TGCTTATGGTCTCGGTATGG	TAACGGCTTCACAACTGCTC
AAT/A5GMaT	AT3G29590	AAAGATGCCGTGTATCTCACGG	CGAGGTTCATCTCCGGAAAGA
AAT1/A3GOCT	AT1G03940	AACAAAGGCCAACGAGGAAGA	CAGGAGCCATACAGTTGCCAA
A3GCOT	AT1G03495	TTGGCAACTGTATGGCTCCTG	GCAGCCATGACGCATTTTTC
ABA1	AT5G67030	TTTGTTTCTTCGGATGTTGG	GAATGGCTTCCTCCTCAGTC
ABA2	AT1G52340	TAGTGTGGGAGGTGTTGTGG	CAAATGAGCCAAAGCGAGT
*ABI1**	AT4G26080	AGCTGCTGATATAGTCGTCGTTGATA	GAGGATCAAACCGACCATCTAACA
ABI2	AT5G57050	GTTCTTGTTCTGGCGACGGAGC	CCATTAGTGACTCGACCATCAAG
ABI5	AT2G36270	AGAGGGATAGCGAACGAGTCTAGTC	GTTCGGGTTTGGATTAGGTTTAGG
ACT2	AT3G18780	CTTGCACCAAGCAGCATGAA	CCGATCCAGACACTGTACTTCCTT
AGL68 Intron	AT5G65080	TTTTTTGCCCCCTTCGAATC	ATCTTCCGCCACCACATTGTAC
ANS/TT18	AT4G22870	GGCTGTGTTTTGTGAGCCACCA	CCTTGGAGGAAACTTAGCCGGAGA
APX1	AT1G07890	TGCCACAAGGATAGGTCTGG	CCTTCCTTCTCTCCGCTCAA
APX2	AT4G09010	TTGCTGTTGAGATCACTGGAGGA	TGAGGCAGACGACCTTCAGG

Table 11. Continued.

Gene	AGI number	Forward sequence (5'-3')	Reverse sequence (5'-3')
bHLH/TT8	AT4G09820	TGGAGACACCATTGCGTACGT	TCTTACAAGTACGCGTCCGCT
CAT1	AT1G20630	AAGTGCTTCATCGGGAAGGA	CTTCAACAAAACGCTTCACGA
CAT2	AT4G35090	CCGCCTGCTGTCTGTTCT	AATCGTTCTTGCCTCTCTGGT
CBF1	AT4G25490	GTCAACATGCGCCAAGGATA	TCGGCATCCCAAACATTGTC
CBF2	AT4G25470	GAATCCCGGAATCAACCTGT	CCCAACATCGCCTCTTCATC
CBF3	AT4G25480	CAACTTGCGCTAAGGACA	TCTCAAACATCGCCTCAT
CBF4	AT5G51990	TGGTCGCTCTGCTTGTCTCAATTT	GTCTCAGGAATACGAAGCCGCCAA
CHI/TT5	AT3G55120	CTCTCTTACGGTTGCGTTTTCG	CACCGTTCTTCCCGATGATAGA
CHS/TT4	AT5G13930	GGAGAAGTTCAAGCGCATGTG	ATGTGACGTTTCCGAATTGTCG
COR15A	AT2G42540	AACGAGGCCACAAAGAAAGC	CAGCTTCTTTACCCAATGTATCTGC
COR15B	AT2G42530	CCACAACGTAGGAGCAAAGCA	TTCTTGCGCTGAGCAACGA
COR47	AT1G20440	ACAAGCCTAGTGTCATCGAAAAGC	TCTTCATCGCTCGAAGAGGAAG
COR6.6	AT5G15970	GAGACCAACAAGAATGCCTTCC	TGCTCTTCTCCTCAGCTTTGC
COR78	AT5G52310	GCACCAGGCGTAACAGGTAAAC	AAACACCTTTGTCCCTGGTGG
CSD1	AT1G08830	TCCATGCAGACCCTGATGAC	CCTGGAGACCAATGATGCC
CYP707A1	AT4G19230	AATCCATCGCTCAAGACTCTCTCC	GCAACGCAACGTTGAAGGTGTATG
CYP707A2	AT2G29090	TTTCCGGCGAATCCATCACTCC	TGGTGCCACCTCGAATCTAGAAG
CYP707A3	AT5G45340	CGGCCAGTAAAGAGAGGATG	TGATTCAATGTGAGGGACCA
CYP707A4	AT3G19270	GGGATGGAAAGTGATGCCACTG	TGTATTCGGCTTCGGATTTACCTC
DFR/TT3	AT5G42800	CGTTTGAAGGTGTTGATGAGAATC	TCCGTCAGCTTCTTGGAACTG
DHAR1	AT1G19570	CTCTGACAAACCCCAGTGGTTC	CAACGATGACGTCGGAATCA
EF1A	AT5G60390	TGAGCACGCTCTTCTTGCTTTCA	GGTGGTGGCATCCATCTTGTTACA
ERF102, ERF5	AT5G47230	GAAACGGAAGAGAGACGATG	GAAACCCCGTTAAATCCC
ERF103, ERF6	AT4G17490	TAATCGATCTCGTCACTCCC	TGAACAGTAACGCGAGGAG
*ERF104**	AT5G61600	GTATTCCTCCGTTATCTCCG	TGCACACTACCGCTACCTT
ERF105	AT5G51190	AGCTGCAAGAGGTTATGAC	TTCATCCTCCGTCACCTGTC
ESK1	AT3G55990	TGGAGATTCCCTAAACCGGAACC	CCGTCGCATTATAATCCTCGACTC
F3H/TT6	AT3G51240	GCTACAAGACCAAGTCGGTGGA	GCTCAAAAAATGGCCGTGG
F3'H/TT7	AT5G07990	GACAGGAAGAGGTTGGAACGCT	CCAACTGGCCTAAATTCACGG
FLS	AT5G08640	TTCTGAGGTTGAGTAATGGGAGG	CCGTCGTCCTATGCAACACAT
*FRY2***	AT4G21670	ATCTCAGCGTCAGCTTCCATCTG	ACGCCCATCTATTTCAACCTGAGC
FSD1	AT4G25100	CTCCCAATGCTGTGAATCCC	TGGTCTTCGGTTCTGGAAGTC
FSD2	AT5G51100.1	TTGGAAAGGTTCAAGTCGGCT	CATTTGCAACGTCAAGTCTATTCG
FSD3	AT4G25100	AACGGGAATCCTTTACCCGA	TGTCTCCACCACCAGGTTGC
GA20OX1	AT4G25420	AGATTACTTCTGCGATGCGTTGG	TCTTGATACACCTTCCCAAATGGC
GA20OX2	AT5G51810	CAAGAGTTCGAGCAGTTTGGGAAG	TCGGAAATAGTCTCGGTTTACGC
GA2OX1	AT1G78440	AACGTTGGTGACTCTCTCCAGGTG	AACCCTATGCCTCACGCTCTTG
GA2OX2	AT1G30040	AGATGGAAGTTGGGTCGCTGTC	CCCGTTAGTCATAACCTGAAGAGC
GA3OX1	AT1G15550	CCCAACATCACCTCAACTACTGC	GGCCCATTCAATGTCTTCTTCGC
GA3OX2	AT1G80340	CCAGCCACCACCTCAAATACTGTG	ATTAGGCCCGGCCCATTGTATG
GAPDH 5'	AT1G13440	TCTCGATCTCAATTTCGCAAAA	CGAAACCGTTGATTCCGATTC
GAPDH 3'	AT1G13440	TTGGTGACAACAGGTCAAGCA	AAACTTGTCGCTCAATGCAATC
HOS1	AT2G39810	TTACCGTGGAACCCAGATGAGG	GGATGTAACGGTAGCGCTGAAG

Table 11. Continued.

Gene	AGI number	Forward sequence (5'-3')	Reverse sequence (5'-3')
*ICE1**	AT3G26744	TCCTAAAGGCCAGCAAGCTA	CTCTTGTCCTTCTTGGCATTG
ICE2	AT1G12860	TTCCGCGCTGAGCAATGTCAAG	ACCAAACCAGCGTAACCTGCTG
LDOX	AT4G22880	AAGCTCACACCGATGTAAGC	TTTGCAGTGACCCATTTGCC
LOS4	AT3G53110	TCAACTTGCTGCTTGATGATGGC	TCTGAGTTCCACGACTTGATCTCC
MDAR1	AT3G52880	TTGGGTTCAAGGTGGTAAAGTGG	TCGAGCTTTGGCGACTTTAGC
MDAR2	AT5G03630	GGAAAGTGGTTGGAGCATTTTTAG	CACTTCAAGGCTCTCAACAGAAGG
MDAR3	AT3G09940	CTGAAGCCTGGTGAACTCGC	GGTCGGATTGACTTCGAGGTC
MYB11	AT3G62610	GGCGATTGTAACCCAAGCATT	TCACATGAGGACACGTGGACA
MYB111	AT5G49330	CGGCCTCACAATGTTTCTCAC	CCACTCATAAGGCCCCAAAGA
MYB12	AT2G47460	AACAGGTGGTCACTAATCGCG	TTCGTTGTCTGTTCTCCCTGG
*MYB15***	AT3G23250	GGTGCGGATATCGATGAAAG	CATTATTAGCGGAGCCCAAG
MYB96	AT5G62470	CAAGAGCTGCAGATTGAGATGGAC	TGCTATGGCTGCCCATCTGTTG
NCED3	AT3G14440	GCTACACCCGCTTCCTAAAA	CGTGAACCATACCGTCTCC
OMT	AT5G54160	CAATCCCGGAGGCAAAGAA	GAAGCCTGATGCTTTGGCTA
PAP1/MYB75	AT1G56650	TGTAAGAGCTGGGCTAAACC	GAAGATCGACTTCATCAGAGC
PAP2/MYB90	AT1G66390	TGGGCTAAATCGATGCAGAAAGA	CCAGCAATCAAGGACCACCTAT
PP2AA2	AT3G25800	CCATTAGATCTTGTCTCTCTGCT	GACAAAACCCGTACCGAG
RAB18	AT5G66400	GCAGTATGACGAGTACGGAAATCC	CCTTGTCCATCATCCGAGCTAGA
RBOHD	AT5G47910	CGGGATAGTCGTCGGTGTT	TTCCATCGGCTCATAGGTGT
RBOHF	AT1G64060	AGAATACAGCACAGGAAGCAAC	GAGAGCAGAACGAGCATCAC
RD22	AT5G25610	AACACTCCCATTCCCAACTC	CCACCTCCGTGACCTTTT
RD29B	AT5G52300	TGGAGGAGGAGGAGAGAAGA	TTACCACCGAGCCAAGAAGT
SIZ1	AT5G60410	GCCCCGCTAAAACTTGGAAT	ACGCTTGCATCATCACCATC
TT19/GST26	AT5G17220	GAACATCTTCTTCGTCAGCC	GTAGTATCTCGCGATGGCTC
TTG1/WD40	AT5G24520	TCGATATTCGTTCGCCGACT	GCCTGTGTATCATCACCACCAG
TTG2/WRKY44	AT2G37260	CGGTTGCAAGAGTAGCCAATG	CCTTGCGATACTCCTGCTTCA
UBC10	AT5G53300	CCATGGGCTAAATGGAAA	TTCATTTGGTCCTGTCTTCAG
UGT75C1/A5GT	AT4G14090	TTTTGGCGCATTGTGCTGT	TCAGCAAACTGCGGAAACG
UGT78D1/F3RT	AT1G30530	TGCTGAAACACGAGGCAATG	ATCCGCCAAAATCGGTCTG
UGT78D2/Fd3GT	AT5G17050	CGGAGCAAACTCACTCTCTGCT	CCTACTTCTTTGACACCGATGGTT
UGT79B1	AT5G54060	CAGCAACCGTTGGTGTTGAAC	GCGGAACCAAAACGATCTGAC
UGT89C1/F7RT	AT1G06000	TTCTTTAACACGACGCTCATCG	CAAAATCCTAGCGAGCTTGTCC
ZAT6	AT5G04340	TGTGAAGTCGCACGTTTGCTCTAT	GCCTCCGTTCTTTCCTTCGTAGTG
ZAT12	AT5G59820	GTGCGAGTCACAAGAAGCCTAACA	GCGACGACGTTTTCACCTTCTTCA

2.11 Establishment of transgenic lines

This chapter contains detailed information about the generation of transgenic lines used in this study. All PCR amplifications were conducted with Phusion high-fidelity DNA polymerase (2.10.2). Primers used for amplifications are listed in Table 9. PCR products were purified as already described (2.10.5), cloned using Gateway® system (2.10.6), sequenced (2.10.8) and

transformed in bacteria (2.9.1). The binary constructs were, if not otherwise stated, transformed into Col-0 plants by *A. tumefaciens* using the floral dip method (2.9.3). Transgenic lines were selected using antibiotics or herbicides.

2.11.1 Generation of ERF102:GUS *to* ERF105:GUS *lines*

To generate *ERF102:GUS, ERF103:GUS* and *ERF104:GUS* lines, the promoter regions of the *ERF* genes (~2 kb upstream of the start codon) were amplified by PCR and cloned into pDONR P4-P1R. To generate the binary destination vectors, the pDONR P4-P1R constructs with the *ERF* promoters and the Gateway® entry clone pEN-L1-SI-L2 harboring the *GUS* reporter gene were then combined with MultiSite Gateway® into the destination vector pK7m24GW,3.

To generate *ERF105:GUS* lines, the promoter region of the *ERF105* gene (~2 kb upstream of the start codon) was amplified by PCR and cloned into pDONR221 and subsequently into pBGWFS7.

2.11.2 Generation of overexpressing lines of ERF102 *to* ERF105

To generate N-terminal fusion constructs overexpressing *ERF102* to *ERF105*, the genomic coding sequences of the *ERF* genes were amplified by PCR (2.10.2). To generate C-terminal fusion constructs overexpressing *ERF102* to *ERF105,* the genomic coding regions without stop codons were amplified. PCR products were cloned into pDONR221 and transferred subsequently into the pK7WGF2 destination vector for N-terminal GFP-fusion, and into the pK7FWG2 for C-terminal GFP-fusion.

2.11.3 Generation of complementation lines

Complementation lines of *erf102* were created by introgressing ERF102ox-1 and ERF102ox-2 into the *erf102* background.

Complementation lines of *erf105* were created by introgressing ERF105ox-1 and ERF105ox-2 into the *erf105* background.

2.11.4 Generation of amiRNA lines of ERF102 *to* ERF105

At the beginning of this study, only T-DNA insertion lines were available for *ERF102* and *ERF105*. In order to analyze lines with a reduced *ERF103* and *ERF104* expression as well, the technique of artificial microRNA (amiRNA) was used (Schwab *et al*. 2006). Two amiRNA constructs were generated for specific gene silencing of *ERF103* and *ERF104* and one amiRNA construct was generated which targets *ERF104* and *ERF105*. The amiRNA sequence targeting *ERF103* was 5'-TAACGTCGTAACTTTCCCCCG-3'. The amiRNA

sequence targeting *ERF104* was 5'-TTGATATTTGCACACTAGCGC-3', and the amiRNA sequence targeting both *ERF104* and *ERF105* was 5'-TCCCATCCAACTTGACGGCGT-3'. Sequences were selected and expression constructs were made using the Web MicroRNA Designer (WMD3) and the protocol available under http://wmd3.weigelworld.org. The amiRNA precursor was cloned into pDONR221 (Invitrogen/Thermo Fisher Scientific, Waltham, US) and subsequently into pH2GW7 (Karimi *et al.*, 2007b) harbouring the cauliflower mosaic virus (CaMV) *35S* promoter to yield *35S:*amiERF103, *35S:*amiERF104 and *35S:*amiERF104/105, respectively. Finally, the amiRNA constructs were also transformed into *erf102* and *erf105* to generate higher order mutants.

2.12 Histochemical analysis of GUS expression

Histochemical analysis to detect GUS reporter enzyme activity was performed as described by Jefferson *et al.* (1987) with some modifications. Sample tissues were fixed with cold 90 % acetone for 1 h at -20 °C and washed twice with 100 mM Na_3PO_4 buffer pH 7.4. The enzymatic reaction was conducted with staining solution (50 mM Na_3PO_4 buffer pH 7.4, 5 mM $K_4[Fe(CN)]_6$, 5 mM $K_3[Fe(CN)_6]$, 0.2 % (v/v) Triton X-100, 0.05 % (w/v) X-Gluc (5-bromo-4-chloro-3-indolyl-β-D-glucoronide)) for 4 h to overnight at 37 °C in the dark. After staining, plant material was destained with 70 % ethanol and cleared with a chloral hydrate : glycerole : water solution (8:1:2, w:v:v). The GUS staining pattern was documented with a stereomicroscope (SZX12; Olympus, Shinjuku, JP) or a microscope (Axioskop 2 plus; Zeiss, Jena, DE) equipped with an Olympus C-4040ZOOM (Olympus, Shinjuku, JP) photographic device.

The quantitative GUS activity assay of plant extracts was performed as described by Blázquez (2007) using 4-methylumbelliferyl-β-D-glucuronide (MUG) as a substrate.

2.13 Confocal laser scanning microscopy

To determine the subcellular protein localization, leaf discs from *N. benthamiana* were used three days after their transformation with *A. tumefaciens* (2.9.4). Subcellular protein localization could be detected by microscopic analyses using an inverted fluorescence microscope (Leica DMI 6000 CS), equipped with a Leica TCS SP5 laser scan unit (Leica Microsystems, Wetzlar, DE) and operated with the Leica Application Software. Images were obtained with a HC PL APO 20X/0.70 IMM CORR water-immersion objective and a 488 nm argon laser in combination with a 500 nm to 530 nm bandpass filter set.

2.14 Protein interaction studies

Protein interaction studies were performed using the yeast two-hybrid system, which comprised a LexA DNA-binding domain encoding bait vector (pBTM116-D9) and a Gal4 activation domain encoding prey vector (pACT2) adapted to the Gateway® system in the *S. cerevisiae* strain L40ccaU. The cDNAs were *in vitro* recombined from the pDONR221 into the bait and prey vectors. Subsequently, yeast transformations were performed (2.9.2) and preselection of bait and prey hybrid proteins was done by testing for autoactivation on interaction medium by coexpression of the bait hybrid proteins with the Gal4 activation domain encoded by the empty prey vector, and by coexpression of the prey hybrid proteins with the LexA DNA-binding domain encoded by the empty bait vector. Weakly autoactivating hybrid proteins were totally suppressed by supplementing 2 mM 3-amino-1,2,4-triazole (3-AT) to the interaction medium, whereas strong autoactivating hybrid proteins were omitted from the matrix screen. All yeast clones were incubated for seven days at 30 °C.

2.15 Plant experiments

2.15.1 Hormone experiments

For analyzing the hormonal regulation of genes, plants were grown *in vitro* in half strength MS liquid medium containing 0.1 % sucrose. Ten days after germination, the respective hormone was added to the medium and seedlings were harvested after various incubation times. Control seedlings were treated with the respective mock solution.

2.15.2 Analysis of growth and developmental parameters

Plants were grown on soil in the greenhouse under long day (LD) conditions (16 h light/8 h dark) at 130–160 µmol m^{-2} s^{-1} and 21 °C. During the life cycle of the plants the phenotype was monitored. 14, 21, 28, and 35 days after germination the rosette diameter, the shoot height and the fresh weight were determined as well as photos were made. 42 days after germination, the number of adventitious shoots, lateral shoots, and siliques were examined. Furthermore, during the whole life cycle the plants were observed regarding their flowering time and their onset of leaf senescence. The flowering time was defined as the point of time where the first flower was visible. For determination of the onset of senescence, the 6th and the 10th leaf were marked with small twines and observed for signs of senescence (Lim *et al.*, 2007), namely yellowing of the leaves (chlorosis).

For analysis of root characteristics, plants were grown *in vitro* (2.7.3.1) in vertically placed square petri dishes on half strength MS medium containing 10g/l phytagel. The elongation of the primary root was determined between four and ten days after germination using the

software ImageJ (Abràmoff *et al.*, 2004). The number of lateral roots was determined ten days after germination.

2.15.3 Cold stress experiments

For examining the kinetics of transcriptional responses of selected genes, plants were grown on soil under short day (SD) conditions (8 h light/16 h dark) in a growth chamber (AR-41L, CLF Plantclimatics GmbH, Wertingen, DE) at 130 µmol m^{-2} s^{-1} and 21 °C for four weeks, and then transferred to 4 °C (AR-41L, CLF Plantclimatics GmbH, Wertingen, DE) and cultivated under the same light conditions. After different time points, leaf number five, six and seven were pooled and used for transcriptional analyses.

For *in vitro* survival experiments, plants were grown on MS medium without sucrose. After two weeks, seedlings were transferred to a customary freezer (-18 °C) for 60 min and transferred back for recovery to the previous conditions. Three days later the number of surviving seedlings was counted and photos were taken.

For *in vivo* survival experiments, plants were grown on soil under SD conditions in a growth chamber (AR-41L, CLF Plantclimatics GmbH, Wertingen, DE) at 130 µmol m^{-2} s^{-1} and 21 °C. Five-week-old plants were exposed to -3 °C for four days in constant darkness (to avoid additional photo-oxidative damage) according to Le *et al.* (2008) and transferred back for recovery to the previous conditions for ten days. The amount of surviving plants was counted and photos were taken.

For electrolyte leakage experiments, proline, carbohydrates, anthocyanin, malondialdehyde, chlorophyll and ABA measurements as well as for analyses of transcriptional regulation of selected genes, plants were grown for two weeks under SD conditions and then for four weeks under LD conditions at 200 µmol m^{-2} $s^{-}1$ and 20 °C during the day, 18 °C during the night (non-acclimated plants). For cold acclimation, plants were transferred to a cold chamber and cultivated under LD at 90 µmol m^{-2} s^{-1} at 4 °C for additional 14 or 21 days (acclimated plants). Samples were taken from non-acclimated plants and acclimated plants for the measurements and analyses mentioned above.

2.15.4 Drought stress experiments

In order to analyze the regulation of genes by drought, plants were grown *in vitro* on MS medium. Eleven days after germination, seedlings were transferred to drought or moist (control plants) filter paper, incubated 15 min or 1 h and harvested.

For examining the loss of fresh weight in detached leaves, plants were grown on soil under LD conditions. After four weeks, leaf number six was cut and weighed at different timepoints to determine the time course of percental reduction of fresh weight.

For *in vivo* survival experiments, plants were grown on soil under LD conditions. Three-week-old plants were exposed to drought stress by withholding water for nine days, followed by a period of rewatering of one week. Photos were taken from fully watered plants, from plants after the drought stress phase and from plants after the recovery phase. After the recovery phase, the amount of surviving plants was counted and photos were taken.

2.15.5 Further stress experiments

The analysis of transcriptional regulation of genes by other abiotic stresses was performed by growing plants *in vitro* on MS medium. Eleven days after germination, seedlings were exposed to stress. Stress treatments were performed by incubation of seedlings by 1000 µE, 42 °C and darkness, by spraying with 500 mM H_2O_2 or by transferring seedlings to MS medium including 200 mM NaCl or 200 mM mannitol for different time periods. Control plants were treated with the respective control conditions (standard light conditions in the high light experiment, 21 °C in the heat stress experiment, spraying with mock solution in the oxidative stress experiment and transferring to mock medium in the salt and osmotic stress experiment).

Further stress experiments comprised of watering plants with different chemicals. Therefore, plants were grown on soil under LD conditions. Two-week-old plants were exposed to stress by watering with 50 mM NaCl, mannitol or H_2O_2. The concentration of chemicals was gradually increased every four days from 50 mM to 100 mM up to 200 mM. Control plants were watered normally all the time. 26 days after germination, growth parameters were determined and photos were taken.

2.16 Evaluation of stress parameters

2.16.1 Electrolyte leakage

Electrolyte leakage measurements were performed following a method of Thalhammer *et al.* (2014b). Fully expanded detached rosette leaves taken from three individual plants were placed in glass tubes containing 200 µl of ddH_2O. (Control experiments have been shown that there was no significant difference in electrolyte leakage between young and old fully expanded leaves from plants of the same age (Rohde *et al.*, 2004). For temperature equilibration, the glass tubes were transferred to a programmable cooling bath (Huber, Offenburg, DE) set to -1 °C. Glass tubes with unfrozen control samples were kept on ice during the entire experiment. After 30 min, ice crystals were added to the tubes in the cooling bath to initiate freezing. After further 30 min, samples were cooled at a rate of 4 °C/h over a temperature range from -1 to -16 °C for non-acclimated plants and from -2 to -22 °C for cold acclimated plants. Leaves were slowly thawed on ice. For electrolyte leakage

measurements, leaves were immersed in 7 ml ddH_2O and incubated at 4 °C on a shaker at 50 rpm for 24 h. Electrolyte leakage was determined as the ratio of conductivity measured in the water before and after boiling using a conductivity meter (SI Analytics, Mainz, DE) and normalized to the unfrozen control samples. Four replicates for each temperature point and for each genotype were analyzed. The temperature of 50 % electrolyte leakage (LT_{50}) was calculated as the log EC50 value of sigmoidal curves fitted to the leakage values using the software GraphPad Prism3 (GraphPad Software, Inc., La Jolla, US).

2.16.2 Proline measurement

For analysis of proline, whole rosettes of individual plants (five biological replicates of each genotype) were harvested at midday on the day of the respective electrolyte leakage experiment. Samples were frozen immediately in liquid nitrogen and homogenized using a Retsch mill (Retsch, Haan, DE). Proline measurements were performed photometrically (Bates *et al*., 1973) with the modifications as described: 45–75 mg of rosette samples were weighed out and 1 ml of 80 % ethanol was added. The sample was thoroughly mixed. After incubation in a waterbath at 80 °C for 30 min, the sample was centrifuged at 4.000 rpm for 5 min at RT. The supernatant was transferred into a new 2 ml reaction tube. 1 ml of 80 % ethanol was added to the pellet. The sample was thoroughly mixed, incubated at 80 °C for 30 min and centrifuged at 4.000 rpm for 5 min at RT. The supernatant was pipetted to the first supernatant and the pellet was discarded. Subsequently, the sample was transferred into a vacuum concentrator (Thermo Fisher Scientific, Waltham, US) and dried out over night at RT. The dried sample was resuspended in 1 ml ddH_2O and have been used for proline and sugar analyses. For proline analysis, 10 µl of the resuspended sample were mixed with 90 µl ddH_2O, 100 µl 100 % acetic acid and 100 µl acid ninhydrine reagent (1 g ninhydrine, 24 ml 100 % acetic acid, 16 ml 6 M phosphoric acid). The mixture was incubated at 95 °C for 1 h and afterwards put on ice for 30 min. Proline was extracted with 500 µl toluene and by vigorously shaking for 1 min. 400 µl of the upper phase were transferred into a glass cuvette and the absorbance was measured at 520 nm. Pure toluene was used as blank. The determination of proline content was calculated using a proline standard curve (0–200 µM proline). Standards, samples and blanks were measured in triplicates.

2.16.3 Carbohydrate analysis

Sugar measurements were performed on the same rosette samples as were used for proline measurements. Sugars were extracted by ethanol as described for proline (2.16.2). For sugar quantification, 500 µl of the in 1 ml ddH_2O resuspended extract were added to 7 mg ion exchange resins AG 501-X8 (Bio-Rad, Munich, DE) and shaken at 1.000 rpm for 15 min at RT. The sugar extract was transferred into a new reaction tube and ion exchange resins

were discarded. In a final volume of 100 µl dilutions of sugar extracts were prepared: 1:20 dilution for samples of cold-acclimated plants and 1:5 dilution for samples of non-acclimated plants. Sugars were analyzed in technical duplicates by high performance anion exchange chromatography (HPAEC) using a CarboPac PA-100 column on the Dionex DX-500 gradient chromatography system (Dionex, Sunnyvale, US) coupled with pulsed amperometric detection by a gold electrode. The column was equilibrated in 0.05 M NaOH and was eluted with a linear gradient from 0.05 M to 0.2 M NaOH.

2.16.4 Anthocyanin measurement

Anthocyanin measurements were performed on the same rosette samples that were used for proline (2.16.2) and carbohydrate (2.16.3) measurements. The relative anthocyanin content was analyzed according to Kant *et al.* (2006) with slight modifications: 45–75 mg of homogenized rosette samples were weighed out and 300 µl 80 % ethanol and 8 µl 37 % HCl were added. The sample was thoroughly mixed on a shaker at 1.000 rpm for 15 min at RT. Anthocyanins were separated from chlorophylls by adding 600 µl ddH_2O and extracting with 900 µl chloroform followed by vigorously shaking and centrifugation at 4.000 rpm for 5 min at RT. The upper phase (~800 µl) was transferred into a glass cuvette and the absorbance was measured at 530 nm. Samples and blanks were measured in triplicates. The relative amount of anthocyanin was expressed as absolute absorption at 530 nm per g fresh weight.

2.16.5 Chlorophyll measurement

Chlorophyll measurements were performed on the same rosette samples as were used for proline (2.16.2), carbohydrate (2.16.3) and anthocyanin (2.16.4) measurements. The relative chlorophyll a and b content was analyzed according to Porra *et al.* (1989) with slight modifications: 45–75 mg of homogenized rosette samples were weighed out and 1 ml 100 % methanol was added and incubated at 4 °C overnight on a shaker. The next day, the samples were centrifuged at 13.000 rpm for 5 min at 4 °C. 200 µl of the samples (or blank) were quickly pipetted in triplicates in microtiter plates. The absorbance was measured using a microplate reader (BioTek, Winooski, US) at 750 nm, 652 nm and 665 nm. To determine the pathway correction factor, a control plate with water was measured at 977 nm and 900 nm. The chlorophyll content was calculated according to Porra *et al.* (1989) using the chlorophyll extinction coefficients (22.12 l mol^{-1} cm^{-1} for chlorophyll a and 2.71 l mol^{-1} cm^{-1} for chlorophyll b).

2.16.6 Determination of oxidative stress

2.16.6.1 Lipid Peroxidation

To determine the level of oxidative stress in leaf tissue the content of malondialdehyde (MDA) was measured. MDA content was determined by the reaction with thiobarbituric acid (TBA) according to Heath and Packer (1968) with modifications. Measurements were performed on the same rosette samples as were used for proline (2.16.2), carbohydrate (2.16.3), anthocyanin (2.16.4) and chlorophyll (2.16.5) measurements. A 45–75 mg rosette sample was cooled with liquid nitrogen and homogenized using a Retsch mill (Retsch, Haan, DE). 650 µl of 0.1 % trichloroacetic acid (TCA) were added to the homogenized leaf material and thoroughly mixed. The homogenate was centrifuged at 13.000 rpm for 10 min at RT. To 125 µl of the supernatant 500 µl 0.5 % TBA (0.5 % TBA in 20 % TCA) were added. The samples were incubated at 95 °C for 30 min and then quickly cooled down on ice and centrifuged at 13.000 rpm for 10 min at 4 °C. 170 µl of the samples (or blank) were measured in duplicates in microtiter plates (170 µl = path length of 1 cm). The absorbance was measured using a microplate reader (BioTek, Winooski, US) at 532 nm and the value for the non-specific absorption at 600 nm was subtracted. The concentration of MDA was calculated using the extinction coefficient $\varepsilon = 155\ l\ mM^{-1}\ cm^{-1}$.

2.16.6.2 Detection of superoxide

The detection of superoxide was performed by qualitative nitroblue tetrazolium (NBT) histochemical staining method as described by Bournonville and Diaz-Ricci, 2011.

2.16.7 Abscisic acid measurement

Measurements of abscisic acid (ABA) and its metabolites were performed on the same rosette samples that were used for proline (2.16.2), carbohydrate (2.16.3), anthocyanin (2.16.4), chlorophyll (2.16.5) and MDA (2.16.6.1) measurements. Extracting and purifying of (+)-abscisic acid (ABA) and five ABA metabolites – phaseic acid (PA), dihydrophaseic acid (DPA), neophaseic acid (neoPA), ABA-glucose ester (ABAGE) and 7'-hydroxy-ABA (7'-OH-ABA) were performed as described by Turečková *et al.* 2009. ABA and its metabolites were identified and quantified by ultra-performance liquid chromatography-electrospray ionisation tandem mass spectrometry (UPLC-ESI-MS/MS). An Acquity UPLC™ System (Waters, Milford, US), including a Binary solvent manager, sample manager, and 2996 PDA detector, combined with a Micromass Quattro micro™ API mass spectrometer (Waters MS Technologies, Manchester, UK), was used to analyze ABA and its metabolites. All data acquired were processed using the QuanLynx™ module within the MassLynx™ software

(version 4.1, Waters, Milford, US). Detailed UPLC-ESI-MS/MS conditions are described by Turečková *et al.* 2009.

2.17 Statistical analyses

Statistical analyses were performed using SAS or GraphPad Instat Software (one-way ANOVA or two-way repeated measures ANOVA with Tukey's post hoc test). Normality and homogeneity of variance were tested using the Shapiro-Wilk and Levene tests (Neter *et al.*, 1996). In order to meet the assumptions, data sets were transformed using log or square-root transformation. If assumptions were not met, a nonparametric Kruskal-Wallis test was performed followed by a Mann-Whitney test to perform a pairwise comparison.

2.18 Contributions

Most of the evaluations of stress parameters (see 2.16, except 2.16.6) were enabled by the collaboration with Dr. Dirk Hincha and Dr. Ellen Zuther (Max Planck Institute of Molecular Plant Physiology, Golm, DE). Plant material for the evaluation of stress parameters was grown in the greenhouse and growth chambers of the MPI Golm. Dr. Ellen Zuther introduced me in the methods of electrolyte leakage, proline and carbohydrate analyses. Extractions, measurements and calculations were conducted by myself.

The measurements of ABA and its metabolites were carried out in collaboration with Prof. Dr. Miroslav Strnad and Dr. Veronika Turečková (Laboratory of Growth Regulators, Palacký University & Institute of Experimental Botany AS CR, Olomouc, CZ). The plant growth, treatment and sampling as well as calculations were conducted by myself (see also 2.16.7).
Prof. Dr. Nicolaus von Wirén and Dr. Seyed Abdollah Hosseini (IPK Gatersleben, DE) performed drought recovery experiments similar to those performed in this study. They analyzed transcript levels of genes involved in ABA biosynthesis and selected ABA regulated transcription factors and performed ABA measurements after drought stress. These data are not shown in this study, but are mentioned in the discussion, since these data exactly confirm the results of this study.

3 RESULTS

3.1 *ERF102* to *ERF105* show a similar transcriptional regulation pattern

3.1.1 Hormonal transcriptional regulation of ERF102 *to* ERF105

In a microarray study, the four phylogenetically closely related genes *ERF102* to *ERF105* were identified to be rapidly upregulated by CK (Brenner *et al*., 2005). In this study, the *ERF102* to *ERF105* regulation by CK was retested using qRT-PCR. This analysis revealed that the steady state levels of the *ERF102*, *ERF103* and *ERF105* genes were rapidly upregulated by CK (BA) after 15 min about to 4-fold (*ERF102* and *ERF105*) or 12-fold (*ERF103*), but lowered at the later time point (2 h). The transcript level of *ERF105* was strongly reduced to 10 % of the initial level after 2 h. *ERF104* did not respond to CK treatment (Fig. 6A).

The regulation of the *ERF* genes by further hormones was tested: Treatment with the metabolic precursor of ET, ACC (1-aminocyclopropane-1-carboxylic acid), caused a reduction of the *ERF103* to *ERF105* transcript abundances to about 50 % of the initial levels after 2 h (Fig. 6B). JA (MeJa) induced only an about 2.5-fold *ERF105* expression after 2 h while all other genes did not respond to MeJa (Fig. 6C). In contrast, the steady state mRNA levels of all four *ERF* genes were strongly reduced by ABA treatment already at the early time point. 30 min of ABA treatment caused an about 80–90 % reduction of the transcript levels of *ERF102*, *ERF104* and *ERF105*. *ERF103* responded a bit slower, but the transcript levels of all four genes were still low after 2 h of treatment (Fig. 6D). Gibberellin (GA_3) provoked a rapid upregulation of *ERF105* of about 3.5-fold within 30 min (Fig. 6E). A similar result was obtained using a mixture of the biologically active metabolites GA_4 and GA_7, which provoked a rapid upregulation of *ERF104* and *ERF105* of about 4-fold and 3-fold, respectively, within 30 min (Fig. 6F). Auxin (NAA) rapidly and strongly induced the transcript abundances of all four *ERF* genes after 30 min about 180-fold (*ERF102*), 100-fold (*ERF103*), 13-fold (*ERF104*) and 130-fold (*ERF105*) and reduced the transcript abundances at the later time point (2 h) (Fig. 6G). In contrast, the transcript levels of all four *ERF* genes were downregulated by SA to about 50 % of the initial level after 2 h (Fig. 6H). Brassinolide (24-epi-BL) reduced transcript levels of *ERF102*, *ERF103* and *ERF105* to about 60 % of the initial level and recovered after 2 h in the case of *ERF102* and *ERF105*. *ERF104* did not respond to brassinolide treatment (Fig. 6I).

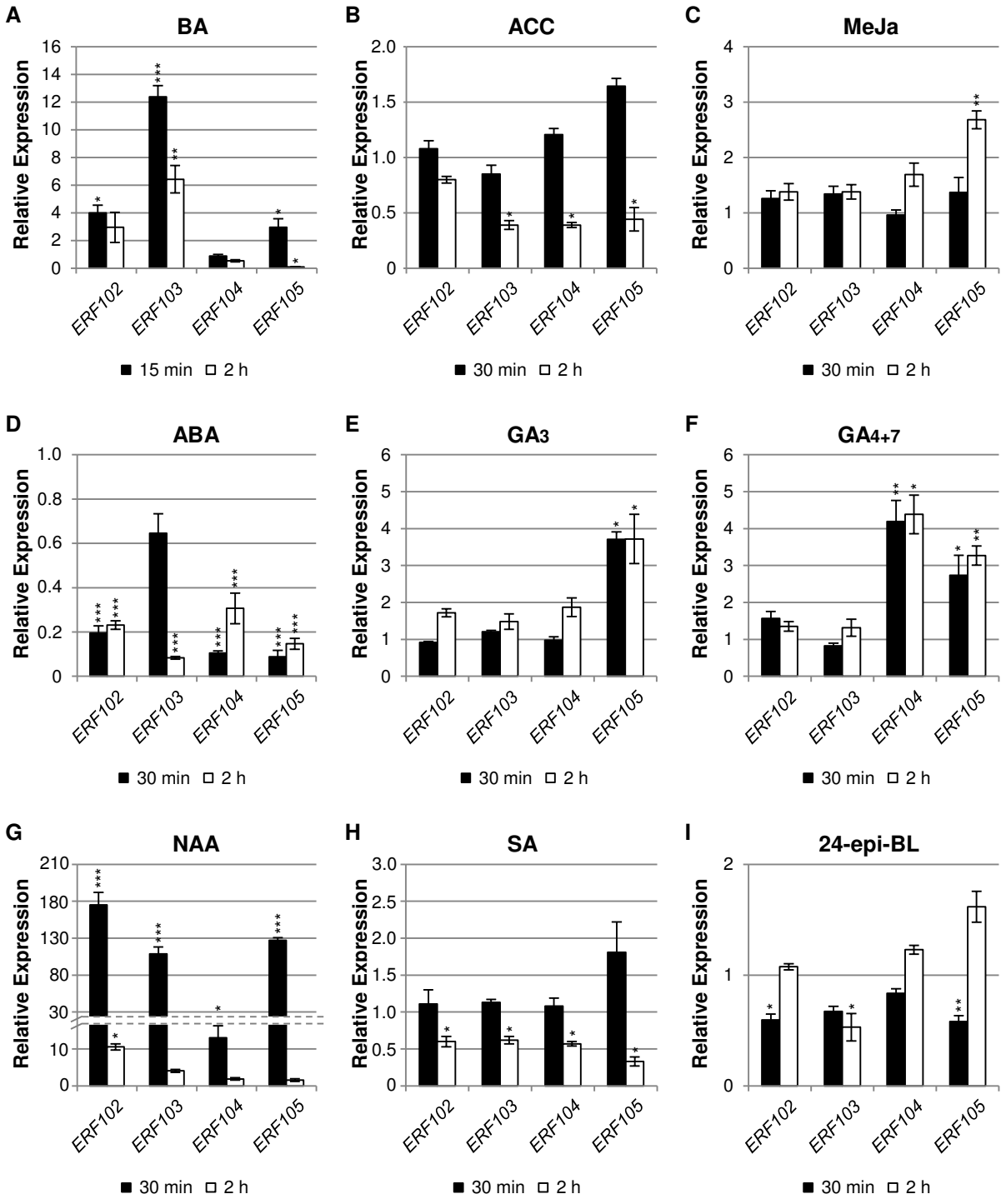

Figure 6. Hormonal regulation of the *ERF102* to *ERF105* genes. Relative expression of *ERF102* to *ERF105* in eleven-day-old wild-type seedlings (eight pooled seedlings per sample) after hormone treatment. **(A)** Cytokinin (1 µM BA), **(B)** ethylene (50 µM ACC), **(C)** jasmonate (100 µM MeJa), **(D)** abscisic acid (10 µM ABA), **(E)** gibberellin (100 µM GA_3), **(F)** gibberellin (10 µM GA_{4+7}; GA_4:GA_7=65:35), **(G)** auxin (10 µM NAA), **(H)** salicylic acid (10 mM SA), **(I)** brassinolide (0.1 µM 24-epi-BL). Transcript levels of wild-type samples under control conditions were set to 1 ($n \geq 4$). Asterisks indicate significant differences to the respective mock treatment (*, $p < 0.05$; **, $p < 0.01$; ***, $p < 0.001$). Error bars represent SE.

Taken together, the four *ERF* genes showed individual response profiles to hormonal treatment, but the majority shared significant aspects such as the rapid induction by CK or auxin and a rapid or slow downregulation by ABA and ET, respectively.

3.1.2 Stress-induced transcriptional regulation of ERF102 *to* ERF105

In order to get more information about the transcriptional regulation of *ERF102* to *ERF105*, stress treatments were performed. During cold stress, the transcript levels of all four *ERF* genes were significantly upregulated, all reaching their highest expression level after about 1 h and being gradually reduced thereafter. *ERF105* showed the fastest and strongest response of these genes. It was significantly upregulated about 3-fold as early as 15 min after the beginning of the cold treatment, was induced 14-fold after 1 h and was back to the initial level after 24 h (Fig. 7A). *ERF103* showed the weakest response with an about 2.5-fold increase of its transcript level after 1 h to 4 h of cold treatment. Heat stress induced an upregulation of *ERF104* and *ERF105* of about 5-fold and 8-fold, respectively, after 2 h (Fig. 7B). High light provoked a rapid upregulation of all four genes about 4-fold (*ERF102*), 3-fold (*ERF103*), 3-fold (*ERF104*) and 4.5-fold (*ERF105*) after 30 min and reduced the transcript abundances back to the initial level at the later time point (2 h) (Fig. 7C). Oxidative stress imposed by H_2O_2 treatment resulted in a rapid upregulation of all four genes after 15 min about 3.5-fold (*ERF102*), 4.5-fold (*ERF103*), 6.5-fold (*ERF104*) and 8.5-fold (*ERF105*). After 2 h transcript levels increased further to about 5-fold (*ERF102*), 9-fold (*ERF103*), 10-fold (*ERF104*) and 12-fold (*ERF105*) compared to the initial level (Fig. 7D). Oxidative stress imposed by treatment with the superoxide-generating herbicide paraquat showed a similar result (data not shown). A fast transcriptional response of the *ERF* genes could also been observed after drought stress that led to an about 2-fold (*ERF102*), 3.5-fold (*ERF103*), 2-fold (*ERF104*) and 5.5-fold (*ERF105*) upregulation within 15 min, respectively. Transcript levels of *ERF102* and *ERF105* lowered at the later time point (1 h) to 2-fold and 3.5-fold, while *ERF103* and *ERF104* transcript levels were back to the initial levels (Fig. 7E). Salt stress was imposed by application of NaCl leading to a rapid upregulation of *ERF* genes of about 7-fold (*ERF102* and *ERF103*), 2-fold (*ERF104*) and 6-fold (*ERF105*) after 30 min and reduced the transcript abundances at the later time point (2 h) (Fig. 7F). *ERF* genes also responded rapidly to mannitol application. After 15 min, *ERF102* and *ERF105* transcript levels were increased 3-fold and 3.5-fold, respectively, and were lowered after 2 h. *ERF103* and *ERF104* did not respond to mannitol (Fig. 7G).

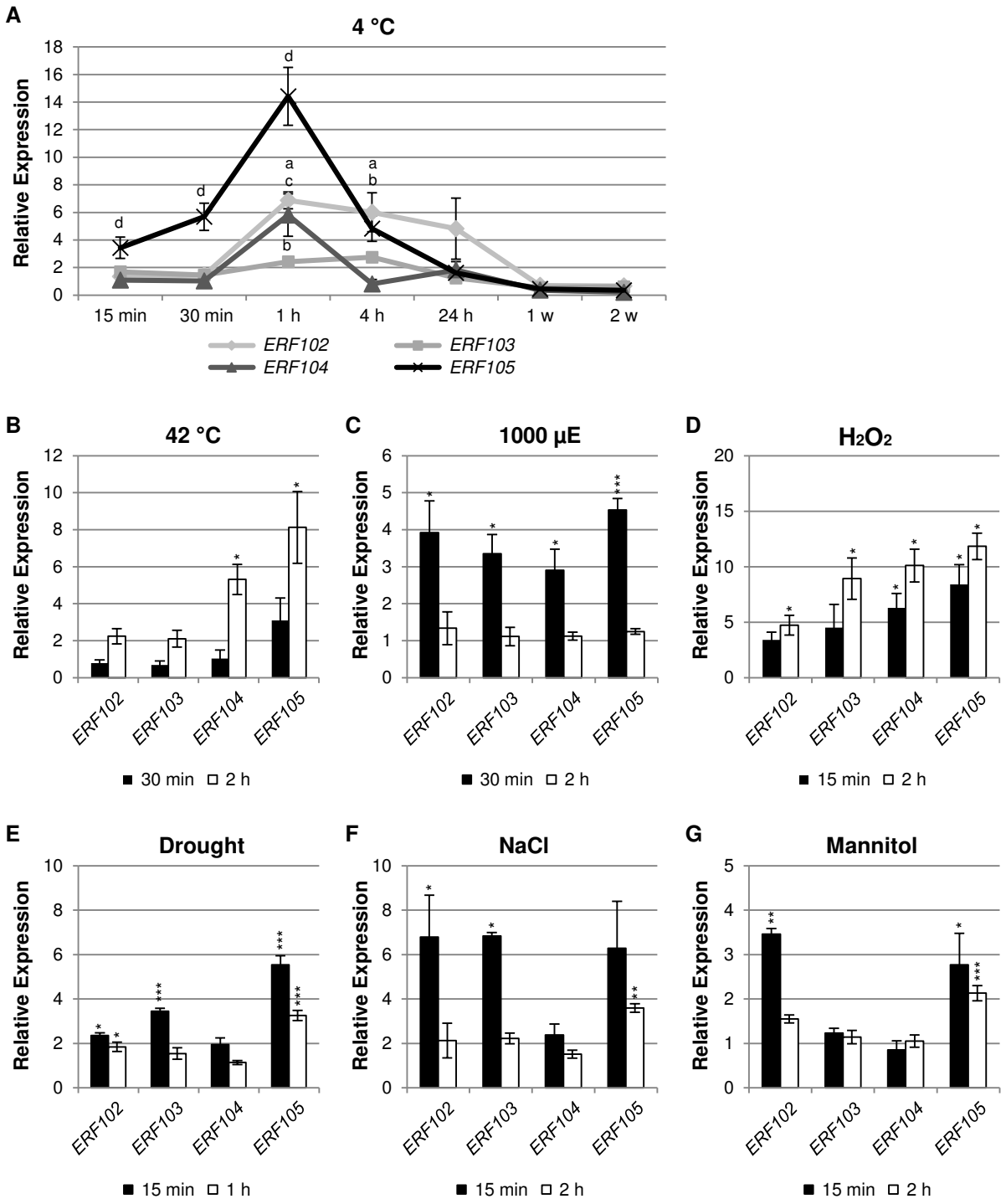

Figure 7. Stress-induced regulation of the *ERF102* to *ERF105* genes. (A) Time course of expression levels of *ERF102* to *ERF105* in four-week-old leaves (pooled leaves five, six and seven) after cold treatment at 4 °C. **(B–G)** Relative expression of *ERF102* to *ERF105* in eleven-day-old wild-type seedlings (eight pooled seedlings per sample) after stress treatment. **(B)** heat (42 °C), **(C)** high light (1000 µE), **(D)** oxidative stress (500 mM H_2O_2), **(E)** drought, **(F)** salt (200 mM NaCl), and **(G)** osmotic stress (200 mM mannitol). Transcript levels of wild-type samples under control conditions were set to 1 ($n \geq 4$). Letters in (A) indicate significant differences ($p < 0.01$) to the respective control (time point zero) (a = *ERF102*, b = *ERF103*, c = *ERF104*, d = *ERF105*). Asterisks indicate significant differences to the respective mock treatment in (B–G) (*, $p < 0.05$; **, $p < 0.01$; ***, $p < 0.001$). Error bars represent SE.

Taken together, the four *ERF* genes showed, on the one hand, similar response profiles to stress treatment, for instance, the rapid and transient regulation by cold or the rapid

upregulation by high light or H_2O_2. On the other hand, the four *ERF102* to *ERF105* showed individual response profiles. Thus, not all four *ERF* genes were transcriptionally regulated by heat, drought, NaCl, or mannitol.

3.2 *ERF102:GUS* to *ERF105:GUS* reporter genes are expressed in different tissues in *Arabidopsis thaliana*

Transgenic plants expressing the *GUS* reporter gene under the control of ~2 kb of the *ERF102* to *ERF105* promoters upstream of the coding regions were analyzed to determine the tissue-specific expression of these *ERF102:GUS* to *ERF105:GUS* reporter genes.

30 h after imbibition, strong GUS activity of *ERF102:GUS* plants was detected in the radicle-to-hypocotyl transition zone of germinated seeds (Fig. 8A) and expanded within the next 30 h within the radicle (Fig. 8B). Ten days after germination, *ERF102:GUS* was expressed in all root tissues except root tips and root hairs. The highest GUS activity was observed in the primary root, particularly in the vascular bundle and in cortex cells that surround emerging lateral roots (Fig. 8C–E). A weak GUS signal was detected in the shoot apical meristem (SAM) (Fig. 8F).

As plants matured, GUS activity was evident in the same tissues as in young seedlings but declined (data not shown). *ERF102:GUS* expression was not detected in cotyledons, leaves, shoot, reproductive organs, mature green, dry or imbibed seeds.

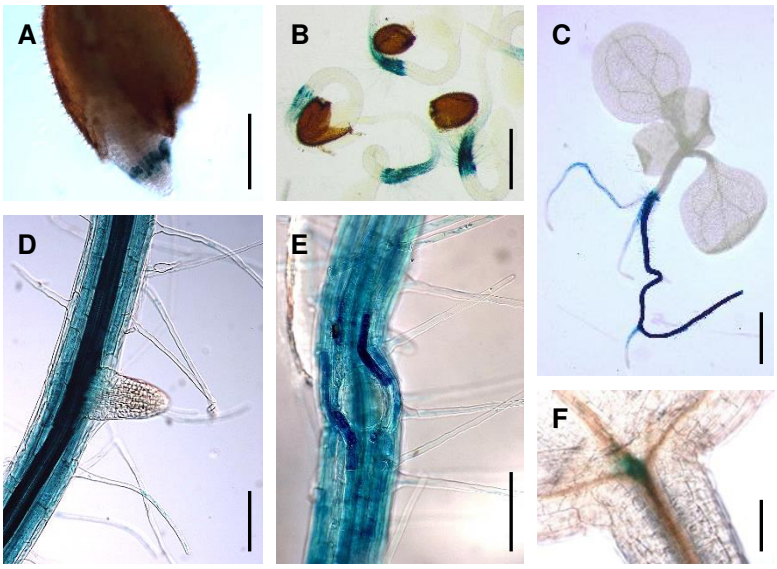

Figure 8. Tissue-specific expression of an *ERF102* driven reporter gene. Histochemical localization of GUS activity in *ERF102:GUS Arabidopsis* seedlings 30 h **(A)** and 60 h **(B)** after imbibition and ten days after germination **(C–F)**. **(A)** and **(B)** germinating seeds, **(C)** whole seedling, **(D)** and **(E)** primary root with emerging lateral roots, and **(F)** shoot apical meristem. Scale bars = 100 µm in (A), (D), (E); 400 µm in (B); 1 mm in (C); 50 µm in (F).

ERF103:GUS activity is shown in Figure 9: 60 h after imbibition, strong GUS activity was detected in the radicle tip (Fig. 9A). Seven days after germination, *ERF103:GUS* was expressed in the meristematic zone of primary root tips with a very high activity in the root apical meristem (RAM) (Fig. 9B and E). *ERF103:GUS* was also expressed in the root tip of lateral roots, but only after stage VIII of lateral root development (Péret *et al.*, 2009) (Fig. 9F and G). Further GUS activity was observed in the vasculature of primary roots (Fig. 9D), but not in the vasculature of lateral roots, in cortex cells that surround emerging lateral roots (Fig. 9F) as well as a weak expression in the SAM (Fig. 9C).

GUS activity in matured plants was evident in the same tissues as in young seedlings but declined (data not shown). *ERF103:GUS* expression was not detected in cotyledons, leaves, shoot, reproductive organs, mature green, dry or imbibed seeds.

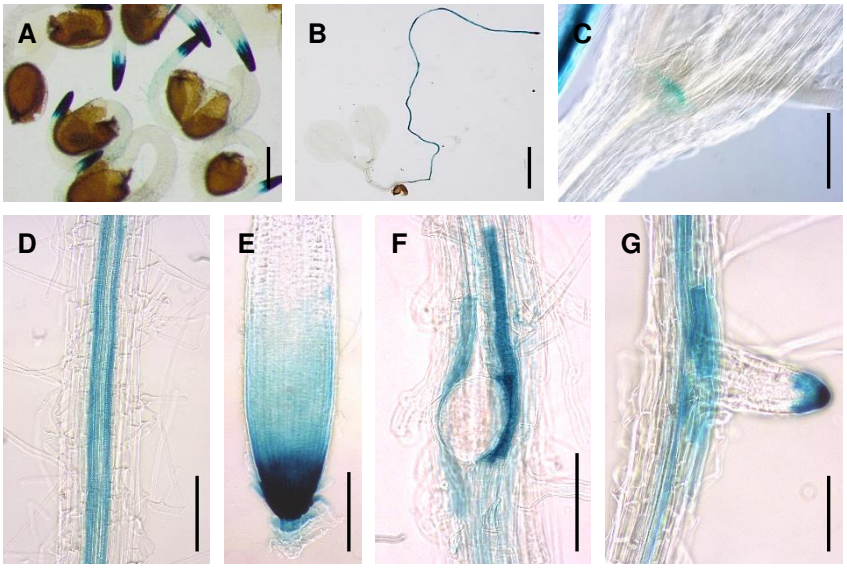

Figure 9. Tissue-specific expression of an *ERF103* driven reporter gene. Histochemical localization of GUS activity in *ERF103:GUS Arabidopsis* seedlings 60 h after imbibition **(A)** and seven days after germination **(B–G)**. **(A)** Germinating seeds, **(B)** whole seedling, **(C)** shoot apical meristem, **(D)** primary root, **(E)** primary root tip, **(F)** and **(G)** primary root with emerging lateral roots. Scale bars = 200 µm in (A); 2 mm in (B); 100 µm in (C–G).

The *ERF104:GUS* expression analysis in Figure 10 clearly shows that *ERF104:GUS* was also detected early after germination. 60 h after imbibition, *ERF104:GUS* was weakly expressed in the vasculature of hypocotyls and cotyledons and slightly higher in the vasculature of radicles (Fig. 10A). Older (seven-day-old) seedlings also showed GUS activity in the vascular tissues as well as in the SAM and in the quiescent center of roots (Fig. 10B–F).

As plants matured, GUS activity was present in the same tissues as in seedlings but declined (data not shown). In addition, GUS activity was present in the base of siliques and in the apex of siliques (Fig. 10G and H). *ERF104:GUS* was not expressed in the shoot, mature green, dry or imbibed seeds.

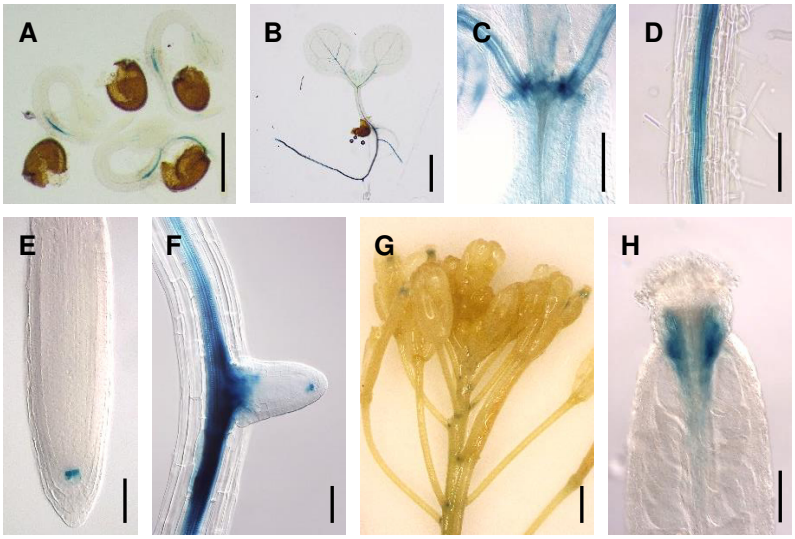

Figure 10. Tissue-specific expression of an *ERF104* driven reporter gene. Histochemical localization of GUS activity in *ERF104:GUS Arabidopsis* seedlings 60 h after imbibition **(A)**, seven days **(B–F)** and 21 days after germination **(G and H)**. **(A)** Germinating seeds, **(B)** whole seedling, **(C)** shoot apical meristem, **(D)** primary root, **(E)** primary root tip, **(F)** primary root tip with emerging lateral root, **(G)** floral stem, and **(F)** apex of a silique. Scale bars = 400 µm in (A); 2 mm (B) and (G); 100 µm in (C), (D) and (H); 50 µm in (E) and (F).

The *ERF105:GUS* expression was detected 60 h after imbibition in the radicle and in the root-to-hypocotyl transition zone of young seedlings (Fig. 11A). At a later developmental stage (seven days after germination) *ERF105:GUS* was expressed in the SAM, in the guard cells and vascular tissue of the hypocotyl, cotyledons and primary leaves as well as in the vascular tissue of roots, in cortex cells that surround emerging lateral roots and in the root apical meristem (Fig. 11A–G). A similar pattern but weaker expression was observed in the fully developed leaves and adult roots (data not shown). Moreover, GUS activity was evident in the shoot (Fig. 11H). During reproductive development, *ERF105:GUS* expression was detected in the pedicles of inflorescences and in the base of siliques (Fig. 11H). *ERF105:GUS* was not expressed in mature green, dry or imbibed seeds.

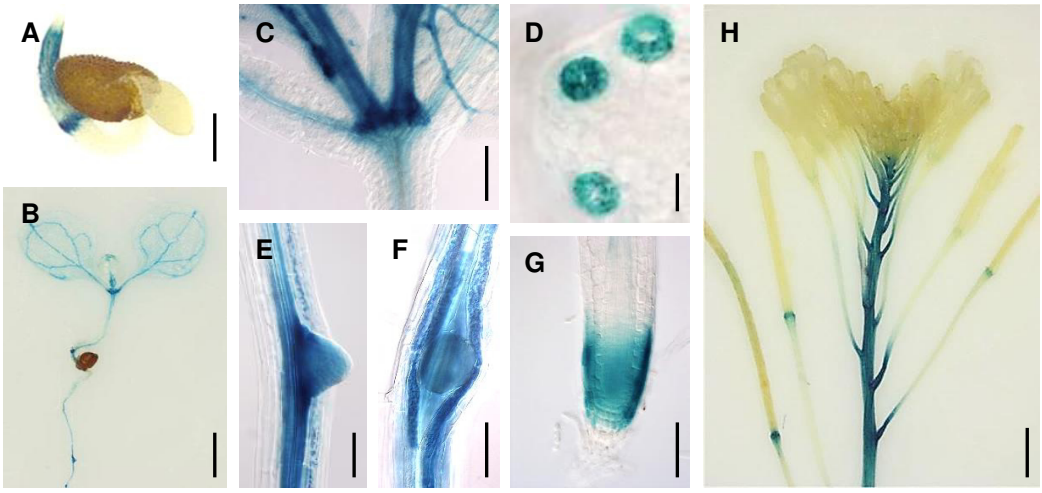

Figure 11. Tissue-specific expression of an *ERF105* driven reporter gene.

Figure 11. Continued. Histochemical localization of GUS activity in *ERF105:GUS Arabidopsis* seedlings 60 h after imbibition **(A)**, seven days **(B–F)** and 21 days after germination **(G)**. **(A)** Germinating seed, **(B)** whole seedling, **(C)** apical shoot, **(D)** stomata of cotyledons, **(E and F)** lateral root, **(G)** primary root tip, **(H)** floral stem and the basis of pedicels during the reproductive stage. Scale bars = 200 µm in (A); 1 mm in (B); 100 µm in (C), (E), (F); 10 µm in (D); 3 mm in (G).

Collectively, *ERF102:GUS* to *ERF105:GUS* showed partly similar expression patterns. All four *ERF* driven reporter genes were expressed shortly after germination, after endosperm rupture respectively. Strong expressions were observed in seedlings, particularly in roots, and became weaker in the course of development, indicating that *ERF102* to *ERF105* expression is under developmental control. However, *ERF102:GUS* to *ERF105:GUS* demonstrated distinct expression patterns suggesting a functional diversity of *ERF102* to *ERF105.* Thus, the observed expressions of *ERF102:GUS* to *ERF105:GUS* in roots, for instance, were restricted to different cell types.

3.3 ERF102-GFP to ERF105-GFP are located to the nucleus

To examine the subcellular localization of the ERF102 to ERF105 proteins, full-length cDNAs of *ERF102* to *ERF105* were fused in frame to the 3' end of the *GREEN FLUORESCENT PROTEIN* (*GFP*) coding sequence. The resulting *GFP-ERF102*, *GFP-ERF103*, *GFP-ERF104* and *GFP-ERF105* fusion genes driven by the cauliflower mosaic virus (CaMV) *35S* promoter were transiently expressed in *Nicotiana benthamiana* leaf cells. Confocal imaging of GFP fluorescence in leaf cells of tobacco plants showed that the GFP-ERF102 to GFP-ERF105 fusion proteins were located in the cytosol and predominantly located to the nucleus (Fig. 12).

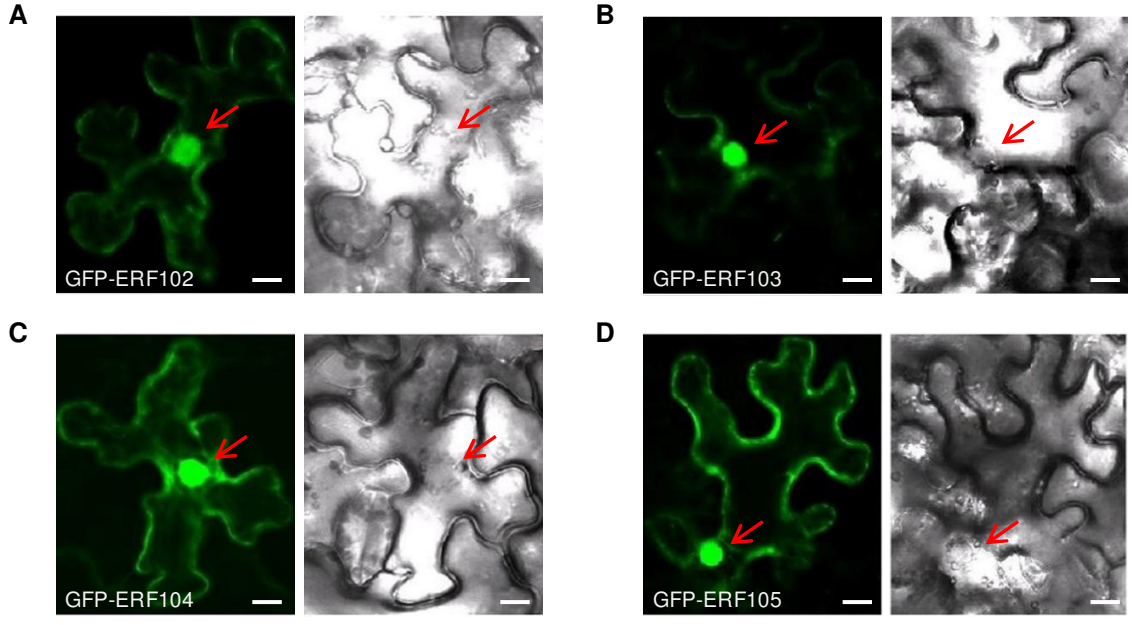

Figure 12. Subcellular localization of GFP-ERF102 to GFP-ERF105 fusion proteins.

Figure 12. Continued. Transient expression of **(A)** *35S:GFP-ERF102,* **(B)** *35S:GFP-ERF103,* **(C)** *35S:GFP-ERF104*, and **(D)** *35S:GFP-ERF105* in leaf epidermis cells of *N. benthamiana* was analyzed by confocal laser scanning microscopy. Left, fluorescence of GFP; right, bright field picture. The red arrows indicate the nucleus. Scale bars = 10 µm.

ERF102 to *ERF105* fusion to the 5' end of the *GFP* coding sequence did not change the nuclear localization of the studied proteins (data not shown).

3.4 Analysis of protein interactions of the ERF102 to ERF105 proteins

3.4.1 Formation of ERF102 to ERF105 dimers in yeast

The majority of proteins interact with other proteins for proper biological activity. As a prelude to examining protein interactions of ERF102 to ERF105, full-length cDNAs for each *ERF* gene were successfully cloned into the yeast two-hybrid (Y2H) bait and prey vectors and first tested for autoactivation. All four ERF proteins showed autoactivating activity in the bait vector that could be inhibited with 2 mM 3-amino-1,2,4-triazole (3-AT). ERF proteins cloned into the prey vector did not show autoactivation (Fig. 13). To examine the possibility of the ERF proteins to form homo- or heterodimers, each possible bait–prey combination was tested at least twice. Interactions were tested using two different reporter genes (*HIS* and *URA*) and growth was evaluated using several dilution steps to reduce the number of false positive interactions. Using this approach, 16 interactions were tested. Of these, ten interactions were positively detected with four of them showing the capability of ERF102 to ERF105 to interact with themselves (Fig. 13). The other six interactions showed the capability of ERF102 to ERF105 to form heterodimers. Formation of heterodimers was tested in both directions, in the bait–prey and in the prey–bait direction. The following heterodimer interaction pairs were identified: ERF102/ERF103, ERF103/ERF102, ERF104/ERF102, ERF104/ERF105, ERF105/ERF102, and ERF105/ERF104. Two heterodimerization tests took place only in one direction (protein interaction between ERF104 and ERF102 as well as interaction between ERF105 and ERF102), whereas two took place in both directions (protein interactions between ERF102 and ERF103 as well as ERF104 and ERF105). A protein interaction between ERF103 and ERF105 could not be detected, neither in the bait–prey nor in the prey–bait direction.

Because the Y2H system tend to produce false-positive interactions (Sprinzak *et al.*, 2003), the interaction data presented in Figure 13 need to be validated by other methods.

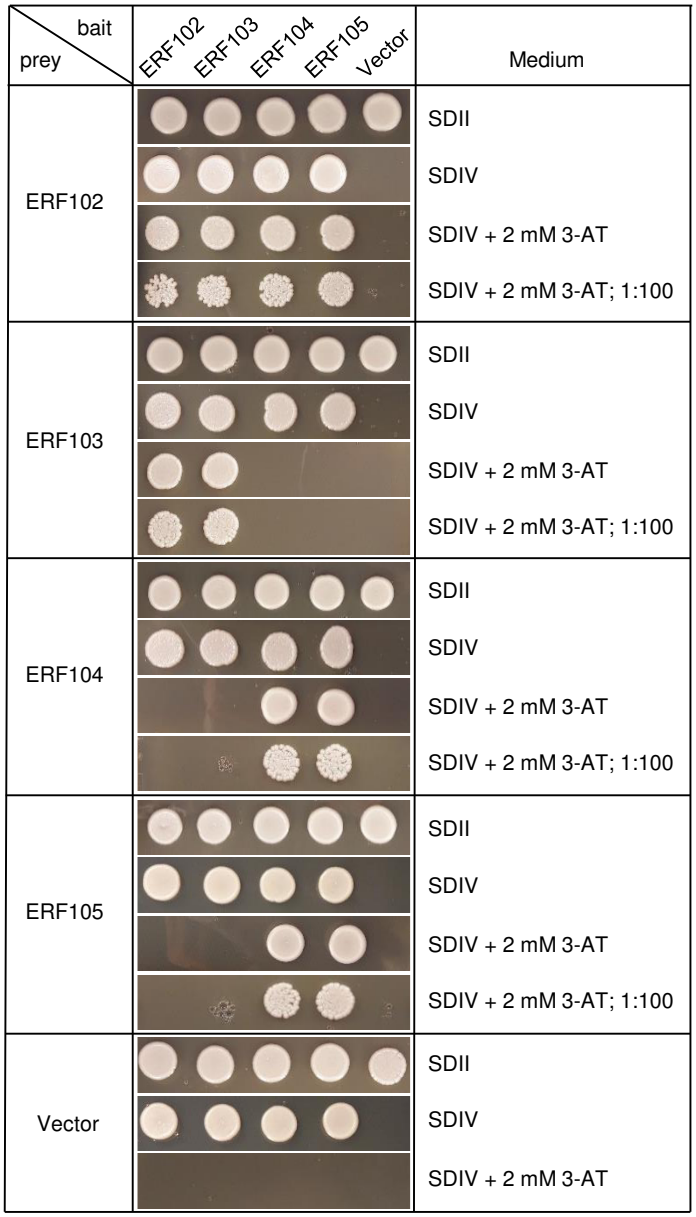

Figure 13. Formation of ERF102 to ERF105 dimers in yeast. Yeast two-hybrid analysis on the ERF102 to ERF105 proteins to examine the formation of homo- or heterodimers. A cell suspension with an OD_{600} of 1.0 was prepared for each clone. 10 µl of each cell suspension was transferred to SDII control (+His, +Ura, -Leu, -Trp) and SDIV interaction (-His, -Ura, -Leu, -Trp) media supplemented with 2 mM 3-AT to inhibit autoactivation. In addition, a 1:100 dilution of each cell suspension was prepared and transferred to SDIV with 2 mM 3-AT interaction medium.

3.4.2 Interaction of ERF102 to ERF105 with MPK6

A previous study has shown that MPK6 interact with and phosphorylates ERF104 to control defense responses (Bethke *et al*., 2009). Thus, the question arose whether MPK6 interacts also with ERF102, ERF103 and ERF105. Therefore, *MPK6* cDNA was cloned into the Y2H bait and prey vectors. Firstly, autoactivation was analyzed. MPK6 showed strong autoactivating activity in the bait configuration and therefore could not be used as bait. Hence, MPK6 was used in the prey configuration. Different 3-AT concentrations were used to inhibit the autoactivation of the ERF proteins in the bait configuration on the one hand, and to examine the strength of interaction on the other hand. Interactions were detected between MPK6 and ERF104, which was tested again as positive control, as well as between MPK6 and the other three ERF proteins. Moreover, interactions between MPK6 and the ERF proteins were strong, since high concentrations of up to 10 mM 3-AT were not able to inhibit

those interactions (Fig. 14). Since it has been shown that ERF102 and ERF103 are phosphorylated by MPK6 (Son *et al*., 2012; Meng *et al*., 2013; Wang *et al*., 2013), only the interaction between MPK6 and ERF105 and the phosphorylation of ERF105 by MPK6, respectively, need to be validated.

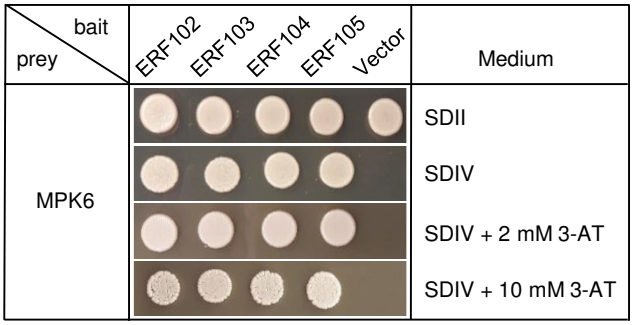

Figure 14. Protein-protein interactions of ERF102 to ERF105 with MPK6 in yeast. Yeast two-hybrid analysis on the ERF102 to ERF105 proteins to examine the protein-protein interaction with MPK6. A cell suspension with an OD_{600} of 1.0 was prepared for each clone. 10 µl of each cell suspension was transferred to SDII control (+His, +Ura, -Leu, -Trp) and SDIV interaction (-His, -Ura, -Leu, -Trp) media supplemented with different 3-AT concentrations to inhibit autoactivation and to show the strength of interaction.

3.5 Generation and phenotypical analysis of plant development of loss-of-function, gain-of-function and complementation lines of *ERF102* to *ERF105*

3.5.1 Generation and verification of lines with a reduced or increased ERF102 *to* ERF105 *gene expression*

A widely-used approach to get insights into possible functions of a protein is the examination of plant lines in which the respective gene is knocked out/down or overexpressed. Therefore, to study the biological function of *ERF102* to *ERF105*, two homozygous T-DNA insertion lines (*erf102*; SAIL_46_C02 and *erf105*; GABI_680C11) were obtained. Lines with a reduced *ERF103* or *ERF104* as well as lines with reduced *ERF104* and *ERF105* expression were constructed (2.11.4) using the technique of artificial microRNA (amiRNA) (Schwab *et al*. 2006). Moreover, lines overexpressing *ERF102* to *ERF105* under control of the CaMV *35S* promoter were constructed (2.11.2).

Verification of the annotated locations of the T-DNA insertions in *erf102* and *erf105* by sequencing revealed that the T-DNAs are located at position +507 (*erf102*) and +356 (*erf105*), both within the AP2/ERF domain (Fig. 15A and C). RT-PCR analyses did not detect any expression of *ERF102* in *erf102* or *ERF105* in *erf105* plants, suggesting that these are nullalleles (Fig. 15B and D). Two independent homozygous lines of generated amiRNA and overexpressing lines with the lowest expression and strongest overexpression, respectively, were selected for further experiments. The expression levels of selected lines are shown in Figure 15: Plants with reduced *ERF103* expression showed a reduced expression to approximately 40 % or 25 % of the wild-type level (Fig. 15E). Plants with reduced *ERF104* expression showed a reduced expression to about 50 % or 30 % of the wild-type level (Fig. 15F). *ERF104* and *ERF105* expressions are downregulated in lines expressing

*35S:*amiERF104/105, in *35S:*amiERF104/105-1 to approximately 30 % (*ERF104*) and 30 % (*ERF105*) and in *35S:*amiERF104/105-2 to 40 % (*ERF104*) and 60 % (*ERF105*) of the wild-type level (Fig. 15G). Plants overexpressing *ERF102* exhibited a 66-fold or 380-fold increase of *ERF102* expression compared to wild-type level (Fig. 15H). ERF103ox-1 and ERF103ox-2 exhibited an about 200-fold or 430-fold increase of *ERF103* expression compared to wild-type level (Fig. 15I). Plants overexpressing *ERF104* showed a 45-fold or 65-fold increase of *ERF104* expression (Fig. 15J), whereas ERF105ox-1 and ERF105ox-2 exhibited an about 15-fold or 22-fold increase of *ERF105* expression compared to wild-type level (Fig. 15K).

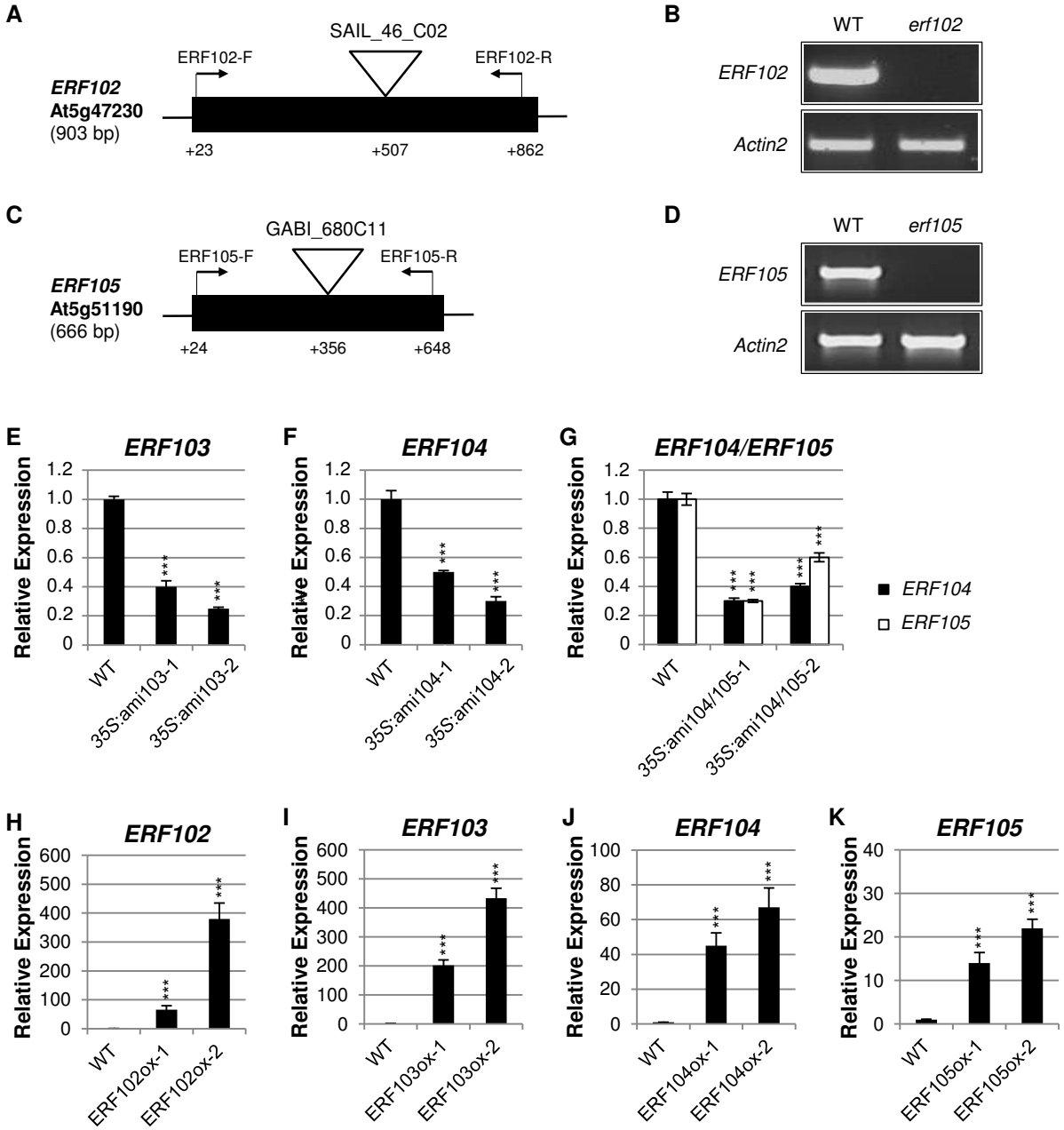

Figure 15. Verification of lines with a reduced or increased *ERF102* to *ERF105* gene expression.

Figure 15. Continued. (A and C) Description of the *ERF102* and *ERF105* genes and the *erf102* and *erf105* insertional mutants. Structure of the *Arabidopsis ERF102* (AT5G47230) and *ERF105* (AT5G51190) genes. Black lines denote the untranslated regions, the black boxes represent the exons, the T-DNA insertions at position +507 and +356 are shown by a triangle. The positions of primers (F = forward; R = reverse) that were used for RT-PCR are indicated by arrows. **(B and D)** RT-PCR analyses of *ERF102* and *ERF105* expression using total RNA extracted from seedlings of wild type, *erf102* and *erf105*. The *Actin2* gene was used as internal control. **(E–K)** Relative expression of *ERF102* to *ERF105* in eight pooled eleven-day-old seedlings of wild type, amiRNA and overexpressing lines of *ERF102* to *ERF105*. Transcript levels of wild-type samples were set to 1 ($n \geq 4$). Asterisks indicate significant differences to the wild type (***, $p < 0.001$). Error bars represent SE.

Double mutants with reduced expression of *ERF* genes – namely *erf102,35S:*amiERF103; *erf102,35S:*amiERF104; *35S:*amiERF103,*erf105* and *35S:*amiERF104/105 – were generated by crossing amiRNA lines with T-DNA insertion lines or in case of *erf104/105* by generating one amiRNA construct which has *ERF104* and *ERF105* as target. Reduced expression levels of the target genes were reconfirmed in the hybrids (data not shown).

3.5.2 Mutants and transgenic plants of ERF102 *to* ERF105 *genes have an altered phenotype*

Phenotypic analyses under long day conditions revealed that 35 days after germination the *erf102* mutant exhibited an about 10 % reduced shoot height compared to the wild type. Overexpressing lines of *ERF102* exhibited a slightly but not significantly increased shoot height as well as 10 % (ERF102ox-1) and 8 % (ERF102ox-2) bigger rosettes (Fig. 16A–C). There were no significant differences in fresh weight (Fig. 16D), number of adventitious shoots, side shoots, time of flowering, number of siliques on the main shoot, or senescence (data not shown) between *erf102*, *ERF102* overexpressing plants and wild type. The analysis of primary root elongation, which was determined between four and ten days after germination revealed no significant differences (Fig. 16E). However, *erf102* exhibited 27 % less lateral roots ten days after germination. In contrast, ERF102ox-1 and ERF102ox-2 exhibited 51 % and 48 %, respectively, more lateral roots compared to wild type (Fig. 16F). Complementation of *erf102* plants by introgression of the ERF102ox-1 allele restored wild-type expression levels of *ERF102*, and the complemented plants were phenotypically indistinguishable from wild type (Fig. 16A–F).

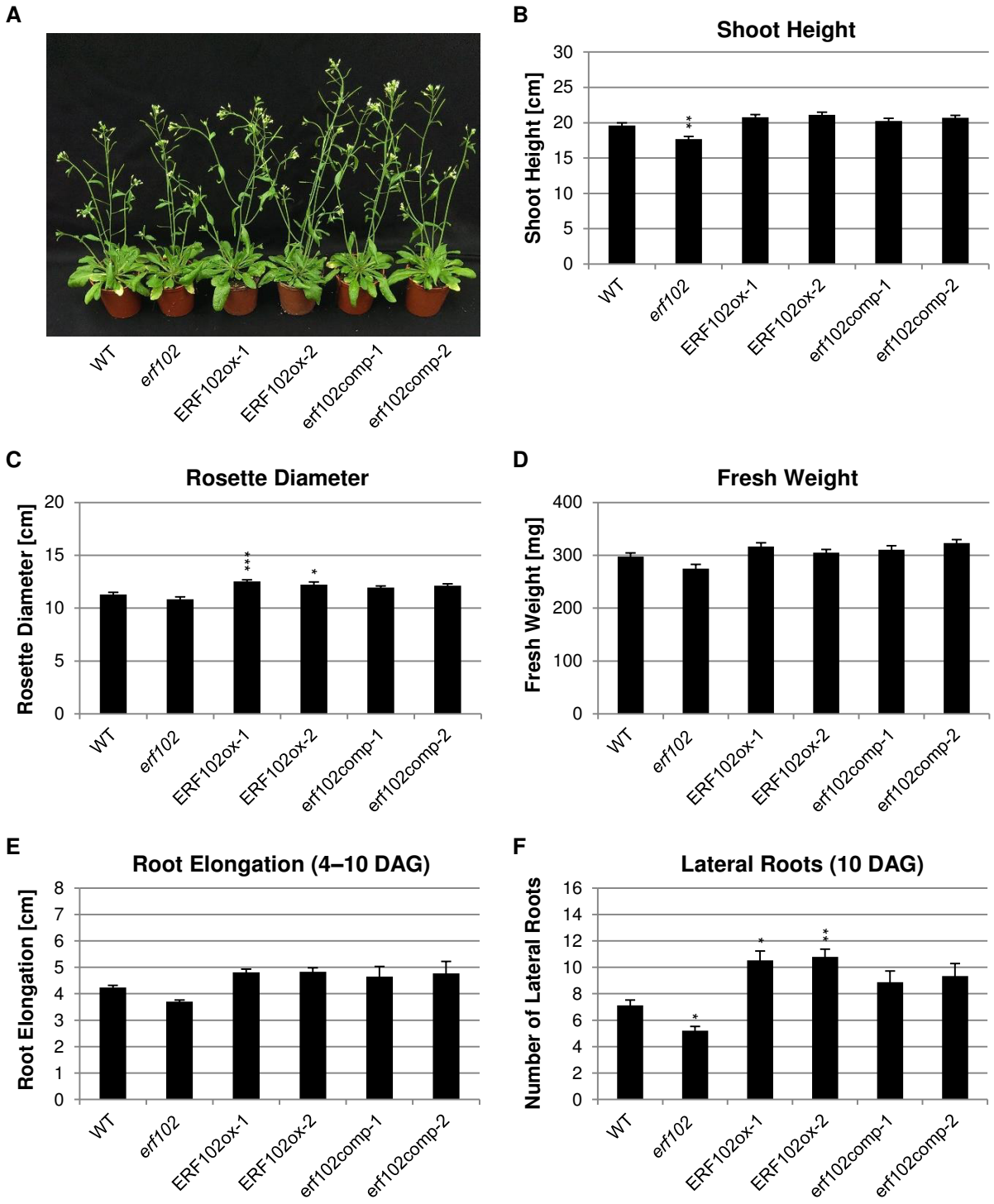

Figure 16. Characterization of lines with altered *ERF102* expression levels and complementation test of the *erf102* mutant. (A) Morphological phenotype of plants grown 35 days under long day conditions. Shoot height **(B)**, rosette diameter **(C)** and fresh weight **(D)** of 35-day-old plants. **(E and F)** Root growth analysis of ten-day-old plants grown on half-strength MS medium. **(E)** The elongation of the primary root was determined between four days and ten days after germination (4–10 DAG). **(F)** The number of lateral roots was determined ten days after germination (10 DAG). Asterisks indicate significant differences to the wild type ($n \geq 30$), (*, $p < 0.05$; **, $p < 0.01$; ***, $p < 0.001$). Error bars represent SE.

The *35S:*ami103 lines were smaller in size. Both *35S:*ami103 lines had an 8 % reduced shoot height and an about 9 % (*35S:*ami103-1) and 6 % (*35S:*ami103-2) reduced rosette size compared to the wild type. *ERF103* overexpression showed no phenotypic differences in shoot height and rosette size compared to wild type (Fig. 17A–D). There were no significant differences in fresh weight (Fig. 17D), number of adventitious shoots, side shoots, time of flowering, number of siliques on the main shoot or senescence between *35S:*ami103 lines, *ERF103* overexpressing plants and wild type (data not shown). Root growth analyses demonstrated that the primary root elongation was about 13 % lower in both *35S:*ami103 lines whereas ERF103ox-1 and ERF103ox-2 exhibited 12 % and 17 %, respectively, longer primary roots compared to wild type (Fig. 17E). Similar results were obtained regarding lateral root analyses. The *35S:*ami103-1 plants had 32 % less lateral roots than wild type. In contrast, ERF103ox-1 showed 31 % more lateral roots than wild type (Fig. 17F).

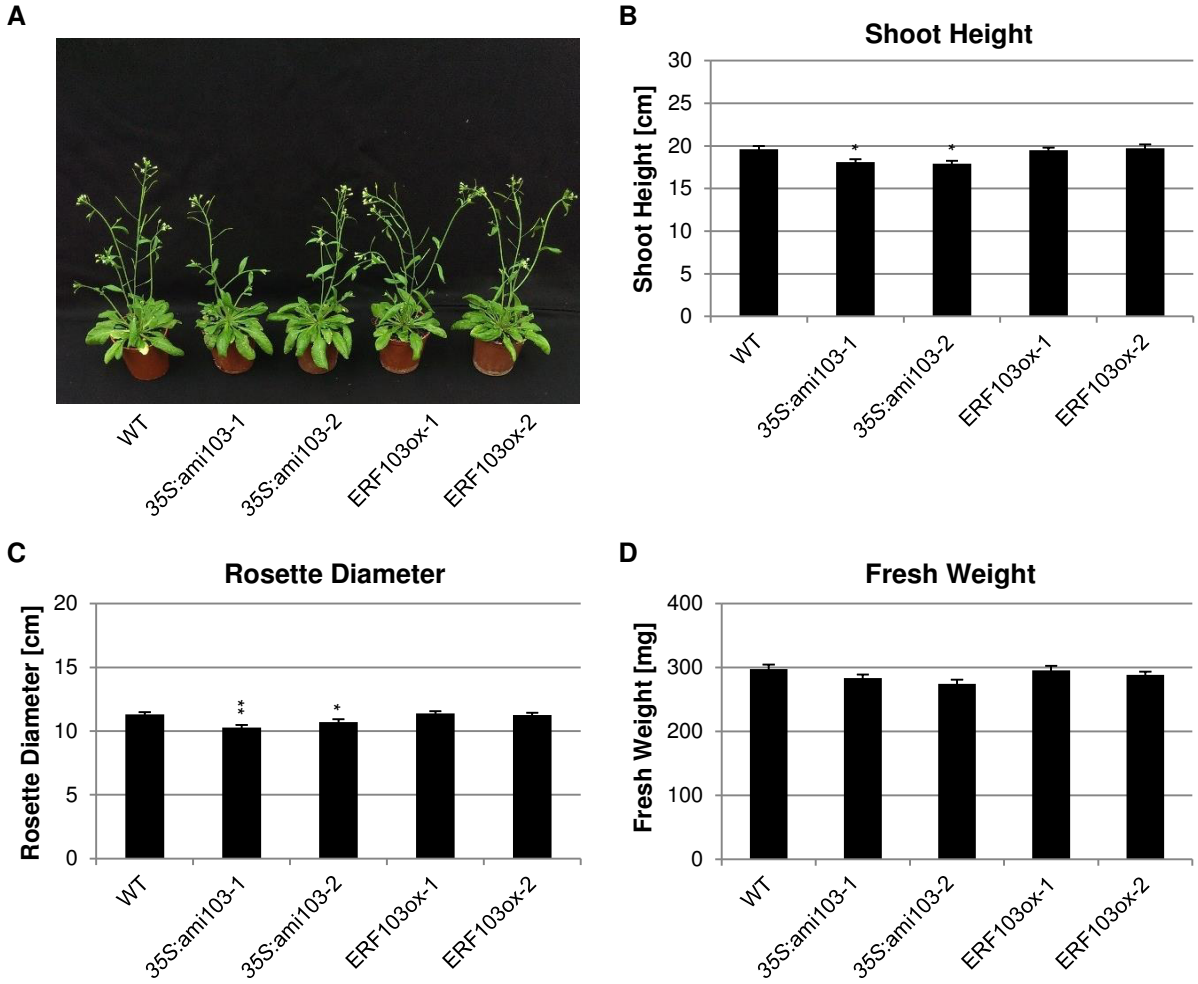

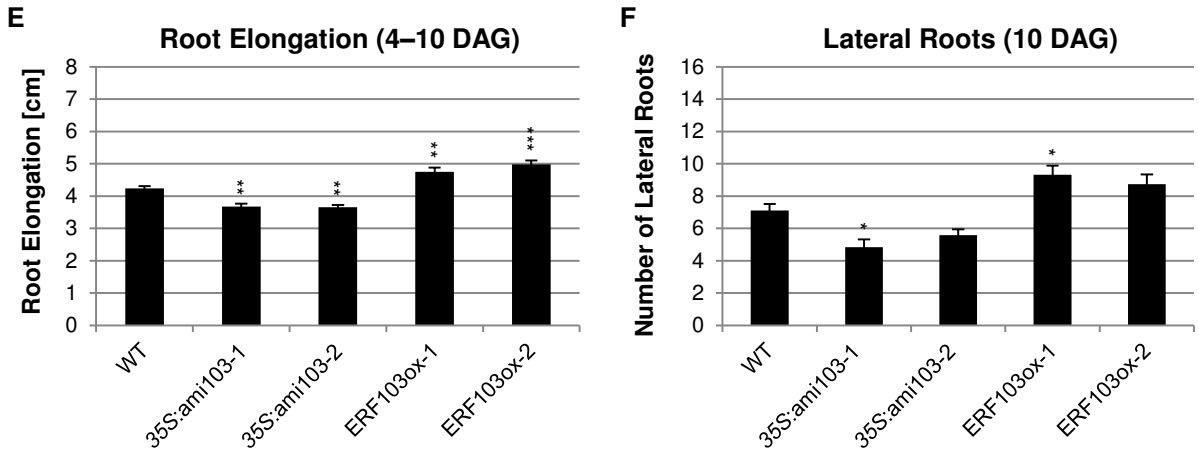

Figure 17. Characterization of lines with altered *ERF103* expression levels. (A) Morphological phenotype of plants grown 35 days under long day conditions. Shoot height **(B)**, rosette diameter **(C)** and fresh weight **(D)** of 35-day-old plants. **(E and F)** Root growth analysis of ten-day-old plants grown on half-strength MS medium. **(E)** The elongation of the primary root was determined between four days and ten days after germination (4–10 DAG). **(F)** The number of lateral roots was determined ten days after germination (10 DAG). Asterisks indicate significant differences to the wild type ($n \geq 30$), (*, $p < 0.05$; **, $p < 0.01$; ***, $p < 0.001$). Error bars represent SE.

The phenotypic analysis of *35S:*ami104 lines demonstrated a 9 % (*35S:*ami104-1) and 18 % (*35S:*ami104-2) reduced shoot height as well as a 12 % (*35S:*ami104-1) and 18 % (*35S:*ami104-2) reduced fresh weight (Fig. 18A, B and D). *ERF104* overexpressing plants did not show an altered shoot height or fresh weight compared to wild type (Fig. 18A, B and D). Rosette diameter (Fig. 18C), number of adventitious shoots, side shoots, time of flowering, number of siliques on the main shoot or senescence of *35S:*ami104 lines and *ERF104* overexpressing plants were phenotypically indistinguishable from wild type (data not shown). Primary roots of both *35S:*ami104 lines were about 13 % shorter, although the reduction was only for *35S:*ami104-2 significant. Primary roots of *ERF104* overexpressing lines were 22 % (ERF104ox-1) and 29 % (ERF104ox-2) longer than wild-type roots (Fig. 18E). The number of lateral roots were reduced to 20 % in both *35S:*ami104 lines. ERF104ox-1 and ERF104ox-2 exhibited 57 % and 53 %, respectively, more lateral roots compared to wild type (Fig. 18F).

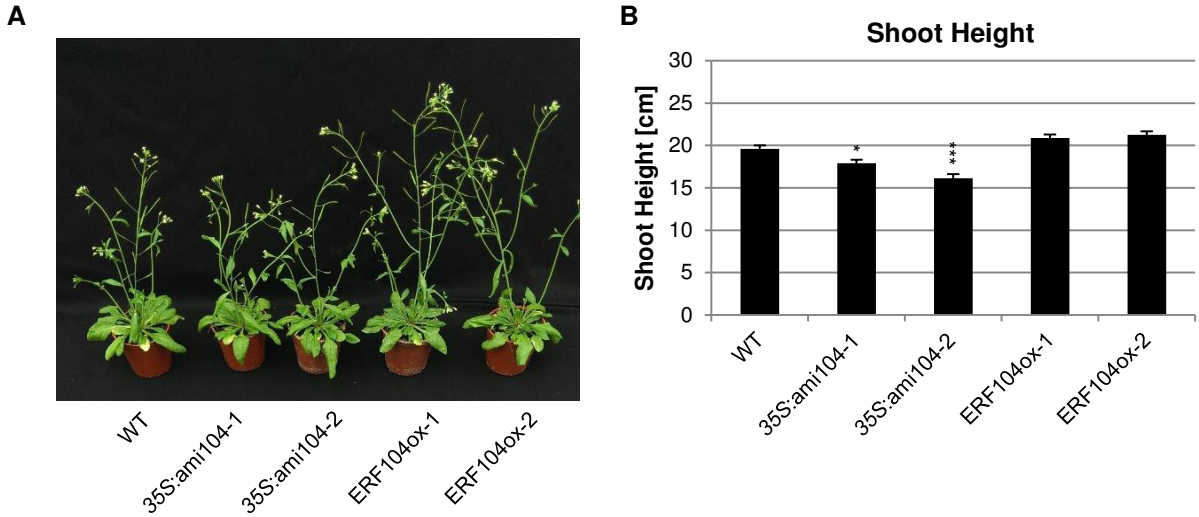

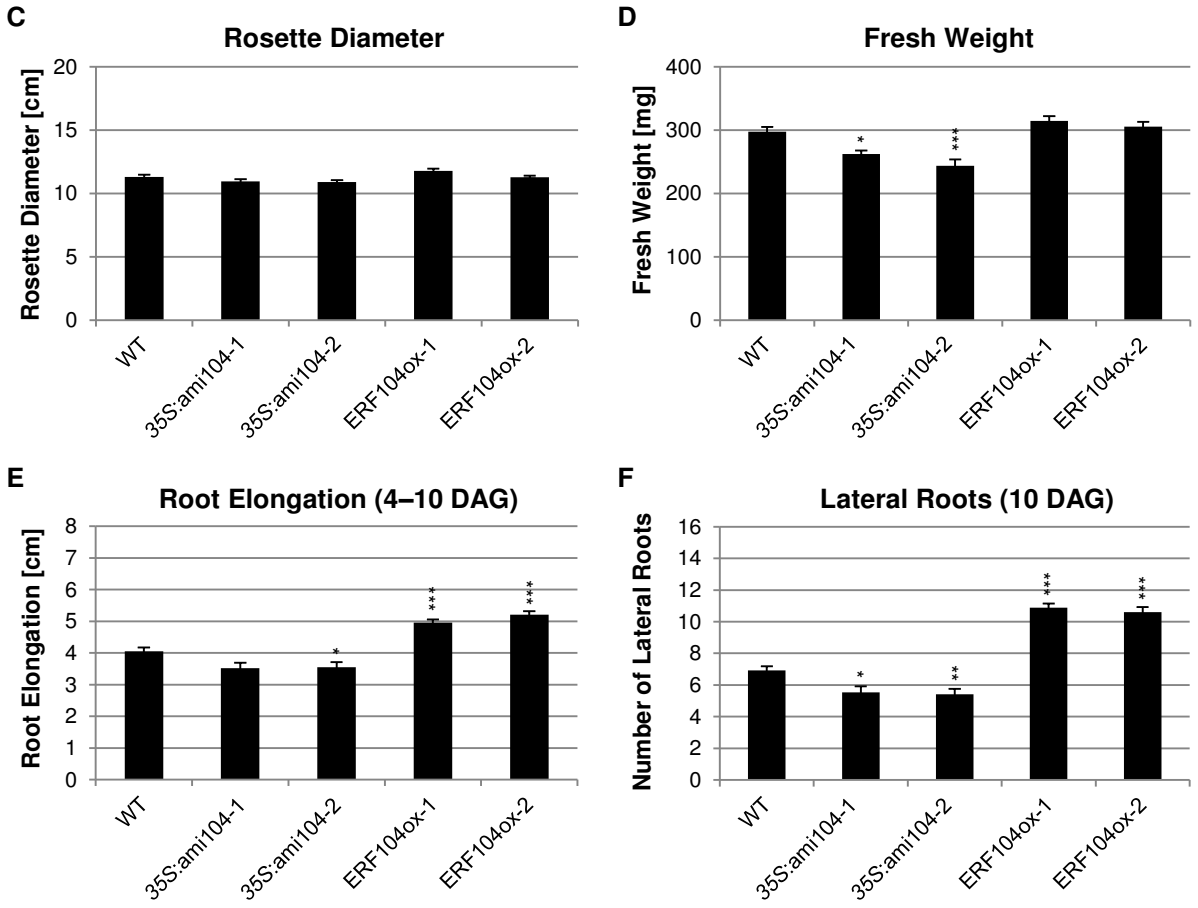

Figure 18. Characterization of lines with altered *ERF104* expression levels. (A) Morphological phenotype of plants grown 35 days under long day conditions. Shoot height **(B)**, rosette diameter **(C)** and fresh weight **(D)** of 35-day-old plants. **(E and F)** Root growth analysis of ten-day-old plants grown on half-strength MS medium. **(E)** The elongation of the primary root was determined between four days and ten days after germination (4–10 DAG). **(F)** The number of lateral roots was determined ten days after germination (10 DAG). Asterisks indicate significant differences to the wild type ($n \geq 30$), (*, $p < 0.05$; **, $p < 0.01$; ***, $p < 0.001$). Error bars represent SE.

The *ERF105* loss of function caused striking phenotypic alterations in the plant shoot and root system. The *erf105* mutant had a 24 % shorter shoot, a 20 % smaller rosette, about 50 % less lateral shoots, 24 % less siliques on the main stem and the fresh weight of *erf105* mutant plants was only 65 % of wild-type plants (Fig. 19). Moreover, *erf105* started with senescence 21 days after germination whereas senescence was observed two weeks later in wild-type plants (Fig. 19A and G). Regarding the root system, *erf105* exhibited 21 % less lateral roots compared to wild type (Fig. 19E and F). Overexpression of *ERF105* caused 8 % (ERF105ox-1) and 11 % (ERF105ox-2) longer shoots, 8 % (ERF105ox-1) and 10 % (ERF105ox-2) bigger rosettes, 7 % (ERF105ox-1) and 23 % (ERF105ox-2) more side shoots, 10 % (ERF105ox-1) and 7 % (ERF105ox-2) more siliques on the main stem, 8 % (ERF105ox-1) and 10 % (ERF105ox-2) more fresh weight, 24 % (ERF105ox-1) and 33 % (ERF105ox-2) longer primary roots and 56 % (ERF105ox-1) and 87 % (ERF105ox-2) more lateral roots (Fig. 19). *ERF105* overexpressing lines did not show an altered senescence phenotype. Additionally, there were no significant differences in number of adventitious

shoots or flowering time between *erf105*, *ERF105* overexpressing plants and wild type (data not shown).

Complementation of *erf105* plants by introgression of the ERF105ox-1 allele restored wild-type expression levels of *ERF105*, and the complemented plants were basically phenotypically indistinguishable from wild type (Fig. 19A–I). Due to the CaMV *35S* promoter of the ERF105ox-1 allele, a slight over-complementation was only observed regarding the lateral root development (Fig. 19F).

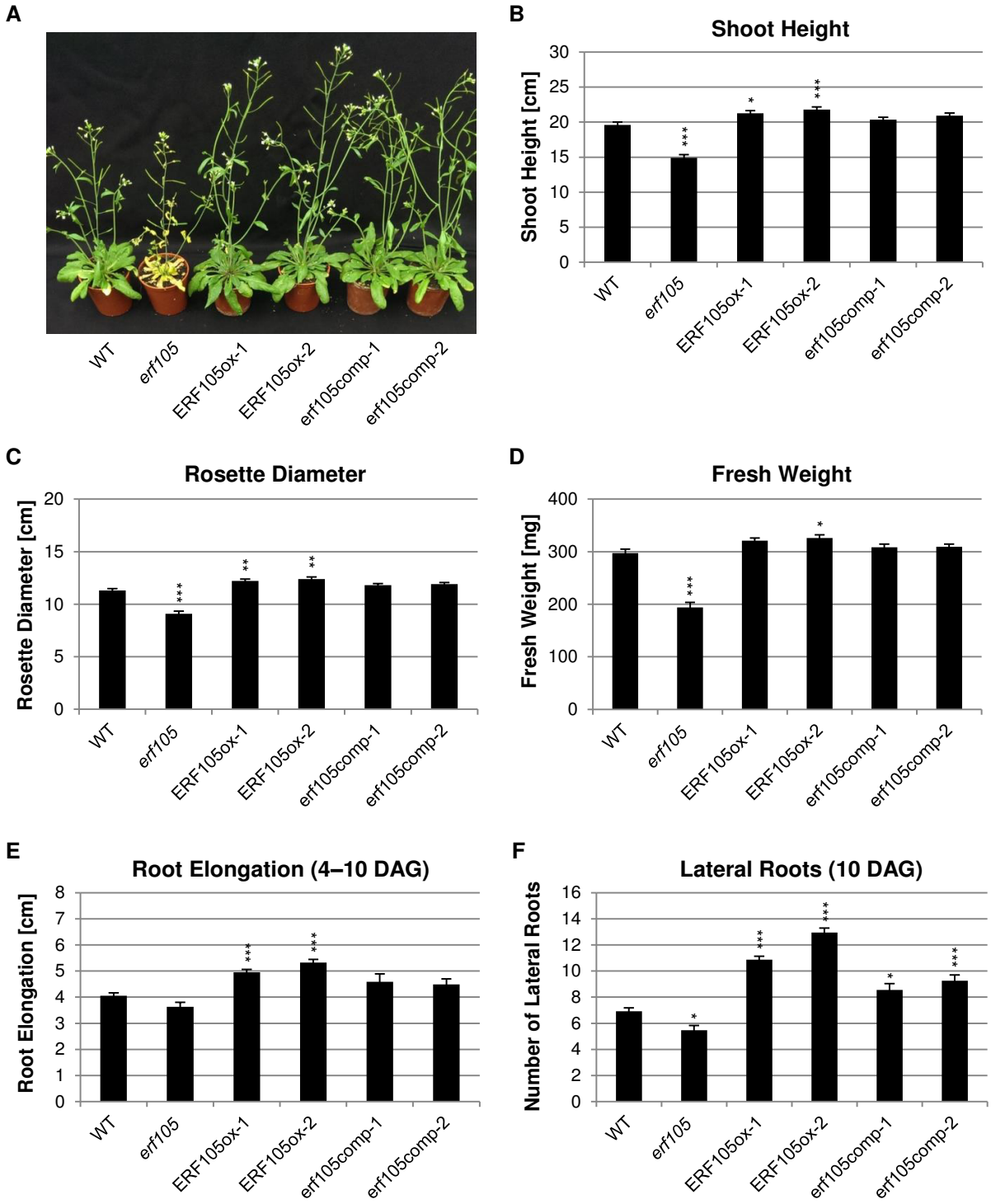

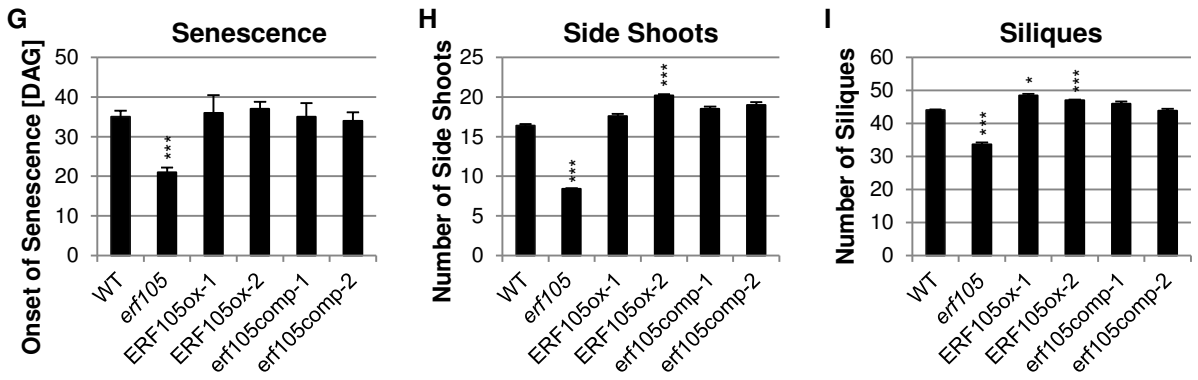

Figure 19. Characterization of lines with altered *ERF105* expression levels and complementation test of the *erf105* mutant. (A) Morphological phenotype of plants grown 35 days under long day conditions. Shoot height **(B)**, rosette diameter **(C)** and fresh weight **(D)** of 35-day-old plants. **(E and F)** Root growth analysis of ten-day-old plants grown on half-strength MS medium. **(E)** The elongation of the primary root was determined between four days and ten days after germination (4–10 DAG). **(F)** The number of lateral roots was determined ten days after germination (10 DAG). **(G)** Onset of senescence. 42 days after germination**,** number of side shoots **(H)**, and number of siliques on main stem **(I)** were determined. Asterisks indicate significant differences to the wild type ($n \geq 30$), (*, $p < 0.05$; **, $p < 0.01$; ***, $p < 0.001$). Error bars represent SE.

Together, the mutants and transgenic lines of the studied *ERF102* to *ERF105* genes showed similar alterations in plant development. Reduced *ERF* expression led to a slightly reduced plant growth, whereas an increased *ERF* expression led to an improved growth. These developmental alterations were already visible in the early stages of development (data not shown) and were more obvious in later stages (see Figures above). A correlation between phenotype and expression level of *ERF* genes was only observed in lines with altered *ERF105* expressions. In fact, ERF105ox-2 showed a higher expression level of *ERF105* and exhibited a stronger phenotype (Figs. 15K and 19).

To examine a potential redundant role of the four *ERF* genes, double mutants with reduced expression of *ERF* genes – namely *erf102,35S:*amiERF103; *erf102,35S:*amiERF104; *35S:*amiERF103,*erf105* and *35S:*amiERF104/105 – were generated and examined in this study. Double mutants did not show a phenotypic additive effect compared to the respective single mutants (data not shown). These results suggest that either *ERF102* to *ERF105* are not redundant or that the knockout/knockdown of two of the four *ERF* genes is not sufficient.

3.6 Functional and molecular characterization of *ERF105*

During the course of the study, several functions of *ERF102*, *ERF103* and *ERF104* have been published (Son *et al.*, 2012; Moffat *et al.*, 2012; Meng *et al.*, 2013; Dubois *et al.*, 2013; Vogel *et al.*, 2014; Moore *et al.*, 2014; Dubois *et al.*, 2015). Thus, the focus of this thesis was set on the detailed characterization of the molecular function of *ERF105*.

3.6.1 ERF105 and its role in cold stress

3.6.1.1 ERF105 positively regulates Arabidopsis *cold tolerance and cold acclimation*

The analysis of transcriptional regulation of *ERF105* by cold stress (3.1.2) revealed that *ERF105* is a fast cold-responsive gene. Cold treatment (4 h, 4 °C) did not change the expression pattern of *ERF105:GUS* lines (data not shown), but a higher GUS activity was measured in cold-treated *ERF105:GUS* plants (Fig. 20). This confirmed the cold responsiveness of the *ERF105* promoter and showed that its activity following cold treatment stays limited to the same tissues as without cold treatment.

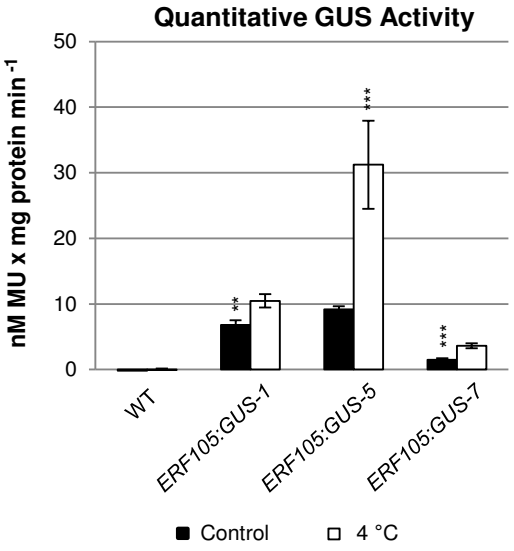

Figure 20. Quantitative GUS activity assay of *ERF105:GUS* lines. GUS activity determined by the MUG assay in ten-day-old seedlings (five pooled seedlings per sample) from wild type and different *ERF105:GUS* lines after cold treatment for 4 h at 4 °C in the dark. Asterisks indicate significant differences to the control conditions (**, $p < 0.01$; ***, $p < 0.001$). Error bars represent SE ($n \geq 4$). Abbreviation: MU, methylumbelliferone.

Subsequently, the consequences of loss and gain of function of *ERF105* on plant sensitivity to freezing stress were investigated. Initially, five-week-old plants grown under short day conditions were placed at -3 °C for 4 days, returned for recovery to normal growth conditions and analyzed for survival ten days later. 73 % of wild-type plants survived the treatment but only 15 % of *erf105* mutants, which indicates their freezing sensitivity. In contrast, more plants of the ERF105ox-1 and ERF105ox-2 lines (100 % and 99 %, respectively) survived, indicating an improved freezing tolerance (Fig. 21A and C). This was also shown by *in vitro* experiments, whereas two-week-old plants were incubated 1 h at -18 °C. Three days after recovery, 44 % of wild-type plants survived the treatment, only 15 % of *erf105* mutants, 78 % of ERF105ox-1 and 65 % of ERF105ox-2 plants (Fig. 21B and D).

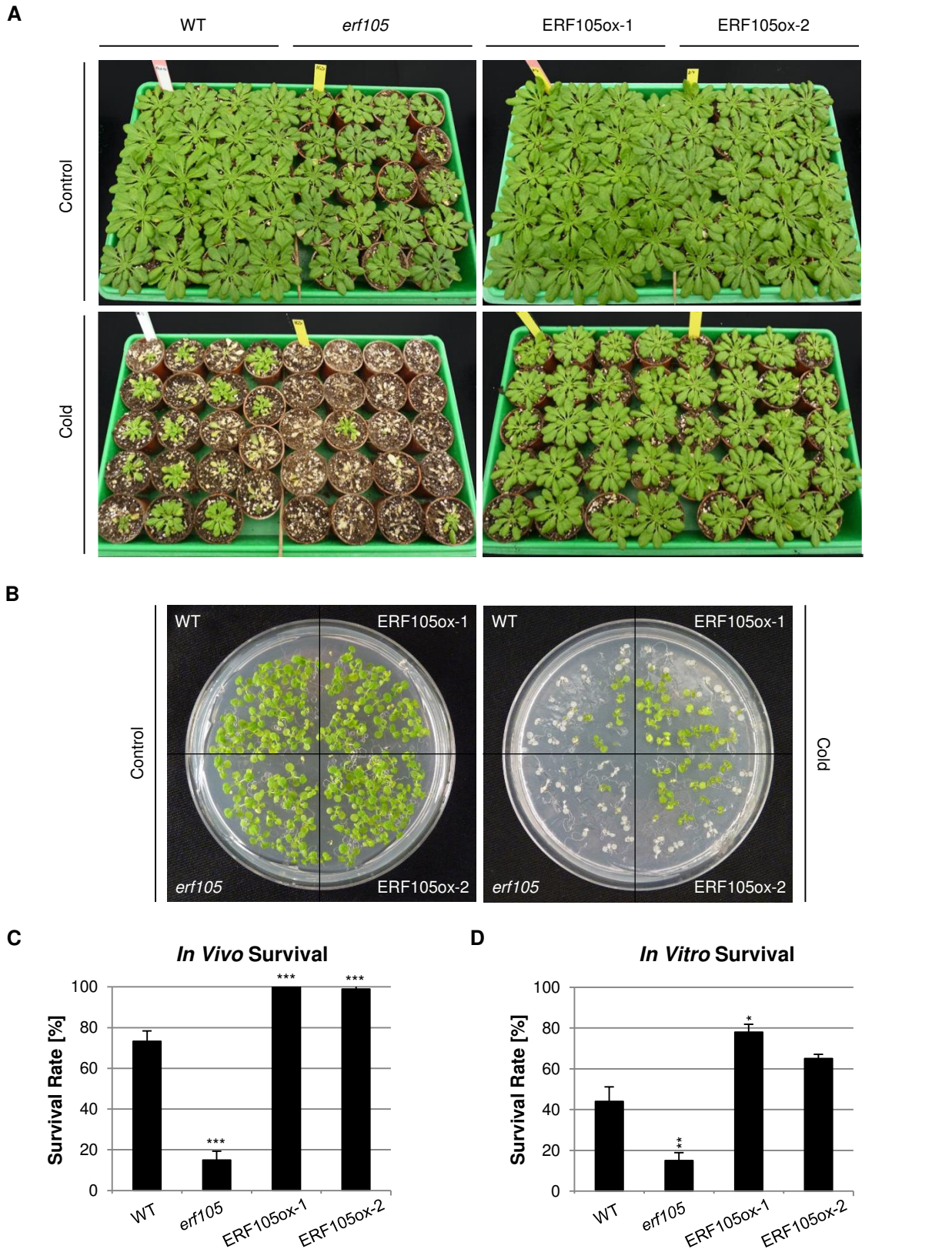

Figure 21. *S*urvival of the *erf105* mutant and *ERF105* overexpressing plants. (A) *In vivo* survival experiment. Phenotype of five-week-old plants that were cultivated 4 days at -3 °C. Photos were taken ten days after recovery and show one exemplary experiment. **(B)** *In vitro* survival experiment. Phenotype of two-week-old plants that were incubated 1 h at -18 °C. Photos were taken three days after recovery and show one exemplary petri dish from one experiment. **(C)** Survival rates of the experiment described and shown in (A). **(D)** Survival rates of the experiment described and shown in (B). Survival rates were calculated from results of three independent experiments (n ≥ 19 for each experiment). Error bars represent SE. Asterisks indicate significant differences to the wild type (*, $p < 0.05$; **, $p < 0.01$; ***, $p < 0.001$).

Furthermore, the freezing tolerance was determined by an electrolyte leakage assay on detached leaves of the *erf105* mutant and *ERF105* overexpressing plants before (non-acclimated, NA) and after 14 days and 21 days of cold acclimation (acclimated, ACC14 and ACC21, respectively) at 4 °C (Thalhammer *et al.*, 2014b). To take into account the almost complete arrest of plant growth at 4 °C, the electrolyte leakage assay was performed at the same developmental state for both NA and ACC plants (see 2.15.3). Figure 22A shows the resulting LT_{50} (temperature of 50 % electrolyte leakage) values. In NA plants, LT_{50} values ranged from -4.23 ±0.18 °C in *erf105* leaves to -4.88 ±0.14 °C in wild-type leaves, -5.21 ±0.12 °C in ERF105ox-1 and -5.16 ±0.10 °C in ERF105ox-2 leaves. This confirmed the results obtained from survival experiments, namely a lower freezing tolerance of *erf105* plants and a higher freezing tolerance of *ERF105* overexpressing plants as compared to wild type.

For all genotypes, 14 days and 21 days acclimated plants performed better than the non-acclimated counterparts, although the increase in freezing tolerance of *ERF105* overexpressing plants was lower than in wild type. In ACC14 plants, the LT_{50} value measured in *erf105* leaves (-8.71 ±0.46 °C) was highest while wild type (-9.76 ±0.22 °C), ERF105ox-1 (-9.48 ±0.27 °C) and ERF105ox-2 (-9.9 ±0.2 °C) showed comparable values. In ACC21 plants similar results were obtained as in ACC14 plants. Interestingly, *erf105* plants responded to low temperature by acclimation despite their lower freezing tolerance. However, the differences of LT_{50} values between wild type and *erf105* plants were higher in ACC14 and ACC21 plants than in NA plants (1.02 °C in ACC14 plants and 0.89 °C in ACC21 plants compared to 0.65 °C in NA plants) indicating a reduced ability to become fully acclimated. Importantly, the freezing sensitive phenotype of *erf105* could be fully complemented by introgression of the ERF105ox-1 allele (Fig. 22B). Further support for a role of *ERF105* in freezing tolerance was obtained from lines expressing an amiRNA directed against *ERF104* alone or against both *ERF104* and *ERF105*. Measurement of LT_{50} showed a significant reduction in *35S:*amiERF104/105 but not in *35S:*ERF104 lines (Fig. 22C). Thus, decreased freezing tolerance was critically dependent on downregulation of *ERF105*.

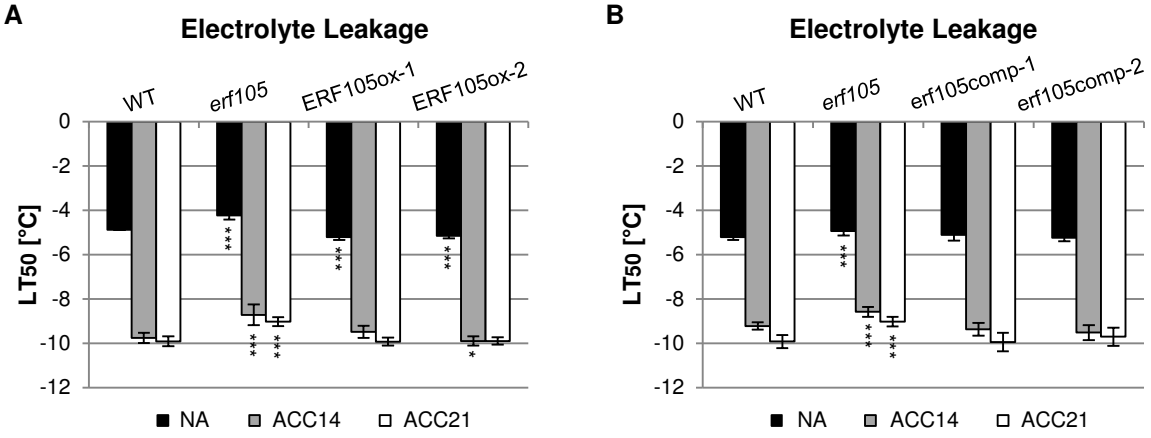

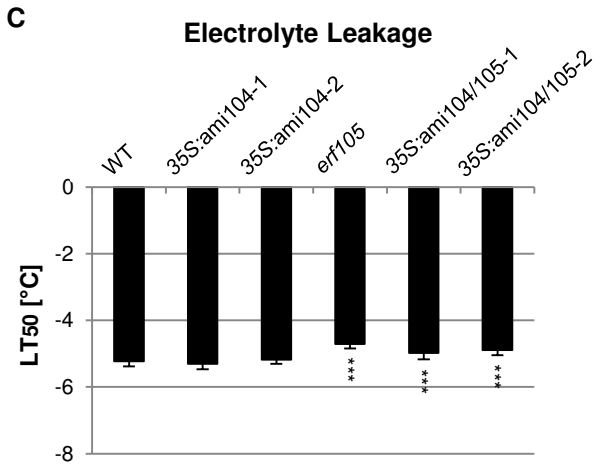

Figure 22. Electrolyte leakage assay of the *erf105* mutant, *ERF105* overexpressing lines, *erf105comp* lines, and lines with reduced *ERF104* and *ERF105* expression levels. (A and B) Electrolyte leakage assay on detached leaves before (non-acclimated, NA) and after (acclimated, ACC) 14 days or 21 days of cold acclimation at 4 °C. **(C)** Electrolyte leakage assay on detached leaves of non-acclimated plants. The bars represent the means ± SE from four replicate measurements where each replicate comprised leaves from three plants. Error bars represent SE. Asterisks indicate significant differences to the wild type (*, $p < 0.05$; ***, $p < 0.001$).

Together, these results indicate that ERF105 is a positive regulator of freezing tolerance and cold acclimation in *Arabidopsis*.

3.6.1.2 The erf105 *mutant and* ERF105 *overexpressing plants show an altered expression of cold-responsive genes*

To gain insight into the molecular function of *ERF105* in the cold stress signaling pathway, the role of *ERF105* in gene regulation was examined and compared to the expression levels of selected cold-responsive genes in NA, ACC14 and ACC21 plants of the *erf105* mutant, *ERF105* overexpressing plants and wild type by qRT-PCR. Most of the tested genes included in particular those of the CBF regulatory pathway known to play an important role in cold signaling (Thomashow, 1999; Chinnusamy *et al.*, 2003; Chinnusamy *et al.*, 2007; Shi *et al.*, 2014). These analyses revealed that in *erf105* plants under non-acclimated conditions the steady state mRNA levels of several tested cold-responsive genes were decreased compared to those of the wild type (Fig. 23 and Tab. A1). Particularly strong reductions of transcript level were found for *CFB1* and *CFB2*, which attained only 16 % and 15 % of the expression level of wild type. The expression level of several other genes including *COR15A*, *COR47*, *ZAT6*, *ZAT12* and *MYB15* was lowered to about 30 % to 60 % of the level found in wild type. Expression level of *RD29B* was increased about 5.5-fold in *erf105*. Interestingly, the expression of the *CBF1* and *CBF2* genes was also reduced in the *ERF105* overexpressing plants. The expression level of *COR47*, *ICE2*, *HOS1*, *SIZ1* and *FRY2* were also slightly but not significantly reduced in *ERF105* overexpressing plants. The expression of most other cold-responsive genes was slightly higher, for instance, up to a more than 2-fold increase in *CBF3* transcript level. Notably, this weak upregulation was not sufficient to cause dwarfism, a phenotype associated with strong overexpression of *CBF3* (Liu *et al.*, 1998; Gilmour *et al.*, 2000).

After 14 days and 21 days of acclimation at 4 °C (ACC14, ACC21), the expression levels of several cold-responsive genes were elevated in wild type compared to NA plants, which is

consistent with an earlier report (Zuther *et al.*, 2012). Particularly strongly elevated transcript levels in the range of a 26-fold to over 40-fold induction were found in ACC14 plants for *CBF1*, *CBF2*, *CBF3* and *COR15A* (Fig. 23 and Tab. A1). Some other genes did not respond or – in case of *MYB96* and *ESK1* – showed a reduced transcript level to about 28 % and 24 %, respectively, compared to non-acclimated plants. In ACC14 *erf105* plants the expression levels of several cold-responsive genes were elevated as well, but to a much lower extend than in wild type. For example, expression levels of *CFB1* to *CFB3* reached only the levels of NA wild-type plants. A notable exception is *ZAT12* which showed in ACC14 *erf105* plants even a stronger increase of transcript abundance than in wild type. After 21 days at 4 °C, the expression levels of cold-responsive genes were still elevated compared to NA conditions in wild type, generally to a similar extent. Some genes, for instance *COR78* and *MYB15*, showed a stronger or lower expression, respectively, in ACC21 plants than in ACC14 and NA plants. In the *erf105* mutant, the expression levels of most of the cold-responsive genes such as the *CBF* or *COR* genes were still lower in ACC21 plants compared to ACC21 wild-type plants, whereas expression of *ZAT12* was still increased but to a lower extend.

Regarding ERF105ox lines, the most prominent differences in expression levels of the cold-responsive genes were detected after 21 days of acclimation at 4 °C. At this time point, expression of most genes but in particular of *CBF3*, *COR6.6*, *COR15A, COR15B*, *COR47* and *COR78* was higher in both transgenic lines compared to ACC21 wild-type plants, ERF105ox-2 showing generally a stronger effect.

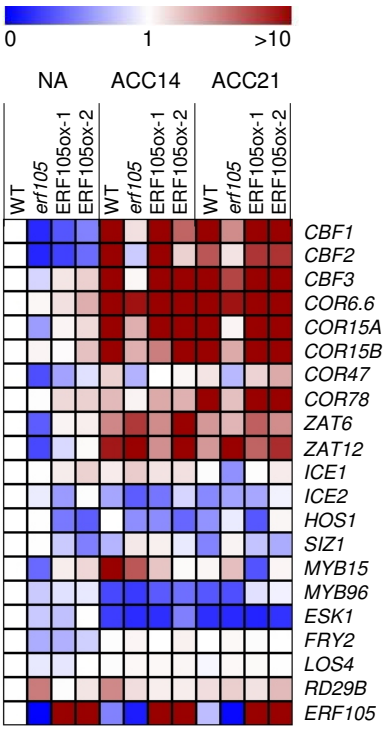

Figure 23. Expression of selected cold-responsive genes in the *erf105* mutant and *ERF105* overexpressing plants. Heat map of relative gene expression in the *erf105* mutant and *ERF105* overexpressing plants before (non-acclimated, NA) and after (acclimated, ACC) 14 days or 21 days of cold acclimation at 4 °C. The relative fold changes are shown compared to transcript levels of wild-type samples under control conditions which were set to 1 ($n \geq 4$). The expression values represented in the heat map are shown in Table A1.

Next, the expression characteristics of selected genes (*CBF1*, *CBF2*, *CBF3*, *COR15A*, *COR15B* and *ZAT12*) were examined in more detail in wild type and the *erf105* mutant. The expression levels of these genes were compared at early and late time points following transfer of plants to cold conditions (4 °C) (Fig. 24 and Tab. A2). The levels of *CBF1*, *CBF2*, and *CBF3* transcripts peaked at 4 h after shifting plants to low temperature and decreased again thereafter but stayed elevated for more than one week in the cold. In wild type, the *COR* and *ZAT12* gene transcripts began to accumulate between 1 h and 4 h after the transfer to cold and reached their maximum between one day and one week later. Comparison of the amplitudes of expression levels of the cold-responsive genes in these two genotypes clearly shows that expression levels of *CBF1*, *CBF2*, *CBF3*, *COR15A* and *COR15B* were dramatically decreased in *erf105*, reaching only between 10 % and 50 % of the wild-type levels. In contrast, the expression of *ZAT12* was 2-fold increased in the *erf105* mutant as compared to wild type.

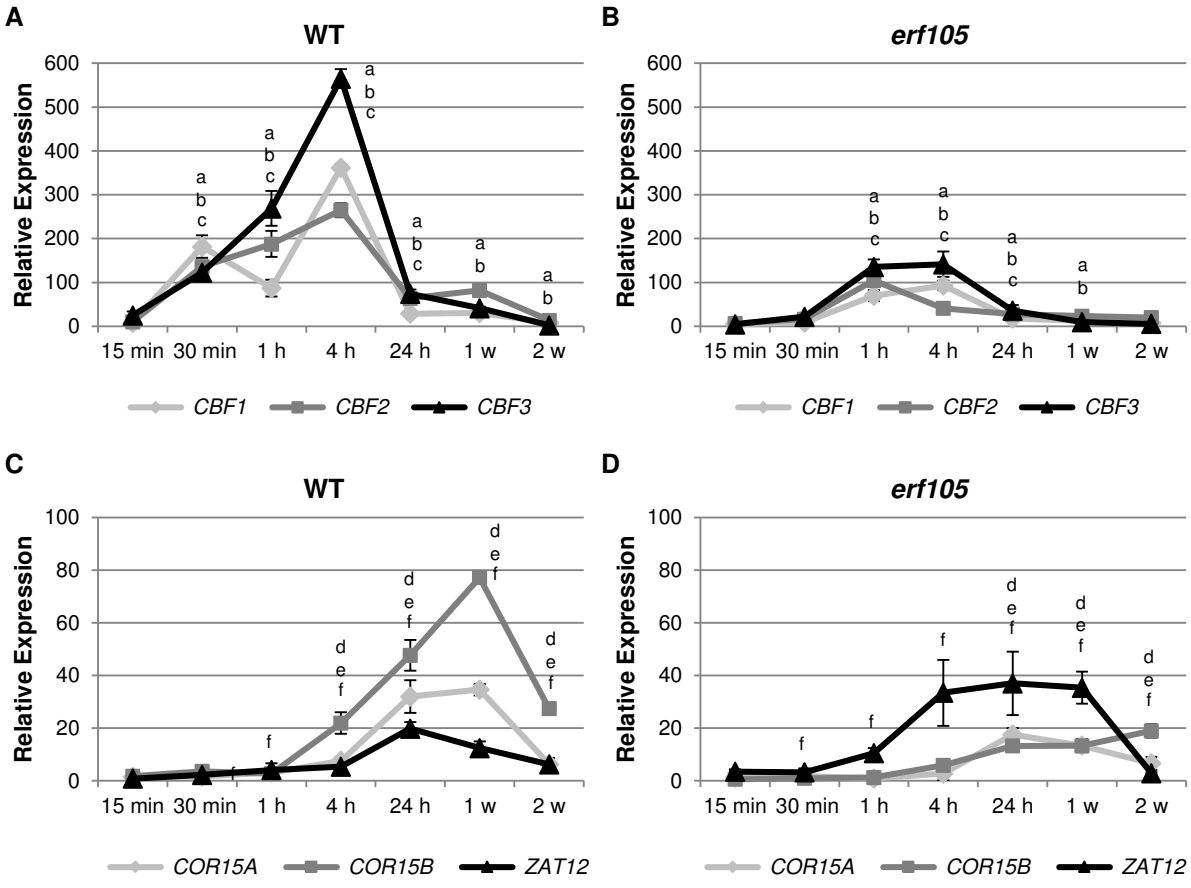

Figure 24. Kinetics of selected cold-responsive genes in wild type and the *erf105* mutant. Time course of expression of *CBF1*, *CBF2*, *CBF3*, *COR15A*, *COR15B* and *ZAT12* in four-week-old leaves (pooled leaves five, six and seven) after cold treatment at 4 °C in wild type **(A and C)** and *erf105* **(B and D)**. Transcript levels of control conditions were set to 1 ($n \geq 4$). Quantitative data corresponding to this figure are shown in Table A2. Letters indicate significant differences ($p < 0.05$) to the respective control (time point zero) (a = *CBF1*, b = *CBF2*, c = *CBF3*, d = *COR15A,* e = *COR15B*, f = *ZAT12*). Error bars represent SE.

Collectively, the results described in this chapter clearly point to a putative role of *ERF105* in the CBF cold signaling pathway.

3.6.1.3 The erf105 *mutant and* ERF105 *overexpressing plants show an altered content of osmoprotectants*

During cold acclimation, the content of osmoprotectants such as proline (Pro) and soluble sugars increases in *Arabidopsis* leaves to protect plants from future freezing stress (Nanjo *et al.*, 1999; Wanner and Junttila, 1999). Therefore, the content of Pro and of the sugars glucose (Glc), fructose (Fru), sucrose (Suc), and raffinose (Raf) was compared in the *erf105* mutant, the *ERF105* overexpressing plants and wild type before and after cold acclimation. With few exceptions the metabolite profiles showed a similar pattern in all genotypes. In NA plants, there were no significant differences in Pro, Glc, Fru and Suc content between the different genotypes (Fig. 25), except for the 2-fold to 4-fold increased Raf content under non-acclimated conditions in the *erf105* mutant and the *ERF105* overexpressing plants. In contrast, the *erf105* mutant and the *ERF105* overexpressing plants showed an about 2-fold to 4-fold increased Raf content under non-acclimated conditions. ACC14 and ACC21 plants of all genotypes showed an increased concentration of osmoprotectants, with the exception of Raf in the *erf105* mutant and the *ERF105* overexpressing lines where the concentration did not increase further but rather decreased. A notable peculiarity was the 3-fold stronger increase of Glc and Fru in *erf105* plants during acclimation (ACC14, ACC21) compared to wild type.

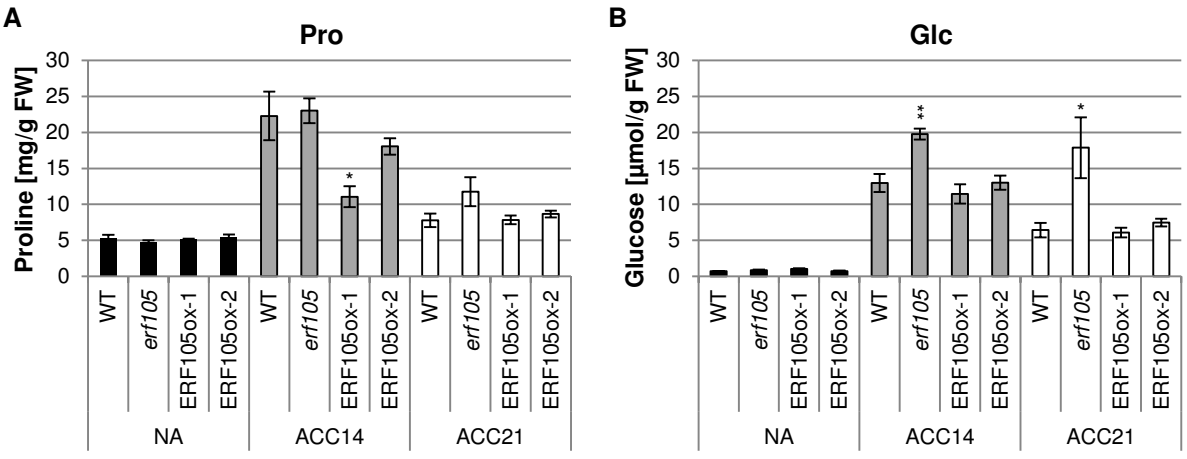

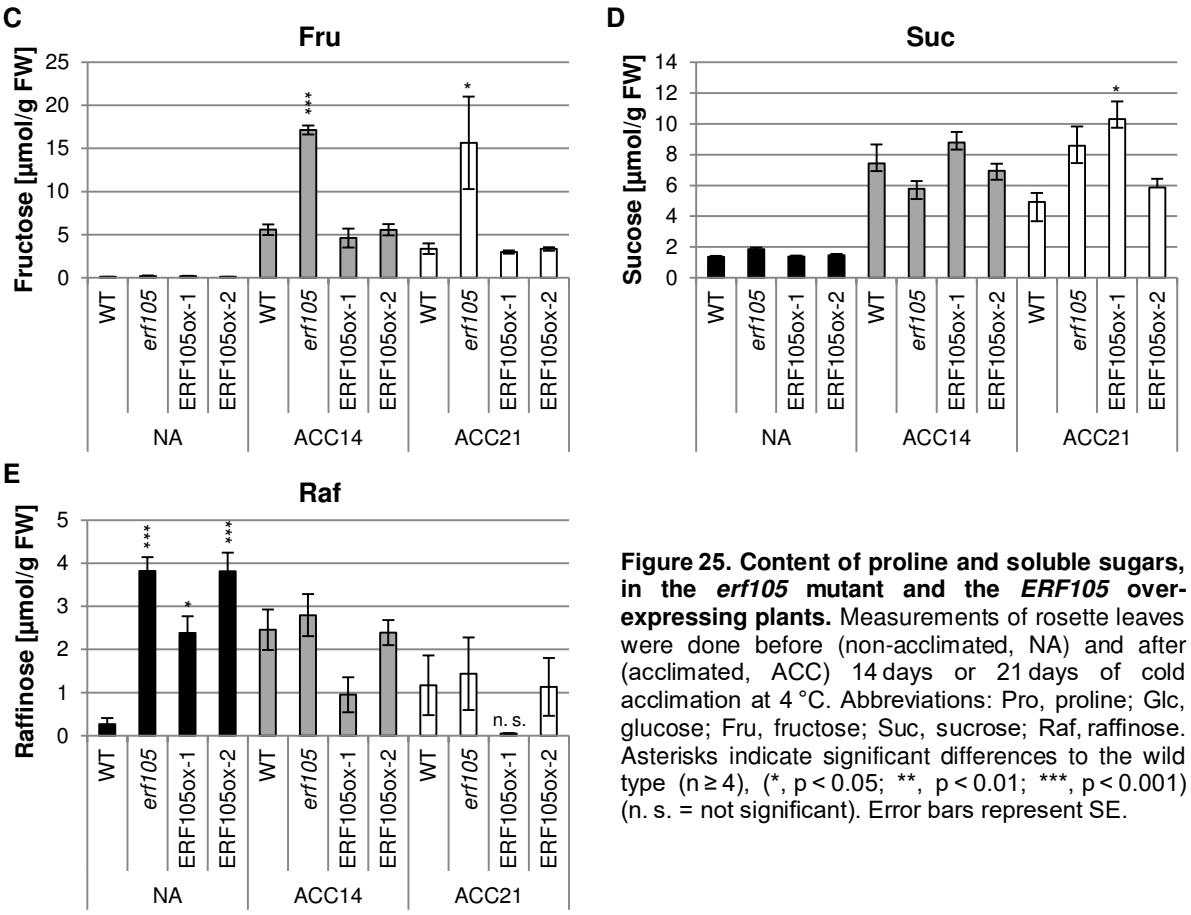

Figure 25. Content of proline and soluble sugars, in the *erf105* mutant and the *ERF105* over-expressing plants. Measurements of rosette leaves were done before (non-acclimated, NA) and after (acclimated, ACC) 14 days or 21 days of cold acclimation at 4 °C. Abbreviations: Pro, proline; Glc, glucose; Fru, fructose; Suc, sucrose; Raf, raffinose. Asterisks indicate significant differences to the wild type ($n \geq 4$), (*, $p < 0.05$; **, $p < 0.01$; ***, $p < 0.001$) (n. s. = not significant). Error bars represent SE.

3.6.1.4 The expression of genes of the flavonol and anthocyanin biosynthesis is altered in the erf105 *mutant but the anthocyanin level is not changed*

Flavonoids accumulate under cold conditions, however the molecular function of these metabolites during cold stress is not well understood. It is suggested that these substances may function as antioxidants and membrane stabilizers (Winkel-Shirley 2002; Schulz *et al*., 2015). Therefore, the transcript abundance of genes involved in the flavonol and anthocyanin biosynthesis before and after 14 days and 21 days of cold acclimation was analyzed in the *erf105* mutant, *ERF105* overexpressing plants and wild type by qRT-PCR and summarized in Figure 26A and Table A3. This analysis revealed that in NA plants, the *erf105* mutant and to some extent *ERF105* overexpressing plants showed decreased transcript abundances of several genes involved in the flavonol and anthocyanin biosynthesis. In the NA *erf105* mutant, particularly strong reductions of transcript level were found for *PAP2/MYB90*, *bHLH/TT8* and *MYB11*, which attained only 1 % to 11 % of the expression level of wild type. During cold acclimation, particularly after 21 days of cold treatment, the transcript abundances of genes involved in the flavonol and anthocyanin biosynthesis increased in all genotypes as it has been described by Schulz *et al*. (2015). Notably, in *erf105* plants most of the genes of the flavonol and anthocyanin biosynthesis were not as strongly induced as in

wild type and attained only expression levels between 2 % and 70 % of the expression level of wild type (Fig. 26A and Tab. A3). Therefore, the question arose whether the *erf105* mutant accumulates less flavonoids. For that, the anthocyanin content was determined and revealed no notable differences between *erf105*, the *ERF105* overexpressing plants and wild type, neither in NA nor in ACC14 or ACC21 plants (Fig. 26B). Flavonols, another group of flavonoids, were not quantified in this study.

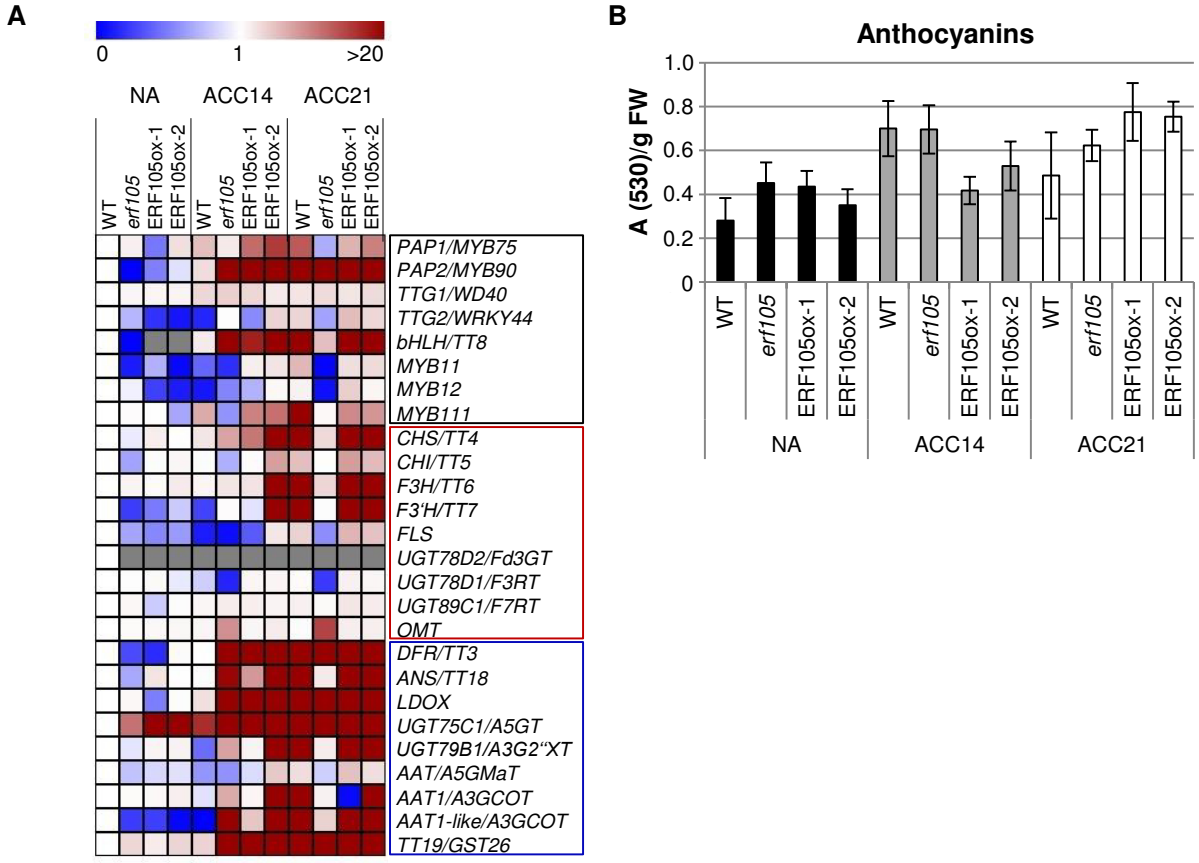

Figure 26. Expression of selected genes involved in the flavonol and anthocyanin biosynthesis pathway and anthocyanin content in the *erf105* mutant and *ERF105* overexpressing plants. (A) Heat map of relative gene expression in the *erf105* mutant and *ERF105* overexpressing plants before (non-acclimated, NA) and after (acclimated, ACC) 14 days or 21 days of cold acclimation at 4 °C. The relative fold changes are shown compared to transcript levels of wild-type samples under control conditions which were set to 1 (n ≥ 4). Genes encoding transcription factors are framed in black, flavonol biosynthesis genes in red and anthocyanin biosynthesis genes in blue. Grey boxes indicate missing values. The expression values represented in the heat map are shown in Table A3. **(B)** Content of anthocyanins in the *erf105* mutant and the *ERF105* overexpressing plants. Measurements of rosette leaves were done before (non-acclimated, NA) and after (acclimated, ACC) 14 days or 21 days of cold acclimation at 4 °C. Error bars represent SE.

3.6.1.5 The accumulation of ROS is elevated in the erf105 *mutant*

Environmental stresses, cold stress included, enhance the production of reactive oxygen species (ROS) (Prasad *et al*., 1994; Mittler, 2002). The ROS such as oxygen ions, free radicals and peroxides can directly attack membrane lipids and increase lipid peroxidation (Mittler, 2002). Stress-induced overproduction of ROS increases the content of malon-dialdehyde (MDA). MDA is a secondary end product of the oxidation of polyunsaturated fatty acids and has been considered as an indicator of oxidative damage and a suitable marker for membrane lipid peroxidation (Heath and Packer, 1968; Møller *et al*., 2007; Anjum *et al*., 2011).

To compare the accumulation of ROS in the different genotypes before and after 14 days and 21 days of cold acclimation, the content of malondialdehyde (MDA) was quantified. Figure 27A shows that MDA levels were elevated in NA *erf105* plants to about 66 % compared to wild type. However, both NA *ERF105* overexpressing lines showed a similar MDA profile as wild type. As described above, cold stress leads to oxidative stress due to an enhanced ROS production and a higher lipid peroxidation, respectively. Thus, after cold treatment all genotypes showed an almost doubled MDA level. The MDA level in the *erf105* mutant was elevated to about 34 % (ACC14) and 48 % (ACC21) compared to wild type, whereas the *ERF105* overexpressing lines exhibited a similar MDA content as wild type.

Additionally, for detection of superoxide, rosette leaves were stained with nitroblue tetrazolium (NBT) and demonstrated that NA *erf105* mutants accumulate more superoxide compared to the wild type. NA *ERF105* overexpressing lines showed a similar staining intensity as wild type. Cold treatment led to an increased level of superoxide in all genotypes. Due to the strong intensity of the staining, it was not possible to detect quantitative differences (Fig. 27B).

To find out whether the higher ROS accumulation in *erf105* is caused by a misregulation of genes involved in the ROS homeostasis, the transcript abundance of selected genes coding for ROS-producing and ROS-scavenging enzymes was determined. This analysis revealed that under non-acclimated conditions there were no notable differences in expression levels between *erf105*, *ERF105* overexpressing lines and wild type. However, after 14 days and 21 days of cold acclimation the transcript abundance of *RBOHD*, a key factor in ROS production in *Arabidopsis* leaves (Miller *et al*., 2009), showed stronger expression in the *erf105* mutant (2-fold in ACC14 *erf105,* and 3.5-fold in ACC21 *erf105*) than in wild-type plants (Tab. A4).

Since the *erf105* mutant showed a higher lipid peroxidation and accumulates more superoxide and ROS causes chlorophyll degradation (Sevengor *et al*., 2011), the assumption arose that *erf105* has a lower chlorophyll content. However, chlorophyll measurements did not reveal notable differences (Fig. 27C).

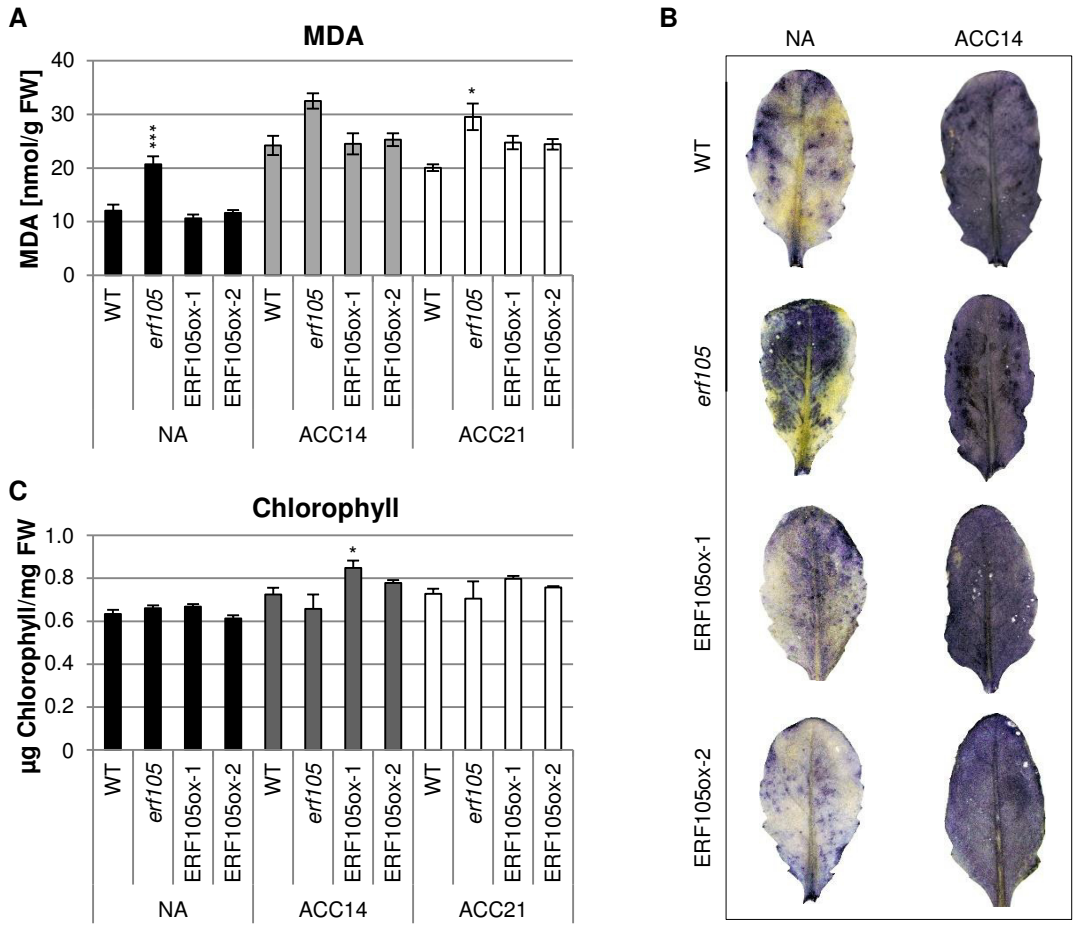

Figure 27. Content of malondialdehyde, superoxide and chlorophyll in the *erf105* mutant and the *ERF105* overexpressing plants. (A) Measurements of malondialdehyde (MDA) as indicator of lipid peroxidation. **(B)** Nitroblue tetrazolium (NBT) histochemical staining patterns of fully developed rosette leaves for detection of superoxide. **(C)** Chlorophyll content. Measurements of rosette leaves were done before (non-acclimated, NA) and after (acclimated, ACC) 14 days or 21 days of cold acclimation at 4 °C. Asterisks indicate significant differences to the wild type ($n \geq 4$), (*, $p < 0.05$; ***, $p < 0.001$). Error bars represent SE.

The results of the MDA measurement and the NBT staining indicate that *ERF105* might also play a role in oxidative stress response.

3.6.1.6 Changes in transcript levels of ABA-related genes in the erf105 *mutant lead to altered ABA levels in* erf105

Levels of the plant hormone ABA are transiently elevated in response to cold (Chen *et al.*, 1983) and exogenous application of ABA at non-acclimating temperatures has been shown to enhance freezing tolerance (Lang *et al.*, 1994) and to induce many of the cold-responsive genes (Heino *et al.*, 1990; Gilmour and Thomashow 1991). Therefore, transcript levels of selected genes of the ABA biosynthesis, the ABA signaling and the ABA catabolic pathway were determined in NA, ACC14 and ACC21 plants of the *erf105* mutant, *ERF105* overexpressing plants and wild type by qRT-PCR (Fig. 28 and Tab. A5). These analyses

revealed that in *erf105* plants under non-acclimated conditions the steady state mRNA levels of *NCED3* and *RAB18* were about 2-fold increased compared to the wild type. A strong reduction of transcript level was found for *CBF4*, which attained only 15 % of the expression level of wild type. *CBF4* expression was also strongly reduced in *ERF105* overexpressing plants compared to wild type.

After cold acclimation, genes of the ABA biosynthesis, the ABA signaling and the ABA catabolic pathway were differentially expressed. Remarkable differences between the genotypes were particularly observed in ACC14 plants. Thus, the transcript abundances of *NCED3*, *ABI1*, *ABI2*, *CYP707A1*, and *CYP707A4* showed a stronger expression in the ACC14 *erf105* mutant than in ACC14 wild-type plants. To name one example, expression level of *NCED3* was 20-fold increased in ACC14 *erf105* plants, whereas expression level of ACC14 wild-type plants did not change. Moreover, expression levels of *RD22* and *CBF4* were stronger reduced in the ACC14 *erf105* mutant compared to ACC14 wild type. Regarding ACC14 and ACC21 *ERF105* overexpressing lines, most of the analyzed genes did not show an altered expression level. Only the expression level of *ABI5* was stronger increased in ACC *ERF105* overexpressing lines than in ACC wild type.

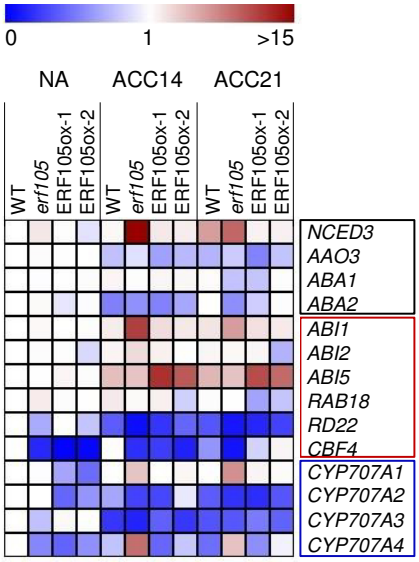

Figure 28. Expression of selected genes of the ABA biosynthesis, the ABA signaling and the ABA catabolic pathway in the *erf105* mutant and *ERF105* overexpressing plants. Heat map of relative gene expression in the *erf105* mutant and *ERF105* overexpressing plants before (non-acclimated, NA) and after (acclimated, ACC) 14 days or 21 days of cold acclimation at 4 °C. The relative fold changes are shown compared to transcript levels of wild-type samples under control conditions which were set to 1 ($n \geq 4$). Genes of the ABA biosynthesis are framed in black, genes encoding transcription factors in red, and genes of the ABA catabolism in blue. The expression values represented in the heat map are shown in Table A5.

The altered transcript abundances of ABA-related genes in the *erf105* mutant and partially in the *ERF105* overexpressing lines suggest an altered ABA content in these lines. Accordingly, the contents of the biologically active ABA and its hydroxylated catabolites phaseic acid (PA), and dihydrophaseic acid (DPA) as well as the physiologically inactive conjugate ABA glucosyl ester (ABA-GE) were quantified (Fig. 29). Indeed, the *erf105* mutant exhibited an altered ABA content. NA *erf105* plants accumulated twice as much ABA than the wild type. Cold acclimation led to an accumulation of ABA and its metabolites in all genotypes. Notably, *erf105* exhibited an about 2-fold to 15-fold stronger accumulation of ABA, PA, DPA and

ABA-GE. *ERF105* overexpressing lines did not show an altered ABA accumulation compared to wild type.

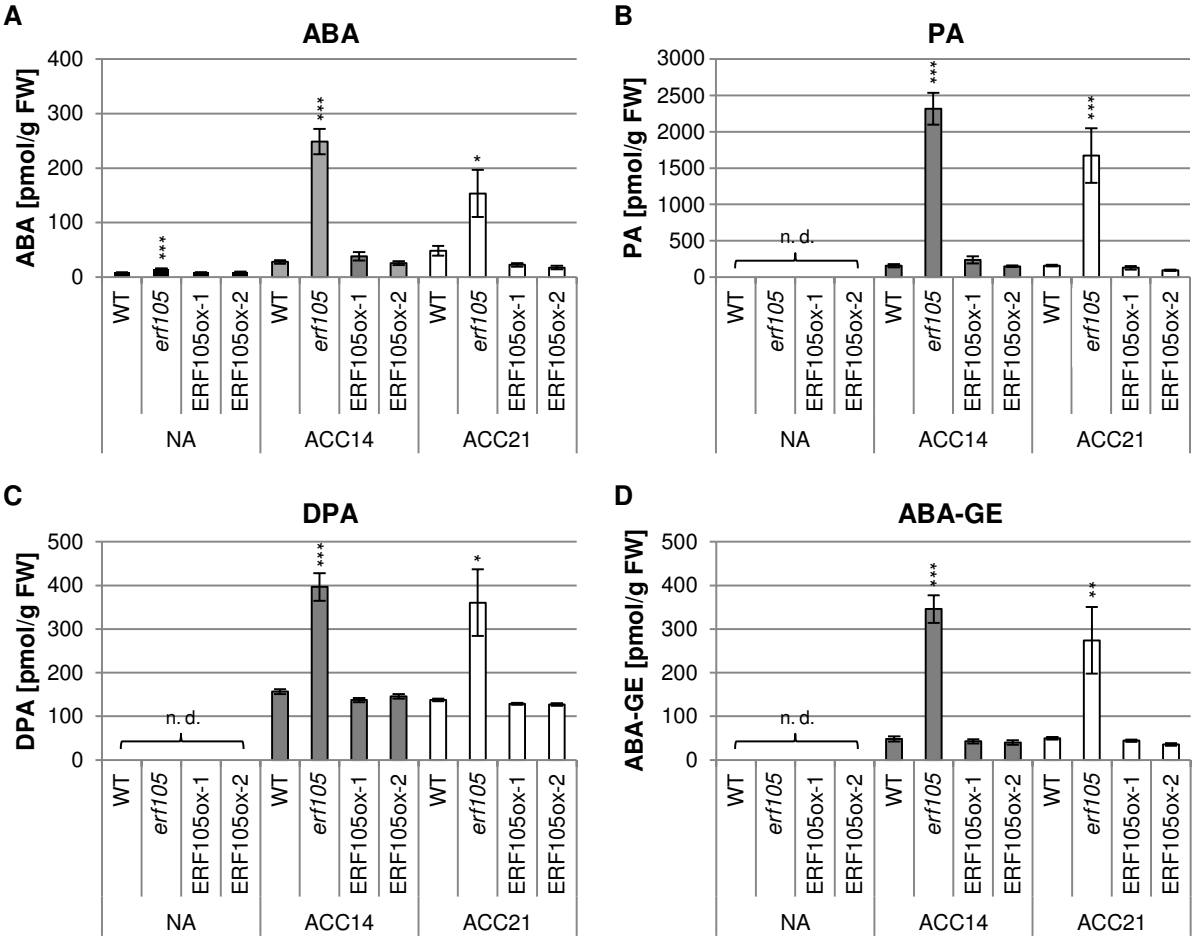

Figure 29. Content of ABA and ABA metabolites in the *erf105* mutant and *ERF105* overexpressing plants. Measurements of rosette leaves were done before (non-acclimated, NA) and after (acclimated, ACC) 14 days or 21 days of cold acclimation at 4 °C. Abbreviations: ABA, abscisic acid; PA, phaseic acid; DPA, dihydrophaseic acid; ABA-GE, abscisic acid glucosyl ester; n. d., not detectable. Asterisks indicate significant differences to the wild type (n ≥ 4), (*, $p < 0.05$; **, $p < 0.01$; ***, $p < 0.001$). Error bars represent SE.

In sum, changes in transcript levels of ABA-related genes in the *erf105* mutant led to altered ABA levels in *erf105.*

3.6.1.7 The erf105 *mutant shows an altered expression of several GA-related genes*

One of the major counteracting hormone of ABA is GA (Weiss and Ori, 2007). In *Medicago sativa* seedlings, Waldman *et al.* (1975) concluded that the cold acclimation capacity is regulated by the ABA/GA balance. Both GA signaling and metabolism are targeted by cold stress, and there is evidence for a participation of the *CBF* genes (Achard *et al.*, 2008).

The expression of selected genes of the GA metabolism (Yamaguchi, 2008) was determined in NA, ACC14 and ACC21 plants of the *erf105* mutant, *ERF105* overexpressing plants and wild type by qRT-PCR (Fig. 30 and Tab. A6). These analyses revealed that in NA plants, there were no significant differences in expression levels of genes of the GA metabolism

between the different genotypes. 14 days after cold acclimation, transcript abundance of *GA3OX2* was increased about 3-fold in wild type and ERF105ox-2 plants. In contrast, *GA3OX2* expression was reduced to 30 % of the initial level in *erf105* plants. 21 days after cold acclimation, expression of *GA3OX2* was back to the initial level in all genotypes. The transcript abundance of all other analyzed genes involved in the GA metabolism was decreased in ACC14 and ACC21 wild-type, *ERF105* overexpressing, and mostly in *erf105* plants. Notable exceptions were the stronger reduction of *GA3OX1* and the about 7.5-fold increased expression of *GA2OX2* in ACC14 *erf105* plants compared to ACC14 wild type.

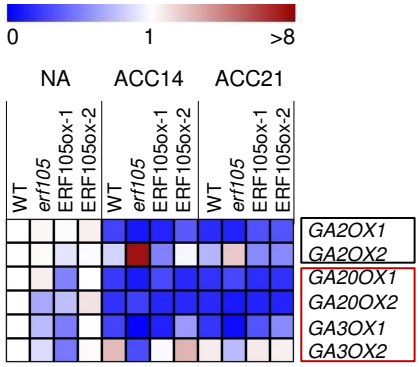

Figure 30. Expression of selected genes of the GA metabolism in the *erf105* mutant and *ERF105* overexpressing plants. Heat map of relative gene expression in the *erf105* mutant and *ERF105* overexpressing plants before (non-acclimated, NA) and after (acclimated, ACC) 14 days or 21 days of cold acclimation at 4 °C. The relative fold changes are shown compared to transcript levels of wild-type samples under control conditions which were set to 1 ($n \geq 4$). Genes of the GA catabolism are framed in black, genes of the GA biosynthesis are framed in red. The expression values represented in the heat map are shown in Table A6.

Collectively, the *erf105* mutant shows an altered expression of some GA-related genes. This raises the question whether or not the GA content in *erf105* is altered as well. Measurements of the GA content were not performed in this study.

3.6.2 ERF105 and its role in other abiotic stresses

In addition to cold, the analysis of transcriptional regulation of *ERF105* revealed a regulation of *ERF105* by different abiotic stresses (3.1.2). To gain insight whether ERF105 plays a role in other abiotic stresses, the *erf105* mutant and *ERF105* overexpressing lines underwent different stress treatments.

3.6.2.1 ERF105 is a positive regulator of drought tolerance

Initially, three-week-old plants were exposed to drought stress by stop watering for nine days. As shown in Figure 31A, the drought stress led to a drastic water loss of plants. Particularly, the *erf105* mutants showed a severe drought-induced phenotype denoted by a massive loss of turgor and strongly wilted and convoluted leaves, respectively. Wild-type plants were affected by the drought period as well but not that strong. *ERF105* overexpressing plants exhibited the least attenuated phenotype. These plants looked fittest. Following a period of rewatering of one week, the surviving plants were counted. 55 % of wild-type plants, only 27 % of *erf105* mutants, and 73 % and 85 %, respectively, of *ERF105*

overexpressing plants survived (Fig. 31B). Another experimental approach was to determine a time course of percental reduction of fresh weight from four-week-old cut leaves. The result is shown in Figure 31C. This analysis revealed that, at any time, the loss of fresh weight was higher in the *erf105* mutant and lower in the *ERF105* overexpressing plants compared to the wild type.

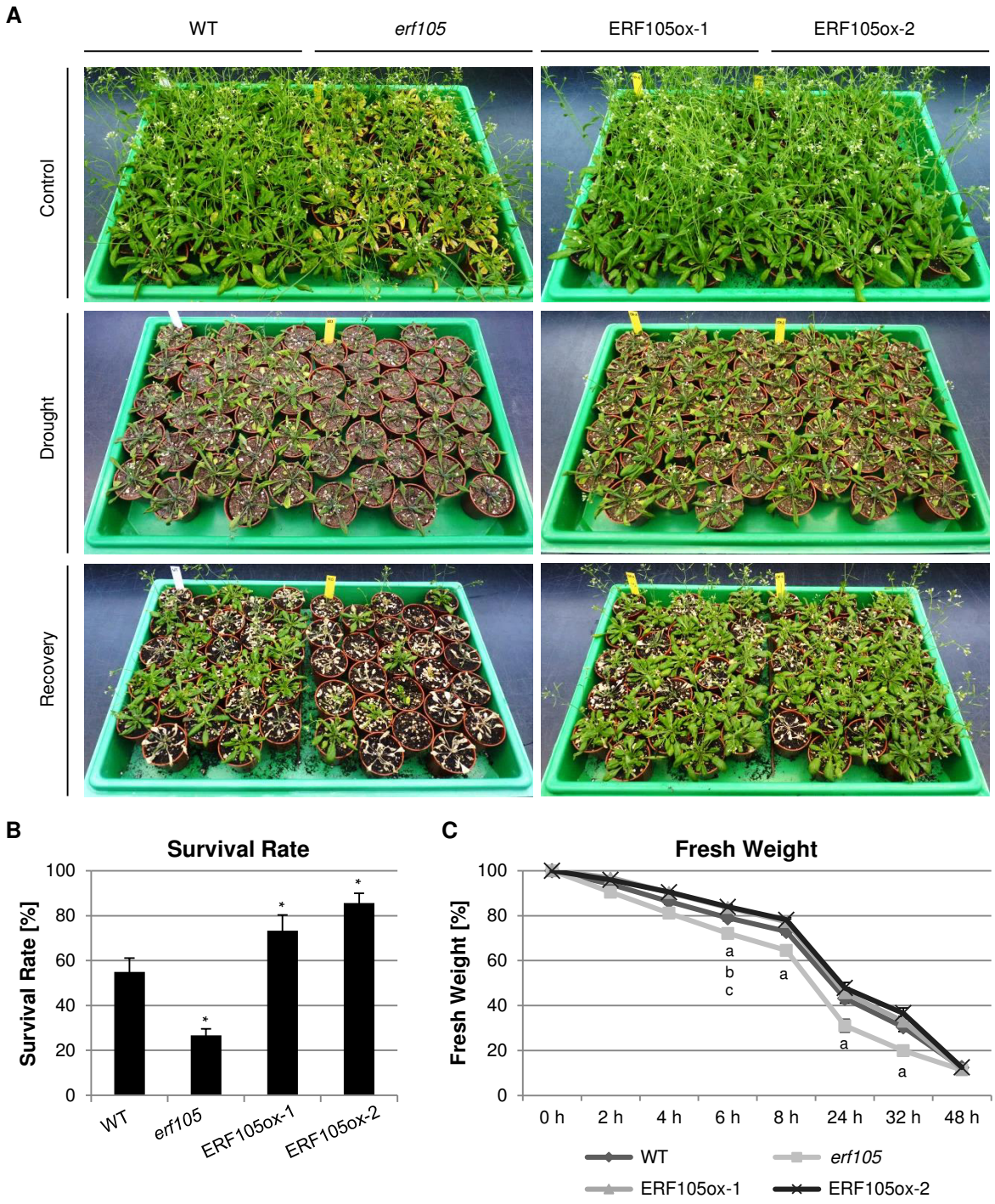

Figure 31. Drought tolerance of the *erf105* mutant and *ERF105* overexpressing plants.

Figure 31. Continued. (A) Phenotype of three-week-old plants that were exposed to drought stress by withholding water for nine days, followed by a period of rewatering of seven days. Photos were taken from fully watered plants, from plants after the drought stress phase and from plants after the recovery phase. Photos show one exemplary experiment. **(B)** Survival rates of the experiment described and shown in (A). Survival rates were calculated from results of three independent experiments ($n \geq 30$ for each experiment). Error bars represent SE. Asterisk indicates significant difference to the wild type (*, $p < 0.05$). **(C)** Time course of percental reduction of fresh weight from four-week-old cut leaves (leaf number six). Error bars represent SE. Letters indicate significant differences ($p < 0.05$) to the wild type (a = *erf105*, b = ERF105ox-1, c = ERF105ox-2).

Collectively, these results indicate that ERF105 is a positive regulator of drought tolerance in *Arabidopsis*.

3.6.2.2 ABA-related genes are differentially expressed in the erf105 *mutant during drought*

Levels of the plant hormone ABA are elevated in response to drought, primarily to promote stomatal closure and to induce the expression of drought stress-related genes, which are responsible for drought tolerance (Giraudat *et al.*, 1994; Shinozaki and Yamaguchi-Shinozaki, 1996). Accordingly, transcript levels of selected genes of the ABA biosynthesis, the ABA signaling and the ABA catabolic pathway were determined in the *erf105* mutant, *ERF105* overexpressing plants and wild type before and after drought treatment. This analysis revealed that in *erf105* non-treated plants the steady state mRNA levels of the ABA biosynthesis gene *NCED3* and of the transcription factor gene *ABI1* were about 2-fold increased compared to the wild type (Fig. 32 and Tab. A7). Transcript abundance of the ABA biosynthesis gene *ABA1* and of the transcription factor genes *ABI2, CBF4* and *RD29B* were reduced in *erf105* non-treated plants to about 37 %, 11 % and 28 %, respectively. *ERF105* overexpressing plants did not show notable differences in transcript levels compared to wild type. Drought provoked an increased expression of most ABA-related genes in all genotypes, except *ABA2*. However, the *erf105* mutant showed a stronger increase of *NCED3*, *ABI1*, *ABI5* and *RAB18* expression compared to wild type. In contrast, the expression of *CBF4* and *CYP707A3* were reduced in drought-treated *erf105* plants to 42 % and 54 %, respectively. The expression of ABA-related genes in drought-treated *ERF105* overexpressing plants was mostly similar to wild-type levels. Remarkable differences were the lower increase of *ABI5* and *RAB18* as well as the stronger increase of *CBF4* and *CYP707A3* expression compared to wild type.

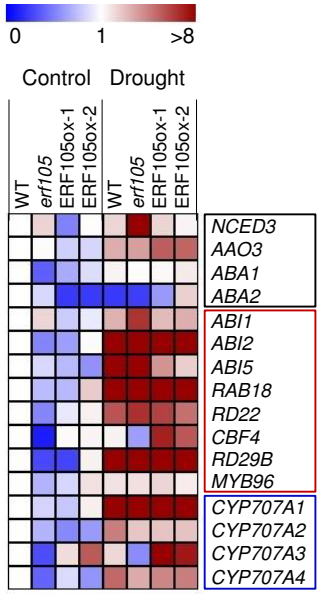

Figure 32. Expression of selected genes of the ABA biosynthesis, the ABA signaling and the ABA catabolic pathway in the *erf105* mutant and *ERF105* overexpressing plants before and after drought stress. Heat map of relative gene expression in the *erf105* mutant and *ERF105* overexpressing plants before and after drought stress by withholding water for nine days. The relative fold changes are shown compared to transcript levels of wild-type samples under control conditions which were set to 1 ($n \geq 4$). Genes of the ABA biosynthesis are framed in black, genes encoding transcription factors in red, and genes of the ABA catabolism in blue. The expression values represented in the heat map are shown in Table A7.

3.6.2.3 ERF105 might be a positive regulator of salt, osmotic and oxidative stress

Further stress experiments comprised watering plants with different chemicals. Two-week-old plants were exposed to stress by watering plants with NaCl or H_2O_2 (2.15.5). 26 days after germination, the phenotype of the *erf105* mutant, *ERF105* overexpressing lines and wild type were photographically documented and are shown in Figure 33A. The pictures document that watering plants with NaCl or H_2O_2 led to a retarded growth of all genotypes. These observations could be confirmed by determining the growth parameters shoot height, rosette diameter and fresh weight (Fig. 33B–D). Comparing the different genotypes, *erf105* plants exhibited the most retarded phenotype. Treatment with NaCl led to a 7 % shorter shoot, a 26 % smaller rosette and 30 % lower fresh weight compared to wild type. Similar, but stronger effects could be observed after H_2O_2 treatment which led to a 50 % shorter shoot, a 32 % smaller rosette and consequently a 58 % lower fresh weight. Furthermore, watering *erf105* plants with NaCl or H_2O_2 provoked a stress-induced leaf senescence (Fig. 33A). *ERF105* overexpressing lines did not exhibit an altered phenotype after NaCl or H_2O_2 treatment compared to wild type.

Additionally, plants were also treated with mannitol using the same experimental set up as described above and with the same outcome as observed in the NaCl and H_2O_2 experiments. Due to the redundancy of the results, the data are not shown.

In conclusion, these results indicate that ERF105 is a positive regulator of salt, osmotic and oxidative stress.

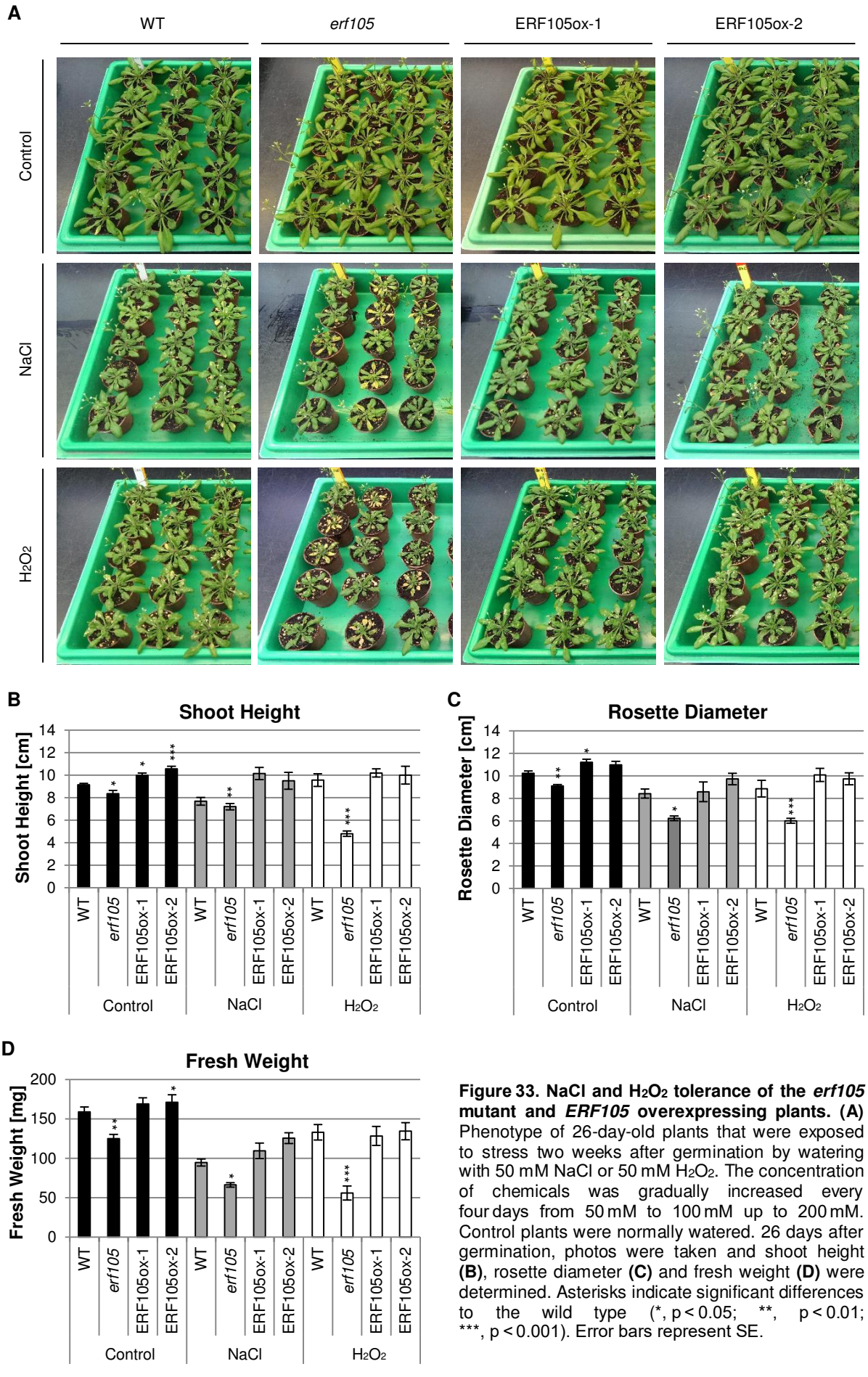

Figure 33. NaCl and H_2O_2 tolerance of the *erf105* mutant and *ERF105* overexpressing plants. (A) Phenotype of 26-day-old plants that were exposed to stress two weeks after germination by watering with 50 mM NaCl or 50 mM H_2O_2. The concentration of chemicals was gradually increased every four days from 50 mM to 100 mM up to 200 mM. Control plants were normally watered. 26 days after germination, photos were taken and shoot height **(B)**, rosette diameter **(C)** and fresh weight **(D)** were determined. Asterisks indicate significant differences to the wild type (*, $p < 0.05$; **, $p < 0.01$; ***, $p < 0.001$). Error bars represent SE.

4 DISCUSSION

In the following chapters, the results obtained in this study will be discussed. The first part is addressed to the question whether the four studied *ERF* transcription factor genes might have partially redundant functions, taken into account the results of *in silico* analyses, transcriptional and *promoter:GUS* expression analyses, protein interactions, and phenotypic investigations. The second part is focused on the *ERF105* gene which has been identified to play an important role in *Arabidopsis* freezing tolerance and cold acclimation. This is briefly summarized by Bolt *et al*., 2017 and described more detailed in this study. Furthermore, a role of *ERF105* in further abiotic stress responses will be discussed.

4.1 Characterization of *ERF102* to *ERF105* and the question of their functional redundancy

4.1.1 Evolutionary relationship and high sequence similarities suggest a functional redundancy of ERF102 *to* ERF105

The present study deals with the characterization of four phylogenetically closely related *ERF* genes. These genes are *ERF102* (AT5G47230; also known as *ERF5*), *ERF103* (AT4G17490; identical to *ERF6*), *ERF104* (AT5G61600), and *ERF105* (AT5G51190) and according to the classification of Nakano *et al*. (2006), they are members of group IXb of the *ERF* gene family. Sequence analyses have shown that just like a variety of other *ERF* transcription factor genes, *ERF102* to *ERF105* emerged from duplication events. Polyploidy studies in *Arabidopsis* by Blanc *et al*. (2003) indicated that *ERF102* and *ERF103* as well as *ERF104* and *ERF105* form gene pairs, which are the result of duplication events (Nakano *et al*., 2006). Amino acid sequence alignments of ERF102 to ERF105 using MUSCLE (Edgar, 2004) revealed a sequence similarity of 40 % between all four proteins with high conservation of the AP2/ERF domain. The protein pairs share 67 % (ERF102 and ERF103) and 52 % (ERF104 and ERF105) amino acid similarity (data not shown).

The evolutionary relationship and the high sequence similarities with conserved motifs such as the AP2/ERF domain, acidic regions that might function as transcriptional activation domains (Fujimoto *et al*., 2000) and putative MPK phosphorylation sites (Fig. 4B) indicate that ERF102 to ERF105 proteins might have redundant functions.

In addition to the phylogenetic relationship, this work revealed further aspects suggesting a functional redundancy of these four proteins. This will be discussed in the following sections.

4.1.2 ERF102 to ERF105: A potential regulatory hub in hormone and stress signaling

Phytohormones, or more often referred to as plant hormones, are small organic molecules produced by the plants themselves. They act either at their site of synthesis or, following their transport, elsewhere in plants (Wani *et al*., 2016). Plant hormones play important roles in regulating plant growth and developmental processes (Bari and Jones, 2009). Several plant hormones such as CK (Jeon *et al*., 2010; Wu *et al*., 2014), auxin (He *et al*., 2005), ET (Zhao and Schaller, 2004; Cheng *et al*., 2013), JA (Cela *et al*., 2011), ABA (Wu *et al*., 2007), GAs (Magome *et al*., 2008), SA (Jayakannan *et al*., 2015), and brassinosteroids (BR) (Divi *et al*., 2010) have been reported to be involved in stress signaling.

This study revealed that *ERF102* to *ERF105* are regulated by a number of hormones (Fig. 6). The four *ERF* genes showed individual response profiles to hormonal treatment but the majority shared significant aspects such as a rapid induction by CK and auxin and a rapid or slow downregulation by ABA and ET, respectively. Regarding the transcriptional regulation by abiotic stress, this study demonstrated that *ERF102* to *ERF105* are regulated by a variety of stress types (Fig. 7). All four genes were (rapidly and) transiently upregulated by cold and high light as well as upregulated by ROS 2 h after treatment. Heat, drought, salt, and osmotic stress treatments led to an increased expression level of individual *ERF* genes. The analyses of transcriptional regulation suggest that *ERF102* to *ERF105* play a role in multiple hormone and stress responses. In other studies, it has been shown that *ERF102* to *ERF104* were identified to be involved in plant immunity (Bethke *et al*. 2009; Son *et al*., 2012; Moffat *et al*., 2012; Meng *et al*., 2013). Regarding abiotic stress, ERF102 and ERF103 were shown to be regulators in osmotic stress response (Dubois *et al*., 2013; 2015). However, in this study *ERF103* was not regulated by the osmoticum mannitol, at least not after 2 h. ERF103 is also a regulator of oxidative stress (Wang *et al*., 2013; Sewelam *et al*., 2013) and was elucidated, in addition to ERF104 and ERF105, to be involved in the fast retrograde signaling response and acclimation response to high light (Vogel *et al*., 2014; Moore *et al*., 2014). A function for ERF105 in freezing tolerance and cold acclimation has been found in this study and has been recently published (Bolt *et al*., 2017).

The results of the transcriptional expression analyses of this work indicate pleiotropic functions of ERF102 to ERF105. Besides ERF102 to ERF105, several ERF transcription factors have been shown to be involved in hormone and stress signaling and thus to have pleiotropic functions. The most extensively studied ERF transcription factor is ERF1 (ERF100), a member of the ERF family group IXc (Nakano *et al*., 2006). ERF1 is involved in ET, JA, ABA and auxin signaling (Cheng *et al*., 2013; Mao *et al*., 2016) and regulates defense against necrotrophic pathogens (Berrocal-Lobo *et al*., 2002; Lorenzo *et al*., 2003) as well as salt, drought and heat tolerance (Cheng *et al*., 2013).

Thus, ERF102 to ERF105 may act as it was recently suggested (Müller and Munné-Bosch, 2015) for many other published ERF transcription factors as a regulatory hub, integrating hormone signaling in the plant response to a number of abiotic stresses. In this context, they may act partially in a functionally redundant manner.

4.1.3 The tissue-specific expression patterns of ERF102:GUS *to* ERF105:GUS *indicate a variety of functions*

The analysis of tissue-specific expression of *ERF102:GUS* to *ERF105:GUS* using *promoter:GUS* reporter lines showed partly similar expression patterns (Fig. 8–11). Expression of all four *ERF* driven reporter genes was detected shortly after germination in different cell types of the radicle of germinating seeds. Expression of *ERF102* to *ERF105* driven reporter genes could also be detected in distinct cell types of later developed roots.

To name two examples, *ERF102*, *ERF103* and *ERF105* driven reporter genes were expressed in the cortex cells that surround emerging lateral roots indicating that those genes may promote lateral root emergence. Interestingly, *ERF102*, *ERF103* and *ERF105* are regulated by CK and auxin, the key hormones with antagonistic functions of the regulation of, for instance, lateral root development (Casimiro *et al*., 2003; Benková *et al*., 2003; Swarup *et al*., 2008). Indeed, *erf102*, *35S*:ami103 lines and *erf105* had a reduced number of lateral roots (Fig. 16F, 17F and 19F).

ERF104 driven reporter gene showed a specific expression in the quiescent centers (QCs) of roots. Many functions have been attributed to the QC of the root apical meristem (RAM), from stem cell reservoir to pattern-generating center. It acts to suppress differentiation and to maintain the surrounding initial cells as stem cells (Doerner, 1998). The maintenance of the QC of the RAM is well characterized and involves two parallel pathways: the PLETHORA (PLT) pathway and the SHORT ROOT (SHR)/SCARECROW (SCR) pathway (Sabatini *et al*., 2003; Aida *et al*., 2004; Galinha *et al*., 2007). QCs of lateral roots and adventitious roots have equivalent functions and involve expression of the same genes that control QC and stem cell niche defintion and functioning in the RAM (Goh *et al*., 2016; Rovere *et al*., 2016).

The expression of the *ERF104* driven reporter gene in the QCs indicate that *ERF104* might support the function of the QCs by being involved in the well-characterized PLT or SHR/SCR network. However, in microarray analyses from Nawy *et al*. (2005) *ERF104* transcripts were not enriched in cells of the QC. Very interestingly, it has recently been published that *SCR* is a direct target of ERF104, but whether ERF104 functions as an activator or repressor of *SCR* has not been validated yet (Sparks *et al*., 2016). A further interesting point comes from yeast two-hybrid (Y2H) analyses performed in this study (data not shown). In two independent Y2H screens using a cDNA library from root callus cultures (Csaba Koncz, MPI Cologne, Germany, unpublished) MYB56 was identified to interact with ERF104. This interaction still has to be

validated *in planta*. MYB56, or also known as BRASSINOSTEROIDS AT VASCULAR AND ORGANIZING CENTER (BRAVO), acts through the BR signaling pathway and represses QC divisions which are mediated by, for instance, SCR (Di Laurenzio *et al.*, 1996; Vilarrasa-Blasi *et al.*, 2014). Consequently, it might be possible that ERF104 forms a heterodimer with MYB56 to regulate the expression of *SCR*.

Another example for the specific and non-redundant expression is the expression of the *ERF105* driven reporter gene in the stomata. This indicates a function of *ERF105* in regulating the exchange of water and CO_2 between the plant and atmosphere, albeit *ERF105* expression was not detected in published microarrays of guard cells (Yang *et al.*, 2008; Wang *et al.*, 2011).

Taken together, *ERF102* to *ERF105* driven reporter genes demonstrated similar but distinct expression patterns which support the hypotheses of a partial redundancy of the four *ERF* genes but also of functional diversity, respectively. Best examples for functional diversity are the expression of *ERF104:GUS* in the QCs and the expression of *ERF105:GUS* in the stomata. Further expression results suggest an involvement of the *ERF* genes in the development of the above-ground aerial organs such as shoot, leaves and reproductive organs. This is supported by analyses of loss-of-function and partly gain-of-function mutants (Fig. 16–19) and will be discussed later (see 4.1.5).

4.1.4 Protein interaction analyses of ERF102 to ERF105 indicate formation of homo- and heterodimers and protein interaction with MPK6

Proteins control all biological systems and rarely act in isolation but bind other biomolecules to elicit specific cellular responses. These biomolecules are often other proteins and a vast majority of proteins interact with others for proper biological activity (Marianayagam *et al.*, 2004). Thus, the capability of ERF102 to ERF105 to form dimers was also analyzed in this study (Fig. 13) and revealed that all proteins are capable to form homodimers in yeast. Heterodimerization was not noted in this experimental system between all four ERF proteins but, for instance, the highly homologue protein pairs ERF102/ERF103 as well as ERF104/ERF105 were identified to form heterodimers.

The capability of transcription factors to form heterodimers with other closely related transcription factors is described for many transcription factor families. For instance, members of the basic leucine-zipper (bZIP) (Dietrich *et al.*, 2011), WRKY (Chen *et al.*, 2010), basic helix-loop-helix (bHLH) (Liu *et al.*, 2013) as well as ERF transcription factor family (Cutcliffe *et al.*, 2011) are known to form heterodimers with members of their family. During the course of this study, the heterodimerization between ERF102 and ERF103 was published (Son *et al.*, 2012). The other identified formations of heterodimers, namely ERF104/ERF102, ERF104/ERF105, and ERF105/ERF102 as well as formation of homodimers need to be demonstrated using, for instance, bimolecular fluorescence complementation experiments (BiFC) (Ohad *et al.*, 2007)

not only to validate the interactions, but also to show that these interactions occur in plant cells. Moreover, an interesting point is to find out through which protein domain the interactions between the four ERF proteins occur. Since the AP2 domain has not only been considered for DNA-binding (Jofuku *et al*., 1994) but has also been demonstrated to be involved in protein-protein interactions (Okamuro *et al*., 1997; Chandler *et al*., 2007), it might be that the homo- and heterodimerization between ERF102, ERF103, ERF104, and ERF105 occurs through the AP2 domain. To investigate this in more detail, deletion analysis, mutagenesis and bioinformatics can be used to map the interaction domain.

The MPK cascades play important roles in mediating a broad spectrum of signals, including hormonal signals during development and biotic and abiotic stress signals in higher plants (Jia *et al*., 2016a). They transduce these signals into adaptive and programmed responses. The basic MPK module is composed of three sequentially activated kinases: MAPK kinase kinase (MAPKKK), MAPK kinase (MKK) and MPK. The MPK phosphorylates downstream substrates to elicit biological responses to various developmental requirements and environmental stimuli (Rodriguez *et al*., 2010; Jia *et al*., 2016a).

The *Arabidopsis* genome comprises 20 MPKs encoding genes (Jia *et al*., 2016a), one of these encoded MPKs, namely MPK6 was shown to interact with and to phosphorylate ERF104 to control defense responses (Bethke *et al*., 2009). Interactions of MPK6 with ERF102, ERF103 and ERF105 were demonstrated in this study (Fig. 14). During the course of this work, the interactions of MPK6 with ERF102 and ERF103 and their phosphorylation by MPK6 were published as well (Son *et al*., 2012; Wang *et al*., 2013). It was also published that the phosphorylation by MPK6 is important for the protein activation and stability of ERF103 and ERF104 (Bethke *et al*., 2009; Son *et al*., 2012; Wang *et al*., 2013). Thus, only the interaction between MPK6 and ERF105 needs to be validated using another method, for instance, co-immunoprecipitation (Co-IP) (Fiil *et al*., 2008) or BiFC. Additionally, the phosphorylation of ERF105 by MPK6 needs to be validated. For this purpose, immunoprecipitation-protein kinase assay can be used (Dickson, 2008). Based on the sequence homologies of ERF105 to the other three ERF proteins, and particular to ERF104, it is likely that ERF105 can also be phosphorylated by MPK6.

MPK6 is involved in multiple processes, including the regulation of shoot branching, plant height, lateral root development, flower filament elongation, hypocotyl gravitropism, and basipetal polar auxin transport in seedlings and main roots (Jia *et al*., 2016a). Moreover, MPK6 plays a role in the osmotic stress response (Zhao *et al*., 2017), pathogen defense (Bethke *et al*., 2009), oxidative stress response (Wang *et al*., 2013), the response to high light (Moore *et al*., 2014; Vogel *et al*., 2014), wounding (Li *et al*., 2017) as well as salt and cold stress (Teige *et al*., 2004; Furuya *et al*., 2014; Kim *et al*., 2017). This leads to the assumption that ERF102

to ERF105 might play a role in these processes as well. As mentioned above, for ERF102 to ERF105 it was indeed already shown that they are involved in some of these processes (4.1.2).

4.1.5 ERF102 *to* ERF105 *are probably involved in developmental processes*

In order to examine the biological functions of *ERF102* to *ERF105*, loss-of-function and gain-of-function mutants were analyzed regarding their growth phenotype under standard growth conditions (Fig. 16–19). Loss-of-function mutants of *ERF102* to *ERF104* tended to show a slightly reduced growth of shoot and/or roots, but the differences compared to wild type were subtle and the corresponding overexpressing lines did not all show the opposing phenotype and were indistinguishable from wild type. In contrast, *erf105* and *ERF105* overexpressing lines demonstrated a more severe phenotype. The *erf105* mutant exhibited a reduced shoot growth, a reduced number of side shoots and reduced numbers of siliques on the main stem as well as a smaller rosette, a reduced root growth and an early senescence. *ERF105* overexpressing lines mostly showed the opposing phenotype, but a delayed senescence could not be observed (Fig. 19).

The examined growth phenotypes correspond in part to the in the course of the study published growth phenotypes of loss-of-function and gain-of-function mutants of *ERF102* and *ERF103*. Thus, Son *et al*. (2012) also observed bigger rosettes of *ERF102* overexpressing lines. In contrast to this study, they additionally observed a slightly later flowering time of *erf102* and a slightly earlier flowering time of *ERF102* overexpressing plants compared to wild type. Sewelam *et al*. (2013) revealed smaller rosettes of a T-DNA insertion line of *ERF103* as observed in this work. In contrast, Dubois *et al*. (2013) could not detect any phenotypical differences in single knockout lines of *ERF102* and *ERF103*.

Some discrepancies between the observed phenotypes of this work and those of the publications can be explained by different growth conditions (for example soil composition, light intensities), lower/stronger expression levels of used overexpressing lines and the usage of different T-DNA insertion lines. For example, the available T-DNA insertion lines for *ERF103* that were used by Sewelam *et al*. (2013) and Dubois *et al*. (2013) were excluded from this study, since these lines were analyzed and either showed residual *ERF103* expression or the antibiotic resistance was lost.

ERF102 to *ERF105* are phylogenetically closely related genes. Particularly the protein pairs ERF102/ERF103 and ERF104/ERF105 are very similar at the amino acid level, interact with each other and are co-expressed in a large number of microarray experiments as analyzed using ATTED II, an *Arabidopsis thaliana* database of co-expressed genes and *cis*-elements for identifying co-regulated gene groups (Obayashi *et al*., 2007). This suggests a functional redundancy of the protein pairs and probably of all four ERF proteins as well. Therefore, double mutants homozygous for the knockout/knockdown for two of the four *ERF* genes were

generated. Due to technical problems, it was not possible to generate a double mutant homozygous for the *ERF103* and *ERF104* knockdown using the amiRNA technology: The cloning strategy was to clone the generated amiRNA precursors against *ERF103* and *ERF104* into two different binary vectors, one into the Gateway®-compatible destination vector pH2GW7 (Karimi *et al*., 2007b), the other into pORE-E4 (Coutu *et al*., 2007), and vice versa. Each of these vectors have a strong and constitutive promoter (pH2GW7: *35S* promoter, pORE-E4: *ENTCUP2* promoter from tobacco) as well as various antibiotic resistances. In order to introduce both amiRNA constructs into the wild type (double transformation), the use of the different antibiotic resistances was necessary for the selection of transformants. A further reason of the use of two different vectors with different promoters was to avoid *trans*-inactivations due to promoter homologies (Daxinger *et al*., 2008). Finally, gene expression analyses demonstrated that target genes that should have been downregulated with an amiRNA driven by the *ENTCUP2* promoter were not downregulated.
Furthermore, since *ERF102* and *ERF105* are coupled genes, it was not feasible to generate the corresponding double mutant by crossing the T-DNA insertion lines. Only in the later course of this study, more efficient genome editing technologies such as TALEN (transcription activator-like effector nucleases) or CRISPR/CAS (clustered regularly interspaced short palindromic repeats/CRISPR-associated protein) were established in plants (Zhang *et al*., 2013; Steinert *et al*., 2015).

The analysis of the growth phenotype of the double mutants *erf102,35S:*amiERF103; *erf102,35S:*amiERF104; *35S:*amiERF103,*erf105* and *35S:*amiERF104/105 did not show a phenotypic additive effect compared to the respective single mutants (data not shown), probably due to the fact that there was a remaining expression in the amiRNA lines. This assumption is supported by results of Dubois *et al*. (2013), which demonstrated a faster growth of the double mutant of *ERF102* and *ERF103* and finally larger rosettes than the wild type. Thus, the question whether or not there is functional redundancy of *ERF102* to *ERF105* has not been resolved yet, since no true null mutant alleles were available for all four *ERF* genes.

4.2 Characterization of ERF105

During the course of the study, several functions of *ERF102*, *ERF103* and *ERF104* have been published (Son *et al*., 2012; Moffat *et al*., 2012; Meng *et al*., 2013; Dubois *et al*., 2013; Vogel *et al*., 2014; Moore *et al*., 2014; Dubois *et al*., 2015). Thus, the focus of this thesis was set on the detailed characterization of the molecular function of *ERF105* and the results will be discussed in the following sections.

4.2.1 ERF105 is a novel regulator involved in the CBF cold signaling pathway and in acquired freezing tolerance

ERF105 is a transcription factor gene with a significant role in the cold stress response. Importantly, an *erf105* loss-of-function mutant showed a strongly reduced survival rate following cold treatment while *ERF105* overexpressing plants were more freezing tolerant (Fig. 21). Similarly, electrolyte leakage assays showed higher and lower LT_{50} values for *erf105* mutants and *ERF105* overexpressing plants, respectively (Fig. 22A). *erf105* mutants also had a lowered ability to adapt to cold conditions although they had not lost this ability. The increased sensitivity of *erf105* in the survival test was comparable to that shown by other mutants of the cold stress response, for example *ice1* (Chinnusamy *et al*., 2003) and even higher than of lines with reduced *CBF1*, *CBF3* or *COR15* expression, which hardly alters the response of non-acclimated plants (Novillo *et al*., 2007; Thalhammer *et al*., 2014a). Together the results indicate that ERF105 encodes a hitherto undiscovered component of the cold stress response pathway acting as a positive regulator of freezing tolerance and cold acclimation in *Arabidopsis*.

In the following sections, it will be proposed to integrate ERF105 into the known cold response network, mainly based on the results obtained with the loss-of-function *erf105* mutant (Fig. 34). Based on transcript data, ERF105 is suggested to play a role upstream of the *CBF* and *COR* genes activating these genes directly and/or indirectly through repression of *ZAT12*. Further, ERF105 was tentatively positioned downstream of a kinase. All close relatives of ERF105 (ERF102, ERF103, ERF104) show interaction with the mitogen-activated protein kinase MPK6 (Bethke *et al*., 2009; Son *et al*., 2012), which has a role in the response to cold stress (Teige *et al*., 2004; Furuya *et al*., 2014; Kim *et al*., 2017). An interaction of ERF105 with MPK6 was shown in this study (Fig. 14).

Several pathways mediating the response to cold are known. Among them the CBF pathway, involving the three transcription factors CBF1, CBF2 and CBF3, is the best characterized. Several regulators operating upstream of the *CBF* genes as well as their downstream targets have been identified. The former includes the transcription factors MYB15, ICE1, ICE2 and CAMTA3, the latter the CBF target genes *COR15A* and *COR15B*. The results of the transcript analyses of this work suggest that ERF105 has a function in this pathway and in the suggested model (Fig. 34), wherein ERF105 was positioned on a separate branch upstream of the *CBF* genes. This is supported by the finding that the transcriptional activation of all three *CBF* genes is strongly dampened in the *erf105* mutant (Figs. 23, 24, Tab. A1 and A2). The mutant showed both a lowered short-term induction of these genes following cold stress and a dampened long-term increase of their transcript levels during acclimation. In non-acclimated *erf105* plants, the initial rapid increase in *CBF* gene transcript levels in response to cold was lower and particularly strongly reduced for *CBF3*. This gene reached only about one fifth of the induction

level found in wild type, while *CBF1* and *CBF2* transcript levels reached about one third to half of the wild-type level. Moreover, the strong increase of *CBF* transcript levels during acclimation was completely missing (in case of *CBF2*) or strongly reduced. Notably, *CBF2* is the most relevant of the *CBF* genes during cold acclimation (Zhao *et al*., 2016). Consistent with the altered *CBF* gene responses, also the induction of CBF target genes, such as *COR15A* and *COR15B*, was lowered in both the short-term and long-term response to cold.

However, it should be noted that an increased expression of genes positioned presumably downstream of ERF105 (Fig. 34) – as suggested by their lowered transcript level in the *erf105* mutant – was not found in *ERF105* overexpressing plants, their transcriptional responses were mostly similar to wild type. It is possible that ERF105 is required but not the rate-limiting factor for the transcriptional activation of these target genes. Alternatively, the protein may possess inherent negative self-regulatory activity masking its action in overexpressing plants unless the negative regulatory domain is removed (for example Sakai *et al*., 2001) or it may function as part of a complex with another transcription factor.

In contrast to the *CBF* and *COR* genes, the transcript levels of other genes of the cold response pathway including *ICE1* and *MYB15* were not or not strongly altered in *erf105* mutants. Conversely, *ERF105* transcript levels are not affected in plants with altered *ICE1* expression (Lee *et al*., 2005). Together, this suggests that ERF105 operates on a branch of the cold signaling pathway that is distinct from these known components but upstream of the *CBF* and *COR* genes (Fig. 34).

A link of *ERF105* to the CBF regulon is also supported by similar kinetics of gene induction and tissue expression pattern of the *ERF105* and *CBF* genes. Following a cold treatment, *CBF1* to *CBF3* are rapidly induced and *ERF105* showed a similar response although the induction level is much lower. Analysis of *promoter:GUS* fusion gene revealed that *ERF105* is most strongly expressed in root tips, in the vascular tissue of roots and leaves, in the shoot apical meristem, in pedicles as well as in guard cells. This pattern is similar to those reported for *CBF1* and *CBF3* (Chow *et al*., 2014; Novillo *et al*., 2007), *ICE1* (Kanaoka *et al*., 2008) and *ZAT12* (Zimmermann *et al*., 2004).

The proposed regulation of the *CBF* genes by ERF105 could be direct or indirect, in the latter case possibly involving ZAT12. The response of the *ZAT12* gene in the *erf105* mutant contrasts with those of the *CBF* and *COR* genes, it was induced earlier and reached a 4-fold higher transcript level in *erf105* mutants than in wild type. ZAT12 encodes a zinc finger protein known to be a negative regulator of the CBF regulon, it is usually induced in parallel with these genes providing a negative regulatory feedback loop (Vogel *et al*., 2005). The transcriptional response of *ZAT12* in the *erf105* mutant suggests that ERF105 may act as a negative regulator of *ZAT12* gene expression and thereby allows for strong *CBF* gene induction upon cold treatment. Thus, high *ZAT12* gene expression in the *erf105* mutant could contribute to the

dampened *CBF* gene induction. ERF105 lacks the best-known plant-specific repressor motif ERF-associated amphiphilic repression (EAR) (Ohta *et al*., 2001; Nakano *et al*., 2006; Kagale and Rozwadowski, 2010) and may repress *ZAT12* via an unknown motif or may recruit a co-repressor protein. The latter option is consistent with the fact that the *ZAT12* gene does not possess the specific DNA-binding motif of ERF transcription factors, the GCC-box or the GCC-box core element in its promoter region (Hao *et al*., 1998), even though a DNA-binding through another *cis*-element might be possible.

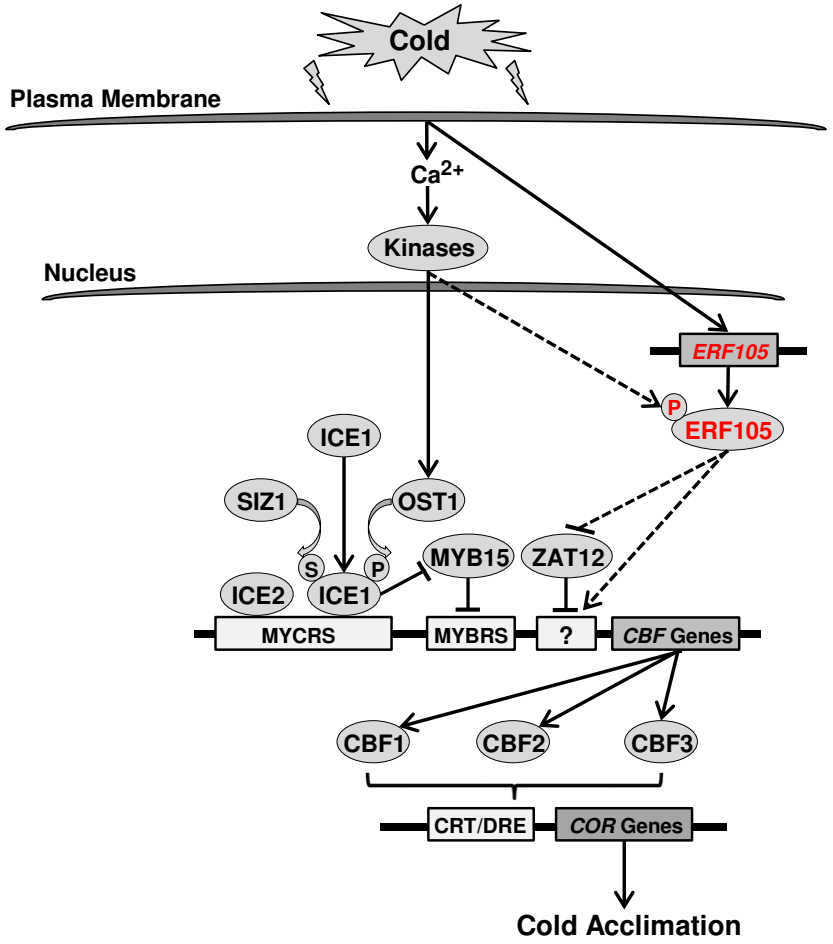

Figure 34. Model showing the proposed role of ERF105 in the known cold-responsive transcriptional network in *Arabidopsis*. Some major components involved in the CBF signaling pathway are shown. Based on transcript data, ERF105 is suggested to play a role upstream of the *CBF* and *COR* genes activating these genes directly and/or indirectly through repression of *ZAT12*. The proposed activation of ERF105 by a kinase is hypothetical but supported by the roles of MPK6 in the response to cold stress (Teige *et al*., 2004; Furuya *et al*., 2014; Kim *et al*., 2017) and the demonstrated interaction of MPK6 with ERF105 in this study. Arrows indicate positive regulation, lines ending with a bar indicate negative regulation. Dashed arrows and lines ending with a bar indicate suggested regulations. Question mark denotes an unknown regulatory *cis*-element. Abbreviations: ICE1/2, INDUCER OF C-REPEAT-BINDING FACTOR EXPRESSION 1/2; OST1, OPEN STOMATA 1; HOS1, HIGH EXPRESSION OF OSMOTICALLY RESPONSIVE GENES 1; ZAT12, ZINC FINGER OF ARABIDOPSIS THALIANA 12; CBF, C-REPEAT-BINDING FACTOR; COR, COLD-REGULATED; CRT/DRE, C-repeat element/dehydration-responsive element; MYBRS, MYB transcription factor recognition sequence; MYCRS, MYC transcription factor recognition sequence; U, ubiquitination; S, sumoylation; P, phosphorylation (Chinnusamy *et al*., 2007; Ding *et al*., 2015; Kim *et al*., 2015).

4.2.2 The increased freezing sensitivity of erf105 is not correlated with the concentration of osmoprotectants

The concentrations of various metabolites in the *erf105* mutants and *ERF105* overexpressing plants did not correlate well with the freezing tolerance phenotypes. During plant cold acclimation, compatible solutes such as Pro or sugars accumulate in leaf cells and there is evidence from several studies that such solutes are important for the development of freezing tolerance (Savouré *et al*., 1997; Xin and Browse, 2000). This conclusion is supported by the positive correlation of the content of Suc and Raf with freezing tolerance in different *Arabidopsis* accessions (Zuther *et al*., 2012). However, although the *erf105* mutant was less freezing tolerant before and after acclimation it contained more Glc and Fru than the wild type. There were also unexpectedly high amounts of Raf in both the non-acclimated *erf105* mutant and *ERF105* overexpressing plants. Together, this indicates that changes in the concentrations of these metabolites are not necessarily required for or linked to altered freezing tolerance. Consistently, others have described that metabolite profiles do not correlate with the cold acclimation capacity of *Arabidopsis* (Hannah *et al*., 2006), although many metabolites are changed (Cook *et al*., 2004; Kaplan *et al*., 2004). In addition, it was shown previously that Raf is not essential for basic freezing tolerance or for cold acclimation of *Arabidpsis thaliana* (Zuther *et al*., 2004) or the closely related species *Eutrema salsugineum*, where Pro seems to play a more dominant role (Lee *et al*., 2012). In *Arabidopsis*, on the other hand, Pro content after cold acclimation was not correlated with freezing tolerance in a collection of natural accessions (Zuther *et al*., 2012). Together, this indicates that metabolites may have a redundant role in plant freezing tolerance and it is possible that ERF105 operates largely independent from metabolic changes investigated here to alter freezing tolerance and cold acclimation. A possible mechanism could involve the regulation of genes such as *COR15A* and *COR15B*. Their expression is strongly reduced in *erf105* mutant plants during cold acclimation and a knockdown of these two genes is sufficient to significantly reduce *Arabidopsis* freezing tolerance in the absence of any changes in compatible solute content (Thalhammer *et al*., 2014a).

4.2.3 ERF105 probably contributes to the initiation of flavonoid biosynthesis by positively regulating the transcription factor genes MYB11, MYB12 and MYB111

Flavonoids are plant secondary polyphenolic metabolites which can be categorized into six major subgroups according to their molecular structures, namely chalcones, flavones, flavonols, flavandiols, anthocyanins, and proanthocyanidins (also called condensed tannins). *Arabidopsis thaliana* mainly accumulates three types of flavonoids, namely flavonols, anthocyanins, and proanthocyanidins (Li, 2014). The different flavonoids have diverse biological functions including coloration of flowers for recruiting pollinators and seed

dispersers, protection against ultraviolet radiation and phytopathogens, and amelioration of stress responses (Gould, 2004; Ferreyra *et al*., 2012). For instance, an accumulation of flavonoids is associated with enhanced resistance to the effect of chilling and freezing, whereby flavonoids may function as antioxidants or membrane stabilizers (Winkel-Shirley 2002; Schulz *et al*., 2015).

The flavonoid biosynthesis is well characterized in *Arabidopsis*. Flavonoids are synthesized through the phenylpropanoid pathway, transforming phenylalanine into 4-coumaroylCoA, which finally enters the flavonoid biosynthetic pathway (Ferreyra *et al*., 2012). The first enzyme of the flavonoid pathway, chalcone synthase (CHS), produces chalcone scaffolds from which all flavonoids derive. The early biosynthetic steps of flavonoid biosynthesis are controlled and activated by three R2R3-MYB proteins (MYB11, MYB12 and MYB111) (Mehrtens *et al*., 2005; Stracke *et al*., 2007). The production of anthocyanins and proanthocyanidins requires a ternary complex called MYB-bHLH-WD40 (MBW) complex, including the proteins PAP1, PAP2, TTG1/WD40, bHLH/TT8, to activate the late biosynthesis genes (Li, 2014). Low temperature leads to an induction of genes coding for transcription factors or enzymes involved in flavonoid biosynthesis, and consequently to an accumulation of flavonoids (Schulz *et al*., 2015).

Studies about the flavonoid biosynthetic pathway using mutant lines that are affected in different steps of this pathway demonstrated that mutations in genes encoding enzymes have only minor effects on the abundance of the transcripts of other genes involved in the flavonoid biosynthesis. In contrast, the triple knockout of the *MYB11*, *MYB12* and *MYB111* transcription factor genes results in a strongly reduced expression of key flavonoid biosynthesis genes such as *CHS/TT4*, *CHI/TT5* and *FLS*, particularly after cold acclimation (Schulz *et al*., 2016). In this study, 21 days cold-acclimated *erf105* plants showed only a weak induction of flavonoid biosynthesis genes compared to wild type (Fig. 26A and Tab. A3). Almost all analyzed genes were not as strongly induced as in wild type. Some genes, including genes coding for the transcription factors MYB11, MYB12 and MYB111, which are responsible for activation of the first enzymatic steps, were not induced in *erf105* plants at all.

A transcriptional regulation of every single component of the flavonoid biosynthesis by ERF105 is very unlikely. More likely, and corresponding to the data of Schulz *et al*. (2016) is that ERF105 regulates the expression of *MYB11*, *MYB12* and *MYB111* at least or particularly during cold stress leading to the weak induction of the downstream genes of the flavonoid biosynthetic pathway. Interestingly, although most of the transcripts of genes of the flavonoid biosynthesis were reduced in the *erf105* mutant 21 days after cold treatment, the content of anthocyanins did not change. Similar observations were made in the *myb11 myb12 myb111* mutant, which shows a strong reduction in the content of all flavonols, but not of anthocyanins (Schulz *et al*., 2016). Thus, the question is whether the flavonols are reduced in *erf105* as well.

Apart from that, flavonols are proposed to be the most important group of flavonoids participating in stress responses (Stafford, 1991; Pollastri and Tattini, 2011).
The transcriptional responses of flavonoid biosynthesis genes and the anthocyanin content in *ERF105* overexpressing plants were mostly similar to wild type. Possible explanations are described above (4.2.1) and include that ERF105 is required but probably not the rate-limiting factor for the transcriptional activation of these target genes.

Together, the striking lowered induction of transcript levels of flavonoid biosynthesis genes after cold treatment, the unchanged anthocyanin content in the *erf105* mutant after cold treatment, together with the data of Schulz *et al*. (2016) suggest that ERF105 probably contributes to the initiation of flavonoid biosynthesis by positively regulating the transcription factor genes *MYB11, MYB12* and *MYB111.* To test this hypothesis the flavonol content in the *erf105* mutant remains to be determined by liquid chromatography-mass spectrometry (LC-MS) analysis. A reduced flavonol content in the *erf105* plants would substantiate this hypothesis. Further evidence could be given by yeast one-hybrid (Y1H) analyses (Reece-Hoyes and Marian Walhout, 2012) by using the promoters of *MYB11, MYB12* and *MYB111* as bait and the ERF105 protein as prey. Another approach could be chromatin immunoprecipitation (Fiil *et al*., 2008) coupled to detection by quantitative real-time PCR (ChIP-qPCR) to study ERF105 binding to the promoters of candidate target genes.

4.2.4 The higher expression of the ROS-producing enzyme coding gene **RBOHD** *might contribute to the elevated ROS accumulation in* **erf105** *during cold*

Reactive oxygen species (ROS), including oxygen ions, free radicals, and peroxides are constantly produced as natural by-products of regular cell metabolism in plants, whereas photosynthesis is one of the main contributers to ROS production (Apel and Hirt, 2004; Giorgio *et al*., 2007). ROS can also be actively produced by enzymes and function as signaling molecules controlling processes such as growth, development, or response to biotic and abiotic environmental stimuli (Prasad *et al*., 1994; Mittler *et al*., 2011).
Cold stress is often accompanied by oxidative stress due to generation of ROS (Prasad *et al*., 1994; Suzuki and Mittler, 2006). In the experiments of this study, it was tried to avoid accessory oxidative stress by performing cold acclimation treatment at a lower light intensity than growth under control conditions. Additionally, for the electrolyte leakage measurements freezing of leaves was performed in the dark to exclude ROS formation in the chloroplast.
Nevertheless, ROS accumulation could be observed in all genotypes after cold acclimation. *erf105* plants accumulated more ROS compared to wild type (Fig. 27A and B). Interestingly, elevated ROS levels in *erf105* plants could also be detected before cold acclimation, indicating an increased stress level in this mutant.

Since high levels of ROS are harmful, plants have developed a sophisticated ROS scavenging system, comprised of enzymatic and non-enzymatic mechanisms to efficiently reduce ROS levels and to maintain ROS homeostasis (Apel and Hirt, 2004; Liu *et al*., 2016). Major enzymatic scavengers of plants are the superoxide dismutase (SOD), glutathione reductase (GR), catalases (CATs), ascorbate peroxidases (APXs), dehydroascorbate reductases (DHARs), and monodehydroascorbate reductases (MDHARs) (Asada, 2006; Sharma *et al*., 2012). *erf105* did not exhibit an altered transcript abundance of selected genes coding for ROS-scavenging enzymes (Tab. A4). Non-enzymatic scavengers of ROS comprise the antioxidants ascorbate, glutathione, tocopherols, carotenoids, alkaloids, and flavonoids (Apel and Hirt, 2004; Wang *et al*., 2006a). As mentioned above (3.6.1.4), the content of anthocyanins, a group of flavonoids, was not altered in *erf105*. No information can be given whether the *erf105* mutant has an altered content of the other numerated antioxidants, since these components were not quantified in this study.

One essential source for ROS during development and under biotic and abiotic stress conditions are ROS-producing NADPH/RESPIRATORY BURST OXIDASE HOMOLOGUES (RBOHs) (Sagi and Fluhr, 2006). Among the ten *RBOH* genes in *Arabidopsis* (Torres and Dangl, 2005), *RBOHD* is constitutively and ubiquitously expressed and shows a high degree of stress responsiveness both in shoots and roots (Suzuki *et al*., 2011). *RBOHD* is induced already after 3 h of cold treatment and after 24 h expression of *RBOHD* is back to the initial level (Suzuki *et al*., 2011). The transcript abundance of *RBOHD* was not altered in the *erf105* mutant under standard growth conditions compared to wild type. However, after 14 days and 21 days of cold acclimation *RBOHD* was induced 3-fold in the *erf105* mutant, whereas wild type did not show a *RBOHD* induction (Tab. A4). This could be a reason for the higher ROS accumulation of *erf105* after cold treatment, but an experimentally proven explanation for the higher ROS levels under standard growth conditions cannot be given yet.

Together, the elevated ROS content in *erf105* plants suggests a role for *ERF105* in regulating ROS homeostasis. The higher ROS content in *erf105* was not sufficient for chlorophyll degradation, probably due to the fact, that the ROS accumulation (Fig. 25C). The elevated ROS levels in *erf105* may probably due to lower amounts of non-enzymatic scavengers of ROS such as flavonols, which need to be analyzed yet (4.2.3). During cold, the higher expression of the ROS-producing enzyme coding gene *RBOHD* might contribute to the elevated ROS accumulation in *erf105*.

4.2.5 A misregulation of hormonal genes and an altered ABA content indicate an imbalance of hormonal homeostasis in the **erf105** *mutant*

Different hormones, including ABA, CK, ET, JA, GA, and BR, all known to have a role in the response to cold stress (Thomashow, 1999; Achard *et al*., 2008; Jeon *et al*., 2010; Li *et al*.,

2012; Shi *et al*., 2012; Hu *et al*., 2013), caused rapid changes in the *ERF105* transcript abundance and mostly also of the other three *ERF* genes (Fig. 6). Notably, the strongest hormonal response of all four genes was shown to ABA, which downregulated *ERF102* to *ERF105* transcript levels within 30 min to 2 h to between 10 % to 30 % of their levels before hormone treatment. The ABA-dependent cold signaling pathway has for long been regarded as operating largely independent of the CBF pathway. However, some downstream genes can be activated by both pathways (Heino *et al*., 1990; Gilmour and Thomashow 1991) and recent work has shown that the transcription factor MYB96 integrates the ABA and CBF pathways (Lee and Seo, 2015). Another evidence for the integration of the ABA pathway into the CBF pathway is OST1, a serine/threonine protein kinase activated by ABA (Mustilli *et al*., 2002), additionally regulates *CBF* expression through phosphorylation and activation of ICE1 (Ding *et al*., 2015).

Levels of the plant hormone ABA are transiently elevated in response to cold (Chen *et al*., 1983) and exogenous application of ABA at non-acclimating temperatures has been shown to enhance freezing tolerance (Lang *et al*., 1994). Intriguingly, under standard growth conditions and particularly after cold treatment, the *erf105* mutant possesses a higher content of physiologically active and inactive forms of ABA than wild type (Fig. 29). This is likely to be in part due to the higher expression of *NCED3*, encoding a key enzyme in the biosynthesis of ABA (Tan *et al*., 1997), as well as the higher expression of *CYP707A1* and *CYP707A4* genes encoding enzymes involved in ABA catabolism (Saito *et al*., 2004), respectively (Fig. 28 and Tab. A5). Interestingly, the elevated ABA content in *erf105* did not lead to a higher freezing tolerance. The elevated content of ABA in the *erf105* mutant suggests that ERF105 might be a negative regulator of ABA metabolism. Conversely, *ERF105* is negatively regulated by ABA, that suggests a negative feedback mechanism between ABA and *ERF105*. Thus, ABA may inhibit the inhibition of its own metabolism. This point is very speculative and needs to be examined in more detail.

Notably, there are crosstalks between the different plant hormones resulting in synergistic or antagonistic interactions (Peleg and Blumwald, 2011). *ERF105* is also regulated by other hormones (Fig. 6). A limited analysis of hormone-related genes (genes of the GA metabolism) revealed that *GA2OX2*, a gene involved in GA catabolism (Thomas *et al*., 1999) was strongly increased, and the GA biosynthesis genes *GA3OX1* (Chiang *et al*., 1995) and *GA3OX2* (Yamaguchi *et al*., 1998) were strongly reduced in *erf105* 14 days after cold acclimation compared to wild type. This indicates that the homeostasis of more than one hormone might be altered. It is conceivable that this might contribute to the cold stress phenotype of *erf105*.

In sum, the misregulations of several hormonal genes of the ABA and GA metabolism as well as the altered ABA content indicate an imbalance of hormonal homeostasis in the *erf105* mutant. It will be interesting to study whether the regulation of ERF105 by ABA and other

hormones has a function in integrating different cold response pathways, possibly in order to fine-tune the cold stress response.

4.2.6 ERF105 is a positive regulator in the drought stress response and might act independent from ABA

Drought is one of the principal abiotic stresses which affects plants in many respects, particularly the growth and yield of plants (Beck *et al*., 1997; Vishwakarma *et al*., 2017). More than half of the terrestrial earth is susceptible to drought each year, resulting in water-supply shortages and losses of agricultural production culminating to human suffering and famine (Kogan, 1997). For this reason, the effects of drought have been studied extensively. So far, many genes have been identified to be involved in the drought stress response, including genes encoding transcription factors from the DREB, ERF, MYB, MYC, WRKY, bZIP, and zinc finger transcription factor families (Joshi *et al*., 2016).

This study revealed the transcription factor ERF105 is involved in the positive regulation of drought tolerance in *Arabidopsis*. The *erf105* mutant showed a strongly reduced survival rate following drought treatment (Figs. 28A and B). Interestingly, a T-DNA insertion mutant of one of the best studied drought response genes, namely *DREB2A,* does not show phenotypic changes under drought stress conditions, probably due to a functional redundancy of *DREB2A* and the other seven *DREB2* gene family members (Sakuma *et al*., 2006a). *ERF105* overexpressing plants exhibited a survival rate of 80 %, and thus were more drought tolerant than wild-type plants, which showed a survival rate of 55 % (Fig. 31). The increased drought tolerance of *ERF105* overexpressing lines was comparable to that of *DREB2A* overexpressing plants (Sakuma *et al*., 2006a).

Drought signaling can be mediated via ABA or independent from ABA (Shinozaki *et al*., 2003). The ABA-dependent pathway involves the ABA-mediated regulation of genes belonging to the *MYB*, *MYC* and *AREB/ABF* transcription factor gene families as well as *CBF4*. These genes in turn regulate the expression of many downstream target genes, including genes from the *COR/LEA* family (Haake *et al*., 2002; Sakuma *et al*., 2006a). ABA-independent drought signaling involves the induction of *DREB2* family genes, which regulate basically the same downstream target genes as the ABA-induced genes (Haake *et al*., 2002; Shinozaki and Yamaguchi-Shinozaki, 2007).

Since *ERF105* is strongly negatively regulated by ABA (Fig. 6D), a potential involvement of *ERF105* in the drought signaling pathway might be ABA-independently, or there might be a regulatory feedback loop between ABA and *ERF105*. It remains to be elucidated whether the *DREB2* genes are regulated differently in the *erf105* mutant and the *ERF105* overexpressing lines, or whether *ERF105* might form a separate branch in the ABA-independent drought signaling pathway.

Despite the importance of a crosstalk between ABA-dependent and ABA-independent pathways, knowledge of how the two signaling pathways regulate each other has been limited until recently (Yoshida *et al.*, 2014). Since *CBF4* is strongly downregulated in the *erf105* mutant before and after drought treatment, and upregulated in *ERF105* overexpressing lines after drought treatment (Fig. 32 and Tab. A7), it might be possible that *ERF105* is a regulatory link between the ABA-dependent and ABA-independent drought signaling pathway. This could be realized, if ERF105 would regulate both, the ABA regulated *CBF4* gene as well as the ABA-independently acting *DREB2* gene(s).

In collaboration with Prof. Dr. Nicolaus von Wirén and Dr. Seyed Abdollah Hosseini (IPK Gatersleben, DE) drought recovery experiments as well as analyses of transcript profiles of ABA-related genes using *erf105* and *ERF105* overexpressing plants were performed similar to those performed in this study. These analyses confirmed the results of this study (data not shown). Moreover, ABA measurements were performed demonstrating that under control conditions the *erf105* mutant had twice as much ABA as observed in the above-mentioned experiment (3.6.1.6 and Fig. 29). After a drought period of three weeks, *erf105* plants accumulated twice as much ABA and its metabolites PA and DPA as wild type, probably due to the higher expression of the ABA biosynthesis gene *NCED3* in *erf105* compared to wild type (Fig. 32 and Tab. A7). *ERF105* overexpressing lines did not show an altered ABA accumulation compared to wild type, neither before nor after drought treatment (data not shown), which is consistent with the results described above (Fig. 29).

Many genes of the drought and cold signaling pathway are induced by both drought and cold stress, suggesting the existence of a complex gene network for specificity and crosstalk in abiotic stress-responsive gene expression (Shinozaki and Yamaguchi-Shinozaki, 2000; Shinozaki *et al.*, 2003). Moreover, response mechanisms of drought and cold stress are similar. Thus, accumulation of osmoprotectants and flavonoids (Verbruggen and Hermans, 2008; Nakabayashi *et al.*, 2014; Schulz *et al.*, 2015) occur in response to both stress types to counteract the common symptom, namely dehydration (Shinozaki *et al.*, 2003). Whether or not there is an altered accumulation of these components as well as of ROS in the *erf105* mutant and *ERF105* overexpressing lines after drought stress, needs to be determined yet. However, it might be that the drought stress response mechanisms in *erf105* are similarly affected to that of the cold stress response.

4.2.7 ERF105 is probably a positive regulator in the osmotic and oxidative stress response

Further stress experiments revealed that ERF105 might additionally be a positive regulator of the osmotic, salt, and oxidative stress response. *erf105* mutants showed not only a strongly

retarded growth compared to wild type after stress treatment by watering plants with mannitol, NaCl, or H_2O_2, but additionally exhibited stress-induced leaf senescence (Fig. 33). *ERF105* overexpressing lines did not exhibit an altered phenotype after mannitol, NaCl, or H_2O_2 treatment compared to wild type. Therefore, it would be interesting to treat particularly wild type and *ERF105* overexpressing plants longer and/or with higher concentrations of those chemicals. The intention of this experiment would be to administer a stronger stress treatment probably revealing phenotypic differences, and probably a higher stress tolerance of *ERF105* overexpressing lines, respectively.

It is not surprising that besides cold and drought stress ERF105 may also be involved in the osmotic and/or salt stress response, since it has often been commented that drought and cold stresses cause osmotic stress. This is why salt, drought and cold stresses induce some common sets of plant genes and thus similar stress tolerance mechanisms (Shinozaki and Yamaguchi-Shinozaki, 1997; Zhu, 2001). The osmotic stress signaling also proceeds via the ABA-dependent and ABA-independent pathway (Yoshida *et al*., 2014). It is well possible that the functional role of ERF105 in response to drought and osmotic stress is similar.

Besides osmotic changes, salt stress leads to a disruption of plant ion homeostasis resulting in an excess of toxic Na^+ in the cytoplasm and a deficiency of essential ions such as K^+ (Zhu, 2002). The ionic stress signaling and tolerance is mediated by the SALT OVERLY SENSITIVE (SOS) pathway that comprises the *SOS1*, *SOS2*, and *SOS3* genes, and that has been proposed to mediate cellular signaling under salt stress to maintain ion homeostasis (Halfter *et al*., 2000; Shi *et al*., 2000; Munns *et al*., 2008). In case of the performed salt stress experiment, it remains to be elucidated whether the higher sensitivity to salt in the *erf105* mutant resulted from the osmotic and/or ionic changes within the plant, and thus whether or not ERF105 has a function during salt stress. Therefore, further experiments, for instance, transcriptional analyses regarding genes involved in the SOS pathway could provide evidence.

A possible role of ERF105 in the oxidative stress response has been described above (4.2.4). The *erf105* mutant possesses an elevated ROS content under standard growth conditions as well as under cold stress conditions (Fig. 27), indicating that ERF105 is involved in the oxidative stress response. Not surprisingly, treatment with H_2O_2 showed a higher susceptibility of *erf105* plants compared to wild type. One could argue that due to the elevated ROS content the *erf105* mutant is already stressed per se, leading to a probably higher susceptibility of this mutant for further stresses. However, the fact that several genes that are specific for the cold signaling (*CBF1*, *CBF2*, *CBF3*), for the drought and osmotic stress signaling (*CBF4*), or genes that are involved in all three stresses (*COR* genes) are differently regulated in the *erf105* mutant, argues against a generally enhanced unspecific stress sensitivity and supports a more specific role of ERF105.

4.3 Conclusions and future perspectives

The following chapter will highlight the most important conclusions and the most promising future perspectives will be suggested.

In the first part of this work, the four phylogenetically closely related ERF transcription factors ERF102 to ERF105 were descriptively characterized. As it is expected for transcription factors, ERF102-GFP to ERF105-GFP fusion proteins were predominantly located to the nucleus (Fig. 12). The results from the analyses of amino acid sequences, the transcriptional regulations, the tissue-specific expression patterns, protein interactions, the growth phenotypes as well as data published by others showed pleiotropic and partly overlapping functions of ERF102 to ERF105 in plant development and the stress response. In conclusion, ERF102 to ERF105 act in a partly redundant fashion, whereas the redundancy is higher between the more closely related protein pairs ERF102/ERF103 and ERF104/ERF105. Therefore, it would be interesting for future experiments to focus on further studies of double mutants as well as higher order mutants.

ERF102 to *ERF105* have been already reported in several recent publications to be associated with the response to biotic and abiotic stresses, their role in regulating plant development has not been well characterized. Since *ERF102* to *ERF105* driven reporter genes were strongly expressed in roots (Figs. 8–11), it might be worthwhile to study in more detail the function(s) of the four *ERF* genes in roots. In this context, it could be of special interest to analyze the potential role of *ERF104* in the QC of roots as the *ERF104* driven reporter gene was specifically expressed in QC cells. In particular, ERF104 is possibly a direct regulator of a well-known regulator of cell specification in roots, which is *SCR*. Recently, in enhanced yeast one-hybrid (eY1H) assays ERF104 has been shown to bind to the promoter of *SCR* (Sparks *et al*., 2016). The question whether *SCR* is activated or repressed by ERF104 could be answered by examining the transcript abundance and expression pattern of *SCR* in *ERF104* loss-of-function and gain-of-function mutants. For this purpose, the generated *35S*:amiERF104 and *ERF104* overexpressing lines could be used. *35S*:amiERF104 and *ERF104* overexpressing lines exhibited an altered root elongation and an altered number of lateral roots (Fig. 18E and F). It would be interesting to take a closer look to the organization of the root meristem and the QC, and to compare it with the *scr* mutant. In this study, it was suggested that ERF104 might form a heterodimer with MYB56 (BRAVO) to regulate the expression of *SCR* (see 4.1.3). If the interaction of ERF104 with MYB56 would be validated *in planta*, it would be informative to perform genetic crossings between loss-of-function mutants of *MYB56* and *ERF104*. Moreover, to visualize the potential phenotypic consequences of the knockout/knockdown of *MYB56* and/or *ERF104,* the analysis of crossings between single and double loss-of-function mutants of *MYB56* and *ERF104* and QC specific promoter trap lines (Sabatini *et al*., 2003) might be informative.

The second part of this study dealt with the more detailed characterization of ERF105, which has been identified to be a positive regulator in the response to cold, drought, osmotic, salt, and oxidative stress. The function of ERF105 during cold stress was examined in more detail and the following questions have been addressed: Is ERF105 involved in the CBF cold signaling pathway, and if so, where can ERF105 be positioned in this pathway? What is/are the reason/s for the higher cold sensitivity of the *erf105* mutant? Does *erf105* accumulate less osmoprotectants, less flavonoids, less ABA and/or more ROS than the wild type? These questions could be answered, however not all results corresponded to the expectations based on the literature. To name one example: Since ABA is transiently elevated in response to cold (Chen *et al*., 1983), and exogenous application of ABA at non-acclimating temperatures has been shown to enhance freezing tolerance (Lang *et al*., 1994), one could expect that *erf105* has a reduced ABA accumulation. In contrast, *erf105* accumulated more ABA, even without cold treatment (4.2.5). Interestingly, the elevated ABA content in *erf105* did not lead to a higher freezing tolerance.

Several parameters contributing to cold tolerance were changed in the *erf105* mutant. However, it is not clear which of these contributes the most to the higher cold sensitivity of *erf105* or which might be indirect consequences. For instance, ABA promotes the ROS production via induction of the ROS producing NADPH oxidase coding genes *RBOHD* and *RBOHF* (Kwak *et al*., 2003; Jiao *et al*., 2013). It might be possible that the increased ROS level in *erf105* is due to the elevated ABA level. However, *ERF105* probably regulates both, genes encoding ABA metabolism as well as *RBOHD*. Whether or not the elevated ABA and/or the elevated ROS content in *erf105* contribute to the cold sensitivity is not yet clarified.

ERF105 has been suggested to be involved in the CBF cold signaling pathway. ERF105 was tentatively positioned downstream of MPK6 and acting independent of ICE1 upstream of the *CBF* and *COR* genes, possibly activating these genes directly and/or indirectly through repression of *ZAT12* (Fig. 33). To test this hypothesis, genetic approaches as well as molecular analyses will be helpful. First, the interaction between MPK6 and ERF105 and the putative phosphorylation of ERF105 need to be validated by an immunoprecipitation-protein kinase assay (Dickson, 2008). Furthermore, cold stress experiments with a *mpk6* mutant harboring the *35S:ERF105* allele can yield information whether the phosphorylation of ERF105 by MPK6 is needed for mediating cold tolerance. Secondly, cold experiments with a genetic crossing of an *ice1* mutant and *erf105* might unravel whether ERF105 acts ICE1-independently on a separate branch in the CBF cold signaling pathway. Thirdly, if the cold sensitivity phenotype of *erf105* would be reversed in cold experiments in the *zat12* mutant background, this would contribute to resolve the question whether *ZAT12* is a target of ERF105. Molecular analyses, for instance ChIP-qPCR, can be used to validate putative ERF105 target genes, not only *ZAT12*. Further candidate genes are the *CBF* genes (from the CBF cold signaling pathway,

Chinnusamy *et al*., 2003), *MYB11*, *MYB12*, *MYB111* (from the flavonoid biosynthetis pathway, Stracke *et al*., 2007), *NCED3* (ABA biosynthesis, Tan *et al*., 1997), *CBF4* (drought stress signaling, Haake *et al*., 2002), and *RBOHD* (encoding a ROS producing NADPH oxidase, Suzuki *et al*., 2011).

It remains to be seen what portion of the cold-responsive transcriptome is controlled by ERF105. Also the potential roles of ERF102, ERF103 and ERF104 need to be explored. Their close phylogenetic relationship to ERF105 and their similar, although weaker, response to different triggers including cold and various hormones as well as further results of this study described above, suggest that these *ERF* genes have partially redundant functions. Indeed, as an outcome of a transcriptomic study two of these genes, *ERF102* and *ERF103*, have been proposed to be a component of the cold signaling pathway (Park *et al*., 2015).

5 SUMMARY

The *ETHYLENE RESPONSE FACTOR* (*ERF*) genes of *Arabidopsis thaliana* form a large family encoding plant-specific transcription factors. In this work, four phylogenetically closely related *ERF* genes were characterized. These genes, *ERF102* (AT5G47230; also known as *ERF5*), *ERF103* (AT4G17490; identical to *ERF6*), *ERF104* (AT5G61600) and *ERF105* (AT5G51190) are members of group IXb of the ERF family.

In the first part of this study, *ERF102* to *ERF105* were descriptively characterized. Transcriptional expression analyses revealed that *ERF102* to *ERF105* were regulated by a number of hormones as well as various abiotic stresses. Analyses of tissue-specific expressions using *promoter:GUS* reporter lines demonstrated similar but distinct expression patterns of *ERF102:GUS* to *ERF105:GUS*, which were particularly expressed in roots. ERF102-GFP to ERF105-GFP fusion proteins were nuclear localized. Protein interaction analyses indicate formation of homo- and heterodimers as well as interaction of all four ERF proteins with the MITOGEN-ACTIVATED PROTEIN KINASE6 (MPK6). In order to examine the biological functions of *ERF102* to *ERF105*, loss-of-function and gain-of-function mutants were analyzed regarding their growth phenotype under standard growth conditions. The loss-of-function of single *ERF* genes resulted in a slightly reduced plant growth, whereas overexpression of the *ERF* genes under control of the CaMV *35S* promoter led to a slightly increased growth. The analysis of the growth phenotype of double mutants did not show a phenotypic additive effect compared to the respective single mutants.
The results from the analyses of amino acid sequences, the transcriptional regulations, the tissue-specific expression patterns, protein interactions, the growth phenotypes as well as data published by others showed pleiotropic and thus overlapping functions of *ERF102* to *ERF105* in plant development and stress response.

The second part of this study dealt with the more detailed functional characterization of *ERF105*, which has a particularly relevant role in the cold stress response. Expression analyses revealed that *ERF105* is early and transiently upregulated by cold. In electrolyte leakage and plant survival tests, loss-of-function and gain-of-function (overexpressing) plants of *ERF105* showed reduced and enhanced freezing tolerance, respectively.
Consistent with the freezing tolerance phenotype, *erf105* mutants showed a decreased expression of numerous cold-responsive genes, such as *CBF1*, *CBF2* and *CBF3* and several *COR* genes in non-acclimated plants as well as after cold acclimation at 4 °C. Based on the examined transcript data and protein interaction analysis with MPK6, ERF105 was suggested to be integrated in the CBF cold signaling pathway. ERF105 was tentatively

positioned downstream of MPK6 and acting independent of ICE1 upstream of the *CBF* and *COR* genes, activating these genes directly and/or indirectly through repression of *ZAT12*.

The increased freezing sensitivity of *erf105* was not correlated with the concentrations of proline, soluble sugars or ABA, which typically accumulate during cold and function as, for instance, osmoprotectants or signaling molecules for regulating gene expression. However, an elevated ROS accumulation in *erf105* could be detected before and after cold acclimation at 4 °C. Flavonoids are accumulated during cold as well and are associated with enhanced resistance to the effect of chilling and freezing, whereby flavonoids may function as antioxidants or membrane stabilizers. ERF105 probably contributes to the initiation of flavonoid biosynthesis by positively regulating the transcription factor genes *MYB11*, *MYB12* and *MYB111*, which control and activate the early biosynthetic steps of flavonoid biosynthesis.

Furthermore, ERF105 has been identified to be a positive regulator in the response to drought, osmotic, salt, and oxidative stress, but its precise molecular function in the response to these stress types needs to be determined yet.

6 ZUSAMMENFASSUNG

Die *ETHYLENE RESPONSE FACTOR* (*ERF*) Gene in *Arabidopsis thaliana* kodieren für eine große pflanzenspezifische Transkriptionsfaktorfamilie. In dieser Arbeit wurden vier phylogenetisch eng verwandte *ERF*-Transkriptionsfaktorgene charakterisiert. Diese Gene sind *ERF102* (AT5G47230; oder auch *ERF5*), *ERF103* (AT4G17490; oder auch *ERF6*), *ERF104* (AT5G61600) sowie *ERF105* (AT5G51190), und sind der Gruppe IXb der ERF-Familie zugehörig.

Der erste Teil dieser Arbeit bestand in der deskriptiven Charakterisierung von *ERF102* bis *ERF105*. Analysen der Expression von *ERF102* bis *ERF105* zeigten, dass diese durch eine Vielzahl von Hormonen sowie verschiedene abiotische Stressarten reguliert wurden. Dies deutet darauf hin, dass diese Gene pleiotrope Funktionen erfüllen. Analysen der gewebespezifischen Expression unter Verwendung von *Promotor:GUS*-Reporterlinien offenbarten, dass *ERF102:GUS* bis *ERF105:GUS* einerseits ähnliche, aber auch distinkte Expressionsmuster aufwiesen und vor allem in der Wurzel exprimiert wurden. ERF102-GFP bis ERF105-GFP Fusionsproteine waren im Zellkern lokalisiert. Proteininteraktionsanalysen wiesen auf die Bildung von Homo- und Heterodimeren sowie die Interaktion aller vier ERF-Proteine mit der MITOGEN-AKTIVIERTEN PROTEIN KINASE6 (MPK6) hin. Um die biologischen Funktionen von *ERF102* bis *ERF105* zu untersuchen, wurden *Loss-of-function*- und *Gain-of-function*-Mutanten hinsichtlich ihres Phänotyps unter normalen Wachstumsbedingungen analysiert. Der Verlust der Funktion einzelner *ERF*-Gene führte zu einem leicht reduzierten Pflanzenwachstum, während die Überexpression der *ERF*-Gene unter Kontrolle des CaMV *35S*-Promotors zu einem leicht verstärkten Wachstum führte. Die Analyse des Wachstumsphänotyps von Doppelmutanten zeigte im Vergleich zu den jeweiligen Einzelmutanten keine additive phänotypische Wirkung.
Die Ergebnisse aus den Analysen der Aminosäuresequenzen, der transkriptionellen Regulation, der gewebespezifischen Expressionsmuster, der Proteininteraktionen, der Wachstumsphänotypen sowie Ergebnisse von anderen veröffentlichten Studien deuten auf pleiotrope und damit zum Teil gleiche Funktionen von *ERF102* bis *ERF105* in der Pflanzenentwicklung und der Stressantwort hin.

Der zweite Teil dieser Studie beschäftigte sich mit der detaillierteren funktionellen Charakterisierung von *ERF105*, das eine besonders relevante Rolle bei der Kältestressreaktion spielt. Expressionsanalysen zeigten, dass *ERF105* schnell und transient durch Kälte hochreguliert wurde. Die *Loss-of-function*-Mutante von *ERF105* zeigte in Elektrolytverlustmessungen und Pflanzenüberlebenstests eine reduzierte Kältetoleranz,

während *Gain-of-function*-Mutanten (Überexpressionsmutanten) eine verbesserte Kältetoleranz aufwiesen.

In Übereinstimmung mit dem Kältephänotyp zeigten sowohl nicht-akklimatisierte *erf105*-Mutanten als auch *erf105*-Mutanten nach einer Kälteakklimatisierung bei 4 °C eine verminderte Expression zahlreicher kälteregulierter Gene, wie beispielsweise *CBF1*, *CBF2* und *CBF3* sowie mehrere *COR*-Gene. Basierend auf den untersuchten Genexpressionsdaten und der Proteininteraktionsanalyse mit MPK6 wird daher zur Diskussion gestellt, ERF105 in den CBF-Kälte-Signaltransduktionsweg zu integrieren. Es wird vorgeschlagen, ERF105 *downstream* von MPK6 zu positionieren. ERF105 agiert vermutlich unabhängig von ICE1 und reguliert die *CBF*- und *COR*-Gene möglicherweise direkt und/oder indirekt durch Repression von *ZAT12*.

Die erhöhte Kälteempfindlichkeit von *erf105* korrelierte jedoch nicht mit den bei Kälte akkumulierenden Konzentrationen von löslichen Zuckern, Prolin oder ABA, welche beispielsweise als Osmo-Schutzmittel oder als Signalmoleküle zur Regulierung der Genexpression fungieren. Allerdings konnte eine erhöhte ROS-Akkumulation in *erf105* sowohl vor als auch nach Kälteakklimatisierung bei 4 °C nachgewiesen werden. Flavonoide akkumulieren ebenfalls bei Kälte und tragen zu einer erhöhten Resistenz gegenüber kühlen Temperaturen unter 10 °C, aber auch Temperaturen unter 0 °C bei, indem sie beispielsweise als Antioxidantien oder Membranstabilisatoren fungieren. Die ersten enzymatischen Schritte der Flavonoidbiosynthese werden durch die für Transkriptionsfaktoren kodierende Gene *MYB11*, *MYB12* und *MYB111* kontrolliert und aktiviert. ERF105 trägt vermutlich zur Initiierung der Flavonoidbiosynthese bei, indem es die Transkriptionsfaktorgene *MYB11*, *MYB12* und *MYB111* positiv reguliert.

Darüber hinaus wurde ERF105 in dieser Arbeit auch als positiver Regulator in der Reaktion auf Trockenstress, osmotischen Stress, Salz- und oxidativen Stress identifiziert. Die genaue molekulare Funktion von ERF105 in der Reaktion auf diese Stressarten muss jedoch noch näher analysiert werden.

7 REFERENCES

Abràmoff MD, Magalhaes PJ, Ram SJ (2004) Image processing with ImageJ. J Biophotonics **11:** 36–43

Achard P, Gong F, Cheminant S, Alioua M, Hedden P, Genschik P (2008) The cold-inducible CBF1 factor-dependent signaling pathway modulates the accumulation of the growth-repressing DELLA proteins via its effect on gibberellin metabolism. Plant Cell **20:** 2117–2129

Adams RM, Hurd BH, Lenhart S, Leary N (1998) Effects of global climate change on agriculture: an interpretative review. Clim Res **11:** 19–30

Agarwal M, Hao Y, Kapoor A, Dong CH, Fujii H, Zheng X, Zhu JK (2006) A R2R3 type MYB transcription factor is involved in the cold regulation of *CBF* genes and in acquired freezing tolerance. J Biol Chem **281:** 37636–37645

Aida M, Beis D, Heidstra R, Willemsen V, Blilou I, Galinha C, Nussaume L, Noh YS, Amasino R, Scheres B (2004) The *PLETHORA* genes mediate patterning of the *Arabidopsis* root stem cell niche. Cell **119:** 109–120

Allen MD, Yamasaki K, Ohme-Takagi M, Tateno M, Suzuki M (1998) A novel mode of DNA recognition by a beta-sheet revealed by the solution structure of the GCC-box binding domain in complex with DNA. EMBO J **17:** 5484–5496

Anchordoguy TJ, Rudolph AS, Carpenter JF, Crowe JH (1987) Modes of interaction of cryoprotectants with membrane phospholipids during freezing. Cryobiology **24:** 324–331

Anjum SA, Xie X, Wang L, Saleem MF, Man C, Lei W (2011) Morphological, physiological and biochemical responses of plants to drought stress. Afr J Agric Res **6:** 2026–2032

Apel K, Hirt H (2004) Reactive oxygen species: metabolism, oxidative stress, and signal transduction. Annu Rev Plant Biol **55:** 373–399

Arvidsson S, Kwasniewski M, Riaño-Pachón DM, Mueller-Roeber B (2008) QuantPrime - a flexible tool for reliable high-throughput primer design for quantitative PCR. BMC Bioinformatics **9:** 465

Asada K (2006) Production and scavenging of reactive oxygen species in chloroplasts and their functions. Plant Physiol **141:** 391–396

Bari R, Jones JDG (2009) Role of plant hormones in plant defence responses. Plant Molecular Biology **69:** 473–488

Bates LS, Waldren RP, Teare ID (1973) Rapid determination of free proline for water-stress studies. Plant Soil **39:** 205–207

Beck EH, Fettig S, Knake C, Hartig K, Bhattarai T (2007) Specific and unspecific responses of plants to cold and drought stress. J Biosci **32:** 501–510

Benková E, Michniewicz M, Sauer M, Teichmann T, Seifertová D, Jürgens G, Friml J (2003) Local, efflux-dependent auxin gradients as a common module for plant organ formation. Cell **115:** 591–602

Bernard P, Couturier M (1992) Cell killing by the F plasmid CcdB protein involves poisoning of DNA-topoisomerase II complexes. J Mol Biol **226:** 735–745

Berrocal-Lobo M, Molina A, Solano R (2002) Constitutive expression of *ETHYLENE-RESPONSE-FACTOR1* in *Arabidopsis* confers resistance to several necrotrophic fungi. Plant J **29:** 23–32

Bertani G (1951) Studies on lysogenesis I. The mode of phage liberation by lysogenic *Escherichia coli.* J Bacteriol **62:** 293–300

Bethke G, Unthan T, Uhrig JF, Pöschl Y, Gust AA, Scheel D, Lee J (2009) Flg22 regulates the release of an ethylene response factor substrate from MAP kinase 6 in *Arabidopsis thaliana* via ethylene signaling. Proc Natl Acad Sci U S A **106:** 8067–8072

Bieniawska Z, Espinoza C, Schlereth A, Sulpice R, Hincha DK, Hannah MA (2008) Disruption of the *Arabidopsis* circadian clock is responsible for extensive variation in the cold-responsive transcriptome. Plant Physiol **147:** 263–279

Blanc G, Hokamp K, Wolfe KH (2003) A recent polyploidy superimposed on older large-scale duplications in the *Arabidopsis* genome. Genome Res **13:** 137–144

Blázquez M (2007) Quantitative GUS activity assay in intact plant tissue. CSH Protoc **1:** prot4688

Bolt S, Zuther E, Zintl S, Hincha DK, Schmülling T (2017) *ERF105* is a transcription factor gene of *Arabidopsis thaliana* required for freezing tolerance and cold acclimation. Plant Cell Environ **40:** 108–120

Bournonville CF, Díaz-Ricci JC (2011) Quantitative determination of superoxide in plant leaves using a modified NBT staining method. Phytochem Anal **22:** 268–271

Bowers JE, Chapman BA, Rong J, Paterson AH (2003) Unravelling angiosperm genome evolution by phylogenetic analysis of chromosomal duplication events. Nature **422:** 433–438

Bray EA (1997) Plant responses to water deficit. Trends Plant Sci **2:** 48–54

Brenner WG, Romanov GA, Köllmer I, Bürkle L, Schmülling T (2005) Immediate-early and delayed cytokinin response genes of *Arabidopsis thaliana* identified by genome-wide expression profiling reveal novel cytokinin-sensitive processes and suggest cytokinin action through transcriptional cascades. Plant J **44:** 314–333

Casimiro I, Beeckman T, Graham N, Bhalerao R, Zhang H, Casero P, Sandberg G, Bennett MJ (2003) Dissecting *Arabidopsis* lateral root development. Trends Plant Sci **8:** 165–171

Catalá R, Medina J, Salinas J (2011) Integration of low temperature and light signaling during cold acclimation response in *Arabidopsis*. Proc Natl Acad Sci U S A **108:** 16475–16480

Cela J, Chang C, Munné-Bosch S (2011) Accumulation of γ-rather than α-tocopherol alters ethylene signaling gene expression in the *vte4* mutant of *Arabidopsis thaliana*. Plant Cell Physiol **52:** 1389–1400

Chandler JW, Cole M, Flier A, Grewe B, Werr W (2007) The AP2 transcription factors DORNRÖSCHEN and DORNRÖSCHEN-LIKE redundantly control *Arabidopsis* embryo patterning via interaction with PHAVOLUTA. Development **134:** 1653–1662

Chen H, Lai Z, Shi J, Xiao Y, Chen Z, Xu X (2010) Roles of *arabidopsis* WRKY18, WRKY40 and WRKY60 transcription factors in plant responses to abscisic acid and abiotic stress. BMC Plant Biol **10:** 281

Chen HH, Li PH, Brenner ML (1983) Involvement of abscisic acid in potato cold acclimation. Plant Physiol **71:** 362–365

Cheng MC, Liao PM, Kuo WW, Lin TP (2013) The *Arabidopsis* ETHYLENE RESPONSE FACTOR1 regulates abiotic stress-responsive gene expression by binding to different *cis*-acting elements in response to different stress signals. Plant Physiol **162:** 1566–1582

Chiang H-H, Hwang I, Goodman HM (1995) Isolation of the *Arabidopsis GA4* locus. Plant Cell **7:** 195–201

Chinnusamy V, Ohta M, Kanrar S, Lee BH, Hong X, Agarwal M, Zhu JK (2003) ICE1: a regulator of cold-induced transcriptome and freezing tolerance in *Arabidopsis*. Genes Dev **17:** 1043–1054

Chinnusamy V, Zhu J, Zhu JK (2007) Cold stress regulation of gene expression in plants. Trends Plant Sci **12:** 444–451

Chow BY, Sanchez SE, Breton G, Pruneda-Paz JL, Krogan NT, Kay SA (2014) Transcriptional regulation of *LUX* by CBF1 mediates cold input to the circadian clock in *Arabidopsis*. Curr Biol **24:** 1518–1524

Cook D, Fowler S, Fiehn O, Thomashow MF (2004) A prominent role for the CBF cold response pathway in configuring the low-temperature metabolome of *Arabidopsis*. Proc Natl Acad Sci U S A **101:** 15243–15248

Coutu C, Brandle J, Brown D, Brown K, Miki B, Simmonds J, Hegedus DD (2007) pORE: a modular binary vector series suited for both monocot and dicot plant transformation. Transgenic Res **16:** 771–781

Cowan IR, Preston RD, Woolhouse HW (1978) Stomatal behaviour and environment. Adv Bot Res **4:** 117–228

Cucinotta M, Manrique S, Guazzotti A, Quadrelli NE, Mendes MA, Benkova E, Colombo L (2016) Cytokinin response factors integrate auxin and cytokinin pathways for female reproductive organ development. Development **143:** 4419–4424

Cutcliffe JW, Hellmann E, Heyl A, Rashotte AM (2011) CRFs form protein-protein interactions with each other and with members of the cytokinin signalling pathway in *Arabidopsis* via the CRF domain. J Exp Bot **62:** 4995–5002

Davies B, Schwarz-Sommer Z (1994) Control of floral organ identity by homeotic MADS-box transcription factors. Results Probl Cell Differ **20:** 235–258

Davis AM, Hall A, Millar AJ, Darrah C, Davis SJ (2009) Streamlined subprotocols for floral-dip transformation and selection of transformants in *Arabidopsis thaliana.* Plant Methods **5:** 1–7

Daxinger L, Hunter B, Sheikh M, Jauvion V, Gasciolli V, Vaucheret H, Matzke M, Furner I (2008) Unexpected silencing effects from T-DNA tags in *Arabidopsis*. Trends Plant Sci **13:** 4–6

Derkx MPM, Vermeer E, Karssen CM (1994) Gibberellins in seeds of *Arabidopsis thaliana*: Biological activities, identification and effects of light and chilling on endogenous levels. Plant Growth Regul **15:** 223–234

Di Laurenzio L, Wysocka-Diller J, Malamy JE, Pysh L, Helariutta Y, Freshour G, Hahn MG, Feldmann KA, Benfey PN (1996) The *SCARECROW* gene regulates an asymmetric cell division that is essential for generating the radial organization of the *Arabidopsis* root. Cell **86:** 423–433

Dickson C (2008) Protein techniques: immunoprecipitation, *in vitro* kinase assays, and western blotting. Methods Mol Biol **461:** 735–744

Dietrich K, Weltmeier F, Ehlert A, Weiste C, Stahl M, Harter K, Dröge-Laser W (2011) Heterodimers of the *Arabidopsis* transcription factors bZIP1 and bZIP53 reprogram amino acid metabolism during low energy stress. Plant Cell **23:** 381–395

Dinakar C, Bartels D (2013) Desiccation tolerance in resurrection plants: new insights from transcriptome, proteome and metabolome analysis. Front Plant Sci **4:** 482

Ding Y, Li H, Zhang X, Xie Q, Gong Z, Yang S (2015) OST1 kinase modulates freezing tolerance by enhancing ICE1 stability in *Arabidopsis*. Dev Cell **32:** 278–289

Dinh TT, Girke T, Liu X, Yant L, Schmid M, Chen X (2012) The floral homeotic protein APETALA2 recognizes and acts through an AT-rich sequence element. Development **139:** 1978–1986

Divi UK, Rahman T, Krishna P (2010) Brassinosteroid-mediated stress tolerance in *Arabidopsis* shows interactions with abscisic acid, ethylene and salicylic acid pathways. BMC Plant Biol **10:** 151–165

Doerner P (1998) Root development: quiescent center not so mute after all. Curr Biol **8:** 42–44

Doherty CJ, Van Buskirk HA, Myers SJ, Thomashow MF (2009). Roles for *Arabidopsis* CAMTA transcription factors in cold-regulated gene expression and freezing tolerance. Plant Cell **21:** 972–984

Dong CH, Agarwal M, Zhang Y, Xie Q, Zhu JK (2006) The negative regulator of plant cold responses, HOS1, is a RING E3 ligase that mediates the ubiquitination and degradation of ICE1. Proc Natl Acad Sci U S A **103:** 8281–8286

Dortay H, Mehnert N, Bürkle L, Schmülling T, Heyl A (2006) Analysis of protein interactions within the cytokinin-signaling pathway of *Arabidopsis thaliana*. FEBS J **273:** 4631–4644

Dubois M, Skirycz A, Claeys H, Maleux K, Dhondt S, De Bodt S, Vanden Bossche R, De Milde L, Yoshizumi T, Matsui M, Inzé D (2013) Ethylene Response Factor6 acts as a central regulator of leaf growth under water-limiting conditions in *Arabidopsis*. Plant Physiol **162:** 319–332

Dubois M, Van den Broeck L, Claeys H, Van Vlierberghe K, Matsui M, Inzé D (2015) The ETHYLENE RESPONSE FACTORS ERF6 and ERF11 antagonistically regulate mannitol-induced growth inhibition in *Arabidopsis*. Plant Physiol **169:** 166–179

Dure L 3rd, Greenway SC, Galau GA (1981) Developmental biochemistry of cottonseed embryogenesis and germination: changing messenger ribonucleic acid populations as shown by *in vitro* and *in vivo* protein synthesis. Biochemistry **20:** 4162–4168

Edgar RC (2004) MUSCLE: multiple sequence alignment with high accuracy and high throughput. Nucleic Acids Res **32:** 1792–1797

Emiliani J, Grotewold E, Falcone Ferreyra ML, Casati P (2013) Flavonols protect *Arabidopsis* plants against UV-B deleterious effects. Mol Plant **6:** 1376–1379

Eremina M, Rozhon W, Poppenberger B (2016) Hormonal control of cold stress responses in plants. Cell Mol Life Sci **73:** 797–810

Fan LM, Zhao Z, Assmann SM (2004) Guard cells: a dynamic signaling model. Curr Opin Plant Biol **7:** 537–546

Farquhar GD, Sharkey TD (1982) Stomatal conductance and photosynthesis. Annu Rev Plant Physiol **33:** 317–345

Ferreyra MLF, Rius SP, Casati P (2012) Flavonoids: biosynthesis, biological functions, and biotechnological applications. Frontiers Plant Sci **3:** 222

Fiil BK, Qiu JL, Petersen K, Petersen M, Mundy J (2008) Coimmunoprecipitation (co-IP) of nuclear proteins and chromatin immunoprecipitation (ChIP) from *Arabidopsis*. CSH Protoc **3:** prot5049

Fowler S, Thomashow MF (2002) *Arabidopsis* transcriptome profiling indicates that multiple regulatory pathways are activated during cold acclimation in addition to the CBF cold response pathway. Plant Cell **14:** 1675–1690

Fujimoto SY, Ohta M, Usui A, Shinshi H, Ohme-Takagi M (2000) *Arabidopsis* ethylene-responsive element binding factors act as transcriptional activators or repressors of GCC box-mediated gene expression. Plant Cell **12:** 393–404

Furihata T, Maruyama K, Fujita Y, Umezawa T, Yoshida R, Shinozaki K, Yamaguchi-Shinozaki K (2006) Abscisic acid-dependent multisite phosphorylation regulates the activity of a transcription activator AREB1. Proc Natl Acad Sci U S A **103:** 1988–1993

Fursova OV, Pogorelko GV, Tarasov VA (2009) Identification of *ICE2*, a gene involved in cold acclimation which determines freezing tolerance in *Arabidopsis thaliana.* Gene **429:** 98–103

Furuya T, Matsuoka D, Nanmori T (2014) Membrane rigidification functions upstream of the MEKK1-MKK2-MPK4 cascade during cold acclimation in *Arabidopsis thaliana*. FEBS Lett **588:** 2025–2030

Galinha C, Hofhuis H, Luijten M, Willemsen V, Blilou I, Heidstra R, Scheres B (2007) PLETHORA proteins as dose-dependent master regulators of *Arabidopsis* root development. Nature **449:** 1053–1057

Geiger D, Scherzer S, Mumm P, Stange A, Marten I, Bauer H, Ache P, Matschi S, Liese A, Al-Rasheid KA, Romeis T, Hedrich R (2009) Activity of guard cell anion channel SLAC1 is controlled by drought-stress signaling kinase-phosphatase pair. Proc Natl Acad Sci U S A **106:** 21425–21430

George M, Burke MJ (1977) Cold-hardiness and deep supercooling in xylem of shagbark hickory. Plant Physiol **27:** 507–528

Gietz RD, Woods RA (2002) Transformation of yeast by lithium acetate/single-stranded carrier DNA/polyethylene glycol method. Methods Enzymol **350:** 87–96

Gilmour SJ, Thomashow MF (1991) Cold-acclimation and cold-regulated gene-expression in *aba* mutants of *Arabidopsis thaliana*. Plant Mol Biol **17:** 1233–1240

Gimble FS (2000). Invasion of a multitude of genetic niches by mobile endonuclease genes. FEMS Microbiol Lett **185:** 99–107

Giorgio M, Trinei M, Migliaccio E, Pelicci PG (2007) Hydrogen peroxide: a metabolic by-product or a common mediator of ageing signals? Nat Rev Mol Cell Biol **8:** 722–728

Giraudat J, Parcy F, Bertauche N, Gosti F, Leung J, Morris P-C, Bouvier-Durand M, Vartanian N (1994) Current advances in abscisic acid action and signaling. Plant Mol Biol **26:** 1557–1577

Goehler H, Lalowski M, Stelzl U, Waelter S, Stroedicke M, Worm U, Droege A, Lindenberg KS, Knoblich M, Haenig C, Herbst M, Suopanki J, Scherzinger E,

Abraham C, Bauer B, Hasenbank R, Fritzsche A, Ludewig AH, Buessow K, Coleman SH, Gutekunst CA, Landwehrmeyer BG, Lehrach H, Wanker EE (2004) A protein interaction network links GIT1, an enhancer of huntingtin aggregation, to Huntington's disease. Molecular Cell **15:** 853–865

Goh T, Toyokura K, Wells DM, Swarup K, Yamamoto M, Mimura T, Weijers D, Fukaki H, Laplaze L, Bennett MJ, Guyomarc'h S (2016) Quiescent center initiation in the *Arabidopsis* lateral root primordia is dependent on the SCARECROW transcription factor. Development **143:** 3363–3371

Gould KS (2004) Nature's swiss army knife: The diverse protective roles of anthocyanins in leaves. Plant Signal Behav **9:** e27522

Guy CL (1990) Cold acclimation and freezing stress tolerance: role of protein metabolism. Annu Rev Plant Physiol Plant Mol Biol **41:** 187–223

Haake V, Cook D, Riechmann JL, Pineda O, Thomashow MF, Zhang JZ (2002) Transcription factor CBF4 is a regulator of drought adaptation in *Arabidopsis*. Plant Physiol **130:** 639–648

Halfter U, Ishitani M, Zhu J-K (2000) The *Arabidopsis* SOS2 protein kinase physically interacts with and is activated by the calcium-binding protein SOS3. Proc Natl Acad Sci U S A **97:** 3735–3740

Hanahan D (1983) Studies on transformation of *Escherichia coli* with plasmids. J Mol Biol **166:** 557–580

Handa S, Handa AK, Hasegawa PM, Bressan RA (1986) Proline accumulation and the adaptation of cultured plant cells to water stress. Plant Physiol **80:** 938–945

Hannah MA, Wiese D, Freund S, Fiehn O, Heyer AG, Hincha DK (2006) Natural genetic variation of freezing tolerance in *Arabidopsis*. Plant Physiol **142:** 98–112

Hao D, Ohme-Takagi M, Sarai A (1998) Unique mode of GCC box recognition by the DNA-binding domain of ethylene-responsive element-binding factor (ERF domain) in plant. J Biol Chem **273:** 26857–26861

Harris D, Tripathi RS, Joshi A (2002). On-farm seed priming to improve crop establishment and yield in dry direct-seeded rice. In: Pandey S, Mortimer M, Wade L, Tuong TP, Lopes K, Hardy B (eds), Direct seeding: Research strategies and opportunities, International Research Institute, Manila, Philippines, 231–240

Haupt-Herting S, Fock HP (2002) Oxygen exchange in relation to carbon assimilation in water-stressed leaves during photosynthesis. Ann Bot **89:** 851–859

He X, Jiang J, Wang CQ, Dehesh K (2017) ORA59 and EIN3 interaction couples jasmonate-ethylene synergistic action to antagonistic salicylic acid regulation of PDF expression. J Integr Plant Biol **59:** 275–287

He XJ, Mu RL, Cao WH, Zhang ZG, Zhang JS, Chen SY (2005) AtNAC2, a transcription factor downstream of ethylene and auxin signaling pathways, is involved in salt stress response and lateral root development. Plant J **44:** 903–916

Heath RL, Packer L (1968) Photoperoxidation in isolated chloroplasts. I. Kinetics and stoichiometry of fatty acid peroxidation. Arch Biochem Biophys **125:** 189–198

Heino P, Sandman G, Lang V, Nordin K, Palva ET (1990) Abscisic acid deficiency prevents development of freezing tolerance in *Arabidopsis thaliana*. Theor Appl Genet **79:** 801–806

Henderson IR, Dean C (2004) Control of *Arabidopsis* flowering: the chill before the bloom. Development **131:** 3829–3838

Hernandez I, Alegre L, van Breusegem F, Munne-Bosch S (2009) How relevant are flavonoids as antioxidants in plants? Trends Plant Sci **14:** 125–132

Heyne EG, Brunson AM (1940) Genetic studies of heat and drought tolerance in maize. J Am Soc Agro **32:** 803–814

Hincha DK, Hagemann M (2004) Stabilization of model membranes during drying by compatible solutes involved in the stress tolerance of plants and microorganisms. Biochem J **383:** 277–283

Hincha DK, Höfner R, Schwab KB, Heber U, Schmitt JM (1987) Membrane rupture is the common cause of damage to chloroplast membranes in leaves injured by freezing or excessive wilting. Plant Physiol **83:** 251–253

Hincha DK, Thalhammer A (2012) LEA proteins: IDPs with versatile functions in cellular dehydration tolerance. Biochem Soc Trans **40:** 1000–1003

Horton P, Park KJ, Obayashi T, Fujita N, Harada H, Adams-Collier CJ, Nakai K (2007) WoLF PSORT: protein localization predictor. Nucleic Acids Res **35:** 585–587

Howe E, Holton K, Nair S, Schlauch D, Sinha R, Quackenbush J (2010) MeV: MultiExperiment Viewer. In: Ochs MF, Casagrande JT, Davuluri RV (eds), Biomedical Informatics for Cancer Research, Springer, 267–277

Hu Y, Jiang L, Wang F, Yua D (2013) Jasmonate regulates the inducer of cbf expression-C-repeat binding factor/DRE binding factor1 cascade and freezing tolerance in *Arabidopsis*. Plant Cell **25:** 2907–2924

Huala E, Dickerman AW, Garcia-Hernandez M, Weems D, Reiser L, LaFond F, Hanley D, Kiphart D, Zhuang M, Huang W, Mueller LA, Bhattacharyya D, Bhaya D, Sobral BW, Beavis W, Meinke DW, Town CD, Somerville C, Rhee SY (2001) The *Arabidopsis* Information Resource (TAIR): a comprehensive database and web-based information retrieval, analysis, and visualization system for a model plant. Nucleic Acids Res **29:** 102–105

Hundertmark M, Hincha DK (2008) LEA (late embryogenesis abundant) proteins and their encoding genes in *Arabidopsis thaliana*. BMC Genomics **9:** 118

Hussain M, Malik MA, Farooq M, Ashraf MY, Cheema MA (2008). Improving drought tolerance by exogenous application of glycinebetaine and salicylic acid in sunflower. J Agron Crop Sci **194:** 193–199

Ingram J, Bartels D (1996) The molecular basis of dehydration tolerance in plants. Annu Rev Plant Physiol Plant Mol Biol **47:** 377–403

Inoue H, Nojima H, Okayama H (1990) High efficiency transformation of *Escherichia coli* with plasmids. Gene **96:** 23–28

Jaglo-Ottosen KR, Gilmour SJ, Zarka DG, Schabenberger O, Thomashow MF (1998) *Arabidopsis CBF1* overexpression induces *COR* genes and enhances freezing tolerance. Science **280:** 104–106

Jaleel CA, Gopi R, Sankar B, Gomathinayagam M, Panneerselvam R (2008) Differential responses in water use efficiency in two varieties of *Catharanthus roseus* under drought stress. C R Biol **331:** 42–47

Jayakannan M, Bose J, Babourina O, Shabala S, Massart A, Poschenrieder C, Rengel Z (2015) The NPR1-dependent salicylic acid signalling pathway is pivotal for enhanced salt and oxidative stress tolerance in *Arabidopsis*. J Exp Bot **66:** 1865–1875

Jefferson RA, Kavanagh TA, Bevan MW (1987) GUS fusions: beta-glucuronidase as a sensitive and versatile gene fusion marker in higher plants. EMBO J **6:** 3901–3907

Jeon J, Cho C, Lee MR, Van Binh N, Kim J (2016) CYTOKININ RESPONSE FACTOR2 (CRF2) and CRF3 regulate lateral root development in response to cold stress in *Arabidopsis*. Plant Cell **28:** 1828–1843

Jeon J, Kim NY, Kim S, Kang NY, Novák O, Ku SJ, Cho C, Lee DJ, Lee EJ, Strnad M, Kim J (2010) A subset of cytokinin two-component signaling system plays a role in cold temperature stress response in *Arabidopsis*. J Biol Chem **285:** 23371–23386

Jia W, Li B, Li S, Liang Y, Wu X, Ma M, Wang J, Gao J, Cai Y, Zhang Y, Wang Y, Li J, Wang Y (2016a) Mitogen-activated protein kinase cascade MKK7-MPK6 plays important roles in plant development and regulates shoot branching by phosphorylating PIN1 in *Arabidopsis*. PLoS Biol **14:** e1002550

Jia Y, Ding Y, Shi Y, Zhang X, Gong Z, Yang S (2016b) The *cbfs* triple mutants reveal the essential functions of *CBF*s in cold acclimation and allow the definition of CBF regulons in *Arabidopsis*. New Phytol **212:** 345–353

Jiao Y, Sun L, Song Y, Wang L, Liu L, Zhang L, Liu B, Li N, Miao C, Hao F (2013) *AtrbohD* and *AtrbohF* positively regulate abscisic acid-inhibited primary root growth by affecting Ca^{2+} signalling and auxin response of roots in *Arabidopsis*. J Exp Bot **64:** 4183–4192

Jofuku KD, den Boer BG, Van Montagu M, Okamuro JK (1994) Control of *Arabidopsis* flower and seed development by the homeotic gene *APETALA2.* Plant Cell **6:** 1211–1225

Joshi R, Wani SH, Singh B, Bohra A, Dar ZA, Lone AA, Pareek A, Singla-Pareek SL (2016) Transcription factors and plants response to drought stress: current understanding and future directions. Front Plant Sci **14:** 1029

Kagale S, Rozwadowski K (2010) Small yet effective: the ethylene responsive element binding factor-associated amphiphilic repression (EAR) motif. Plant Signal Behav **5:** 691–694

Kagaya Y, Ohmiya K, Hattori T (1999) RAV1 a novel DNA-binding protein, binds to a bipartite recognition sequence through two distinct DNA-binding domains uniquely found in higher plants. Nucleic Acids Res **27:** 470–478

Kanaoka MM, Pillitteri LJ, Fujii H, Yoshida Y, Bogenschutz NL, Takabayashi J, Zhu JK, Torii KU (2008) SCREAM/ICE1 and SCREAM2 specify three cell-state transitional steps leading to arabidopsis stomatal differentiation. Plant Cell **20:** 1775–1785

Kant S, Kant P, Raveh E, Barak S (2006) Evidence that differential gene expression between the halophyte, *Thellungiella halophila*, and *Arabidopsis thaliana* is responsible for higher levels of the compatible osmolyte proline and tight control of Na^+ uptake in *T. halophila.* Plant Cell Environ **29:** 1220–1234

Kaplan F, Kopka J, Haskell DW, Zhao W, Schiller KC, Gatzke N, Sung DY, Guy CL (2004) Exploring the temperature-stress metabolome of *Arabidopsis*. Plant Physiol **136:** 4159–4168

Kaplan F, Kopka J, Sung DY, Zhao W, Popp M, Porat R, Guy CL (2007) Transcript and metabolite profiling during cold acclimation of *Arabidopsis* reveals an intricate relationship of cold regulated gene expression with modifications in metabolite content. Plant J **50:** 967–981

Karimi B, Bleys A, Vanderhaeghen R, Hilson P (2007a) Building blocks for plant gene assembly. Plant Physiol **145:** 1183–1191

Karimi M, De Meyer B, Hilson P (2005) Modular cloning in plant cells. Trends Plant Sci **10:** 103–105

Karimi M, Depicker A, Hilson P (2007b) Recombinational cloning with plant Gateway vectors. Plant Physiol **145:** 1144–1154

Kasuga M, Liu Q, Miura S, Yamaguchi-Shinozaki K, Shinozaki K (1999) Improving plant drought, salt, and freezing tolerance by gene transfer of a single stress-inducible transcription factor. Nat Biotechnol **17:** 287–291

Khan MA, Gemenet DC, Villordon A (2016) Root system architecture and abiotic stress tolerance: Current knowledge in root and tuber crops. Front Plant Sci **7:** 1584

Kidokoro S, Yoneda K, Takasaki H, Takahashi F, Shinozaki K, Yamaguchi-Shinozaki K (2017) Different cold-signaling pathways function in the responses to rapid and gradual decreases in temperature. Plant Cell **29:** 760–774

Kim HJ, Kim YK, Park JY, Kim J (2002) Light signalling mediated by phytochrome plays an important role in cold-induced gene expression through the C-repeat/dehydration responsive element (C/DRE) in *Arabidopsis thaliana*. Plant J **29:** 693–704

Kim SH, Kim HS, Bahk S, An J, Yoo Y, Kim JY, Chung WS (2017) Phosphorylation of the transcriptional repressor MYB15 by mitogen-activated protein kinase 6 is required for freezing tolerance in *Arabidopsis*. Nucleic Acids Res **in press**

Kim YS, Lee M, Lee JH, Lee HJ, Park CM (2015) The unified ICE-CBF pathway provides a transcriptional feedback control of freezing tolerance during cold acclimation in *Arabidopsis*. Plant Mol Biol **89:** 187–201

Kogan FN (1997) Global drought watch from space. Bull Am Meteorol Soc **78:** 621–636

Konsc C, Schell J (1986) The promoter of TL-DNA gene 5 controls the tissue-specific expression of chimaeric genes carried by a novel type of *Agrobacterium* binary vector. Mol Genet Genomics **204:** 383–396

Kozlowski TT (1968) Water deficit and plant growth. In: Kozlowski TT (ed), Development, control and measurement Vol.1, Acad Press NY, 195–234

Krause GH, Grafflage S, Rumich-Bayer S, Somersalo S (1988) Effects of freezing on plant mesophyll cells. Symp Soc Exp Biol **42:** 311–327

Kreps JA, Wu Y, Chang HS, Zhu T, Wang X, Harper JF (2002) Transcriptome changes for *Arabidopsis* in response to salt, osmotic, and cold stress. Plant Physiol **130:** 2129–2141

Krömer T, Kessler M, Herzog SK (2006) Distribution and flowering ecology of bromeliads along two climatically contrasting elevational transects in the bolivian Andes. Biotrophica **38:** 183–195

Kumar MN, Jane W-N, Verslues P (2012) Role of the putative osmosensor *Arabidopsis* Histidine Kinase 1 (AHK1) in dehydration avoidance and low water potential response. Plant Physiol **161:** 942–953

Kwak JM, Mori IC, Pei ZM, Leonhardt N, Torres MA, Dangl JL, Bloom RE, Bodde S, Jones JD, Schroeder JI (2003) NADPH oxidase *AtrbohD* and *AtrbohF* genes function in ROS-dependent ABA signaling in *Arabidopsis*. EMBO J **22:** 2623–2633

Lang V, Mantyla E, Welin B, Sundberg B, Palva E (1994) Alterations in water status, endogenous abscisic acid content and expression of *RAB18* gene during the development of freezing tolerance in *Arabidopsis thaliana*. Plant Physiol **104:** 1341–1349

Lawlor DW, Cornic G (2002) Photosynthetic carbon assimilation and associated metabolism in relation to water deficits in higher plants. Plant Cell Environ **25:** 275–294

Le MQ, Engelsberger WR, Hincha DK (2008) Natural genetic variation in acclimation capacity at sub-zero temperatures after cold acclimation at 4 °C in different *Arabidopsis thaliana* accessions. Cryobiol **57:** 104–112

Lee B, Henderson DA, Zhua J (2005) The *Arabidopsis* cold-responsive transcriptome and its regulation by ICE1. Plant Cell **17:** 3155–3175

Lee HG, Seo PJ (2015) The MYB96-HHP module integrates cold and abscisic acid signaling to activate the CBF-COR pathway in *Arabidopsis*. Plant J **82:** 962–977

Lee YP, Babakov A, de Boer B, Zuther E, Hincha DK (2012) Comparisons of freezing tolerance, compatible solutes and polyamines in geographically diverse collections of *Thellungiella sp.* and *Arabidopsis thaliana* accessions. BMC Plant Biol **12**: 131

Levitt J (1980) Responses of plants to environmental stresses. Vol.1 2nd edn. Academic Press. New York, NY.

Li B, Zhang C, Cao B, Qin G, Wang W, Tian S (2012) Brassinolide enhances cold stress tolerance of fruit by regulating plasma membrane proteins and lipids. Amino Acids **43:** 2469–2480

Li R-h, Guo P-g, Michael B, Stefania G, Salvatore C (2006) Evaluation of chlorophyll content and fluorescence parameters as indicators of drought tolerance in barley. Agric Sci China **5:** 751–757

Li S (2014) Transcriptional control of flavonoid biosynthesis: fine-tuning of the MYB-bHLH-WD40 (MBW) complex. Plant Signal Behav **9:** e27522

Li S, Han X, Yang L, Deng X, Wu H, Zhang M, Liu Y, Zhang S, Xu J (2017) Mitogen-activated protein kinases and calcium-dependent protein kinases are involved in wounding-induced ethylene biosynthesis in *Arabidopsis thaliana*. Plant Cell Environ **in press**

Licausi F, Ohme-Takagi M, Perata P (2013) APETALA2/Ethylene responsive factor (AP2/ERF) transcription factors: mediators of stress responses and developmental programs. New Phytol **199:** 639–649

Lim PO, Kim HJ, Nam HG (2007) Leaf senescence. Annu Rev Plant Biol **58:** 115–136

Lindquist S (1986) The heat-shock response. Annu Rev Biochem **55:** 1151–1191

Lindquist S, Craig EA (1988). The heat-shock proteins. Annu Rev Genet **22:** 631–677

Liu J, Li J, Wang H, Fu Z, Liu J, Yu Y (2011) Identification and expression analysis of ERF transcription factor genes in petunia during flower senescence and in response to hormone treatments. J Exp Bot **62:** 825–840

Liu L, White MJ, MacRae TH (1999) Transcription factors and their genes in higher plants functional domains, evolution and regulation. Eur J Biochem **262:** 247–257

Liu Q, Kasuga M, Sakuma Y, Abe H, Miura S, Yamaguchi-Shinozaki K, Shinozaki K (1998) Two transcription factors, DREB1 and DREB2, with an EREBP/AP2 DNA binding

domain separate two cellular signal transduction pathways in drought- and low-temperature-responsive gene expression, respectively, in *Arabidopsis*. Plant Cell **10:** 1391–1406

Liu Y, He C (2016) Regulation of plant reactive oxygen species (ROS) in stress responses: learning from *AtRBOHD*. Plant Cell Rep **35:** 995–1007

Liu Y, Li X, Li K, Liu H, Lin C (2013) Multiple bHLH proteins form heterodimers to mediate CRY2-dependent regulation of flowering-time in *Arabidopsis*. PLoS Genet **9:** e1003861

Lorenzo O, Piqueras R, Sánchez-Serrano JJ, Solano R (2003) ETHYLENE RESPONSE FACTOR1 integrates signals from ethylene and jasmonate pathways in plant defense. Plant Cell **15:** 165–178

Lu G, Moriyama EN (2004) Vector NTI, a balanced all-in-one sequence analysis suite. Brief Bioinform **5:** 378–388

Magnani E, Sjölander K, Hake S (2004) From endonucleases to transcription factors: Evolution of the AP2 DNA binding domain in plants. Plant Cell **16:** 2265–2277

Magome H, Yamaguchi S, Hanada A, Kamiya Y, Oda K (2008) The DDF1 transcriptional activator upregulates expression of a gibberellin deactivating gene, *GA2ox7*, under high-salinity stress in *Arabidopsis*. Plant J **56:** 613–626

Mao JL, Miao ZQ, Wang Z, Yu LH, Cai XT, Xiang CB (2016) *Arabidopsis* ERF1 mediates cross-talk between ethylene and auxin biosynthesis during primary root elongation by regulating *ASA1* expression. PLoS Genet **12:** e1005760

Marianayagam NJ, Sunde M, Matthews JM (2004) The power of two: protein dimerization in biology. Trends Biochem Sci **29:** 618–625

McKhann HI, Gery C, Bérard A, Lévêque S, Zuther E, Hincha DK, De Mita S, Brunel D, Téoulé E (2008) Natural variation in *CBF* gene sequence, gene expression and freezing tolerance in the Versailles core collection of *Arabidopsis thaliana*. BMC Plant Biol **8:** 105

Mehrtens F, Kranz H, Bednarek P, Weisshaar B (2005) The *Arabidopsis* transcription factor MYB12 is a flavonol-specific regulator of phenylpropanoid biosynthesis. Plant Physiol **138:** 1083–1096

Meng X, Xu J, He Y, Yang KY, Mordorski B, Liu Y, Zhang S (2013) Phosphorylation of an ERF transcription factor by *Arabidopsis* MPK3/MPK6 regulates plant defense gene induction and fungal resistance. Plant Cell **25:** 1126–1142

Miller G, Schlauch K, Tam R, Cortes D, Torres MA, Shulaev V, Dangl JL, Mittler R (2009) The plant NADPH oxidase RBOHD mediates rapid systemic signaling in response to diverse stimuli. Sci Signal **2:** ra45

Mittler R (2006) Abiotic stress, the field environment and stress combination. Trends Plant Sci **11:** 15–19

Mittler R, Vanderauwera S, Suzuki N, Miller G, Tognetti VB, Vandepoele K, Gollery M, Shulaev V, Van Breusegem F (2011) ROS signaling: the new wave? Trends Plant Sci **16:** 300–309

Miura K, Jin JB, Lee J, Yoo CY, Stirm V, Miura T, Ashworth EN, Bressan RA, Yun DJ, Hasegawa PM (2007) SIZ1-mediated sumoylation of ICE1 controls *CBF3/DREB1A* expression and freezing tolerance in *Arabidopsis*. Plant Cell **19:** 1403–1414

Moffat AS (2002) Finding new ways to protect drought-stricken plants. Science **296:** 1226–1229

Moffat CS, Ingle RA, Wathugala DL, Saunders NJ, Knight H, Knight MR (2012) ERF5 and ERF6 play redundant roles as positive regulators of JA/Et-mediated defense against *Botrytis cinerea* in *Arabidopsis*. PLoS One **7:** e35995

Møller IM, Jensen PE, Hansson A (2007) Oxidative modifications to cellular components in plants. Annu Rev Plant Biol **58:** 459–481

Moore M, Vogel M, Dietz K (2014) The acclimation response to high light is initiated within seconds as indicated by upregulation of AP2/ERF transcription factor network in *Arabidopsis thaliana.* Plant Signal Behav **9:** 976479

Müller M, Munné-Bosch S (2015) Ethylene response factors: A key regulatory hub in hormone and stress signaling. Plant Physiol **169:** 32–41

Mullis KB, Faloona FA (1987) Specific synthesis of DNA in vitro via a polymerase catalyzed chain reaction. Methods Enzymol **155:** 335–350

Munns R, Tester M (2008) Mechanisms of salinity tolerance. Annu Rev Plant Biol **59:** 651–681

Murashige T, Skoog F (1962) A revised medium for rapid growth and bioassays with tobacco tissue cultures. Physiol Plant **15:** 473–497

Mustilli AC, Merlot S, Vavasseur A, Fenzi F, Giraudat J (2002) *Arabidopsis* OST1 protein kinase mediates the regulation of stomatal aperture by abscisic acid and acts upstream of reactive oxygen species production. Plant Cell **14:** 3089–3099

Nakabayashi R, Mori T, Saito K (2014) Alternation of flavonoid accumulation under drought stress in *Arabidopsis thaliana*. Plant Signal Behav **9:** e29518

Nakano T, Suzuki K, Fujimura T, Shinshi H (2006) Genome-wide analysis of the *ERF* gene family in *Arabidopsis* and rice. Plant Physiol **140:** 411–432

Nakashima K, Shinwari ZK, Sakuma Y, Seki M, Miura S, Shinozaki K, Yamaguchi-Shinozaki K (2000) Organization and expression of two *Arabidopsis DREB2* genes encoding DRE-binding proteins involved in dehydration- and high-salinity-responsive gene expression. Plant Mol Biol **42:** 657–665

Nakayama K, Okawa K, Kakizaki T, Honma T, Itoh H, Inaba T (2007) Arabidopsis Cor15am is a chloroplast stromal protein that has cryoprotective activity and forms oligomers. Plant Physiol **144:** 513–523

Nanjo T, Kobayashi M, Yoshiba Y, Sanada Y, Wada K, Tsukaya H, Kakubari Y, Yamaguchi-Shinozaki K, Shinozaki K (1999) Biological functions of proline in morphogenesis and osmotolerance revealed in antisense transgenic *Arabidopsis thaliana*. Plant J **18:** 185–193

Nawy T, Lee JY, Colinas J, Wang JY, Thongrod SC, Malamy JE, Birnbaum K, Benfey PN (2005) Transcriptional profile of the *Arabidopsis* root quiescent center. Plant Cell **17:** 1908–1925

Neter J, Kutner MH, Nachtsheim CJ, Wasserman W (1996) Applied Linear Statistic Models. McGraw-Hill, New York

Novillo F, Medina J, Salinas J (2007) *Arabidopsis CBF1* and *CBF3* have a different function than *CBF2* in cold acclimation and define different gene classes in the CBF regulon. Proc Natl Acad Sci U S A **104:** 21002–21007

Obayashi T, Kinoshita K, Nakai K, Shibaoka M, Hayashi S, Saeki M, Shibata D, Saito K, Ohta H (2007) ATTED-II: A database of co-expressed genes and *cis* elements for identifying co-regulated gene groups in *Arabidopsis*. Nucleic Acids Res **35:** D863–D869

Ober ES, Sharp RE (2003) Electrophysiological responses of maize roots to low water potentials: relationship to growth and ABA accumulation. J Exp Bot **54:** 813–824

Ohad N, Shichrur K, Yalovsky S (2007) The analysis of protein-protein interactions in plants by bimolecular fluorescence complementation. Plant Physiol **145:** 1090–1099

Ohme-Takagi M, Shinshi H (1995) Ethylene-inducible DNA binding proteins that interact with an ethylene-responsive element. Plant Cell **7:** 173–182

Ohta M, Matsui K, Hiratsu K, Shinshi H, Ohme-Takagi M (2001) Repression domains of class II ERF transcriptional repressors share an essential motif for active repression. Plant Cell **13:** 1959–1968

Okamuro JK, Caster B, Villarroel R, Van Montagu M, Jofuku KD (1997) The AP2 domain of APETALA2 defines a large new family of DNA binding proteins in *Arabidopsis.* Proc Natl Acad Sci U S A **94:** 7076–7081

Ossowski S, Schwab R, Weigel D (2008) Gene silencing in plants using artificial microRNAs and other small RNAs. Plant J **53:** 674–690

Park S, Lee CM, Doherty CJ, Gilmour SJ, Kim Y, Thomashow MF (2015) Regulation of the *Arabidopsis* CBF regulon by a complex low-temperature regulatory network. Plant J **82:** 193–207

Peleg Z, Blumwald E (2011) Hormone balance and abiotic stress tolerance in crop plants. Curr Opin Plant Biol **14:** 290–295

Péret B, De Rybel B, Casimiro I, Benková E, Swarup R, Laplaze L, Beeckman T, Bennett MJ (2009) *Arabidopsis* lateral root development: an emerging story. Trends Plant Sci **14:** 399–408

Pollastri S, Tattini M (2011) Flavonols: old compounds for old roles. Ann Bot **108:** 1225–1233

Popescu SC, Popescu GV, Bachan S, Zhang Z, Gerstein M, Snyder M, Dinesh-Kumar SP (2009) MAPK target networks in *Arabidopsis thaliana* revealed using functional protein microarrays. Genes Dev **23:** 80–92

Porra RJ, Thompson WA, Kriedemann PE (1989) Determination of accurate extinction coefficients and simultaneous equations for assaying chlorophylls a and b extracted with four different solvents: verification of the concentration of chlorophyll standards by atomic absorption spectroscopy. Biochim Biophys Acta **975:** 384–394

Prasad TK, Anderson MD, Martin BA, Stewart CR (1994) Evidence for chilling-induced oxidative stress in maize seedlings and a regulatory role for hydrogen peroxide. Plant Cell **6:** 65–74

Pré M, Atallah M, Champion A, De Vos M, Pieterse CM, Memelink J (2008) The AP2/ERF domain transcription factor ORA59 integrates jasmonic acid and ethylene signals in plant defense. Plant Physiol **147:** 1347–1357

Quamme H (1974) An exothermic process involved in the freezing injury to flower buds of several *Prunus* species. J Am Soc Hort Sci **99:** 315–318

Raines T, Shanks C, Cheng CY, McPherson D, Argueso CT, Kim HJ, Franco-Zorrilla JM, López-Vidriero I, Solano R, Vaňková R, Schaller GE, Kieber JJ (2016) The cytokinin response factors modulate root and shoot growth and promote leaf senescence in *Arabidopsis*. Plant J **85:** 134–147

Rashotte AM, Goertzen LR (2010) The CRF domain defines cytokinin response factor proteins in plants. BMC Plant Biol **10:** 74

Rashotte AM, Mason MG, Hutchison CE, Ferreira FJ, Schaller GE, Kieber JJ (2006) A subset of *Arabidopsis* AP2 transcription factors mediates cytokinin responses in concert with a two-component pathway. Proc Natl Acad Sci U S A **103:** 11081–11085

Reece-Hoyes JS, Marian Walhout AJ (2012) Yeast one-hybrid assays: a historical and technical perspective. Methods **574:** 441–417

Riechmann JL, Meyerowitz EM (1998) The AP2/EREBP family of plant transcription factors. Biol Chem **379:** 6336–6346

Rodriguez MC, Petersen M, Mundy J (2010) Mitogen-activated protein kinase signaling in plants. Annu Rev Plant Biol **61:** 621–649

Rohde P, Hincha DK, Heyer AG (2004) Heterosis in the freezing tolerance of crosses between two *Arabidopsis thaliana* accessions (Columbia-0 and C24) that show differences in nonacclimated and acclimated freezing tolerance. Plant J **38:** 790–799

Rovere FD, Fattorini L, Ronzan M, Falasca G, Altamura MM (2016) The quiescent center and the stem cell niche in the adventitious roots of *Arabidopsis thaliana*. Plant Signal Behav **11:** e1176660

Sabatini S, Heidstra R, Wildwater M, Scheres B (2003) SCARECROW is involved in positioning the stem cell niche in the *Arabidopsis* root meristem. Genes Dev **17:** 354–358

Sagi M, Fluhr R (2006). Production of reactive oxygen species by plant NADPH oxidases. Plant Physiol **141:** 336–340

Saito S, Hirai N, Matsumoto C, Ohigashi H, Ohta D, Sakata K, Mizutani M (2004) *Arabidopsis CYP707A*s encode (+)-abscisic acid 8'-hydroxylase, a key enzyme in the oxidative catabolism of abscisic acid. Plant Physiol **134:** 1439–1449

Sakai H, Honma T, Aoyama T, Sato S, Kato T, Tabata S, Oka A (2001) ARR1, a transcription factor for genes immediately responsive to cytokinins. Science **294:** 1519–1521

Sakuma Y, Liu Q, Dubouzet JG, Abe H, Shinozaki K, Yamaguchi-Shinozaki K (2002) DNA-binding specificity of the ERF/AP2 domain of *Arabidopsis* DREBs, transcription factors involved in dehydration- and cold-inducible gene expression. Biochem Biophys Res Commun **290:** 998–1009

Sakuma Y, Maruyama K, Osakabe Y, Qin F, Seki M, Shinozaki K, Yamaguchi-Shinozaki K (2006a) Functional analysis of an *Arabidopsis* transcription factor, DREB2A, involved in drought-responsive gene expression. Plant Cell **18:** 1292–1309

Sakuma Y, Maruyama K, Qin F, Osakabe Y, Shinozaki K, Yamaguchi-Shinozaki K (2006b) Dual function of an *Arabidopsis* transcription factor DREB2A in water-stress-responsive and heat-stress-responsive gene expression. Proc Natl Acad Sci U S A **103:** 18822–18827

Sambrook J, Russell D (2001) Molecular cloning: a laboratory manual. 3rd edn: Cold Spring Harbor Laboratory Press

Saradhi A, Saradhi PP (1991) Proline accumulation under heavy metal stress. J Plant Physiol **138:** 554–558

Saradhi PP, Alia, Arora S, Prasad KV (1995) Proline accumulates in plants exposed to UV radiation and protects them against UV induced peroxidation. Biochem Biophys Res Commun **209:** 1–5

Savouré A, Hua XJ, Bertauche N, Van Montagu M, Verbruggen N (1997) Abscisic acid-independent and abscisic acid-dependent regulation of proline biosynthesis following cold and osmotic stresses in *Arabidopsis thaliana*. Mol Gen Genet **254:** 104–109

Schobert B, Tschesche H (1978) Unusual solution properties of proline and its interactions with proteins. Biochem Biophys Acta **541:** 270–277

Schulz E, Tohge T, Zuther E, Fernie A, Hincha DK (2015) Natural variation in flavonol and anthocyanin metabolism during cold acclimation in a wide range of *Arabidopsis* accessions. Plant Cell Environ **38**: 1658–1672

Schulz E, Tohge T, Zuther E, Fernie AR, Hincha DK (2016) Flavonoids are determinants of freezing tolerance and cold acclimation in *Arabidopsis thaliana*. Sci Rep **6:** 34027

Schwab R, Ossowski S, Riester M, Warthmann N, Weigel D (2006) Highly specific gene silencing by artificial microRNAs in *Arabidopsis.* Plant Cell **18:** 1121–1133.

Scott IM, Clarke SM, Wood JE, Mur LAJ (2004) Salicylate accumulation inhibits growth at chilling temperature in *Arabidopsis*. Plant Physiol **135:** 1040–1049

Sevengor S, Yasar F, Kusvuran S, Ellialtioglu S (2011) The effect of salt stress on growth, chlorophyll content, lipid peroxidation and antioxidative enzymes of pumpkin seedling. Afr J Agric Res **6:** 2026–2032

Sewelam N, Kazan K, Thomas-Hall SR, Kidd BN, Manners JM, Schenk PM (2013) Ethylene response factor 6 is a regulator of reactive oxygen species signaling in *Arabidopsis*. PLoS One **8:** e70289

Shaikhali J, Heiber I, Seidel T, Ströher E, Hiltscher H, Birkmann S, Dietz KJ, Baier M (2008) The redox-sensitive transcription factor Rap2.4a controls nuclear expression of 2-Cys peroxiredoxin A and other chloroplast antioxidant enzymes. BMC Plant Biol **8:** 48

Sharma P, Dubey RS (2005). Drought induces oxidative stress and enhances the activities of antioxidant enzyme in growing rice seedling. Plant Growth Regul **46:** 209–221

Sharma P, Jha AB, Dubey RS, Pessarakli M (2012) Reactive oxygen species, oxidative damage, and antioxidative defense mechanism in plants under stressful conditions. J Bot **2012:** 1–26

Shi H, Ishitani M, Kim C, Zhu J-K (2000) The *Arabidopsis thaliana* salt tolerance gene *SOS1* encodes a putative Na^+/H^+ antiporter. Proc Natl Acad Sci U S A **97:** 6896–6901

Shi H, Wang X, Ye T, Chen F, Deng J, Yang P, Zhang Y, Chan Z (2014) The Cysteine2/Histidine2-Type transcription factor ZINC FINGER OF ARABIDOPSIS THALIANA6 modulates biotic and abiotic stress responses by activating salicylic acid-related genes and C-REPEAT-BINDING FACTOR genes in *Arabidopsis*. Plant Physiol **165:** 1367–1379

Shi Y, Tian S, Hou L, Huang X, Zhang X, Guo H, Yanga S (2012) Ethylene signaling negatively regulates freezing tolerance by repressing expression of *CBF* and type-A *ARR* genes in *Arabidopsis.* Plant Cell **24:** 2578–2595

Shinozaki K, Yamaguchi-Shinozaki K (1996) Molecular responses to drought and cold stress. Curr Opin Biotechnol **7:** 161–167

Shinozaki K, Yamaguchi-Shinozaki K (1997) Gene expression and signal transduction in water-stress response. Plant Physiol **115:** 327–334

Shinozaki K, Yamaguchi-Shinozaki K (2000) Molecular responses to dehydration and low temperature: Differences and cross-talk between two stress signaling pathways. Curr Opin Plant Biol **3:** 217–223

Shinozaki K, Yamaguchi-Shinozaki K (2007) Gene networks involved in drought stress response and tolerance. J Exp Bot **58:** 221–227

Shinozaki K, Yamaguchi-Shinozaki K, Seki M (2003) Regulatory network of gene expression in the drought and cold stress responses. Curr Opin Plant Biol **6:** 410–41

Šimášková M, O'Brien JA, Khan M, Van Noorden G, Ötvös K, Vieten A, De Clercq I, Van Haperen JM, Cuesta C, Hoyerová K, Vanneste S, Marhavý P, Wabnik K, Van Breusegem F, Nowack M, Murphy A, Friml J, Weijers D, Beeckman T, Benková E (2015) Cytokinin response factors regulate PIN-FORMED auxin transporters. Nat Commun **6:** 8717

Smallwood M, Bowles DJ (2002) Plants in a cold climate. Philos Trans R Soc Lond B Biol Sci **357:** 831–847

Smirnoff N, Cumbes QJ (1989) Hydroxyl radical scavenging activity of compatible solutes. Phytochemistry **28:** 1057–1060

Solanke AU, Sharma AK (2008) Signal transduction during cold stress in plants. Physiol Mol Biol Plants **14:** 69–79

Solano R, Stepanova A, Chao Q, Ecker JR (1998) Nuclear events in ethylene signaling: a transcriptional cascade mediated by ETHYLENE INSENSITIVE3 and ETHYLENE-RESPONSE-FACTOR1. Genes Dev **12:** 3703–3714

Son GH, Wan J, Kim HJ, Nguyen XC, Chung WS, Hong JC, Stacey G (2012) Ethylene-responsive element-binding factor 5, ERF5, is involved in chitin-induced innate immunity response. Mol Plant Microbe Interact **25:** 48–60

Sparkes IA, Runions J, Kearns A, Hawes C (2006) Rapid, transient expression of fluorescent fusion proteins in tobacco plants and generation of stably transformed plants. Nat Protoc **1:** 2019–2025

Sparks EE, Drapek C, Gaudinier A, Li S, Ansariola M, Shen N, Hennacy JH, Zhang J, Turco G, Petricka JJ, Foret J, Hartemink AJ, Gordân R, Megraw M, Brady SM, Benfey PN (2016) Establishment of expression in the SHORTROOT-SCARECROW

transcriptional cascade through opposing activities of both activators and repressors. Dev Cell **395:** 585–596

Sprinzak, E, Sattah S, Margalit H (2003) How reliable are experimental protein–protein interaction data? J Mol Biol **327:** 919–923

Stafford HA (1991) Flavonoid evolution: an enzymic approach. Plant Physiol **96:** 680–685

Steinert J, Schiml S, Fauser F, Puchta H (2015) Highly efficient heritable plant genome engineering using *Cas9* orthologues from *Streptococcus thermophilus* and *Staphylococcus aureus*. Plant J **84:** 1295–1305

Steponkus PL (1984) Role of the plasma membrane in freezing injury and cold acclimation. Annu Rev Plant Physiol **35:** 543–584

Steponkus PL, Uemura M, Joseph RA, Gilmour SJ, Thomashow MF (1998) Mode of action of the *COR15a* gene on the freezing tolerance of *Arabidopsis thaliana*. Proc Natl Acad Sci U S A **95:** 14570–14575

Steponkus PL, Uemura M, Webb MS (1993) A contrast of the cryostability of the plasma membrane of winter rye and spring oat – two species that widely differ in their freezing tolerance and plasma membrane lipid composition. In: Steponkus PL (ed), Advances in low-temperature biology, JAI Press Ltd., 211–312

Stockinger EJ, Gilmour SJ, Thomashow MF (1997) *Arabidopsis thaliana CBF1* encodes an AP2 domain-containing transcriptional activator that binds to the C-repeat/DRE, a *cis*-acting DNA regulatory element that stimulates transcription in response to low temperature and water deficit. Proc Natl Acad Sci U S A **94:** 1035–1040

Stracke R, Ishihara H, Huep G, Barsch A, Mehrtens F, Niehaus K, Weisshaar B (2007) Differential regulation of closely related R2R3-MYB transcription factors controls flavonol accumulation in different parts of the *Arabidopsis thaliana* seedling. Plant J **50:** 660–677

Strauss G, Hauser H (1986) Stabilization of lipid bilayer vesicles by sucrose during freezing. Proc Natl Acad Sci U S A **83:** 2422–2426

Sun S, Yu JP, Chen F, Zhao TJ, Fang XH, Li YQ, Sui SF (2008) TINY, a dehydration-responsive element (DRE)-binding protein-like transcription factor connecting the DRE- and ethylene-responsive element-mediated signaling pathways in *Arabidopsis*. J Biol Chem **283:** 6261–6271

Suzuki N, Miller G, Morales J, Shulaev V, Torres MA, Mittler R (2011) Respiratory burst oxidases: the engines of ROS signaling. Curr Opin Plant Biol **14:** 691–699

Suzuki N, Mittler R (2006) Reactive oxygen species and temperature stresses: a delicate balance between signaling and destruction. Physiol Plant **126:** 45–51

Swarup K, Benková E, Swarup R, Casimiro I, Péret B, Yang Y, Parry G, Nielsen E, De Smet I, Vanneste S, Levesque MP, Carrier D, James N, Calvo V, Ljung K, Kramer E, Roberts R, Graham N, Marillonnet S, Patel K, Jones JD, Taylor CG, Schachtman

DP, May S, Sandberg G, Benfey P, Friml J, Kerr I, Beeckman T, Laplaze L, Bennett MJ (2008) The auxin influx carrier LAX3 promotes lateral root emergence. Nat Cell Biol **10:** 946–954

Tamura K, Stecher G, Peterson D, Filipski A, Kumar S (2013) MEGA6: Molecular evolutionary genetics analysis version 6.0. Mol Biol Evol **30:** 2725–2729

Tan B, Schwartz S, Zeevaart J, McCarty D (1997) Genetic control of abscisic acid biosynthesis in maize. Proc Natl Acad Sci U S A **94:** 12235–12240

Taylor HM, Klepper B, Brady NC (1979) The role of rooting characteristics in the supply of water to plants. Adv Agron **30:** 99–128

Teige M, Scheikl E, Eulgem T, Dóczi R, Ichimura K, Shinozaki K, Dangl JL, Hirt H (2004) The MKK2 pathway mediates cold and salt stress signaling in *Arabidopsis*. Mol Cell **15:** 141–152

Thalhammer A, Bryant G, Sulpice R, Hincha DK (2014a) Disordered cold regulated15 proteins protect chloroplast membranes during freezing through binding and folding, but do not stabilize chloroplast enzymes *in vivo*. Plant Physiol **166:** 190–201

Thalhammer A, Hincha DK, Zuther E (2014b) Measuring freezing tolerance: electrolyte leakage and chlorophyll fluorescence assays. Methods Mol Biol **1166:** 15–24

Thomas SG, Phillips AL, Hedden P (1999) Molecular cloning and functional expression of gibberellin 2-oxidases, multifunctional enzymes involved in gibberellin deactivation. Proc Natl Acad Sci U S A **96:** 4698–4703

Thomashow MF (1999) Plant cold acclimation: Freezing tolerance genes and regulatory mechanisms. Annu Rev Plant Physiol Plant Mol Biol **50:** 571–599

Torres MA, Dangl JL (2005) Functions of the respiratory burst oxidase in biotic interactions, abiotic stress and development. Curr Opin Plant Biol **8:** 397–403

Tunnacliffe A, Wise MJ (2007) The continuing conundrum of LEA proteins. Naturwissenschaften **94:** 791–812

Turečková V, Novák O, Strnad M (2009) Profiling ABA metabolites in *Nicotiana tabacum* L. leaves by ultra-performance liquid chromatography-electrospray tandem mass spectrometry. Talanta **80:** 390–399

Uemura M, Joseph RA, Steponkus PL (1995) Cold acclimation of *Arabidopsis thaliana*. Effect on plasma membrane lipid composition and freeze-induced lesions. Plant Physiol **109:** 15–30

Uemura M, Steponkus PL (1997) Effect of cold acclimation on membrane lipid composition and freeze-induced membrane destabilization. In: Li PH, Chen THH (eds), Plant cold hardiness, Molecular biology, biochemistry and physiology. Plenum Press, New York, 171–179

Uemura M, Yoshida S (1984) Involvement of plasma membrane alterations in cold acclimation of winter rye seedlings (*Secale cereale* L. cv Puma). Plant Physiol **75:** 818–826

Urao T, Yakubov B, Satoh R, Yamaguchi-Shinozaki K, Seki M, Hirayama T, Shinozaki K (1999) A transmembrane hybrid-type histidine kinase in *Arabidopsis* functions as an osmosensor. Plant Cell **11:** 1743–1754

Van der Valk A (2009) Herbaceous plant ecology: Recent advances in plant ecology. In: Van der Valk A (ed), Herbaceous plant ecology: Recent advances in plant ecology, Springer

Vandesompele J, De Preter K, Pattyn F, Poppe B, Van Roy N, De Paepe A, Speleman F (2002) Accurate normalization of real-time quantitative RT-PCR data by geometric averaging of multiple internal control genes. Genome Biol **3:** research 0034

Verbruggen N, Hermans C (2008) Proline accumulation in plants: a review. Amino Acids **35:** 753–759

Vilarrasa-Blasi J, González-García MP, Frigola D, Fàbregas N, Alexiou KG, López-Bigas N, Rivas S, Jauneau A, Lohmann JU, Benfey PN, Ibañes M, Caño-Delgado AI (2014) Regulation of plant stem cell quiescence by a brassinosteroid signaling module. Dev Cell **30:** 36–47

Vishwakarma K, Upadhyay N, Kumar N, Yadav G, Singh J, Mishra RK, Kumar V, Verma R, Upadhyay RG, Pandey M, Sharma S (2017) Abscisic acid signaling and abiotic stress tolerance in plants: A review on current knowledge and future prospects. Front Plant Sci **8:** 161

Vision TJ, Brown DG, Tanksley SD (2000) The origins of genomic duplications in *Arabidopsis*. Science **290:** 2114–2117

Vogel JT, Zarka DG, Van Buskirk HA, Fowler SG, Thomashow MF (2005) Roles of the CBF2 and ZAT12 transcription factors in configuring the low temperature transcriptome of *Arabidopsis*. Plant J **41:** 195–211

Vogel MO, Moore M, König K, Pecher P, Alsharafa K, Lee J, Dietz KJ (2014) Fast retrograde signaling in response to high light involves metabolite export, MITOGEN-ACTIVATED PROTEIN KINASE6, and AP2/ERF transcription factors in *Arabidopsis.* Plant Cell **26:** 1151–1165

Waldman A, Rikin A, Dovrat A, Richmond AE (1975) Hormonal regulation of morphogenesis and cold-resistance II. Effect of cold-acclimation and exogenous abscisic acid on gibberellic acid and abscisic acid activities in alfalfa (*Medicago sativa L.*) seedlings. J Exp Bot **26:** 853–859

Wang L, Tu YC, Lian TW, Hung JT, Yen JH, Wu MJ (2006a) Distinctive antioxidant and antiinflammatory effects of flavonols. J Agric Food Chem **54:** 9798–9804

Wang P, Du Y, Zhao X, Miao Y, Song CP (2013) The MPK6-ERF6-ROS-responsive *cis*-acting Element7/GCC box complex modulates oxidative gene transcription and the oxidative response in *Arabidopsis*. Plant Physiol **161:** 1392–1408

Wang RS, Pandey S, Li S, Gookin TE, Zhao Z, Albert R, Assmann SM (2011) Common and unique elements of the ABA-regulated transcriptome of *Arabidopsis* guard cells. BMC Genomics **12:** 216

Wang S, Yang S, Yin Y, Xi J, Li S, Hao D (2009) Molecular dynamics simulations reveal the disparity in specific recognition of GCC-box by AtERFs transcription factors super family in *Arabidopsis*. J Mol Recognit **22:** 474–479

Wang W, Vinocur B, Shoseyov O, Altman A (2004) Role of plant heat-shock proteins and molecular chaperones in the abiotic stress response. Trends Plant Sci **9:** 244–252

Wang X, Li W, Li M, Welti R (2006b) Profiling lipid changes in plant response to low temperatures. Physiol Plant **126:** 90–96

Wani SH, Kumar V, Shriram V, Sah SK (2016) Phytohormones and their metabolic engineering for abiotic stress tolerance in crop plants. Crop J **4:** 162–176

Wanner LA, Junttila O (1999) Cold-induced freezing tolerance in *Arabidopsis*. Plant Physiol **120:** 391–400

Weigel D (1995) The APETALA2 domain is related to a novel type of DNA binding domain. Plant Cell **7:** 388–389

Weigel D, Glazebrook J (2002) *Arabidopsis*: A laboratory manual. Cold Spring Harbour Labaratory Press

Weiss D, Ori N (2007) Mechanisms of cross talk between gibberellin and other hormones. Plant Physiol **144:** 1240–1246

Welsch R, Maass D, Voegel T, Dellapenna D, Beyer P (2007) Transcription factor RAP2.2 and its interacting partner SINAT2: stable elements in the carotenogenesis of *Arabidopsis* leaves. Plant Physiol **145:** 1073–1085

Winkel-Shirley B (2002) Biosynthesis of flavonoids and effects of stress. Curr Opin Plant Biol **5:** 218–223

Wohlbach DJ, Quirino BF, Sussman MR (2008) Analysis of the *Arabidopsis* histidine kinase ATHK1 reveals a connection between vegetative osmotic stress sensing and seed maturation. Plant Cell **20:** 1101–1117

Wu L, Chen X, Ren H, Zhang Z, Zhang H, Wang J, Wang XC, Huang R (2007) ERF protein JERF1 that transcriptionally modulates the expression of abscisic acid biosynthesis-related gene enhances the tolerance under salinity and cold in tobacco. Planta **226:** 815–825

Wu X, He J, Chen J, Yang S, Zha D (2014) Alleviation of exogenous 6-benzyladenine on two genotypes of eggplant (*Solanum melongena* Mill.) growth under salt stress. Protoplasma **251:** 169–176

Xin Z, Browse J (2000) Cold comfort farm: the acclimation of plants to freezing temperatures. Plant Cell Environ **23:** 893–902

Xin Z, Mandaokar A, Chen J, Last RL, Browse J (2007) *Arabidopsis ESK1* encodes a novel regulator of freezing tolerance. Plant J **49:** 786–799

Yamaguchi S (2008) Gibberellin metabolism and its regulation. Annu Rev Plant Biol **59:** 225–251

Yamaguchi S, Smith MW, Brown RGS, Kamiya Y, Sun T-p (1998) Phytochrome regulation and differential expression of gibberellin 3β-hydroxylase genes in germinating *Arabidopsis* seeds. Plant Cell **10:** 2115–2126

Yamaguchi-Shinozaki K, Shinozaki K (2006) Transcriptional regulatory networks in cellular responses and tolerance to dehydration and cold stresses. Annu Rev Plant Biol **57:** 781–803

Yamauchi Y, Ogawa M, Kuwahara A, Hanada A, Kamiya Y, Yamaguchi S (2004) Activation of gibberellin biosynthesis and response pathways by low temperature during imbibition of *Arabidopsis thaliana* seeds. Plant Cell **16:** 367–378

Yamori W, Hikosaka K, Way DA (2014) Temperature response of photosynthesis in C3, C4, and CAM plants: temperature acclimation and temperature adaptation. Photosynth Res **119:** 101–117

Yang Y, Costa A, Leonhardt N, Siegel RS, Schroeder JI (2008) Isolation of a strong *Arabidopsis* guard cell promoter and its potential as a research tool. Plant Methods **4:** 6

Yoshida T, Mogami J, Yamaguchi-Shinozaki K (2014) ABA-dependent and ABA-independent signaling in response to osmotic stress in plants. Curr Opin Plant Biol **21:** 133–139

Zarei A, Körbes AP, Younessi P, Montiel G, Champion A, Memelink J (2011) Two GCC boxes and AP2/ERF-domain transcription factor ORA59 in jasmonate/ethylene-mediated activation of the *PDF1.2* promoter in *Arabidopsis*. Plant Mol Biol **75:** 321–331

Zhang S, Outlaw WH (2008) Abscisic acid introduced into the transpiration stream accumulates in the guard-cell apoplast and causes stomatal closure. Plant Cell Environ **24:** 1045–1054

Zhang Y, Zhang F, Li X, Baller JA, Qi Y, Starker CG, Bogdanove AJ, Voytas DF (2013) Transcription activator-like effector nucleases enable efficient plant genome engineering. Plant Physiol **161:** 20–27

Zhao C, Zhu JK (2016) The broad roles of *CBF* genes: From development to abiotic stress. Plant Signal Behav **11:** e1215794

Zhao L, Wang C, Zhu F, Li Y (2017) Mild osmotic stress promotes 4-methoxy indolyl-3-methyl glucosinolate biosynthesis mediated by the MKK9-MPK3/MPK6 cascade in *Arabidopsis*. Plant Cell Rep **36:** 543–555

Zhao XC, Schaller GE (2004) Effect of salt and osmotic stress upon expression of the ethylene receptor ETR1 in *Arabidopsis thaliana*. FEBS Lett **562:** 189–192

Zhou J, Tang X, Martin GB (1997) The Pto kinase conferring resistance to tomato bacterial speck disease interacts with proteins that bind a *cis*-element of pathogenesis-related genes. EMBO J **16:** 3207–3218

Zhu JK (2001) Cell signaling under salt, water and cold stresses. Curr Opin Plant Biol **4:** 401–406

Zhu JK (2002) Salt and drought stress signal transduction in plants. Annu Rev Plant Biol **53:** 247–273

Zhu JK (2016) Abiotic stress signaling and responses in plants. Cell **167:** 313–324

Zimmermann P, Hirsch-Hoffmann M, Hennig L, Gruissem W (2004) GENEVESTIGATOR. *Arabidopsis* microarray database and analysis toolbox. Plant Physiol **136:** 2621–2632

Zuther E, Büchel K, Hundertmark M, Stitt M, Hincha DK, Heyer AG (2004) The role of raffinose in the cold acclimation response of *Arabidopsis thaliana*. FEBS Lett **576:** 169–173

Zuther E, Schulz E, Childs LH, Hincha DK (2012) Natural variation in the non-acclimated and cold-acclimated freezing tolerance of *Arabidopsis thaliana* accessions. Plant Cell Environ **35:** 1860–1878

Zwack PJ, Compton MA, Adams CI, Rashotte AM (2016) Cytokinin response factor 4 (CRF4) is induced by cold and involved in freezing tolerance. Plant Cell Rep **35:** 573–584

Zwack PJ, Robinson BR, Risley MG, Rashotte AM (2013) Cytokinin response factor 6 negatively regulates leaf senescence and is induced in response to cytokinin and numerous abiotic stresses. Plant Cell Physiol **54:** 971–981

PUBLICATIONS

Bolt S, Zuther E, Zintl S, Hincha DK, Schmülling T (2017) *ERF105* is a transcription factor gene of *Arabidopsis thaliana* required for freezing tolerance and cold acclimation. Plant Cell Environ **40:** 108–120

Table A1. Expression of selected cold-responsive genes in the *erf105* mutant and *ERF105* overexpressing plants. Relative expression values in the *erf105* mutant and *ERF105* overexpressing plants before (non-acclimated, NA) and after (acclimated, ACC) 14 days or 21 days of cold acclimation at 4 °C. The relative fold changes ± SE are shown compared to transcript levels of wild-type samples under control conditions which were set to 1 ($n \geq 4$). Relative expression values of *erf105* mutant and *ERF105* overexpressing plants with a statistical significance of $p < 0.01$ compared to the respective NA and ACC wild type are printed in bold.

		NA				ACC14				ACC21			
		WT	*erf105*	ERF105ox-1	ERF105ox-2	WT	*erf105*	ERF105ox-1	ERF105ox-2	WT	*erf105*	ERF105ox-1	ERF105ox-2
CBF1	AT4G25490	1	**0.16**	**0.34**	0.51	26.64	**2.10**	**10.57**	**6.49**	11.38	**5.11**	12.39	13.27
		± 0.06	± 0.01	± 0.14	± 0.14	± 3.74	± 0.13	± 2.99	± 2.08	± 1.18	± 0.51	± 1.11	± 0.91
CBF2	AT4G25470	1	**0.15**	**0.25**	0.43	35.96	**0.80**	**12.91**	**2.65**	6.97	**2.01**	8.16	8.22
		± 0.01	± 0.02	± 0.14	± 0.14	± 2.73	± 0.10	± 2.51	± 1.01	± 0.47	± 0.10	± 0.58	± 0.72
CBF3	AT4G25480	1	0.84	1.90	**2.67**	43.52	**1.32**	55.44	**14.95**	33.86	**7.58**	**47.27**	**49.64**
		± 0.05	± 0.04	± 0.34	± 0.19	± 4.24	± 0.09	± 4.33	± 3.96	± 4.15	± 0.62	± 1.12	± 1.63
COR6.6	AT5G15970	1	1.30	2.13	**3.90**	24.42	**9.37**	12.13	25.07	24.14	**9.35**	32.67	**54.96**
		± 0.09	± 0.14	± 0.06	± 0.38	± 2.88	± 0.27	± 3.83	± 2.83	± 2.33	± 0.34	± 3.47	± 6.02
COR15A	AT2G42530	1	0.61	1.41	**2.31**	34.99	**3.82**	**11.35**	**15.75**	23.25	**1.40**	24.30	**58.65**
		± 0.13	± 0.05	± 0.21	± 0.13	± 4.86	± 0.36	± 1.92	± 2.60	± 3.87	± 0.35	± 5.79	± 7.76
COR15B	AT2G42540	1	1.40	1.15	**3.22**	12.25	**3.84**	5.56	12.45	16.40	**4.01**	19.35	**55.02**
		± 0.08	± 0.10	± 0.16	± 0.17	± 1.79	± 0.34	± 1.96	± 1.67	± 3.88	± 0.68	± 4.37	± 8.03
COR47	AT1G20440	1	**0.31**	0.64	0.88	2.62	**0.70**	1.03	1.33	1.97	**0.72**	2.58	**4.01**
		± 0.07	± 0.03	± 0.20	± 0.10	± 0.26	± 0.08	± 0.17	± 0.19	± 0.33	± 0.11	± 0.31	± 0.54
COR78	AT5G52310	1	1.09	**2.39**	**2.64**	3.45	1.45	**4.02**	3.76	17.12	**3.25**	23.48	**58.45**
		± 0.12	± 0.09	± 0.08	± 0.17	± 0.57	± 0.25	± 0.31	± 0.56	± 3.12	± 0.56	± 2.34	± 8.05
ZAT6	AT5G04340	1	**0.36**	1.43	1.60	5.25	8.04	5.12	**16.56**	4.64	3.62	6.65	5.09
		± 0.17	± 0.12	± 0.07	± 0.12	± 0.49	± 0.61	± 0.24	± 3.92	± 0.59	± 0.50	± 1.32	± 1.46
ZAT12	AT5G59820	1	0.29	0.85	1.19	9.18	**25.08**	4.98	18.71	4.66	**19.66**	6.51	8.45
		± 0.17	± 0.11	± 0.13	± 0.12	± 1.54	± 1.30	± 0.85	± 3.92	± 1.04	± 2.82	± 1.07	± 1.22

Table A1. Continued.

		NA				ACC14				ACC21			
		WT	*erf105*	ERF105ox-1	ERF105ox-2	WT	*erf105*	ERF105ox-1	ERF105ox-2	WT	*erf105*	ERF105ox-1	ERF105ox-2
ICE1	AT3G26744	1	1.00	1.69	2.59	1.74	2.81	2.00	2.12	1.14	0.57	1.10	1.71
		± 0.05	± 0.15	± 0.48	± 0.89	± 0.29	± 0.79	± 0.40	± 0.39	± 0.11	± 0.32	± 0.11	± 0.37
ICE2	AT1G12860	1	0.93	0.60	1.09	0.65	0.36	0.46	0.84	0.54	0.64	0.66	0.95
		± 0.04	± 0.11	± 0.07	± 0.07	± 0.06	± 0.09	± 0.05	± 0.16	± 0.09	± 0.21	± 0.11	± 0.09
HOS1	AT2G39810	1	1.04	0.48	0.37	1.02	0.56	0.55	0.41	0.58	0.92	0.34	1.33
		± 0.41	± 0.19	± 0.12	± 0.14	± 0.06	± 0.13	± 0.21	± 0.13	± 0.06	± 0.22	± 0.11	± 0.36
SIZ1	AT5G60410	1	1.04	0.79	0.50	0.71	1.81	1.59	0.92	0.52	1.43	0.77	0.68
		± 0.25	± 0.23	± 0.31	± 0.09	± 0.04	± 0.36	± 0.43	± 0.37	± 0.07	± 0.37	± 0.14	± 0.14
MYB15	AT3G23250	1	0.41	1.64	**2.44**	11.26	6.96	3.08	1.19	1.33	3.29	0.33	1.37
		± 0.14	± 0.11	± 0.20	± 0.19	± 3.49	± 1.24	± 0.16	± 0.17	± 0.18	± 1.18	± 0.12	± 0.07
MYB96	AT5G62470	1	0.79	0.88	0.91	0.28	0.23	0.36	0.43	0.34	0.31	0.89	**0.95**
		± 0.11	± 0.09	± 0.06	± 0.04	± 0.03	± 0.02	± 0.03	± 0.14	± 0.05	± 0.05	± 0.16	± 0.10
ESK1	AT3G55990	1	0.79	0.75	1.04	0.24	0.17	0.18	**0.50**	0.18	0.16	0.14	0.20
		± 0.04	± 0.11	± 0.09	± 0.05	± 0.02	± 0.02	± 0.03	± 0.04	± 0.01	± 0.03	± 0.04	± 0.03
FRY2	AT4G21670	1	0.68	0.69	0.82	1.09	1.37	1.03	1.55	1.02	1.27	1.13	1.02
		± 0.05	± 0.03	± 0.04	± 0.06	± 0.14	± 0.18	± 0.12	± 0.35	± 0.13	± 0.09	± 0.14	± 0.09
LOS4	AT3G53110	1	0.91	0.90	1.00	1.12	1.27	1.25	1.32	0.97	1.27	1.22	1.04
		± 0.08	± 0.04	± 0.05	± 0.12	± 0.09	± 0.15	± 0.16	± 0.09	± 0.12	± 0.07	± 0.18	± 0.08
RD29B	AT5G52300	1	**5.65**	1.09	1.94	5.17	2.22	1.62	1.64	2.23	2.72	2.04	3.45
		± 0.04	± 0.56	± 0.19	± 0.43	± 1.80	± 0.56	± 0.24	± 0.31	± 0.58	± 0.45	± 0.26	± 0.36
ERF105	AT5G51190	1	**0.01**	**403.42**	**201.58**	0.51	0.01	**235.05**	**149.18**	0.74	**0.03**	**88.37**	**160.88**
		± 0.11	± 0.00	± 8.16	± 19.87	± 0.13	± 0.02	± 36.37	± 19.76	± 0.04	± 0.02	± 11.69	± 24.24

Table A2. Kinetics of the expression of selected cold-responsive genes in wild type and the *erf105* mutant. The table shows relative expression of genes in four-week-old leaves (pooled leaves five, six and seven) at different time points after the beginning of cold treatment (4 °C) in wild type and *erf105*. The relative fold changes ± SE are shown compared to transcript levels of wild-type samples under control conditions which were set to 1 ($n \geq 4$). Relative expression values of *erf105* mutant plants with a statistical significance of $p < 0.01$ compared to the respective wild-type sample are printed in bold.

		Control		15 min		30 min		1 h		4 h		24 h		1 w		2 w	
		WT	*erf105*	WT	*erf105*	WT	*erf105*	WT	*erf105*	WT	*erf105*	WT	*erf105*	WT	*erf105*	WT	*erf105*
CBF1	AT4G25490	1	0.63	7.92	**5.21**	181.51	**11.54**	86.89	69.44	361.69	**101.45**	28.80	15.68	30.35	**14.69**	7.99	6.57
		± 0.17	± 0.04	± 0.84	± 0.54	± 25.63	± 1.04	± 19.33	± 9.54	± 8.43	± 11.41	± 5.76	± 1.02	± 2.29	± 1.11	± 0.92	± 0.74
CBF2	AT4G25470	1	**0.47**	10.31	**6.05**	136.10	**19.54**	187.74	**101.44**	264.71	**43.58**	63.72	**30.06**	81.77	**22.43**	13.67	**19.35**
		± 0.12	± 0.02	± 1.02	± 0.95	± 2.46	± 1.95	± 29.52	± 5.15	± 16.11	± 9.45	± 4.68	± 0.82	± 7.15	± 2.47	± 1.30	± 2.58
CBF3	AT4G25480	1	0.78	25.02	**4.12**	122.22	**20.84**	268.94	**136.85**	565.22	**146.44**	74.35	**37.80**	41.15	**10.11**	2.12	**4.89**
		± 0.18	± 0.05	± 8.73	± 0.41	± 15.83	± 1.78	± 40.11	± 16.77	± 21.15	± 28.46	± 9.11	± 13.11	± 3.29	± 1.10	± 0.35	± 1.13
COR15A	AT2G42530	1	0.62	1.43	1.19	1.63	1.65	3.02	0.96	7.55	**2.85**	31.99	**18.54**	34.62	**14.21**	6.26	6.41
		± 0.24	± 0.05	± 0.25	± 0.21	± 0.50	± 0.11	± 1.26	± 0.07	± 1.34	± 0.35	± 6.22	± 3.91	± 2.19	± 1.22	± 0.46	± 0.76
COR15B	AT2G42540	1	0.83	1.73	**0.65**	3.57	**1.01**	2.65	**1.12**	21.91	**6.11**	47.68	**13.55**	77.24	**14.02**	27.47	**19.11**
		± 0.15	± 0.09	± 0.25	± 0.14	± 0.62	± 0.14	± 0.19	± 0.27	± 4.13	± 0.88	± 5.87	± 0.92	± 1.85	± 0.92	± 2.38	± 2.63
ZAT12	AT5G59820	1	1.14	0.83	**3.51**	2.18	3.25	4.05	**10.65**	5.35	**34.05**	19.81	37.46	12.41	**36.65**	6.16	**2.96**
		± 0.20	± 0.12	± 0.11	± 0.82	± 0.15	± 1.50	± 0.93	± 1.92	± 1.50	± 12.12	± 3.48	± 11.82	± 0.65	± 6.22	± 0.91	± 0.38

Table A3. Expression of selected genes involved in the flavonol and anthocyanin biosynthesis pathway in the *erf105* mutant and *ERF105* overexpressing plants. Relative expression values in the *erf105* mutant and *ERF105* overexpressing plants before (non-acclimated, NA) and after (acclimated, ACC) 14 days or 21 days of cold acclimation at 4 °C. The relative fold changes ± SE are shown compared to transcript levels of wild-type samples under control conditions which were set to 1 (n ≥ 4). Relative expression values of *erf105* mutant and *ERF105* overexpressing plants with a statistical significance of $p < 0.01$ compared to the respective NA and ACC wild type are printed in bold. (n. d. = not detectable).

		NA				ACC14				ACC21			
		WT	*erf105*	ERF105ox-1	ERF105ox-2	WT	*erf105*	ERF105ox-1	ERF105ox-2	WT	*erf105*	ERF105ox-1	ERF105ox-2
PAP1/MYB75	AT1G56650	1	2.25	0.47	**3.40**	5.91	2.68	**12.00**	**15.61**	13.28	**0.68**	**6.67**	**10.44**
		± 0.05	± 0.64	± 0.20	± 0.09	± 0.54	± 0.11	± 1.05	± 1.09	± 0.12	± 0.05	± 0.10	± 0.15
PAP2/MYB90	AT1G66390	1	**0.01**	0.50	0.88	3.60	**727.40**	63.61	**1584.70**	576.71	406.40	**1400.36**	1016.23
		± 0.04	± 0.002	± 0.06	± 0.14	± 0.13	± 88.09	± 10.25	± 120.08	± 61.11	± 30.10	± 165.23	± 95.56
TTG1/WD40	AT5G24520	1	1.74	1.81	1.86	4.03	4.56	3.99	2.68	3.05	3.78	3.01	3.74
		± 0.06	± 0.11	± 0.24	± 0.31	± 0.09	± 0.11	± 0.21	± 0.81	± 0.21	± 0.34	± 0.24	± 0.27
TTG2/WRKY44	AT2G37260	1	**0.71**	**0.20**	**0.08**	0.15	1.22	0.54	**4.32**	4.19	**0.64**	**6.06**	4.00
		± 0.07	± 0.04	± 0.09	± 0.04	± 0.02	± **0.54**	± 0.02	± 0.21	± 0.26	± 0.01	± 0.34	± 0.38
bHLH/TT8	AT4G09820	1	**0.01**	n. d.	n. d.	2.62	22.26	17.72	**203.57**	197.65	**5.84**	203.95	279.18
		± 0.05	± 0.002			± 0.38	± 8.45	± 2.54	± 22.31	± 25.42	± 1.45	± 27.25	± 21.85
MYB11	AT3G62610	1	**0.11**	0.70	**0.03**	0.40	0.18	**2.30**	**2.99**	6.39	**0.02**	3.49	3.69
		± 0.05	± 0.01	± 0.09	± 0.14	± 0.02	± 0.001	± 0.15	± 0.35	± 1.08	± 0.001	± 0.04	± 0.87
MYB12	AT2G47460	1	0.94	**0.25**	**0.11**	0.09	0.52	0.70	**1.54**	1.99	0.06	**4.72**	1.81
		± 0.07	± 0.05	± 0.11	± 0.21	± 0.04	± 0.22	± 0.03	± 0.08	± 0.13	± 0.003	± 1.05	± 0.15
MYB111	AT5G49330	1	1.34	1.10	0.65	7.38	**0.58**	10.37	11.67	21.55	**1.59**	**9.84**	**8.91**
		± 0.08	± 0.18	± 0.09	± 0.15	± 1.09	± 0.01	± 1.47	± 1.54	± 1.98	± 0.45	± 1.75	± 1.47
CHS/TT4	AT5G13930	1	0.92	**2.31**	1.03	2.88	7.85	11.16	**49.20**	62.53	**3.90**	56.55	66.50
		± 0.12	± 0.09	± 0.18	± 0.05	± 0.57	± 2.45	± 2.11	± 4.13	± 5.47	± 0.94	± 4.42	± 9.35
CHI/TT5	AT3G55120	1	0.64	1.26	**1.73**	1.23	0.69	1.33	**8.21**	5.91	**1.11**	8.41	6.11
		± 0.14	± 0.07	± 0.19	± 0.20	± 0.21	± 0.04	± 0.18	± 1.04	± 0.32	± 0.01	± 1.11	± 1.26
F3H/TT6	AT3G51240	1	1.85	1.38	**2.63**	1.79	2.95	3.09	**33.99**	37.74	**4.12**	54.38	46.97
		± 0.06	± 0.23	± 0.16	± 0.17	± 0.15	± 0.65	± 0.41	± 5.54	± 4.25	± 0.95	± 2.84	± 5.18

Table A3. Continued

		NA				ACC14				ACC21			
		WT	*erf105*	ERF105ox-1	ERF105ox-2	WT	*erf105*	ERF105ox-1	ERF105ox-2	WT	*erf105*	ERF105ox-1	ERF105ox-2
FLS	AT5G08640	1	0.65	0.53	0.61	0.11	0.05	0.35	**2.83**	4.43	**0.55**	6.55	5.61
		± 0.07	± 0.02	± 0.17	± 0.18	± 0.005	± 0.001	± 0.01	± 0.18	± 0.55	± 0.02	± 0.84	± 0.74
UGT78D1/F3RT	AT1G30530	1	1.16	1.52	0.92	0.81	0.14	**1.72**	**1.84**	1.35	**0.22**	**2.07**	1.70
		± 0.09	± 0.15	± 0.16	± 0.14	± 0.04	± 0.03	± 0.18	± 0.21	± 0.10	± 0.07	± 0.17	± 0.12
UGT89C1/F7RT	AT1G06000	1	1.61	0.80	1.23	1.70	2.47	2.27	1.95	2.20	1.48	2.90	2.54
		± 0.12	± 0.14	± 0.09	± 0.31	± 0.09	± 0.62	± 0.30	± 0.18	± 0.19	± 0.31	± 0.24	± 0.15
OMT	AT5G54160	1	1.43	1.53	1.65	1.81	**9.31**	1.73	2.50	1.25	**15.04**	2.30	2.34
		± 0.12	± 0.05	± 0.13	± 0.12	± 0.20	± 1.15	± 0.16	± 0.12	± 0.09	± 1.98	± 0.16	± 0.37
DFR/TT3	AT5G42800	1	**0.29**	**0.18**	1.41	1.06	161.22	41.00	**2655.92**	1259.12	22.97	**3238.73**	2122.32
		± 0.05	± 0.005	± 0.07	± 0.21	± 0.08	± 20.21	± 5.85	± 547.2	± 250.3	± 4.54	± 388.8	± 125.2
ANS/TT18	AT4G22870	1	0.66	**2.96**	1.12	1.27	19.68	8.75	**134.05**	98.44	**2.71**	**173.05**	104.09
		± 0.04	± 0.02	± 0.45	± 0.07	± 0.08	± 3.58	± 1.74	± 16.12	± 8.85	± 1.08	± 20.54	± 11.87
LDOX	AT4G22880	1	1.62	0.49	1.29	3.40	192.09	60.40	**4457.84**	2390.53	**35.60**	**4167.87**	3140.00
		± 0.05	± 0.17	± 0.03	± 0.08	± 0.51	± 21.05	± 5.58	± 652.3	± 210.5	± 4.25	± 355.8	± 342.4
UGT75C1/A5GT	AT4G14090	1	11.53	**30.64**	**22.55**	16.70	2637.85	752.79	**20501.26**	13610.86	**435.37**	**25074.09**	18939.67
		± 0.06	± 4.13	± 2.85	± 1.98	± 1.89	± 240.8	± 68.21	± 3254.2	± 1502.2	± 37.81	± 3584.2	± 1622.1
UGT79B1/A3G2"XT	AT5G54060	1	0.90	**1.87**	**2.04**	0.42	8.04	**1.90**	**26.73**	37.52	**2.49**	**72.93**	46.22
		± 0.04	± 0.05	± 0.21	± 0.15	± 0.02	± 3.75	± 0.15	± 3.42	± 3.51	± 0.46	± 6.42	± 5.44
AAT/A5GMaT	AT3G29590	1	0.76	0.85	0.88	0.59	0.57	0.87	**5.17**	3.58	**0.81**	5.69	3.51
		± 0.08	± 0.05	± 0.06	± 0.07	± 0.02	± 0.02	± 0.06	± 1.02	± 0.24	± 0.01	± 0.53	± 0.56
AAT1/A3GCOT	AT1G03940	1	1.40	1.58	**2.31**	0.89	7.39	1.77	**21.99**	25.24	**2.09**	26.04	25.09
		± 0.06	± 0.11	± 0.09	± 0.18	± 0.04	± 2.64	± 0.15	± 1.48	± 1.98	± 0.25	± 3.11	± 2.16
AAT1-like/A3GCOT	AT1G03495	1	**0.24**	**0.25**	**0.03**	0.002	22.10	5.29	**247.99**	308.83	**4.49**	434.13	280.31
		± 0.06	± 0.002	± 0.10	± 0.01	± 0.001	± 3.25	± 0.68	± 26.41	± 24.21	± 0.24	± 37.25	± 19.41
TT19/GST26	AT5G17220	1	3.98	2.52	4.19	4.31	357.93	105.14	**3080.90**	1307.91	**53.22**	**2767.82**	1550.65
		± 0.10	± 1.32	± 0.35	± 0.11	± 0.41	± 94.21	± 42.87	± 278.5	± 124.2	± 4.74	± 210.4	± 100.3

Table A4. Expression of selected genes of the ROS homeostasis in the *erf105* mutant and *ERF105* overexpressing plants. Relative expression values in the *erf105* mutant and *ERF105* overexpressing plants before (non-acclimated, NA) and after (acclimated, ACC) 14 days or 21 days of cold acclimation at 4 °C. The relative fold changes ± SE are shown compared to transcript levels of wild-type samples under control conditions which were set to 1 (n ≥ 4). Relative expression values of *erf105* mutant and *ERF105* overexpressing plants with a statistical significance of $p < 0.01$ compared to the respective NA and ACC wild type are printed in bold.

		NA				ACC14				ACC21			
		WT	*erf105*	ERF105ox-1	ERF105ox-2	WT	*erf105*	ERF105ox-1	ERF105ox-2	WT	*erf105*	ERF105ox-1	ERF105ox-2
APX1	AT1G07890	1	0.75	0.78	0.61	0.65	0.62	1.02	0.58	0.43	0.52	0.56	0.60
		± 0.03	± 0.12	± 0.10	± 0.16	± 0.07	± 0.02	± 0.06	± 0.12	± 0.03	± 0.08	± 0.02	± 0.14
APX2	AT3G09640	1	2.38	1.27	0.47	0.03	0.11	0.19	0.96	0.41	0.58	0.22	0.82
		± 0.33	± 0.59	± 0.28	± 0.10	± 0.00	± 0.07	± 0.06	± 0.63	± 0.35	± 0.19	± 0.07	± 0.21
CAT1	AT1G20630	1	0.80	**0.54**	0.75	0.70	1.65	0.46	0.68	0.54	1.74	0.28	0.55
		± 0.05	± 0.04	± 0.04	± 0.09	± 0.12	± 0.02	± 0.04	± 0.12	± 0.17	± 0.85	± 0.03	± 0.09
CAT2	AT4G35090	1	0.89	0.67	0.86	0.58	0.16	0.33	0.64	0.44	0.31	0.33	0.33
		± 0.05	± 0.11	± 0.08	± 0.12	± 0.06	± 0.14	± 0.10	± 0.13	± 0.08	± 0.16	± 0.08	± 0.10
CSD1	AT1G08830	1	0.61	0.76	0.77	0.91	1.49	1.04	1.72	0.60	1.33	1.34	1.05
		± 0.15	± 0.05	± 0.21	± 0.13	± 0.17	± 0.21	± 0.22	± 1.09	± 0.16	± 0.31	± 0.47	± 0.15
DHAR1	AT1G19570	1	0.79	0.76	0.75	0.66	0.17	0.43	0.68	0.27	0.17	0.31	0.22
		± 0.09	± 0.11	± 0.10	± 0.12	± 0.06	± 0.07	± 0.06	± 0.15	± 0.04	± 0.05	± 0.01	± 0.06
FSD1	AT4G25100	1	1.54	1.22	0.87	2.39	0.60	2.61	2.56	2.06	1.15	1.72	2.32
		± 0.15	± 0.19	± 0.10	± 0.17	± 0.33	± 0.11	± 0.73	± 0.48	± 0.49	± 0.54	± 0.46	± 0.74
FSD2	AT5G51100	1	0.97	0.55	0.76	0.94	0.45	0.65	1.42	0.68	0.48	0.46	1.19
		± 0.11	± 0.12	± 0.03	± 0.04	± 0.18	± 0.07	± 0.14	± 0.23	± 0.23	± 0.18	± 0.07	± 0.15
FSD3	AT5G23310	1	1.00	0.61	0.56	0.44	0.66	0.59	1.37	0.54	0.48	0.30	0.89
		± 0.14	± 0.16	± 0.12	± 0.04	± 0.11	± 0.17	± 0.21	± 0.26	± 0.22	± 0.12	± 0.05	± 0.33
MDAR1	AT3G52880	1	1.14	0.99	0.91	2.21	2.16	2.16	2.13	1.60	1.87	1.55	1.16
		± 0.06	± 0.01	± 0.05	± 0.08	± 0.19	± 0.10	± 0.04	± 0.32	± 0.17	± 0.15	± 0.16	± 0.19

Table A4. Continued.

		NA				ACC14				ACC21			
		WT	*erf105*	ERF105ox-1	ERF105ox-2	WT	*erf105*	ERF105ox-1	ERF105ox-2	WT	*erf105*	ERF105ox-1	ERF105ox-2
MDAR2	AT5G03630	1	0.98	1.89	1.02	1.11	1.06	2.62	1.47	0.88	0.94	1.57	0.92
		± 0.08	± 0.07	± 0.23	± 0.18	± 0.10	± 0.16	± 0.47	± 0.19	± 0.11	± 0.13	± 0.38	± 0.21
MDAR3	AT3G09940	1	1.25	1.39	0.82	0.67	1.31	1.10	1.36	2.19	2.28	1.70	2.45
		± 0.17	± 0.21	± 0.14	± 0.07	± 0.07	± 0.31	± 0.08	± 0.32	± 0.50	± 0.42	± 0.13	± 0.46
RBOHD	AT5G47910	1	1.00	1.71	1.04	0.72	**2.38**	1.81	1.28	1.17	**3.50**	1.26	1.15
		± 0.06	± 0.09	± 0.11	± 0.10	± 0.09	± 0.04	± 0.31	± 0.27	± 0.34	± 0.55	± 0.17	± 0.27
RBOHF	AT1G64060	1	1.31	1.54	0.78	0.83	1.43	0.82	1.23	1.18	1.71	0.52	0.91
		± 0.08	± 0.14	± 0.21	± 0.12	± 0.07	± 0.14	± 0.12	± 0.26	± 0.15	± 0.27	± 0.02	± 0.10

Table A5. Expression of selected genes of the ABA biosynthesis, the ABA signaling and the ABA catabolic pathway in the *erf105* mutant and *ERF105* overexpressing plants. Relative expression values in the *erf105* mutant and *ERF105* overexpressing plants before (non-acclimated, NA) and after (acclimated, ACC) 14 days or 21 days of cold acclimation at 4 °C. The relative fold changes ± SE are shown compared to transcript levels of wild-type samples under control conditions which were set to 1 ($n \geq 4$). Relative expression values of *erf105* mutant and *ERF105* overexpressing plants with a statistical significance of $p < 0.05$ compared to the respective NA and ACC wild type are printed in bold.

		NA				ACC14				ACC21			
		WT	*erf105*	ERF105ox-1	ERF105ox-2	WT	*erf105*	ERF105ox-1	ERF105ox-2	WT	*erf105*	ERF105ox-1	ERF105ox-2
NCED3	AT3G14440	1	**2.35**	1.11	0.89	1.42	**21.79**	2.23	2.02	6.38	9.42	1.76	1.82
		± 0.08	± 0. 11	± 0.14	± 0.09	± 0.13	± 1.48	± 0.19	± 0.34	± 1.13	± 3.26	± 0.34	± 0.26
AAO3	AT2G27150	1	1.19	1.09	1.05	0.75	0.88	0.63	0.73	0.71	0.80	0.51	0.76
		± 0.06	± 0.10	± 0.08	± 0.17	± 0.06	± 0.10	± 0.03	± 0.06	± 0.07	± 0.10	± 0.35	± 0.18
ABA1	AT5G67030	1	0.99	1.09	1.22	1.56	1.13	1.52	1.48	1.27	0.77	0.77	1.27
		± 0.03	± 0.22	± 0.09	± 0.17	± 0.09	± 0.27	± 0.24	± 0.49	± 0.34	± 0.23	± 0.17	± 0.28
ABA2	AT1G52340	1	1.34	0.91	0.99	0.50	0.57	0.51	0.66	1.00	0.56	0.80	1.18
		± 0.06	± 0.11	± 0.11	± 0.05	± 0.09	± 0.09	± 0.05	± 0.06	± 0.19	± 0.09	± 0.17	± 0.40
ABI1	AT4G26080	1	1.43	1.05	1.13	2.00	**11.57**	2.92	2.21	2.44	**6.40**	2.66	2.13
		± 0.11	± 0.28	± 0.17	± 0.17	± 0.30	± 1.54	± 0.60	± 0.12	± 0.50	± 0.80	± 0.07	± 0.34
ABI2	AT5G57050	1	1.24	1.16	0.85	1.64	**3.00**	1.87	1.09	1.52	1.39	1.54	0.70
		± 0.06	± 0.29	± 0.08	± 0.10	± 0.33	± 0.33	± 0.28	± 0.29	± 0.38	± 0.12	± 0.15	± 0.16
ABI5	AT2G36270	1	1.10	1.58	1.19	4.59	4.33	**12.35**	**10.15**	5.02	4.38	**10.78**	9.23
		± 0.17	± 0.02	± 0.17	± 0.11	± 0.73	± 0.31	± 1.14	± 1.96	± 1.10	± 0.77	± 0.79	± 2.38
RAB18	AT5G66400	1	**2.14**	1.17	1.05	2.25	1.36	1.93	**0.83**	1.20	1.07	0.64	0.77
		± 0.11	± 0.12	± 0.15	± 0.19	± 0.43	± 0.20	± 0.40	± 0.17	± 0.46	± 0.15	± 0.16	± 0.13
RD22	AT5G25610	1	0.66	1.06	0.77	0.37	**0.05**	0.21	0.40	0.34	0.09	0.15	0.26
		± 0.03	± 0.07	± 0.17	± 0.09	± 0.003	± 0.03	± 0.03	± 0.08	± 0.10	± 0.05	± 0.02	± 0.11
CBF4	AT5G51990	1	**0.15**	**0.01**	**0.03**	1.07	**0.18**	0.44	0.53	0.59	**0.08**	0.83	1.64
		± 0.02	± 0.002	± 0.001	± 0.01	± 0.02	± 0.003	± 0.05	± 0.03	± 0.03	± 0.01	± 0.17	± 0.27

Table A5. Continued.

		NA				ACC14				ACC21			
		WT	*erf105*	ERF105ox-1	ERF105ox-2	WT	*erf105*	ERF105ox-1	ERF105ox-2	WT	*erf105*	ERF105ox-1	ERF105ox-2
CYP707A1	AT4G19230	1	0.99	0.65	0.43	1.10	**4.28**	1.02	1.49	0.99	**7.12**	1.61	1.31
		± 0.20	± 0.22	± 0.13	± 0.07	± 0.28	± 0.17	± 0.18	± 0.32	± 0.07	± 0.78	± 0.17	± 0.47
CYP707A2	AT2G29090	1	1.01	0.40	0.59	0.65	0.26	0.28	0.90	0.36	0.20	0.18	0.34
		± 0.25	± 0.24	± 0.04	± 0.12	± 0.17	± 0.08	± 0.07	± 0.13	± 0.07	± 0.07	± 0.04	± 0.13
CYP707A3	AT5G45340	1	0.76	1.34	1.05	0.21	0.14	0.38	0.22	0.33	0.34	0.48	0.39
		± 0.19	± 0.21	± 0.02	± 0.18	± 0.02	± 0.01	± 0.08	± 0.03	± 0.10	± 0.12	± 0.06	± 0.12
CYP707A4	AT3G19270	1	0.53	0.39	0.57	0.77	**8.97**	0.40	0.78	0.43	**4.36**	0.56	0.95
		± 0.12	± 0.23	± 0.09	± 0.14	± 0.20	± 0.57	± 0.05	± 0.28	± 0.15	± 1.76	± 0.14	± 0.31

Table A6. Expression of selected genes of the GA metabolism in the *erf105* mutant and *ERF105* overexpressing plants. Relative expression values in the *erf105* mutant and *ERF105* overexpressing plants before (non-acclimated, NA) and after (acclimated, ACC) 14 days or 21 days of cold acclimation at 4 °C. The relative fold changes ± SE are shown compared to transcript levels of wild-type samples under control conditions which were set to 1 (n ≥ 4). Relative expression values of *erf105* mutant and *ERF105* overexpressing plants with a statistical significance of $p < 0.01$ compared to the respective NA and ACC wild type are printed in bold.

		NA				ACC14				ACC21			
		WT	*erf105*	ERF105ox-1	ERF105ox-2	WT	*erf105*	ERF105ox-1	ERF105ox-2	WT	*erf105*	ERF105ox-1	ERF105ox-2
GA2OX1	AT1G78440	1.00	1.22	0.99	1.44	0.26	0.09	0.14	0.35	0.17	0.13	0.32	0.33
		± 0.07	± 0.16	± 0.05	± 0.10	± 0.03	± 0.05	± 0.01	± 0.06	± 0.05	± 0.03	± 0.10	± 0.07
GA2OX2	AT1G30040	1.00	1.14	0.90	0.99	0.83	**7.51**	0.51	0.97	0.71	2.49	0.54	0.54
		± 0.11	± 0.13	± 0.04	± 0.08	± 0.22	± 1.69	± 0.11	± 0.28	± 0.15	± 0.92	± 0.07	± 0.10
GA20OX1	AT4G25420	1.00	1.48	0.51	1.02	0.23	0.10	0.29	0.16	0.20	0.28	0.18	0.19
		± 0.19	± 0.30	± 0.04	± 0.16	± 0.06	± 0.02	± 0.21	± 0.04	± 0.05	± 0.11	± 0.10	± 0.03
GA20OX2	AT5G51810	1.00	0.66	0.75	1.81	0.20	0.25	0.15	0.16	0.16	0.10	0.14	0.14
		± 0.21	± 0.23	± 0.23	± 0.49	± 0.04	± 0.03	± 0.03	± 0.01	± 0.02	± 0.03	± 0.03	± 0.04
GA3OX1	AT1G15550	1.00	0.73	0.49	1.05	0.26	**0.02**	0.13	0.60	0.21	0.05	0.33	0.54
		± 0.09	± 0.11	± 0.06	± 0.06	± 0.04	± 0.00	± 0.07	± 0.01	± 0.05	± 0.02	± 0.15	± 0.11
GA3OX2	AT1G80340	1.00	0.86	0.47	1.15	2.89	**0.30**	0.98	3.06	1.54	0.73	1.63	1.39
		± 0.04	± 0.18	± 0.05	± 0.06	±0.74	± 0.11	± 0.31	± 0.26	± 0.59	± 0.63	± 0.62	± 0.52

Table A7. Expression of selected genes of the ABA biosynthesis, the ABA signaling and the ABA catabolic pathway in the *erf105* mutant and *ERF105* overexpressing plants before and after drought stress. Relative expression values in the *erf105* mutant and *ERF105* overexpressing plants before and after drought stress by withholding water for 9 days. The relative fold changes ± SE are shown compared to transcript levels of wild-type samples under control conditions which were set to 1 ($n \geq 4$). Relative expression values of *erf105* mutant and *ERF105* overexpressing plants with a statistical significance of $p < 0.05$ compared to the respective wild type are printed in bold.

		Control				Drought			
		WT	*erf105*	ERF105ox-1	ERF105ox-2	WT	*erf105*	ERF105ox-1	ERF105ox-2
NCED3	AT3G14440	1	**2.22**	0.51	1.06	2.15	**8.29**	2.17	1.34
		± 0.21	± 0.06	± 0.05	± 0.18	± 0.26	± 0.31	± 0.59	± 0.55
AAO3	AT2G27150	1	1.13	0.82	0.84	3.25	3.64	5.43	5.24
		± 0.08	± 0.22	± 0.02	± 0.04	± 0.43	± 0.48	± 1.12	± 0.89
ABA1	AT5G67030	1	**0.37**	0.67	0.87	1.34	1.08	1.21	1.60
		± 0.10	± 0.06	± 0.06	± 0.11	± 0.19	± 0.05	± 0.16	± 0.22
ABA2	AT1G52340	1	0.85	0.23	0.24	0.22	0.25	0.60	**2.32**
		± 0.38	± 0.64	± 0.03	± 0.01	± 0.05	± 0.07	± 0.30	± 0.30
ABI1	AT4G26080	1	**2.12**	0.80	0.92	3.15	**6.57**	2.88	3.22
		± 0.22	± 0.16	± 0.02	± 0.06	± 0.33	± 0.34	± 0.52	± 0.39
ABI2	AT5G57050	1	**0.52**	0.62	0.99	11.69	12.06	16.51	**25.18**
		± 0.17	± 0.06	± 0.12	± 0.01	± 1.33	± 0.92	± 1.43	± 1.22
ABI5	AT2G36270	1	0.85	0.73	0.57	16.49	**26.81**	**3.95**	**2.37**
		± 0.17	± 0.09	± 0.16	± 0.10	± 1.99	± 4.22	± 1.10	± 0.74
RAB18	AT5G66400	1	0.74	0.72	2.44	1402.04	**2109.44**	**629.67**	**768.75**
		± 0.20	± 0.24	± 0.20	± 0.74	± 139.10	± 106.88	± 117.76	± 94.13
RD22	AT5G25610	1	0.52	0.91	1.39	5.69	6.68	6.19	4.91
		± 0.20	± 0.12	± 0.10	± 0.24	± 0.45	± 1.09	± 1.48	± 0.06
CBF4	AT5G51990	1	**0.11**	1.14	1.32	1.37	**0.42**	**7.12**	**5.60**
		± 0.09	± 0.03	± 0.03	± 0.13	± 0.08	± 0.05	± 0.30	± 0.32
RD29B	AT5G52300	1	**0.28**	0.27	1.37	380.87	538.70	643.20	681.58
		± 0.06	± 0.08	± 0.05	± 0.25	± 57.91	± 98.74	± 98.21	± 56.18
MYB96	AT5G62470	1	0.70	0.84	1.83	1.80	1.86	2.17	1.57
		± 0.14	± 0.12	± 0.17	± 0.20	± 0.12	± 0.16	± 0.37	± 0.46
CYP707A1	AT4G19230	1	1.83	0.78	1.46	28.76	45.89	53.21	53.60
		± 0.09	± 0.22	± 0.15	± 0.23	± 5.20	± 6.12	± 6.81	± 8.55
CYP707A2	AT2G29090	1	0.70	0.54	0.60	4.57	2.57	2.67	2.67
		± 0.10	± 0.13	± 0.06	± 0.07	± 0.48	± 0.12	± 0.72	± 0.40
CYP707A3	AT5G45340	1	0.31	1.94	**5.52**	2.08	**0.54**	**13.95**	**7.35**
		± 0.19	± 0.15	± 0.31	± 1.18	± 0.17	± 0.01	± 2.08	± 0.59
CYP707A4	AT3G19270	1	0.39	0.86	0.58	5.16	3.31	4.34	4.55
		± 0.10	± 0.04	± 0.01	± 0.04	± 1.06	± 0.46	± 0.12	± 0.93

ACKNOWLEDGEMENTS

First of all I would like to express my gratitude to Prof. Dr. Thomas Schmülling for giving me the opportunity to work on this interesting project. Thank you for giving me the freedom to take my research in any direction I choose, which allowed me to acquire numerous techniques. Thank you so much for the supervision during all those years, the guidance and for all your support during the writing process.

I am very grateful to Prof. Dr. Wolfgang Schuster for reviewing this work but also for being helpful in many other ways. Thanks for your assistance with computer or printer problems and for being encouraging.

My deep thanks go to Stefanie Zintl. Thank you so much for your supervision, your constructive criticism, your advice and for sharing your knowledge.

Special thanks go to Dr. Jan Erik Leuendorf for introducing me to the yeast two-hybrid technology. Many thanks for your hints and motivation and for creating a funny atmosphere in the lab and in the office.

I am very grateful to Dr. Ellen Zuther, Dr. Dirk Hincha and their team (Max Planck Institute of Molecular Plant Physiology, Golm, DE). Thank you for the warm welcome in your lab and for the fruitful collaboration in the cold stress project.

I also want to thank Prof. Dr. Nicolaus von Wirén and Dr. Seyed Abdollah Hosseini (IPK Gatersleben, DE) for the successful collaboration regarding the drought stress experiments.

Thanks also to Prof. Dr. Miroslav Strnad and Dr. Veronika Turečková (Laboratory of Growth Regulators, Palacký University & Institute of Experimental Botany AS CR, Olomouc, CZ) for the ABA measurements.

Thank you, Dr. Anne Cortleven for reading and correcting this thesis as well as for being such a friendly colleague.

Many thanks to the student workers Ulrike Wittkopf and Jennifer Müller, who performed hundreds of RNA extractions and cDNA syntheses.

Many thanks also to the gardeners.

I would like to thank all present and former members of the institute for providing a welcoming, warm, and funny atmosphere, and for being helpful in multiple ways.

I am grateful to the DCPS, the DRS, the Frauenförderung of the FU Berlin and the CRC973 for financing this work.

There are no words to express my endless gratitude to my friends and my family. Thank you for believing in me, encouraging me, and supporting me, for your patience and for simply being there. Thank you, Tobi and Lotti, you are so precious to me!